University of Dundee

DOCTOR OF PHILOSOPHY

The AMPK signalling pathway in cancer and DNA damage

Dandapani, Madhumita

Award date:
2013

Awarding institution:
University of Dundee

[Link to publication](#)

DOCTOR OF PHILOSOPHY

The AMPK signalling pathway in cancer and DNA damage

Madhumita Dandapani

2013

University of Dundee

TABLE OF CONTENTS

LIST OF FIGURES

CHAPTER ONE: INTRODUCTION

CHAPTER THREE: ACTIVATION OF AMPK BY AGENTS THAT CAUSE DOUBLE STRANDED DNA BREAKS

CHAPTER FOUR: AMPK IS A TUMOUR SUPPRESSOR IN A T CELL-SPECIFIC PTEN KNOCKOUT TUMOUR MODEL

CHAPTER FIVE: THE ROLE OF PHOSPHORYLATION OF THE C-TERMINAL TAIL OFLKB1 ON AMPK ACTIVATION

LIST OF TABLES

CHAPTER TWO: MATERIALS AND METHODS

LIST OF AMINO ACIDS

Amino acid	Three letter symbol	One letter symbol
Alanine	Ala	A
Arginine	Arg	R
Asparagine	Asn	N
Aspartic acid	Asp	D
Cysteine	Cys	C
Glutamine	Gln	Q
Glutamic acid	Glu	E
Glycine	Gly	G
Histidine	His	H
Isoleucine	Ile	I
Leucine	Leu	L
Lysine	Lys	K
Methionine	Met	M
Phenylalanine	Phe	F
Proline	Pro	P
Serine	Ser	S
Threonine	Thr	T
Tryptophan	Trp	W
Tyrosine	Tyr	Y
Valine	Val	V

ABBREVIATIONS

ACC	acetyl-Coenzyme A carboxylase
AICAR	5-amino-imidazole carboxamide riboside
AMP	adenosine5'-monophosphate
AMPK	AMP activated protein kinase
APC	Anitgen presenting cell
ARK5	AMPK-related kinase 5
AS160	Akt substrate of 160 kDa
ATM	ataxia telangiectasia mutated protein kinase
ATR	ATM and Rad 3 related protein
ATP	adenosine 5'-triphosphate
AU	arbitrary units
Bis	bis-acrylamide
BRSK	brain-specific kinase
BSA	bovine serum albumin
^{0}C	degree Celsius
C. elegans	Caenorhabdtis elegans
CaMK	Ca^{2+}/Calmodulin dependent protein kinase
CaMKK	Ca^{2+}/Calmodulin dependent protein kinase kinase

cAMP   cyclic adenosine monophosphate

CBS   cystathione-β-synthase

Cdk   cyclin-dependent kinase

ChREBP   carbohydrate responsive element-binding protein

CPT-1   carnitine palmitoyltransferase-1

CREB   cAMP response element-binding protein

C-TAK1   Cdc25C-associated kinase-1

C-terminal   carboxy terminal

DAG   Diacyl glycerol

DAPI   4',6-diamidino-2-phenylindole

DMEM   Dulbecco's modified Eagle's medium

DMSO   dimethyl sulfoxide

DNA   deoxyribonucleic acid

DNA-PK   DNA-dependent protein kinase

Drosophila   Drosophila melanogaster

DTT   dithiothreitol

ECL   enhanced chemiluminescence

E. Coli   Escherechia coli

EDTA   ethyldiaminetetraacetate

EGTA   ethyleneglycol-bis (β-aminoethylether)N',N',N',N'-tetraacetate

EMEM	Eagle's minimum essential medium
ePK	eukaryotic protein kinase
ERK	Extracellular signal-regulated kinase
FACS	fluorescence-activated cell sorting
FBS	foetal bovine serum
FLAG	DYKDDDDKG peptide
GAP	GTPase activating protein
GBD	glycogen binding domain
GFP	green fluorescent protein
GST	glutathione-S-transferase
GEF	Guanine nucleotide exchange protein
H2AX	Histone 2A family member X
HDAC	histone deacetylase
HEK293	human embryonic kidney 293 cells
Hepes	N-2-hydroxyethylpiperazine-N'-2-ethane sulfonic acid
HMGR	3-hydroxy-3-methylglutaryl-CoenzymeA reductase
HNF-4α	hepatocyte nuclear factor-4α
HRP	horse radish peroxidase
Hsp	heat shock protein
IgG	immunoglobulin G

ICAM-1	Intercellular adhesion molecule-1
IPTG	isopropyl-β-D-thiogalactopyranoside
KD	kinase domain
kDa	kilodalton
LAT	Linker of activated T-cells
LCK	Lymphocyte-specific protein tyrosine kinase
LB	Luria-bertani broth
LDS	lithium dodecyl sulphate
LFA-1	Leukocyte function antigen-1
M	molar
MAP	microtubule associated protein
MARK	MAP/microtubule affinity regulating kinase
MEF	mouse embryonic fibroblast
MEF2	myocyte enhancing factor 2
MLCK	myosin light chain kinase
MO25	mouse protein 25
MOPS	3-(n-morpholino) propane sulfonic acid
MRLC	myosin regulatory light chain
mTOR	mammalian target of rapamycin
mTORC1	mTOR complex 1

NLS	nuclear localization sequence
N- terminal	amino terminal
OD	optical density
PAGE	polyacrylamide gel electrophoresis
PBS	phosphate buffered saline
PCR	polymerase chain reaction
PDK1	3-phosphoinositie-dependent kinase1
PEI	polyethylenimine
PFK2	6-phosphofructose-2-kinase
PJS	Peutz-Jeghers syndrome
PKA	cAMP- dependent protein kinase
PKB	protein kinase B
PKC	protein kinase C
PLC	phospholipase C
PMSF	phenylmethanesulfonylflouride
PP2	protein phosphatase-2
PTEN	phosphatase and tensin homologue
PTK	Protein tyrosine kinase
RNA	ribonucleic acid
rpm	rotations per minute

S. cerevisiae   Saccharomyces cerevisiae

S.pombe   Saccharomyces pombe

SBT1   soyabean trypsin inhibitor

SDS   sodium dodecyl sulphate

SEM   standard error of the mean

SIK   salt inducible kinase

siRNA   short interfering RNA

SLP76   SH2 domain containing leukocyte protein of 76kDa

SMC-1   Structural Maintainence of chromosome-1

SNARK   SNF1/AMPK-related kinase

SNF1   sucrose non-fermenting-1

SNRK   SNF-related kinase

SREBP-1   sterol regulatory element binding protein-1

STRAD   ste20-related protein

TAK1   transforming growth factor-β-activated kinase-1

TBS   Tris buffered saline

TNFα tumour necrosis factor α

TORC2   transducer of regulated CREB activity-2

TRAIL   TNF-related apoptosis inducing ligand

Tris   Tris (hydroxymethyl) methylamine

TSC	tuberous sclerosis complex
UBA	ubiquitin associated
V	volt
VEGF	vascular endothelial growth factor
Xenopus	Xenopus laevis
ZAP-70	Zeta-chain-associated protein kinase 70

ACKNOWLEDGEMENTS

DECLARATIONS

I hereby declare that the following thesis is based on results of investigations conducted by myself, and that this thesis is my own composition. Work other than my own is clearly indicated in the text. This dissertation has not in whole, or in part, been previously presented for a higher degree.

Madhumita Dandapani

I certify that Madhumita Dandapani has spent the equivalent of atleast nine terms in research work in the Division of Cell signalling and Immunology, University of Dundee, and that she has fulfilled the conditions of Ordinance No 39 of the University of Dundee and is qualified to submit the accompanying thesis in application for the degree of Doctor of Philosophy.

Professor D.Grahame Hardie

SUMMARY

AMP-activated protein kinase (AMPK) is a master regulator of energy homeostasis and metabolism, both at the cellular and at the whole body level. It acts as a cellular fuel gauge, sensing changes in AMP: ATP or ADP: ATP ratios. Once activated by energy deficit, AMPK switches on catabolic processes, generating ATP, and inhibits biosynthetic processes, consuming ATP, thus conserving cellular energy. AMPK also regulates metabolism at the whole-body level, for example, by controlling appetite and entraining feeding with the circadian clock. AMPK regulates the cell cycle and modulates neuronal excitability. In recent years, it has been found that AMPK acts downstream of the tumour suppressor LKB1, that the AMPK signalling pathway is down-regulated in some tumours, and that diabetics treated with the AMPK-activating drug metformin exhibit a lower incidence of cancer. These results suggest that AMPK may itself be a tumour suppressor, although direct evidence has so far been lacking.

This thesis provides genetic evidence that AMPK functions as a tumour suppressor in vivo. A T cell-specific mouse tumour model was developed to delineate the role of AMPK in cancer. T cell-specific deletion of PTEN in mice causes development of T cell lymphomas at a median age of 85 days (43-214 days), while T cell-specific deletion of AMPK as well as PTEN caused development of lymphomas much sooner, at a median age of 65 days (46-87days, p<0.0001, hazard ratio = 6.3). The distribution of tumours was also significantly different between the two groups; the PTEN-null mice developed lymphomas in the thymus as well as in peripheral lymphoid organs such as lymph nodes and spleen, while the PTEN and AMPK double null lymphomas were largely confined to the thymus (p<0.001). Before the onset of tumours, the PTEN AMPK double null T cells were larger and had greatly increased phospho-S6 levels compared to wild type and PTEN null T cells. These results suggest

that AMPK delays tumour onset in cells with an overactive PI3K pathway by down-regulating the mTOR pathway.

Recent studies have also suggested a role for AMPK in the response to DNA damage, produced by treatments such as ionising radiation and the anti-cancer drug etoposide. However, the molecular mechanism underlying this activation was unclear. This thesis shows that etoposide activates AMPK in a CaMKKβ-dependent manner in HeLa cells and G361 cells, both of which lack LKB1. Activation is restricted to the AMPK-α1 isoform within the nucleus, and this is associated with increased nuclear calcium flux. Taken together the results suggest that release of intra-nuclear calcium activates CaMKK-β, which in turn activates AMPK-α1. In addition, activation of AMPK by the calcium ionophore A23187 increased the survival of mouse embryonic fibroblasts treated with etoposide in an AMPK-dependent manner.

This thesis also investigates the role of C-terminal phosphorylation of LKB1 on Ser-325 and Ser-431. The results presented in this thesis show that mutation of these sites to alanine, did not affect activation of AMPK by LKB1. It also shows that ERK2 does not phosphorylate LKB1 on Ser-325 efficiently, and that phosphorylation of Ser-431 by p90RSK does not affect activation of AMPK. These results do not support the view that phosphorylation of these two residues in the C-terminal tail of LKB1 inhibits AMPK activation.

Overall, the studies performed in this thesis demonstrate that AMPK can be both a "friend" and a "foe" in cancer; On the one hand, it functions as a tumour suppressor delaying the onset of cancer, while on the other hand, it increases the survival of cancer cells treated with the anti-cancer drug etoposide. These distinct effects of AMPK might be exploited therapeutically, both in the prevention and in the treatment of cancer.

CHAPTER 1: INTRODUCTION

1.1 Protein phosphorylation

The molecular process involving the conversion of an extracellular signal to a functional change within the cell is termed signal transduction. Protein phosphorylation, a type of post-translational modification of proteins, mediated by enzymes termed protein kinases is an integral part of this process. Protein phosphorylation is a reversible process by which, a covalently bound phosphate group is transferred from ATP to a serine, threonine or tyrosine residue on a protein by an upstream kinase, generating ADP as the other product. This process is reversed by the removal of the phosphate group by a protein phosphatase that catalyses a hydrolysis reaction (Figure 1.1). Phosphorylation and de-phosphorylation of cellular proteins can modify their function in many ways: it can lead to an increase or decrease in the catalytic activity of the protein, stabilise its structure, target it for degradation, alter its sub-cellular localisation, or affect its interaction with other proteins. Nearly 30% of the proteins encoded by the human genome are thought to be regulated by phosphorylation and abnormal phosphorylation is linked either causally, or as a consequence of many human diseases (Cohen, 2002).
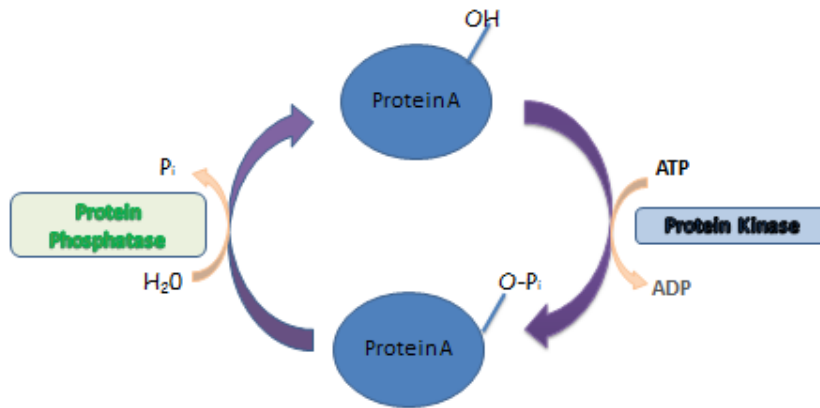
Figure 1.1: Protein phosphorylation

This is a schematic representation of reversible phosphorylation of proteins. Phosphorylation is catalysed by a protein kinase with the phosphate group derived from ATP. Reversal of this process is mediated by protein phosphatases, which dephosphorylate the protein.

Reversible regulation of a protein by phosphorylation was first described by Fischer and Krebs, who showed that phosphorylase kinase converted phosphorylase b to phosphorylase a in the presence of Mg-ATP (Fischer and Krebs, 1955). The reverse reaction was found to be catalysed by protein phosphatase-1 (Ingebritsen and Cohen, 1983). It was then discovered that cyclic-AMP-dependent kinase or protein kinase A itself activated phosphorylase kinase by phosphorylation; thus the concept of a kinase cascade was born (Walsh et al., 1968). This was followed by the discovery of many more such kinases and phosphatases. The genes encoding all of these kinases in the human genome were eventually identified, arranged and depicted as the human kinome.

1.2 The human kinome

The subset of the human genome which encodes protein kinases is termed the kinome (Figure 1.2). Most protein kinases in the human kinome belong to a large superfamily characterized by the presence of a eukaryotic protein kinase (ePK) catalytic domain. There are also 13 families of atypical protein kinases (aPKs) which have biochemical kinase activity but lack sequence similarity to the ePK domain. A total of 518 kinases, comprising 478 ePKs and 40 aPKs have been described (Manning et al., 2002). All kinases are classified into groups, families and subfamilies primarily on the basis of sequence similarity of the catalytic domain, domain structure outside of the catalytic domains and known biological functions. Similar classifications of the yeast and worm kinomes have also been described (Plowman et al., 1999, Breitkreutz et al., 2010). Forty eight ($\approx$ 10%) proteins in the human kinome are considered to be catalytically inactive, as they lack conserved residues required for kinase activity. These 'pseudokinases' have been reported to regulate the activity of other functional kinases, and they also function as scaffolding proteins in multi-protein complexes (Boudeau et al., 2006). One example of a pseudokinase is STRAD (Ste-20 related adapter protein), which is required for the stable assembly and activation of the LKB1 complex. Binding of STRAD and another protein MO25 (mouse protein 25) to LKB1, alters the subcellular localisation of the LKB1 complex from the nucleus to the cytoplasm (Boudeau et al., 2006).

Figure 1.2: The human kinome

Image downloaded from kinase.com (based on the paper by Manning et al 2002) showing the human protein kinome which is classified into groups, mainly based on sequences of the kinase domain. AMPK and the AMPK- related kinase family (ARKs) are shown shaded in green and yellow respectively. LKB1 is shaded in purple and CaMKK1 and 2 are shaded in blue.

1.3 AMP-activated protein kinase

1.3.1 Introduction and historical background

This thesis will focus on the 5'-AMP activated protein kinase (AMPK). AMPK was first described as activities present in rat liver extracts that inhibited the activity of either acetyl- CoA carboxylase (Carlson and Kim, 1973, Lee and Kim, 1977) (Lee and Kim, 1977) or microsomal HMG- CoA reductase activity (Beg et al., 1973) in the presence of Mg-ATP. The HMG-CoA reductase kinase was initially reported to require both ADP and ATP for its activity (Brown et al., 1975), but AMP was confirmed to be the nucleotide required to activate the kinase (Ferrer et al., 1985). The earlier observation by Brown et al was likely due to the presence of adenylate kinase in their extracts which converted ADP to AMP. It was then shown that the acetyl-CoA carboxylase (ACC) kinase and HMG-CoA reductase kinase activities were both functions of a single protein kinase (Carling et al., 1987). This kinase, previously referred to as acetyl-CoA carboxylase kinase-3 was renamed AMP-activated protein kinase (AMPK), as it was known to be allosterically activated by AMP (Munday et al., 1988, Carling et al., 1989).

The first subunit of AMPK to be identified was the α subunit. AMPK was purified from rat liver and the catalytic subunit was identified (using a reactive ATP analogue that labelled the catalytic site) to be a 63 KDa protein, initially termed p63 (Carling et al., 1989). Purification of AMPK to homogeneity using ATP-γ-sepharose affinity chromatography led to the identification of two other subunits of molecular mass 38 and 35 KDa, in addition to p63 (Davies et al., 1994). Purification of AMPK from porcine liver using peptide substrate affinity chromatography also confirmed the

existence of three AMPK subunits with estimated molecular masses of 63, 40 and 38

KDa (Mitchelhill et al., 1994). The three distinct subunits p63, p38 and p35, are now

referred to as the α, β and γ subunits of the AMPK complex (Figure 1.3).

1.3.2 The catalytic α subunit

The catalytic subunit of mammalian (rat) AMPK was first cloned and sequenced in

1994 (Carling et al., 1994). The amino acid sequence was used to identify the AMPK

orthologue in yeast, Sucrose non- fermenting (Snf1) protein. The mammalian AMPK α

subunit has a 59% sequence identity to Snf1. A Snf1 preparation purified from yeast

efficiently phosphorylated the SAMS peptide, a rather specific peptide substrate for

AMPK (Woods et al., 1994). A second, more abundant isoform of the mammalian

catalytic subunit termed α1 was then identified, with the isoform originally identified

by Carling et al being termed α2 (Stapleton et al., 1996). Despite being encoded by

different genes, namely PRKAA1 and PRKAA2, α1 and α2 share 90% sequence

identity in the catalytic domain and ≈60% sequence identity outside the catalytic

domain (Stapleton et al., 1996). Both isoforms contain a threonine residue at position

172, which was shown to be the site at which AMPK is phosphorylated by the upstream

kinase, AMPKK (Hawley et al., 1996). Both isoforms had similar substrate specificity

(Michell et al., 1996). Also, α1 was found to be evenly distributed in most tissues, while

α2 was found to be mainly present in skeletal muscle, liver, heart, brain and kidneys

(Stapleton et al., 1996). The α2, but not the α1 isoform was also enriched in the nucleus,

suggesting a role in the regulation of gene expression (Salt et al., 1998).

The C-terminus of the α subunit (residues 392-548) is required for its interaction with the β subunit. Truncation of α1 at residues 312 or 392 abolished the interaction between the α subunit and the β and γ subunits (Crute et al., 1998). α1 (1-392) had greatly reduced AMPK activity compared to the full length α subunit when co-expressed with β and γ subunits. When expressed as a single subunit, α1(1-312) had 30-fold increased activity compared to α1(1-392) indicating the presence of an auto-inhibitory domain between residues 312 and 392 (Crute et al., 1998). This auto-inhibitory domain was subsequently mapped to residues 313-335 in α1, which corresponds to residues 311-333 in α2. Deletion of residues 313-335 from α1 (1-394) and residues 311-313 from α2 (1-398) was sufficient to restore kinase activity (Pang et al., 2007). Analysis of the crystal structure of the unphosphorylated fragment of the α subunit containing the kinase domain and the auto-inhibitory domain (KD-AID) from *S. p*ombe, revealed multiple interaction sites between the N and C lobes of the kinase domain and the auto-inhibitory domain. The authors propose that this binding of the AID may constrain the mobility of the kinase domain helix αC, causing it to remain in an open, inactive conformation (Chen et al., 2009).

The C-terminal tail of the α subunit has recently been shown to contain a nuclear export sequence (Kazgan et al., 2010). Deletion of the last 14 amino acids in the C-terminal tail led to nuclear sequestration of the α subunit. Moreover, cytoplasmic localisation of AMPK could be restored by other known nuclear export sequences when fused to the truncated AMPK-α subunit missing the last 14 residues (Kazgan et al., 2010).

1.3.3 The β subunit

The β subunit has 2 isoforms termed β1 and β2, encoded by the distinct genes PRKAB1 and PRKAB2 (Hardie, 2007b). The two isoforms share 71% amino acid sequence identity. The original β subunit, now termed β1, was purified as a 38 KDa protein from rat liver with DNA encoding the β2 isoform being subsequently cloned from a skeletal muscle cDNA library (Thornton et al., 1998). The β subunit is related to the Sip1/Sip2/ Gal83p family of proteins found in the budding yeast (Woods et al., 1996b, Gao et al., 1995). The β subunit was shown to interact with both the α and γ subunits, thus functioning as a scaffold. Co-expression of α and β or β and γ subunits in rabbit reticulocytes and subsequent immunoprecipitation of the cell lysates using anti-β antibody revealed the presence of α or γ subunits in the precipitate, thus suggesting that AMPK assembles into a heterotrimeric complex with the β subunit at the core (Woods et al., 1996b). A conserved region within the C-terminus of the AMPK β subunit (residues 180-276) is 90% identical between β1 and β2. This region is homologous to the ASC domain in the Sip1/Sip2/Gal83 complex, and has been shown to be required for the binding of α and γ subunits and the formation of the active AMPK heterotrimeric complex (Iseli et al., 2005, Xiao et al., 2007).

The β subunit also contains another highly conserved domain, originally called the *K*inase *I*nteracting *S*equence (KIS) domain, which is conserved in Gal83 and is now known to mediate the interaction of AMPK with glycogen (Hudson et al., 2003, Polekhina et al., 2003). Co-expression of the full-length β subunit with α and γ subunits caused accumulation of AMPK in large cytoplasmic inclusions, which also stained positive for glycogen and glycogen synthase. These inclusions were lost when the truncated β subunit lacking this domain was expressed with α and γ subunits, although

the kinase activity was unaffected (Hudson et al., 2003). This domain is now termed the glycogen-binding domain (GBD) or carbohydrate-binding module (CBM), and it is related to CBMs found in glycogen-binding proteins in animals and bacteria, and starch binding proteins in plants. The crystal structure of the CBM of β1 has been determined in complex with β-cyclodextrin and is similar to those of several starch-binding enzymes (Polekhina et al., 2005). A high level of glycogen in muscle negatively regulates AMPK activation in response to exercise and AICA riboside, while glycogen and oligosaccharides have been found to inhibit purified AMPK (Wojtaszewski et al., 2002, Mcbride et al., 2009). This has led to proposals that AMPK can act as a cellular glycogen sensor.

Using mass spectrometry, several phosphorylation sites have been mapped on the β subunit, including Ser-24/25, Ser-108 and Ser-182 (Mitchelhill et al., 1997). Mutation of the Ser-24/25 and Ser-182 sites to alanine had no effect on the regulation of kinase activity, but caused a redistribution of the subunit to the nucleus (Warden et al., 2001). Mutation of Ser-108 to alanine reduced the activity of the kinase by 60%. The Ser-108 residue is also required for activation of AMPK by the drugs A-769662 and salicylate (Scott et al., 2008, Hawley et al., 2012). The N-terminus of the β subunits also have glycine residues at position 2, which undergo myristoylation (Mitchelhill et al., 1997). Mutation of this glycine to alanine (G2A) leads to a four-fold increase in AMPK activity (Warden et al., 2001), similar to the effect observed by N-terminal truncation of the β subunit (Hudson et al., 2003). Myristoylation is known to target proteins to cell membranes, and the G2A mutation also alters subcellular localisation of AMPK from a particulate extra-nuclear distribution to a more homogenous cell distribution (Warden et al., 2001). It has also been recently shown that myristoylation of

the β subunit is required for stimulation of phosphorylation of Thr-172 on AMPK by AMP and ADP (Oakhill et al., 2010, Oakhill et al., 2011).

1.3.4 The γ subunit

The γ subunit has three isoforms, i.e. γ1, γ2 and γ3, encoded by three distinct genes PRKAG1, PRKAG2 AND PRKAG3 (Woods et al., 1996a, Cheung et al., 2000). The γ1 and γ2 isoforms are expressed ubiquitously, while γ3 is mainly expressed in skeletal muscle. The γ2 and γ3 isoforms have extended N-terminal regions that do not share sequence identity to one another (Cheung et al., 2000); the exact role of these extended regions is not fully understood. Shorter variants of γ2 and γ3, probably due to alternate transcriptional start sites, have also been identified. The C-terminal region of all three γ isoforms show significant sequence identity. Photoaffinity labelling of partially purified AMPK using the AMP analogue, 8-azido [^{32}P] AMP, resulted in labelling of the γ1 subunit, which was abolished in the presence of AMP (Cheung et al., 2000). This was the first evidence that the γ subunit was involved in AMP binding.

The C-terminal region of the γ subunit contain four tandem repeats of a 60 amino acid sequence motif known as a cystathione β synthase (CBS) motif (Bateman, 1997). These motifs associate in pairs to form two Bateman domains, each of which binds one molecule of AMP (Scott et al., 2004). The two Bateman domains appear to bind AMP with positive cooperativity, with the second site binding AMP with higher affinity after the first site has bound AMP (Scott et al., 2004). The crystal structure of AMPK confirmed the presence of these two sites (site 1, in the cleft between CBS1 and CBS2 and site 3, in the cleft between CBS3 and CBS4) that bind AMP or ATP, but also

identified a third site that has a tightly bound, non-exchangeable molecule of AMP located in site 4 between CBS3 and CBS4 (each nucleotide contacts residues from different CBS motifs, but the sites are numbered according to the CBS motif that bears an aspartate residue containing the 2'- and 3'- hydroxyls of the ribose rings; CBS 2 lacks this aspartate, so there is no site 2). The two exchangeable sites, sites1 and 3, have been recently shown to bind ADP as well as ATP and AMP (Xiao et al., 2011). As ATP is more abundant than ADP or AMP in unstressed cells, under basal conditions, these sites are most likely occupied by ATP and the complex is inactive (Xiao et al., 2007). Binding of AMP (Davies et al., 1995) or ADP at the lower affinity site (site 3) has been shown to protect AMPK against dephosphorylation by protein phosphatases (Xiao et al., 2011). Because ADP is usually present at higher concentrations than AMP, a rise in ADP may be the critical signal that induces that effect. However, binding of AMP (but not ADP) at the higher affinity site, site 1, causes a further allosteric activation (see below).

Mutations with dominant inheritance within the CBS motifs of the γ2 subunit that affect AMP binding have been shown to cause hypertrophic cardiomyopathy and Wolff-Parkinson White syndrome (Gollob et al., 2001). These mutations (e.g. R302Q, H383R and R531G) are associated with reduced AMPK activation by AMP (Daniel and Carling, 2002) and reduced binding of AMP to the γ subunit (Scott et al., 2004) . The R531G mutation also increases the basal activity of the kinase, most likely because it affects binding of the inhibitor, ATP, as well as the activator, AMP (Daniel and Carling, 2002, Hawley et al., 2010). This increase in basal activity was particularly evident with two mutations, R531Q (Burwinkel et al., 2005) and R384T (Akman et al., 2007) that cause severe hypertrophic cardiomyopathy and death within weeks or months of birth. These were new mutations that were not inherited from parents (Akman et al., 2007).

Because the R531G mutation causes insensitivity to changes in adenine nucleotide concentration, cells expressing this variant have been used to identify the mechanism of action of various agents that activate AMPK (Hawley et al., 2010). The region immediately N-terminal to the CBS motifs of the γ subunit contains a conserved sequence of residues required for its binding with the β subunit (Viana et al., 2007), a finding confirmed following crystallisation of a partial heterotrimeric AMPK complex (Xiao et al., 2007).
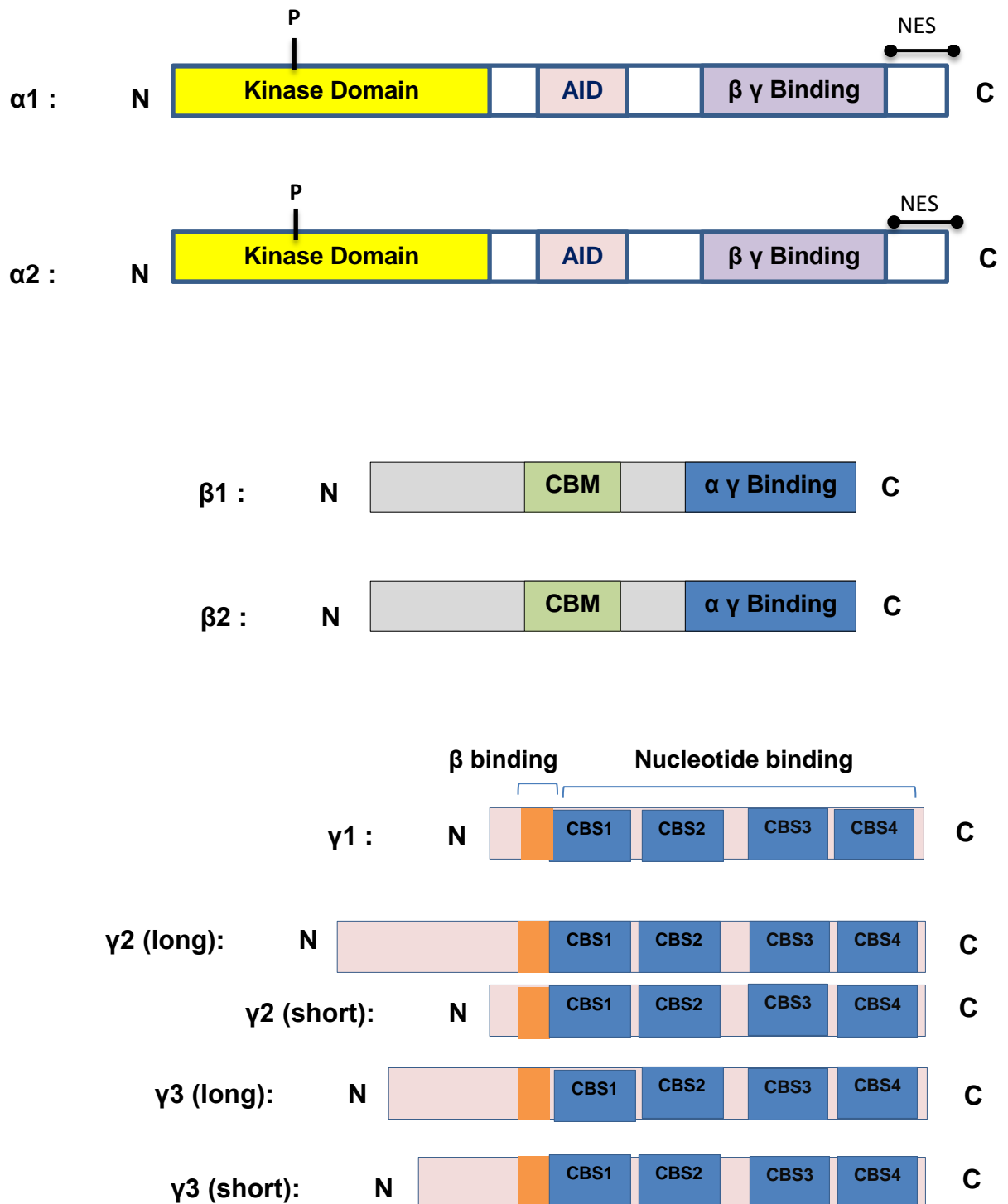
Figure 1.3: AMPK subunit isoforms and splice variants

Schematic diagram adapted from (Towler and Hardie, 2007) showing the AMPK subunit isoforms and splice variants of the γ subunit isoforms.

AID- Auto inhibitory domain, CBM- Carbohydrate binding module, CBS- Cystathione-β-synthase

1.3.5 Phosphorylation by upstream kinases

1.4.5.1 Identification of LKB1 as the main AMPKK

AMPK was shown to be phosphorylated on Thr-172 within the activation loop of the α subunit by an upstream kinase, termed AMPKK, whose identity was at that time unknown (Hawley et al., 1996). Its identity remained elusive for some time, despite the efforts of several research groups. However, in budding yeast, the AMPK orthologue Snf1 was eventually shown to be activated by phosphorylation on Thr-210, the site equivalent to Thr-172 site in rat AMPK by three kinases (Elm1, Pak1p and Tos3), which acted in a partially redundant manner (Sutherland et al., 2003, Hong et al., 2003). Deletion of all three kinases abolishes Snf1 activity and causes the same phenotype as deletion of *SNF*1 gene in budding yeast. Yeast showing the *snf*1 phenotype fail to grow on fermentable carbon sources other than glucose (e.g. sucrose or raffinose), as well as non-fermentable carbon sources like glycerol. The kinases within the human kinome with closest sequence similarity to these three kinases were calmodulin-dependent kinase kinases-α and -β, and LKB1 (Hawley et al., 2003, Hong et al., 2003). Three groups independently identified that LKB1 was the major upstream kinase that phosphorylated the recombinant α subunit of AMPK in cell free assays as well as endogenous AMPK in cells (Woods et al., 2003, Hawley et al., 2003, Shaw et al., 2004b). The ability of LKB1 to phosphorylate AMPK was greatly increased when co-expressed with its accessory proteins STRAD and MO25 (Hawley et al., 2003). Cell-free assays demonstrated that the LKB1: STRAD:MO25 complex activated AMPK about a hundred fold. LKB1-deficient cells, such as the HeLa tumour cell line had very low basal AMPK activity, which was increased by expression of recombinant LKB1 (Hawley et al., 2003). In addition, LKB1-null mouse embryonic fibroblasts had low

basal AMPK activity and were not activated by treatment with AICAR or phenformin, unless LKB1 was re-expressed (Hawley et al., 2003).

These results showed that LKB1 was both necessary and sufficient for AMPK activation in response to energy stress. However, since multiple kinases acted upstream of the SNF1 complex in budding yeast, it seemed likely that AMPK was also likely to be activated by more than one kinase. This was supported by the finding that in mouse heart, under conditions of mild myocardial ischaemia, an AMPKK other than LKB1 was responsible for increase in AMPK activity in heart muscle (Altarejos et al., 2005).

1.4.5.2 CaMKK-β is the alternate upstream kinase for AMPK

Calmodulin-dependent kinase kinase (CaMKK) purified from pig brain had previously been shown to activate AMPK in cell-free assays (Hawley et al., 1995), although the major AMPKK purified from rat liver (which was later identified to be LKB1) did not appear to be calmodulin-dependent and was therefore not thought to be a CaMKK. However, several LKB1-deficient cell lines including HeLa cells, had a detectable level of Thr-172 phosphorylation and activity of AMPK, and exhibited increased Thr-172 phosphorylation and AMPK activation in response to calcium ionophores. These findings suggested that an alternative, calcium-dependent AMPKK was involved. CaMKKβ was identified as the major alternative upstream kinase for AMPK in cells, although CaMKKα does activate AMPK in cell-free assays (Hawley et al., 2005, Hurley et al., 2005, Woods et al., 2005). These studies showed that AMPK was activated by treatment with the calcium ionophore A23187 or ionomycin, and that overexpression of CaMKKβ increased AMPK activity in HeLa cells. The CaMKK inhibitor STO-609 abolished calcium ionophore-mediated AMPK activity. Knockdown

of endogenous CaMKKβ using RNA interference also significantly reduced calcium ionophore-mediated AMPK activation (Hawley et al., 2005, Hurley et al., 2005, Woods et al., 2005). Therefore, it was proposed that CaMKKβ activated AMPK in response to increased Ca^{2+} levels, while LKB1 is normally required for activation of AMPK following an increase in the AMP:ATP ratio (Hawley et al., 2005). However, as CaMKK is not widely distributed in tissues and not abundant in the heart, it is unlikely to be the kinase that Altarejos and colleagues described.

*T*ransforming *g*rowth *f*actor-β- *a*ctivated *k*inase (TAK1) has been proposed as a third upstream kinase that activates AMPK. Expression of mammalian TAK1 in yeast lacking all the three SNF1 kinases (Δ*Elm1*Δ*Pak1*Δ*Tos3*) rescues the *snf*1 phenotype. TAK1 has been shown to activate the SNF1 complex and phosphorylate SAMS peptide in cell-free assays (Momcilovic et al., 2006). Expression of dominant negative TAK1 in cardiac myocytes was associated with inhibition of Thr-172 phosphorylation and AMPK activity (Xie et al., 2006). TAK1 was also shown to be activated by agents such as oligomycin, AICAR and metformin that are known to activate AMPK (Xie et al., 2006). Also, treatment of breast epithelial cells with tumour necrosis factor- related apoptosis-inducing ligand (TRAIL) activates AMPK and induces autophagy in these cells, in an AMPK-dependent manner. This AMPK activation was attenuated when TAK1 levels were reduced by siRNA- mediated silencing (Herrero-Martin et al., 2009). However, clear evidence of AMPK activation by endogenous TAK1 in intact cells is lacking.

1.3.6 Regulation by nucleotides: AMP, ADP and ATP

AMPK is activated by an increase in the AMP:ATP or ADP:ATP ratios due to increases in ATP consumption caused by processes such as exercise or cell growth, or caused by treatments that decrease ATP production, such as hypoxia or glucose deprivation (Hardie, 2007a). ATP is converted to ADP (or in a few synthetase reactions, to AMP plus pyrophosphate) by energy-requiring reactions that are driven by ATP hydrolysis. When ADP is produced, the enzyme adenylate kinase then converts two molecules of ADP into one ATP and one AMP molecule, a reaction that is maintained close to equilibrium in eukaryotic cells and is thought to be the major source of cellular AMP. Because of the adenylate kinase reaction, the cellular AMP: ATP ratio varies approximately as the square of the ADP:ATP ratio (Hardie and Hawley, 2001). In unstressed cells, the concentration of ATP is thought to be 10-fold higher than ADP, and 100-fold higher than AMP. However, studies have shown that the lower affinity site on the $\gamma 1$ subunit (site 3) binds Mg-ATP with 5-10 fold lower affinity than free ATP, ADP or AMP (Xiao et al., 2011). Since free ATP is present at a 20-fold lower concentration than Mg-ATP in cells, ADP (which does not bind Mg^{2+}), would be able to compete with ATP for binding at site 3 even during mild stress, while AMP may be able to compete with ATP and ADP at site 1 when its concentration rises during a more severe stress (Xiao et al., 2011) .

AMP allosterically activates AMPK as confirmed by several studies (Ferrer et al., 1985, Carling et al., 1989). ATP antagonizes this action of AMP but does not inhibit the kinase on its own (Hardie et al., 2011). When AMP binds to the high affinity site on the γ subunit (site 1), it can increases the activity of AMPK via the allosteric effect by as much as 10-fold (Hardie et al., 2011). AMP also increases the net phosphorylation of

AMPK by upstream kinases. By phosphorylating Thr-172, upstream kinases can increase the AMPK activity by >100-fold, which is then enhanced a further 10-fold by AMP resulting in a maximum of >1000-fold increase in AMPK kinase activity overall (Carling et al., 1987, Carling et al., 1989, Suter et al., 2006, Hawley et al., 1996). Mutations in the γ subunit that decrease its ability to bind AMP have shown to reduce the allosteric activation of AMPK (Scott et al., 2004, Sanders et al., 2007). Recently it has been shown that ADP can also bind to site 1 and 3 on the γ subunit and this causes a conformational change that promotes Thr-172 phosphorylation, although ADP does not allosterically activate AMPK (Oakhill et al., 2011). The effects of ADP and AMP to promote phosphorylation require N-terminal myristoylation of the β subunit (Oakhill et al., 2011).

AMP also protects the kinase from dephosphorylation by protein phosphatases (Davies et al., 1995, Suter et al., 2006). When the AMP-binding sites of the γ subunit were mutated in bacterially expressed heterotrimers, the complex showed a reduction in the protection against dephosphorylation of Thr-172 by protein phosphatase 2Cα in cell-free assays (Sanders et al., 2007). The same mutations also prevented allosteric activation of the kinase by AMP. These results suggest that AMP promotes allosteric activation and inhibits dephosphorylation by binding to the same sites on the γ subunit. This effect has been shown to be independent of the upstream kinase. In cells lacking LKB1, increasing AMP levels using phenformin did not affect AMPK activity on its own, but it further increased AMPK activation caused by treatment with a calcium ionophore (Fogarty et al., 2010).

Recent studies of a partial heterotrimeric complex which included the kinase domain has confirmed that ADP can also inhibit dephosphorylation of AMPK (Xiao et al., 2011). This study provided new insights into the conformational change in the

structure of the heterotrimer whereby, binding of AMP or ADP binding to site 3 is proposed to stabilize the close association of the activation loop containing Thr-172 with the C-terminal domains of the α and β subunit. This is thought to shield Thr-172 from the protein phosphatase so that the latter is less able to de-phosphorylate the residue (Xiao et al., 2011).

Previous reports suggested that AMP had an additional third regulatory effect. AMP binding was thought to make AMPK a better substrate for phosphorylation by upstream kinases (Hawley et al., 1995). However, it was subsequently proposed that this may have been an artefact caused by the fact that the kinase preparations might have been contaminated by PP2C (Sanders et al., 2007). AMP did not stimulate the phosphorylation of AMPK by either LKB1 or CaMKKβ using bacterially expressed AMPK heterotrimers (Sanders et al., 2007, Suter et al., 2006). However, it was later shown that AMP did promote phosphorylation of Thr-172 as long as the β subunits were myristoylated, a modification that does not occur in bacteria, unless a mammalian N-myristoyl transferase is co-expressed (Oakhill et al., 2010).

To summarise this section, the current model suggests that AMP and ADP increase Thr-172 phosphorylation both by promoting phosphorylation and by inhibiting dephosphorylation, both effects being antagonized by ATP. AMP also allosterically activates AMPK, an effect that is antagonized by ATP and ADP.
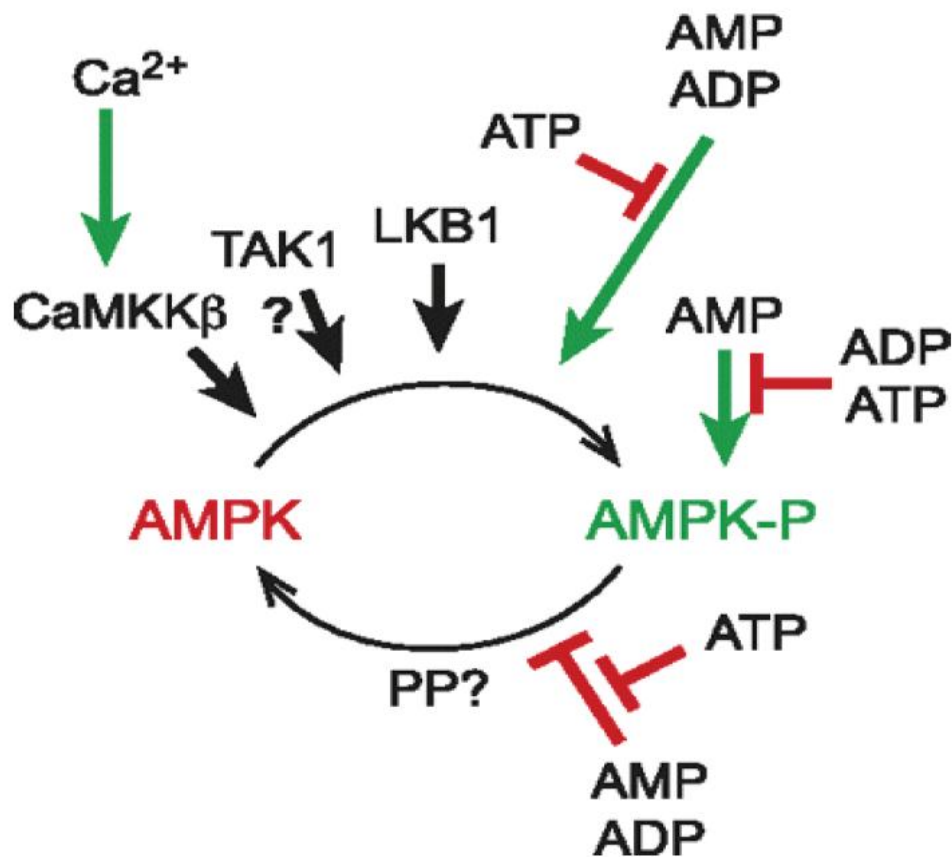
Figure 1.4: Regulation of AMPK by reversible phosphorylation and adenine nucleotides

AMPK is activated ≥100-fold by phosphorylation by upstream kinase in cell-free assays. CaMKKβ is the alternative upstream kinase which activates AMPK following a rise in cytosolic Ca^{2+}. TAK1 has been proposed as the third upstream kinase, although its ability to phosphorylate AMPK in vivo has not been fully established. Adenine nucleotides regulate the kinase in three ways:

1) allosteric activation: AMP activates the kinase allosterically, causing a 10-fold increase in activity. ADP and ATP inhibit AMP-mediated allosteric activation of AMPK;
2) both AMP and ADP cause a conformational change that promotes Thr-172 by upstream kinases- this effect, which is opposed by ATP, is dependent on N- terminal myristoylation of the β subunit;
3) preventing dephosphorylation: AMP and ADP binding to site 3 causes a conformational change in the kinase, protecting it from dephosphorylation by protein phosphatases (PP). ATP antagonises this effect of AMP and ADP.

Adapted from (Hardie, 2011a)

1.3.7. Activators of AMPK

In general, AMPK is activated by metabolic stress. AMPK activation was initially reported during severe pathological metabolic stress such as hypoxia (Marsin et al., 2000) or following addition of mitochondrial inhibitors such as arsenite (Corton et al., 1994). AMPK is activated in cultured cells by glucose deprivation, although total removal of glucose would not be a normal event in vivo. AMPK may however be regulated by glucose in specialised tissues such as pancreatic beta cells and hypothalamic neurons, where, due to the expression of high Km isoforms of glucose transporter (GLUT2) and/or hexokinase (HKIV or glucokinase), the rate of glucose metabolism (and hence ATP production) is affected by physiological variations in blood glucose (Salt et al., 1998, Sun et al., 2010, Mccrimmon et al., 2008). Type I cells of the carotid body also sense physiological variations in blood oxygen levels, and trigger appropriate alterations in breathing, due to activation of AMPK and AMPK-mediated phosphorylation and inhibition of voltage gated BK_{Ca} potassium channels (Ross et al., 2011). AMPK is also activated by muscle contraction during exercise (Winder and Hardie, 1996, Wojtaszewski et al., 2000), most likely due to increase in ATP consumption. In exercise involving rapid, powerful contractions (e.g. sprinting or weightlifting), glycogen is the major fuel and AMPK may not be important. Activation of AMPK in response to muscle contraction becomes more relevant during prolonged endurance exercise, where AMPK mediates increased uptake of glucose from the bloodstream, as well as adaptive responses to regular endurance training. Mice that have had LKB1 conditionally deleted in skeletal muscle, have lower basal AMPK α2 activity in skeletal muscle that is not increased by phenformin, AICAR or muscle contraction (Sakamoto et al., 2005). These mice also showed greatly reduced glucose uptake in

response to muscle contraction or AICAR treatment (Sakamoto et al., 2005). AMPK activation may account for several other beneficial effects of exercise such as increased fatty acid oxidation (Merrill et al., 1997, Aschenbach et al., 2004) and increased mitochondrial biogenesis (Zong et al., 2002).

In addition to regulating cellular energy, AMPK is also activated by cytokines and hormones that regulate energy status at the whole body level (Hardie, 2011b). Leptin, which is released from adipocytes to signal the presence of adequate fat stores, activates AMPK in skeletal muscle leading to fatty acid oxidation (Minokoshi et al., 2002). The hormone adiponectin, which is released from adipocytes with low fat stores, has also been shown to activate AMPK in liver and skeletal muscle, inhibiting gluconeogenesis in the liver and stimulating fatty acid oxidation in both organs (Yamauchi et al., 2002). In contrast to its effects in muscle, leptin acting on neurons in the hypothalamus inhibits AMPK, possibly by binding to leptin receptors on pro-opiomelanocortin-expressing neurons that inhibit food intake, triggering release of opioids onto other neurons where AMPK is inhibited (Hardie, 2011b). Fasting is known to increase AMPK activity in the hypothalamus, while refeeding suppresses it (Minokoshi et al., 2004), suggesting a role for AMPK in the regulation of food intake and appetite (Kahn et al., 2005). Treatments that increase food intake such as ghrelin, cannabinoids and hypoglycaemia all activate AMPK in the hypothalamus, possibly by acting on presynaptic neurons upstream of agouti- related protein (AGRP) -expressing neurons that promote food intake (Hardie, 2011b).

A number of drugs and xenobiotics also activate AMPK. The first agent identified to activate AMPK was AICAR, which is taken up into cells and converted to 5-aminoimidazole-4-carboxamide ribonucleoside monophosphate (ZMP), an AMP analogue that mimics both activating effects of AMP on AMPK (Corton et al., 1995).

The widely used antidiabetic drug metformin, which is prescribed to over 100 million people worldwide, also activates AMPK. Activation of hepatic AMPK was shown to be required for the anti-hyperglycaemic effects of metformin (Zhou et al., 2001, Shaw et al., 2005), although it appears not to be required for the acute effects of metformin on gluconeogenesis (Foretz et al., 2010). Another class of anti-diabetic drugs, the thiazolidinediones, have also been shown to activate AMPK (Fryer et al., 2002). Several xenobiotics or nutraceuticals derived from plants, such as resveratrol in red wine, epigallocatechin 3-gallate from green tea, berberine used in Chinese medicine and quercetin activate AMPK by diverse mechanisms (Hardie, 2011b). Many of these agents including metformin, thiazolidinediones, oligomycin, resveratrol and berberine inhibit mitochondrial respiration and increase cellular AMP:ATP and ADP:ATP ratios, thus activating cells expressing wild type AMPK but not cells expressing the AMP/ADP-insensitive R531G mutant γ subunit (Hawley et al., 2010). Agents such as hydrogen peroxide also appear to activate AMPK indirectly by damaging the respiratory chain (Hawley et al., 2010). Agents such as A23187 and ionomycin increase intracellular calcium and thus activate AMPK by activating the alternative upstream kinase CaMKKβ, whereas A-769662 and salicylate directly bind to AMPK, causing both allosteric activation and inhibition of Thr-172 dephosphorylation. These agents thus activate the R531G mutant as well as wild type AMPK (Hawley et al., 2010, Hawley et al., 2012).

1.3.8 Processes regulated by AMPK

AMPK activation switches on catabolic ATP-generating pathways while switching off ATP-consuming anabolic pathways (Hardie, 2007a). The optimum AMPK substrate motif is Φ (X,β)XXS/TXXX Φ where Φ is a hydrophobic residue (M, L, I, V or F) and β is a basic residue (R, K or H) (Weekes et al., 1993, Dale et al., 1995). Additional determinants upstream of this motif that promote binding but are not essential have also been studied (Scott et al., 2002). AMPK regulates several important cellular processes by phosphorylation-mediated activation or inhibition of numerous downstream targets. Some of these processes and the AMPK target substrates that regulate them are discussed in the next section.

1.3.8.1 Lipid metabolism

Acetyl-CoA carboxylase was the first AMPK substrate to be identified (Carlson and Kim, 1973). ACC catalyses the conversion of acetyl-CoA to malonyl-CoA, which is the first step committed to fatty acid synthesis. AMPK phosphorylates ACC on Ser-79, thus inhibiting the enzyme and consequently inhibiting fatty acid synthesis (Davies et al., 1992). ACC2, another isoform of acetyl-CoA carboxylase mainly expressed in muscle cells, is also phosphorylated and inhibited by AMPK (Winder et al., 1997). Unlike ACC1, ACC2 is associated with mitochondria and it is believed to increase levels of malonyl-CoA at the mitochondrial surface. Malonyl-CoA inhibits carnitine palmitoyl transferase-1 (CPT-1), an enzyme required for fatty acid uptake across the inner mitochondrial membrane and subsequent oxidation in mitochondria (Abu-Elheiga et al., 2000). AMPK activation inhibits ACC2, reducing malonyl-CoA levels and thus

increasing CPT-1-mediated fatty acid oxidation (Merrill et al., 1997). Consistent with

the above findings, mice lacking ACC2 have been shown to have a greatly increased

rate of fatty acid oxidation (Abu-Elheiga et al., 2001). AMPK also phosphorylates and

inhibits HMG-CoA reductase, which is a key enzyme in cholesterol synthesis, thereby

inhibiting this process (Beg et al., 1973, Towler and Hardie, 2007, Carling et al., 1987).

AMPK also negatively regulates hormone-sensitive lipase and thus inhibits hydrolysis

of triglyceride in adipocytes and in muscle (Smith et al., 2005, Corton et al., 1995).

1.3.8.2 Carbohydrate metabolism

During exercise, skeletal muscle cells actively take up glucose, mainly through

glucose transporter GLUT4. Translocation of GLUT4 to the cell membrane is the rate-

limiting step in this process (Steinberg and Kemp, 2009). Activation of AMPK,

particularly $\alpha2$ in muscle in response to contraction or AICAR treatment, increases

glucose uptake by increasing translocation of the glucose transporter GLUT4 from

intracellular GLUT4 vesicles to the cell membrane (Jørgensen et al., 2004). AMPK

phosphorylates TBC1D1 on Ser-237, which enhances 14-3-3 binding; this causes

dissociation of this protein (which contains a Rab-GAP domain) from GLUT4 vesicles,

promoting exchange of GTP for GDP on Rab proteins that trigger fusion of the vesicles

with the plasma membrane (Chen et al., 2008). AMPK has also been shown to

phosphorylate and activate the PFKFB2 and PFKFB3 isoforms of 6-phosphofructo-2-

kinase (PFK2). PFK2 regulates the formation and degradation of fructose 2,6 bis-

phosphate, which in turn activates the glycolytic enzyme PFK1, increasing glycolysis in

heart muscle where PFKFB2 is expressed (Marsin et al., 2000), and in monocytes and

macrophages where expression of PFKFB3 is induced by pro-inflammatory stimuli

(Marsin et al., 2002). Interestingly the latter isoform is also expressed in some tumour cells, and this mechanism may in part explain their high glycolytic rate. AMPK also regulates hepatic glucose production. Mice that lack LKB1 in the liver or are deficient in α2 exhibit fasting hyperglycaemia and increased hepatic glucose production (Shaw et al., 2005, Viollet et al., 2003). AMPK is also involved in glucose sensing in specialised cells in the pancreas and hypothalamus (Mccrimmon et al., 2008, Sun et al., 2010).

1.3.8.3 Mitochondrial Biogenesis, Autophagy and Mitophagy

A role for AMPK in mitochondrial biogenesis was suggested by reports that AICAR treatment in mice increased mitochondrial enzymes levels in skeletal muscle (Winder et al., 2000). Mice expressing wildtype AMPK also showed increased mitochondrial biogenesis in muscle on treatment with AICAR or β-guanidinopropionic acid (a creatine analogue that depletes cellular ATP and thus increases the AMP:ATP ratio) (Zong et al., 2002, Thomson et al., 2007). This effect was lost in mice that lacked α2 or expressed a dominant negative AMPK mutant (Thomson et al., 2007, Zong et al., 2002). Expression of *N*uclear *R*espiratory *f*actor (NRF1), which is a key transcriptional factor controlling mitochondrial biogenesis is increased following AMPK activation (Bergeron et al., 2001). AMPK has also been reported to phosphorylate the "master regulator" of mitochondrial biogenesis, the transcriptional coactivator PGC-1α, which co-activates at genes with binding sites for NRF1 and other transcription factors. Deacetylation of PGC-1α is then proposed to cause activation of its own transcription (Jäger et al., 2007). AMPK also regulates the process of mitophagy, whereby dysfunctional mitochondria are engulfed by autophagic vacuoles which then fuse to lysosomes to be broken down and their contents recycled (Hardie, 2011a). Initiation of

autophagy involves activation of ULK1 and ULK2, proteins that are orthologues of

Atg1 in yeast (Hardie, 2011a). AMPK has been shown to phosphorylate ULK1 at

multiple sites (Egan et al., 2011, Kim et al., 2011). Hepatocytes lacking either AMPK or

ULK1 show increased accumulation of mitochondria with aberrant morphology. Cells

expressing mutant ULK1, where four serine residues phosphorylated by AMPK were

mutated to non-phosphorylatable alanine residues, also showed functional impairment

in the ability to maintain mitochondrial membrane potential (Egan et al., 2011).

1.3.8.4 Regulation of transcription factors

In addition to modulating the effects of target enzymes and proteins by direct

phosphorylation, AMPK also affects the transcription of proteins that regulate the same

cellular processes. Activation of AMPK by metformin suppresses expression of

SREBP-1, a key lipogenic transcription factor (Zhou et al., 2001). AMPK has also been

shown to directly phosphorylate SREBP-1c and SREBP-2 and AMPK activation has

also been shown to decrease the nuclear accumulation of SREBP-1c and SREBP-2 (Li

et al., 2011). AMPK represses transcription of mRNAs encoding enzymes regulating

gluconeogenesis in part by phosphorylating CRTC2, a transcriptional co-activator of

CREB (cyclic AMP response element binding protein), causing binding of 14-3-3

proteins and its exclusion from the nucleus (Koo et al., 2005). AMPK also

phosphorylates Class II HDACs (a family of histone deacetylases comprising HDAC-4,

-5 and -7). Treatment of cells with A-769662, a direct AMPK activator, increases

phosphorylation of Class II HDACs and this causes their nuclear exclusion (Mihaylova

et al., 2011). When present in the nucleus, Class II HDACs acetylate and activate

FOXO transcription factors. AMPK activation by AICAR has also been shown to

decrease the levels of *H*epatocyte *N*uclear *F*actor 4α (HNF-4α) , another transcription factor and decreases the expression of HNF-4α target genes (Leclerc et al., 2001). AMPK inhibits the transcriptional co-activator p300 by direct phosphorylation , preventing its interaction with transcriptional factors such as *p*eroxisome *p*roliferator-*a*ctivated *r*eceptor-γ (PPAR-γ), thyroid hormone receptor and retinoic acid receptor (Yang et al., 2001).

1.3.8.5 Protein synthesis and cell growth

Cell growth and protein synthesis are energy-consuming processes. The mammalian target-of-rapamycin (mTOR) controls cell growth and proliferation in response to growth factors and nutrients (Laplante and Sabatini, 2012). The Rheb-GAP (*G*TP-ase *a*ctivating *p*rotein) heterodimer TSC1/TSC2 (*T*uberous *s*clerosis *p*rotein 1 and 2) is a negative upstream regulator of mTOR, converting Rheb into the inactive GDP bound form, thus disrupting its interaction with mTORC1 (Inoki et al., 2003). AMPK directly phosphorylates TSC2, increasing its GAP activity, thus inhibiting mTOR (Inoki et al., 2003). AMPK has also been shown to directly phosphorylate Raptor (*R*egulatory *a*ssociated *p*rotein of TOR), causing 14-3-3 binding to Raptor and subsequent inhibition of mTORC1 (Gwinn et al., 2008).

1.3.8.6 Regulation of membrane excitability

AMPK has been shown to phosphorylate voltage gated potassium channels in neuronal cells. Activation of AMPK by A-769662 in HEK-293 cells expressing a voltage-gated potassium channel Kv2.1, has been shown to cause the channels to open at more negative membrane potential, thus sensitizing them to depolarization (Ikematsu

et al., 2011). AMPK phosphorylates Kv2.1 on two sites, Ser-440 and Ser-537, although

mutation of Ser-440 to alanine was sufficient to abolish the effect on voltage gating

(Ikematsu et al., 2011). Kv2.1 is a major delayed rectifier K^+ channel in central neurons,

where it regulates the frequency of firing of action potentials. As expected, activation of

AMPK in cultured primary neurons from rat brain reduced the firing of action potentials

(Ikematsu et al., 2011). Since firing of action potentials is a major energy-consuming

process in the brain, AMPK would conserve energy by reducing their frequency.

Interestingly, AMPK has an opposite, inhibitory effect, when it phosphorylates another

voltage-gated K^+ channel, BK_{Ca}, which is expressed in Type I cells in the carotid body

(Ross et al., 2011). These cells are believed to be the primary oxygen-sensing cells that

control breathing. It is proposed that AMPK is activated by hypoxia in the carotid

arteries that supply the brain, causing phosphorylation and inactivation of BK_{Ca}

channels. This triggers depolarization of Type I cells, causing release of

neurotransmitter onto the carotid sinus nerve, that communicates with the brain to elicit

corrective changes in breathing patterns (Ross et al., 2011).

1.3.8.7 Regulation of the cell cycle

Cell division, not unlike cell growth is also an energy consuming process and

AMPK activation has been shown to cause a cell cycle arrest at the G1 phase of the cell

cycle (Imamura et al., 2001). Treatment of HepG2 cells with AICAR caused G1 cell

cycle arrest which was associated with phosphorylation of the p53 tumour suppressor

on Ser-15. However, it is still not clear whether p53 is a direct AMPK substrate. AMPK

has been shown to phosphorylate the cyclin- dependent kinase inhibitor p27, thereby

increasing its stability and inhibiting cell cycle progression (Liang et al., 2007).

Phosphorylation of Raptor by AMPK causes a reduction in the percentage of cells

progressing to G2/M (Gwinn et al., 2008). Activation of CaMKKβ by A23187 in G361

cells (which lack LKB1) also causes a G1 cell cycle arrest (Fogarty S PhD thesis 2008).
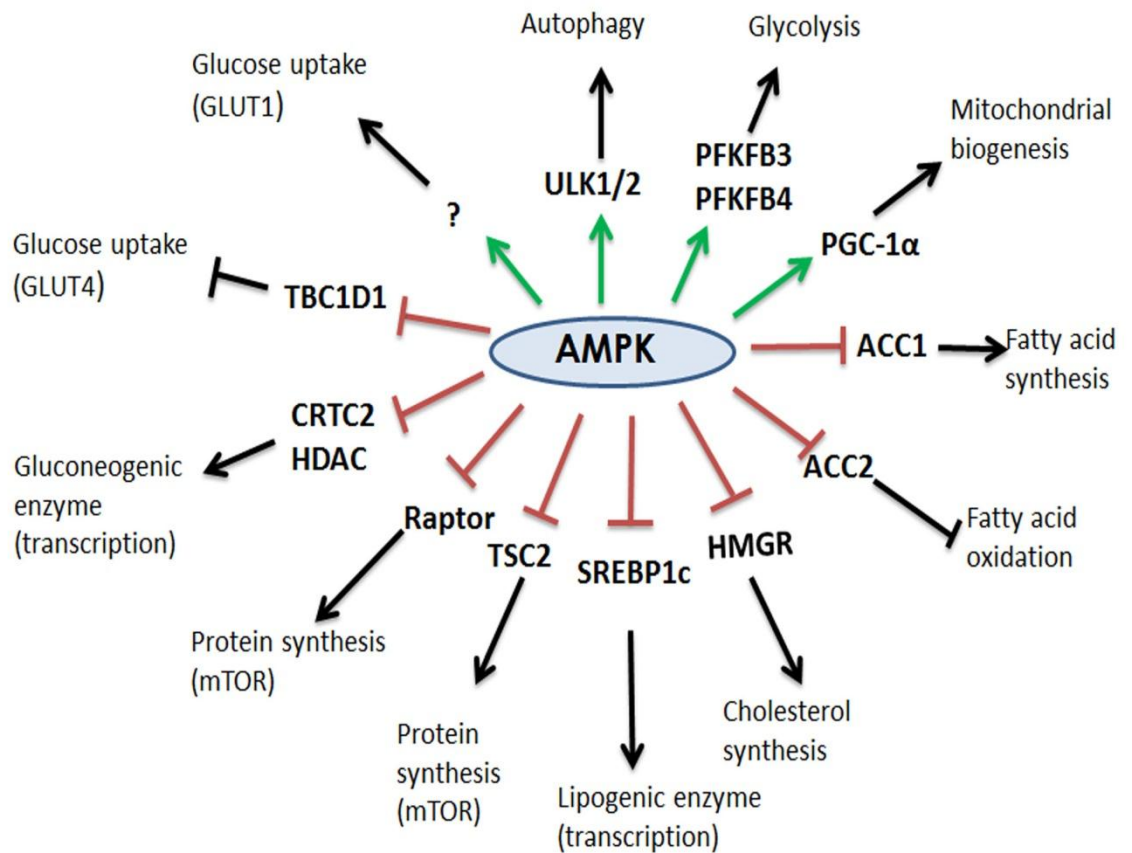
Figure 1.5: Processes regulated by AMPK

This figure shows the effect of AMPK activation on its various downstream targets. Catabolic pathways shown above namely, glucose uptake via glucose transporter type 4 (GLUT4) and GLUT1 glycolysis, fatty acid oxidation, mitochondrial biogenesis and autophagy, are activated by AMPK. Anabolic pathways such as fatty acid synthesis, cholesterol, glycogen and protein synthesis, and transcription of lipogenic and gluconeogenic enzymes are inhibited by AMPK. Adapted from (Hardie et al., 2012)

1.4 AMPK and cancer

The role of AMPK as a master regulator of cell metabolism is well established. Cell proliferation is an energy consuming process and is therefore likely to stress cells and thereby activate AMPK. The link between cellular metabolism and tumourigenesis has been known for decades (Warburg, 1956). However, in recent years, there has been a growing body of evidence linking the AMPK pathway to the regulation of cell growth and proliferation. This has led to interest in AMPK as a potential therapeutic target in cancer. The main reasons for this have been detailed in this section.

1.4.1. LKB1 and Peutz Jeghers syndrome

The discovery that LKB1, a tumour suppressor, was the main upstream kinase for AMPK (Hawley et al., 2003, Woods et al., 2003, Shaw et al., 2004b), was a major finding which prompted interest in the role of the AMPK in cancer. Loss of LKB1 causes Peutz -Jeghers syndrome (PJS), a rare, autosomal dominant inherited cancer syndrome, characterised by the development of benign, hamartomatous polyps and marked pigmentation of mucous membranes (Alessi et al., 2006). Patients with PJS also have a markedly increased risk of cancer especially colon, stomach, small intestinal and pancreatic cancer (Hemminki, 1999). In addition to germ line mutations that cause PJS, somatic mutations of LKB1 have been reported in 30% of non-small cell lung cancers (Matsumoto et al., 2007, Sanchez-Cespedes et al., 2002) and around 20% of cervical tumours (Wingo et al., 2009). 144 different mutations in LKB1 have been identified in patients with PJS and from sporadic tumours, with a substantial proportion being

truncating mutations in the catalytic domain resulting in loss of function (Alessi et al.,

2006). PJS has similar clinical features to Cowden syndrome, another inherited

syndrome which causes hamartomas and a predisposition to cancer, which is caused by

inactivating mutations of the tumour suppressor, *p*hosphatase and *t*ensin homolog

(PTEN). PTEN negatively regulates the PI3-kinase/Akt pathway. The overlap of

clinical features between PJS and Cowden's suggests a common downstream pathway

which may be altered in both these syndromes. The mTOR pathway which regulates

cell growth and proliferation has been identified as the common downstream pathway

regulated by activating signals from the PI3-kinase/Akt pathway in response to nutrients

and growth factors, and inhibitory signals from the LKB1-AMPK pathway, which

responds to energy stress and down-regulates mTOR (Shackelford and Shaw, 2009).

LKB1 is a master upstream kinase, and in addition to AMPK-α1 and

AMPK-α2, LKB1 is known to phosphorylate 12 other protein kinases (BRSK1,

BRSK2, NUAK1, NUAK2, QIK, QSK, SIK, MARK1, MARK2, MARK3, MARK4,

and SNRK) that are located next to AMPK in the human kineome dendrogram and

share significant sequence homology with AMPK (Alessi et al., 2006). However,

evidence suggests that some of the tumour suppressor effects of LKB1 may be mediated

through AMPK. LKB1-deficient mouse embryonic fibroblasts and HeLa cells (which

lack LKB1) show activation of *m*ammalian *t*arget *o*f *r*apamycin *c*omplex 1 (mTORC1),

without increase in PI3-kinase signalling (Corradetti et al., 2004, Shaw et al., 2004a).

Treatment of wild type MEFs with AICAR, which activates AMPK, reduced mTOR

signalling whereas, this reduction in mTOR signalling was not observed in LKB1-

deficient MEFs (Shaw et al., 2004a). Also, lung cancer cells deficient in LKB1 fail to

inactivate mTOR when deprived of glucose, whereas cell lines containing LKB1 show

reduction in mTOR activity which is also associated with increased levels of pACC,

suggesting that activation of AMPK is associated with inhibition of mTOR activity (Carretero et al., 2006). This suggests that AMPK, acting downstream of LKB1, modulates targets downstream of the PI3-kinase/Akt pathway, under conditions of energy stress.

1.4.2 AMPK negatively regulates the mTOR pathway

AMPK has been shown to negatively regulate the mTOR pathway by two ways. Firstly, AMPK phosphorylates TSC2 (Inoki et al., 2003), a Rheb GTPase activating protein (GAP). Rheb increases phosphorylation of mTOR on Ser-2448 and activates the mTORC1 complex. Phosphorylation of TSC2 inhibits its GAP activity towards Rheb, thereby inhibiting mTORC1. Secondly, AMPK directly phosphorylates Raptor, one of the binding partners of mTOR, on two residues Ser-722 and Ser-792, leading to 14-3-3 binding and subsequent suppression of mTORC1 (Gwinn et al., 2008).Phosphorylation of these two residues is required for suppression of mTOR, as cells stably expressing the non-phosphorylatable mutant Raptor, where both phosphorylation sites were mutated to alanine, failed to suppress mTOR signalling when treated with AICAR, while cells stably expressing wildtype Raptor down-regulated mTOR signalling in response to AICAR treatment (Gwinn et al., 2008).

1.4.3 Evidence for the role of AMPK in cancer

There is strong epidemiological data showing that diabetics on metformin have a 30% reduced overall risk of cancer compared to diabetics on other treatments such as insulin

or sulphonylureas (Evans, 2005, Bowker et al., 2006b). Also, in mouse tumour models, metformin and phenformin have been shown to delay the onset of tumours in mice that are heterozygous for PTEN and LKB1 (Huang et al., 2008). This effect of delaying tumour onset was also observed in mice treated with A-769662, a direct activator of AMPK, suggesting that AMPK activation mediated the tumour suppressive action of metformin and phenformin. Moreover, murine ES cells lacking LKB1 not only failed to activate AMPK in response to treatment with AICAR, phenformin or metformin, but they also did not supress mTOR signalling, further supporting the view that AMPK was acting to suppress mTOR signalling and delay tumours in this model (Huang et al., 2008).

1.4.4 Tumour cells down- regulate AMPK

There is a growing body of evidence that tumour cells down-regulate AMPK. Melanoma cells expressing the B-RAF-V600E mutation have been shown to down-regulate AMPK. The authors propose that the c-terminal tail of LKB1 is phosphorylated on Ser-325 and Ser-428 (equivalent to Ser-431 on murine LKB1) by ERK and p90RSK respectively, which are downstream of the constitutively active B-RAF (Zheng et al., 2009). LKB1 when phosphorylated on these two residues fails to activate AMPK (Zheng et al., 2009). Inhibition of the MEK- ERK pathway using the MEK inhibitor U0126 reduced phosphorylation of Ser-428 and restored AICAR induced activation of AMPK in a melanoma cell lines carrying the oncogenic B-RAF mutation (Esteve-Puig et al., 2009). Also, immunostaining for phospho-AMPK in breast tissues taken from patients with breast cancer showed that tumour cells demonstrated less staining for

phospho-AMPK when compared to normal breast tissue contained in the same tissue block from individual patients (Hadad et al., 2009).

Taken together, the evidence suggests that AMPK activation in response to energy stress, downstream of LKB1, leads to suppression of the mTOR pathway, antagonising the PI3-kinase/Akt pathway (Figure 1.6). Dysregulation of the LKB1-AMPK axis is observed in different tumours and AMPK activators may be useful in cancer prevention.

1.5 Experimental aims and objectives

The main aim of this thesis was to investigate the role of AMPK in cancer and in the DNA damage response. A mouse tumour model was utilised to examine the role of AMPK as a tumour suppressor. This thesis also explores mechanisms underlying AMPK activation in response to genotoxic stress caused by anti-cancer drugs, such as etoposide. Finally, the regulatory role of C-terminal phosphorylation of LKB1 on Ser-325 and Ser-431 on AMPK activation was examined.
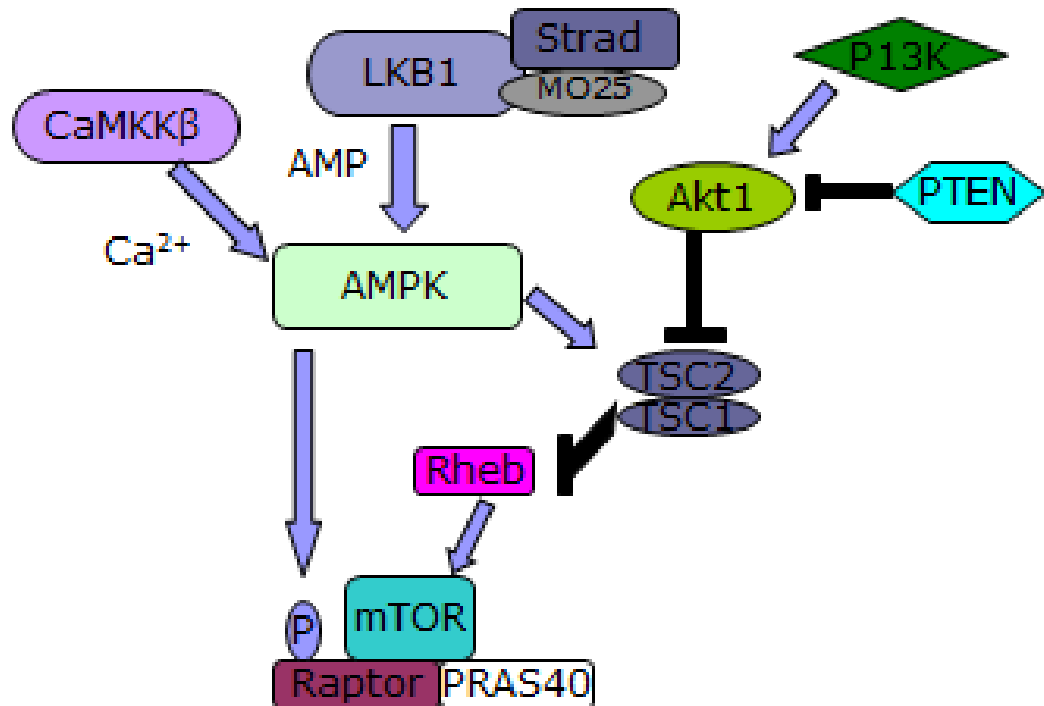
Figure 1.6: The AMPK signalling pathway in cancer

AMPK antagonises the PI3-kinase /Akt pathway and inhibits mTOR in 2 ways:

1) Firstly, AMPK phosphorylates TSC2 (Inoki et al., 2003), a Rheb GTPase activating protein (GAP). Rheb increases phosphorylation of mTOR on Ser-2448 and activates the mTORC1 complex. Phosphorylation of TSC2 inhibits its GAP activity towards Rheb, thereby inhibiting mTORC1
2) Secondly, AMPK directly phosphorylates Raptor, one of the binding partners of mTOR, on two residues Ser-722 and Ser-792, leading to 14-3-3 binding and subsequent suppression of mTORC1.

CHAPTER TWO: MATERIALS AND METHODS

2.1 MATERIALS

2.1.1 Chemicals

Hepes, Tris (hydroxymethyl) methylamine(Tris), Triton X-100, Tween-20, phenylmethylsulphonylfluoride (PMSF), Soya bean trypsin inhibitor, dimethylsulphoxide (DMSO), magnesium chloride, Serva blue G, Brij-35, benzamidine, Propidium iodide, Dithiothreitol, ethidium bromide and A23187 were from Sigma (Poole, UK). Sodium chloride, sodium fluoride, sodium pyrophosphate, glycine, hydrochloric acid, sodium azide, acetic acid, sodium ethylenediaminetetraacetate (EDTA), sodium ethylenebis (oxyethylenenitrilo)-tetraacetate (EGTA) and glycerol were obtained from BDH (Lutterworth UK). Ethanol, methanol, orthophosphoric acid were from VWR, UK. 'Complete' EDTA free protease cocktail inhibitor, Adenosine triphosphate (ATP) and adenosine monophosphate (AMP) was from Roche (Lewisham, UK). Glutathione Sepharose and Optisafe HiSafe II liquid scintillant and [γ-^{32}P] were from Perkin Elmer (Bucks, UK). Effectene transfection reagent and RNAse A were from QIAGEN (Crawley, UK). siPORT transfection reagent was from Ambion, Life Technologies, UK. PEI was from Polysciences Inc (Warrington, PA). Dulbecco's Modified Eagle's Medium (DMEM), McCoy's 5A medium, Fetal Bovine serum (FBS), Optimem reduced serum medium, Dulbecco's PBS, Trypsin EDTA, L-Glutamine and Penicillin/ streptomycin antibiotic solution were from Life Technologies, UK. 75cm^3 and 175 cm^3 tissue culture flasks and 6 well plates were from Invitrogen and 60 and 100mm tissue culture dishes were from Nunc (Lutterworth, UK).

2.1.2 Molecular Biology reagents

Restriction enzymes *KpnI, SpeI*, 1kb and 100bp DNA ladder and 100X buffer were from NEB (Herts, UK). T4 DNA ligase and Blue Orange 6X loading dye were from Promega (Southampton, UK). Top 10F competent E. Coli, XL gold super competent E. Coli, Molecular biology grade agarose and SOC medium were from Invitrogen. QIA prep® Spin Miniprep kit, QIA Quick Gel extraction kit and HiSpeed plasma Maxi kit were from QIAGEN. QuikChange XLII site directed mutagenesis kit and cloned *Pfu* DNA polymerase were from Stratagene (La Jolla, CA). dNTPs were from Fermentas and DMSO from Sigma. Liquid LB medium and agar plates supplemented with 100μg/ml ampicillin and 50X TAE buffer (1X contains 40mM Tris acetate pH 8.0 with 1mM EDTA) were supplied by Media Services, College of Life Sciences, University of Dundee. Oligonucleotides were from Sigma. siRNA constructs against CaMKK-β and ATM were from Ambion, Life Technologies, UK.

2.1.3 Plasmids

Plasmids encoding Wild type and Kinase-dead rat LKB1in the pcDNA3.1 Zeo vector were gifts from Dr. Sarah Fogarty, formerly of University of Dundee. Wild type and Kinase-dead human LKB1 were kind gifts from Prof. Dario Alessi, University of Dundee. Site-directed mutagenesis of LKB1 is described in section and sub-cloning constructs into the pEBG2T vector is described in section. The pEBG2T vector was a gift from Dr. Andrew McBride, formerly of the University of Dundee.

2.1.4 Peptides and Proteins

The AMARA peptide was synthesised by Dr. G. Bloomberg, University of Bristol and was derived from rat acetyl-CoA carboxylase (Dale et al 1995) and has the sequence AMARAASAAALARRR. GST-ERK was provided by the Division of Signal Transduction Therapy (DSTT), University of Dundee.

2.1.5 Protein Biochemistry Reagents

NuPage $^{®}$ LDS sample buffer (4X), NuPage $^{®}$ MOPS Running Buffer (20X), Tris acetate Running Buffer (20X), NuPage $^{®}$ Transfer buffer (20X), SeeBlue Plus 2 Prestained Standard, NuPage $^{®}$ Antioxidant, precast NuPage $^{®}$ Novex 4-12% Bis-Tris gels and 3-8% Tris acetate gels, Xcell Sure Lock™ Mini-Cell, Xcell Blot Module ™ were from Life Technologies, UK. Bovine Serum Albumin (BSA) and Protein G conjugated to horse radish peroxidase were from Sigma, ECL reagent was from Millipore, UK and Hyperfilm™ was from GE Healthcare (Bucks, UK). Li-Cor Odyssey Blocking Buffer was from Li-Cor. IRDye 680 secondary antibodies were from Molecular Probes, Life Technologies, UK. IRDye 800 secondary antibodies were from Rockland Immunochemicals Inc (Gilbertsville, PA).

2.1.6 Antibodies

The source and catalogue number of all antibodies used in the experiments detailed in the thesis are described in Table 1. All non-commercial antibodies used are described in Table 2.

Table 1: Commercial antibodies used in this thesis

Antibody	Species	Recognises	Company	Catalogue No
Actin	Mouse	β-actin	Sigma	A5441
AMPK α(T172-P)	Rabbit	AMPKα1 and α2 phosphorylated at T172	Cell Signalling	A2535
FLAG	Mouse	FLAG	Sigma	3165
Myc	Mouse	Myc tag	Cell Signalling	2276
pSMC-1 (S966-P)	Rabbit	SMC-1 phosphorylated at S966	Bethyl	A300-050A
SMC-1	Rabbit	SMC	Bethyl	A300-055A
ATM	Goat	total ATM	Abcam	Ab2631
pATM (S1981-P)	Mouse	ATM auto-phosphorylated on S-1981	Cell Signalling	4526
γ-H2AX (S139-P)	Rabbit	Histone 2A family member X phosphorylated on S-139	Sigma	H5912
PTEN	Mouse	total PTEN	Sigma	G4414
GSK3β	Mouse	Glycogen synthase Kinase 3	Cell Signalling	9832
PKB (T308-P)	Rabbit	PKB phosphorylated at T308 (by PDK1)	Cell Signalling	4056
PKB (S473-P)	Rabbit	PKB phosphorylated at S473 (by mTORC2)	Cell Signalling	4060
PKB	Rabbit	total PKB	Cell Signalling	4685
FOXO1, 3A (T24/32-P)	Rabbit	FOXO1 phosphorylated on T24, FOXO3 phosphorylated on T 32	Cell Signalling	9464

Table 2: In-house antibodies used in this thesis

Antibody	Species	Recognises
AMPK α1	Sheep	344-358 rat AMPK α1 (immunogen)
AMPK α2	Sheep	352-366 rat AMPK α2 (immunogen)
GST	Sheep	GST-LKB1 (produced as a by-product of GST-LKB1 antibody)
pACC (S79-P)	Sheep	ACC1phosphorylated at S79
LKB1 total	Sheep	1-31 LKB1 (rat)
CaMKKβ	Sheep	Total CAMKK-β

2.1.7 Buffers

Lysis Buffer :   50mM Tris- HCl, pH 7.2, 50mM NaF, 1mM NaPPi, 1mM

EDTA, 1mM EGTA, 1mM DTT, 0.1mM Benzamidine, 0.1mM

PMSF, 5μg/ml soybean trypsin inhibitor, 1%(v/v) Triton X-100

IP Buffer: 50mM Tris- HCl, pH 7.25, 150mM NaCl, 50mM NaF, 1mM

NaPPi, 1mM EDTA, 1mM EGTA, 1Mm DTT, 0.1mM

Benzamidine, 0.1mM PMSF, 5μg/ml soybean trypsin inhibitor,

1% (v/v) Triton X-100

High Salt IP buffer: 50mM Tris- HCl, pH 7.25, 0.5 M NaCl, 50mM NaF, 1mM

NaPPi, 1mM EDTA, 1mM EGTA, 1Mm DTT, 0.1mM

Benzamidine, 0.1mM PMSF, 5μg/ml soybean trypsin inhibitor,

1% (v/v) Triton X-100

Assay Buffer: 50mM Hepes pH7.4, 1mM DTT, 0.02% (v/v) Brij-35.

Affinity purification

Buffer 1:   50mM Tris- HCl, pH 7.25, 150mM NaCl

Buffer 2:   50mM Tris- HCl, pH 7.25, 150mM NaCl, 1mM DTT, 0.5% (v/v) Triton

X-100

Buffer 3:   50mM Tris- HCl, pH 7.25, 150mM NaCl, 1mM DTT, 0.27M sucrose,

0.5% (v/v) Triton X-100

Elution Buffer: 50mM Tris- HCl, pH 7.25, 150mM NaCl, 1mM DTT, 0.27M sucrose,

20mM glutathione.

PBS: 137mM NaCl, 2.7mM KCl, 8.1mM Na_2HPO_4

2.1.8 Microscopy Reagents and Equipment

Glass slides and coverslips were from VWR, UK. Paraformaldehyde and Fish skin gelatin and fluorescent secondary antibodies were from Sigma, UK. Vectashield was from Vector Laboratories, Burlingame, CA. Willco Wells were from Intracel, Herts, UK. Fluo-4 AM was from Invitrogen. The Deltavision wide field deconvolution microscope and the Zeiss LSM 710 confocal microscope were based at the College of Life Sciences, University of Dundee.

2.2 METHODS

2.2.1 Site-directed mutagenesis

Synthetic complimentary oligonucleotides (shown in Table 3) were designed to give specific mutations by making base changes at the appropriate codon. Site-directed mutagenesis was performed using QuikChange®II site directed mutagenesis kit according to manufacturer's instructions. Briefly, the mutagenesis reactions were set up in sterile 0.2 ml PCR tubes; each containing 1x reaction buffer, 15ng dsDNA template, 125 ng of each mutagenic oligonucleotide, 1mM dNTPs, 2.5U Pfu turbo DNA polymerase made upto a final volume of 50µl with sterile de-ionised water. The reactions were incubated in a Hybrid PCR Express thermal cycler using the following parameters- 1cycle 95ºc for 30sec, 18 cycles 95ºc for 30 sec, 55 ºc for 1 min, and 68 º c for 8mins. After cycling, the tube was cooled to below 37ºc after which 10U DpnI restriction endonuclease was added. DpnI digests methylated and hemi-methylated DNA, but leaves non-methylated mutant DNA. The reaction was incubated for 1hour at 37ºc. 2 µl of the reaction mixture was used to transform competent E.coli cells as described in section 2.2.3. pcDNA3.1 Zeo plasmids encoding LKB1 were used as template DNA for all mutagenesis reactions.

Table 3: List of primers used for site-directed mutagenesis of LKB1

LKB1 S325A: 5'- GTGCCCATCCCACCGGCCCCAGACACCAAGGAC

                           3'- GTCCTTGGTGTCTGGCGCCGGTGGGATGGGCAC

LKB1 S431A: 5'- CTGCTGCTTGCAGGCCGCCAGCCGGCGGATCTT

                           3'- GTCCTTGGTGTCTGGGGCCGGTGGGATGGGCAC

2.2.2 Sub cloning of GST-LKB1 constructs

pcDNA3.1 Zeo plasmids encoding wild-type and mutant LKB1 constructs were used as DNA templates and were amplified by PCR using the primers and ligated into pEBG-2T plasmid using the SpeI/KpnI restriction sites. The PCR reaction contained 1x Pfu reaction buffer, 100ng dsDNA template, 1mM dNTPs 1pmol forward primer, 1pmol reverse primer, 5% (v/v) DMSO, 4mM $MgCl_2$ and 2.5U Pfu DNA polymerase made up to a final volume of 50µl with sterile de-ionised water. The reactions were incubated in a Hybrid PCR Express thermal cycler using the following parameters- 1 cycle at 95ºC for 10 minutes, 36 cycles at 95ºC for 1min, 50ºC for 1 min, 72ºC for 2 minutes, followed by a final extension at 72ºC for 10 minutes. The PCR reactions were analysed on 1% agarose gel (as described in section 2.2.6) and the appropriate bands were excised using a sterile scalpel. The PCR products were purified (as described in section 2.2.5). 10 µl of purified PCR product and 1 µg of pEBG-2T vector were digested with SpeI and KpnI at 37ºC for 2 hours. The restriction digest reactions were analysed on 1% agarose gel and linearised plasmids were purified (as described in section 2.2.5). The purified digest products were incubated overnight at 4ºC with 1 µl T4 DNA ligase and 1x ligase buffer at a vector: insert ratio of 1:7 in a final volume of 10 µl. TOP10F E.Coli

were transformed with 2 µl of thee ligation reactions (as described in the next section).

Positive clones were screened by DNA sequencing.

2.2.3 Transformation of competent E.Coli cells

An aliquot of TOP10F E. Coli was allowed to thaw on ice. Ligation reaction (2 µl) or

plasmid (0.5-1 µg) was added to cells and incubated on ice for 30 minutes before being

subjected to 'heat shock' at 42ºC for 1 min. The cells were placed back on ice for a

further 2 minutes and 500 µl of SOCS medium was then added. The samples were

incubated at 37ºC for 1 hour on a shaking platform set at 220rpm. 20-100 µl of cells

were streaked onto LB-kan or LB-amp plates and incubated overnight at 37ºC.

2.2.4 Purification of plasmid DNA from E.Coli

2.2.4.1 Small-scale purification

Transformed E.Coli cells were grown overnight at 37ºC in 2ml LB-amp.

Centrifugation at 2300g (5000rpm) for 2 minutes was used to pellet the cells and

plasmid DNA was purified using the QIAGEN QIA prep Spin Miniprep kit, according

to manufacturer's instructions. Briefly, the cells were resuspended and lysed in 250 µl

of buffers P1 and P2, which contain sodium hydroxide, SDS and RNase A. The SDS

solubilises the phospholipid and protein components of the cell membrane leading to

cell lysis, while the alkaline conditions denature chromosomal and plasmid DNA. The

samples were neutralized by 350 µl buffer N3, which is a high salt buffer that causes

denatured proteins, chromosomal DNA and SDS to precipitate. The precipitate was

separated from the soluble fraction by centrifugation at 16000g for 10 minutes. The

supernatant was applied to a silica membrane column, which selectively binds plasmid

DNA under high salt conditions, and centrifuged at 16000g for 1min. The membrane was washed with 750 µl of the ethanol-based PE buffer to remove any contaminating salts. The plasmid DNA was eluted from the column with 30 µl of sterile de-ionised water. This DNA was used for sub-cloning and DNA sequencing.

2.2.4.2 Large- scale purification

To prepare larger quantities of DNA for transfection into mammalian cells, transformed E.Coli cells were grown overnight at 37 ºC in 200ml LB-amp or LB-kan as required. The cells were pelleted at 6000g for 15 minutes at 4 ºC. Plasmid DNA was purified using the QIAGEN Hispeed plasmid Maxi kit according to manufacturer's instructions. Briefly, the cells were resuspended and lysed in 10mls each of buffers P1 and P2. The suspension was neutralized by the addition of 10mls of buffer P3. The lysate was cleared by filtration and applied to a silica column. The column was washed with 60mls of buffer QC and plasmid DNA was eluted with buffer QF. DNA was precipitated by the addition of 10.5 ml isopropanol and was collected using the QIA precipitator before final elution in 750 µl sterile de-ionised water.

2.2.5 Purification of DNA from agarose gels

DNA was purified from agarose gels using the QIAGEN QIAquick Gel Extraction kit following manufacturer's instructions. Briefly, the desired band was excised from the agarose gel using a sterile scalpel. The band was dissolved in 3 volumes of buffer QG at 50ºC for 10 minutes. After the gel slice was completely dissolved, 1 volume of isopropanol was added and the sample was gently mixed. The mixture was applied to a silica membrane column by centrifugation at 16000g for 1min. the column was washed

with 750 µl of the ethanol based PE buffer. The DNA was eluted in a final volume of 30 µl sterile de-ionised water.

2.2.6 Analysis of DNA by agarose gel electrophoresis

Agarose gel electrophoresis was performed using a horizontal gel electrophoresis system. 1% (w/v) agarose gels containing 0.5 µg/ml ethidium bromide or SyBr green were cast and run in TAE buffer. Samples were loaded in 6X DNA loading buffer and were resolved alongside 1Kb DNA ladder markers at 110 volts for 30 minutes. DNA was visualized using an ultraviolet light transilluminator.

2.2.7 Determination of DNA concentration

Plasmid DNA was diluted in sterile de-ionised water to a final volume of 500 µl and transferred to a quartz cuvette. The absorbance was measured at 260 nm against water blank. A 50 µg/ml solution of double stranded DNA has an absorbance of 1 at 260nm. The quality of DNA (contamination with RNA and protein) was assessed by measuring the absorbance at 280 nm. A 260/280 nm ratio of greater than 1.6 was indicative of highly purified DNA.

2.2.8 DNA Sequencing

DNA Sequencing was performed by the DNA Sequencing Service, College of Life Sciences, University of Dundee; using Applied Biosystems Big-Dye Ver 3.1 chemistry on an Applied Biosystems model 3730 automated capillary DNA Sequencer.

2.2.9 Glycerol Stocks of transformed E.coli

200 µl of sterile glycerol was added to 800 µl from an overnight culture of transformed E.coli and vortexed thoroughly. The mixture was snap frozen in liquid nitrogen and stored at -80ºC.

2.2.10 Tissue culture

All media and buffers used for tissue culture were warmed in a water bath to 37ºC prior to use. Cells were maintained in 75 cm^3 or 175 cm^3 flasks at 37ºC in an incubator with an atmosphere containing 5% CO_2. The cells were grown until 80-90% confluent before splitting for routine maintenance. For passaging of cells, the culture medium was aspirated, 5-10 mls of trypsin-EDTA was added and the cells were returned to the 37ºC incubator for 3-5 minutes. After the cells detached from the surface of the flask, 1 ml of the cell suspension was used to seed a fresh 75 cm^3 or 175 cm^3 flask containing 15 ml or 25 ml of complete culture medium.

2.2.10.1 HeLa cells

HeLa cells were obtained from the Department of Health and were cultured in Dulbecco's Modified Eagle's Medium (DMEM) supplemented with 10% (v/v) Foetal bovine serum and 1% (v/v) antibiotic/ antimycotic solution.

2.2.10. 2 Trex-HeLa stable cell lines

Trex-HeLa parental cells as well as Trex-HeLa cells expressing wild type and kinase-dead (KD) LKB1 were kind gifts from Professor Dario Alessi, University of

Dundee (described by Sapkota et al 2002). These were cultured in Earle's Modified

Eagle's Medium (EMEM) supplemented with 10% (v/v) Foetal bovine serum, 5 µg/ml

blasticidin and 100 µg/ml zeocin.

2.2.10.3 HEK 293 cell line

HEK 293 cells obtained from the Department of Health were cultured in

Dulbecco's Modified Eagle's Medium (DMEM) supplemented with 10% (v/v) Foetal

bovine serum and 1% (v/v) antibiotic/antimycotic solution.

2.2.10.4 G361 melanoma cell line

The human G361 melanoma cell line was cultured in McCoy's 5A medium

supplemented with 2mM glutamine, 5% (v/v) Foetal bovine serum and 1% (v/v)

antibiotic/antimycotic solution.

2.2.10.5 Mouse embryonic fibroblasts

Both wild type and AMPK-α1, -α2 knock out (KO) mouse embryonic cells were

kind gifts from Dr. Benoit Viollet, Universit´e Paris. The fibroblasts were cultured in

Dulbecco's Modified Eagle's Medium (DMEM) supplemented with 10% (v/v) Foetal

bovine serum and 1% (v/v) antibiotic/antimycotic solution. These MEFs were passaged

no more than 10 times before being discarded and a fresh batch of MEFs thawed for

use.

2.2.11 Transfection

Cells were transfected with wild type and mutant LKB1 DNA, along with STRAD and MO25 or GST-ERK2, by one of the two methods listed below.

2.2.11.1 PEI Transfection

Cells were transfected using polyethylimine (PEI) which has been described previously (Durocher et al 2002). PEI is a cationic polymer in which every third atom is an amine nitrogen that can be protonated giving it a substantial buffering capacity at physiological pH. PEI can assemble DNA into compact structures, which allows efficient entry into cells, while its pH buffering properties protects DNA from lysosomal degradation. For a 100 mm diameter dish, 1 ml of serum-free media was incubated with 5-10 µg DNA and 20-30 µl of 1mg/ml PEI at room temperature for 20 minutes. The solution was then added drop wise to each dish and the cells were incubated at 37ºC in an incubator with an atmosphere containing 5% CO_2.

2.2.11.2 Transfection of HeLa and G361 cells using Effectene

HeLa and G361 cells were transfected using Effectene transfection reagent according to manufacturer's instructions. Effectene is a non-liposomal lipid formulation used with an enhancer and DNA condensation buffer (buffer EC). DNA is condensed by its interaction with the enhancer in a defined buffer system. Addition of Effectene leads to the formation of condensed Effectene-DNA complexes, which allow efficient entry of DNA into cells with the Effectene reagent providing a cationic lipid coating . For a 100mm dish, 2µg of DNA was incubated with 300 µl buffer EC and 16 µl

Enhancer for 2 minutes at room temperature. 60 µl of Effectene was then added and the

mixture was incubated at room temperature for 10 minutes. 3mls pre-warmed complete

media was mixed with Effectene-DNA solution and added drop wise to each dish. The

dishes were incubated for 48 hours at 37ºC and 5% CO_2.

2.2.12 Freezing and thawing cell lines

Cells grown to confluence in $75cm^3$ culture flasks were trypsinised in 5ml trypsin-

EDTA solution as described previously. Tubes containing the trypsinised cells were

centrifuged for 5mins at 230g. Trypsin was aspirated and the cells were resuspended in

capped tubes containing 900 µl of pre-warmed culture medium and 100 µl DMSO. The

tubes were transferred to a cell freezer and kept in a -80ºC freezer overnight, after which

it was stored long term in liquid nitrogen. Frozen cell stocks were thawed in a water

bath at 37ºC with gentle shaking and transferred into 10mls of media. Cells were re-

pelleted to remove DMSO and the supernatant discarded. The cells were re-suspended

in fresh media and seeded immediately into $75cm^3$ flasks containing pre-warmed culture

medium.

2.2.13 Lysis of cells

Cells were harvested using a rapid lysis method to minimize activation of AMPK during

cell lysis. Dishes were placed on ice and the culture media was aspirated. The cells were

washed twice with ice cold PBS, lysed in 250-500 µl ice-cold lysis buffer and scraped

into pre-chilled 1.5ml eppendorf tubes. Cell lysate was clarified by centrifugation at

17,600 g for 10mins at 4ºC. The clarified lysate was kept on ice for immediate use or

snap frozen in liquid nitrogen and stored at -80ºC. Frozen lysates were thawed on ice

before use. Protein concentration of the lysates was determined by the Bradford method (section 2.2.15).

2.2.14 Purification of GST-fusion proteins from the cells

100mm dishes containing HEK 293 or HeLa cells were transiently transfected with plasmids encoding GST- tagged wild type and mutant LKB1. 36-48 hours post transfection, the cells were lysed in 0.5 mls of ice-cold lysis buffer as described previously and the clarified lysates were incubated for 2 hours on a rolling platform with glutathione-sepharose (25 μl/100mm dish) previously equilibrated in buffer 1. The beads were washed 3 times in buffer 1, twice in buffer 2 and twice in buffer 3 containing 0.27M sucrose. The resin was incubated with 1-1.5 volumes buffer 4 containing 0.27M sucrose and 20mM glutathione to elute the GST- fusion proteins. The eluate was snap frozen and stored at -80ºC.

2.2.15 Determination of protein concentration

Protein concentration was estimated using the Bradford dye-binding method (Bradford 1976). Bradford reagent was prepared using 30mg Serva Blue G in 50ml of 95% (v/v) ethanol and 85% (w/v) orthophosphoric acid. The solution was made up to a final volume of 1 litre with de-ionised water and stored in a bottle protected from light, as the solution is light sensitive. A standard curve was generated for each preparation of Bradford reagent using a range of concentrations of Bovine serum albumin (1-10 mg/ml). The concentration of BSA was confirmed by measuring absorbance at 280 nm (1mg/ml BSA has an absorbance of 0.68 at 280 nm). Protein concentrations were determined by adding 1ml of Bradford reagent to samples in a volume of 100 μl and

measuring the absorbance at 595nm against a reference containing 1 ml Bradford reagent and 100 µl de-ionised water.

2.2.16 SDS-polyacrylamide gel electrophoresis

SDS-PAGE is used to separate proteins based on their apparent molecular weight. The anionic detergents Sodium dodecyl sulphate (SDS) or lithium dodecyl sulphate (LDS), denature proteins and confer a negative charge in proportion to mass resulting in a constant charge to mass ratio for most proteins. The rate of migration through a polyacrylamide gel matrix is determined by the molecular weight (size) and the charge of the protein. Smaller proteins migrate faster than larger proteins and negatively charged proteins migrate slower than uncharged proteins. Purified proteins, cell lysates and immunoprecipitate prepared in NuPage® LDS sample buffer (4X) and 25mM DTT were heated to 70ºC for 15 minutes. The samples and 5 µl of SeeBlue®Plus Two Prestained molecular weight protein standards were loaded onto a pre-cast gradient gel in an XCell Sure Lock™ Mini-Cell. 4-12% Bis-Tris polyacrylamide gels were used with NuPage® MOPS running buffer. Proteins were resolved at 200V after which gels either stained or the proteins transferred to a nitrocellulose membrane for immunoblotting. For the analysis of acetyl CoA Carboxylase and ATM, 3-8% Tris-acetate polyacrylamide gels were used with tris- acetate running buffer and the proteins were resolved at 150V for 75 minutes, after which the gels were transferred to a nitrocellulose membrane for immunoblotting.

2.2.17 Coomasie staining of gels

Proteins separated by SDS-PAGE on agarose gel were visualized using Coomasie staining. Gels were fixed for 30 minutes in a solution containing 50 % (v/v) methanol, 10% acetic acid (v/v) and 0.1% (w/v) Coomasie Blue on a shaking platform. The gels were then de- stained with a solution containing 10% (v/v) methanol and 10 %(v/v) acetic acid in de-ionised water overnight to remove background staining. The gels were then washed in de-ionised water and visualized on the Li-Cor Odyssey Imaging system.

2.2.18 Transfer of proteins to nitrocellulose membrane

Proteins were transferred following SDS-PAGE onto nitrocellulose membrane using an Xcell II Blot Module™, according to the manufacturer's instructions. Blotting pads, nitrocellulose membrane and 3MM filter paper were pre-soaked in 1X NuPage® transfer buffer containing 20% (v/v) methanol. The gel membrane sandwich was assembled from back to front as follows- blotting pad, filter paper, gel, nitrocellulose membrane, filter paper and blotting pads with the gel towards the cathode and the membrane towards the anode. The blotting module was placed in an Xcell Sure Lock™ Mini Cell and filled with the transfer buffer. Transfers were normally carried out at 34V for 90 minutes. In the case of high molecular weight proteins, transfer was carried out overnight at 12 V in the cold room (at 4°C).

2.2.19 Immunoblotting

Following transfer, nitrocellulose membranes were incubated either in Li-Cor Odyssey buffer or TBS buffer with 5% (w/v) non-fat milk for 1 hour to reduce non-specific antibody binding. Membranes were incubated overnight at 4°C with primary antibody (usually diluted 1:1000 for phospho antibodies and 1:5000 for total antibodies) in Li-

Cor buffer for phospho antibodies and TBS containing 2% (w/v) non-fat milk for total antibodies. Following incubation, membranes were washed in TBS containing 0.1% (v/v) Tween-20 for atleast 30 minutes (3X10 min washes). IRDye680- or IRDye800- conjugated secondary antibodies or Protein G-Sepharose coupled HRP (horse radish peroxidase) antibody were diluted 1:5000 in TBS containing 2% (w/v) non-fat milk. Membranes were washed in TBS containing 0.1% (v/v) Tween-20 for atleast 30 minutes (3 X10 min washes) followed by a final wash in de-ionised water. The signal was detected either using the Li-Cor Odyssey™ system which detects Infra-red IRDye-conjugated secondary antibody, or using enhanced chemiluminescence reagent for HRP conjugated secondary antibody. Briefly, equal volumes of luminol and peroxide were mixed and applied to the membrane for 2-5 minutes. The signal was then detected by placing the membrane with an X-ray film and developing the film after exposure.

2.2.20 Non- covalent coupling of antibodies to protein G-Sepharose

Protein G –Sepharose is commercially available as 66% slurry in ethanol. The required volume of beads was washed in IP buffer 4 times to remove alcohol, centrifuged at 16000g for 30 seconds and the supernatant removed. The beads were resuspended as a 20% slurry in IP buffer. The required antibody was added to the beads at a concentration of 1 μg antibody per μl Protein G-Sepharose resin. The mixture was placed on a roller mixer overnight to allow non-covalent coupling of the antibody to the beads. The beads were then centrifuged at 16000g for 30 seconds and the supernatant aspirated. The beads were then washed 3 times with IP buffer containing 0.5M NaCl to remove unbound antibody. The beads were then washed with IP buffer containing

150mM NaCl twice and finally resuspended in IP buffer containing 0.02% sodium azide and stored at 4°C until required.

2.2.21 AMPK immunoprecipitation assay

AMPK activity was measured by its ability to phosphorylate the AMARA synthetic peptide. AMPK-α1 and -α2 antibodies coupled to protein G-Sepharose (15µg antibody with 15 µl beads) was incubated with 100 µg cell lysate to immunoprecipitate endogenous AMPK. This method has previously been described (Davies et al., 1989); the only change to the described protocol is the use of AMARA synthetic peptide instead of SAMS peptide. The beads were then washed to remove unbound proteins and then aliquoted into 3 eppendorf tubes in assay buffer (5 µl beads in 20 µl buffer). The reactions were started by the addition of 30 µl assay buffer containing 200 µM AMP, 200 µM [γ^{32}P]-ATP, 5 µM $MgCl_2$ and 200 µM AMARA and the mixture was incubated in an orbital shaker at 30°C for 15 minutes. 30 µl of the reaction mixture was spotted onto p81 paper and the reaction was terminated by transfer of the paper to a beaker containing 1% orthophosphoric acid. Following further washes to remove unincorporated ATP, the papers were air-dried before being placed in scintillation vials and radioactivity was measured using an LKB- Wallace 1214 Rackbeta liquid scintillation counter. One unit of activity was defined as that which catalysed the incorporation of one nmole of γ^{32}P into the synthetic peptide.

2.2.22 Mice

All mice were bred in the Wellcome Trust Biocentre Transgenic Unit at the University of Dundee in accordance with UK Home Office Animals (Scientific Procedures) Act

1986. Mice with floxed PTEN alleles (129 ES cells implanted into FVB-N mice) were kindly donated by Hergen Spitz and mice with AMPK-α1 floxed alleles (129 ES cells implanted into C57Bl/6mice) were gifts from Dr. Benoit Viollet. Both mice were backcrossed onto the C57BL/6 background for atleast six generations. These were then crossed onto C57Bl/6 mice with a Cre recombinase under the control of the Lck promoter. This part of the project is co-supervised by Prof. Doreen Cantrell.

2.2.23 Genotyping

PCR reactions were used to amplify DNA extracted from ear clip samples from the mice. The primers listed below were used in the reactions

Table 4: List of Genotyping primers used

AMPKα 1	forward 5'	TAT-TGC-TGC-CAT-TAG-GCT-AC (20)
	reverse 3'	ACC-TGA-CAG-AAT-AGG-ATA-TGC-CCA-ACC-TC (29)
PTEN	forward 5'	GCCTTACCTAGTAAAGCAAG (20)
	reverse 3'	GGCAAAGAATCTTGGTGTTAC (21)
Cre-recombinase	forward 5'	CGGTCGATGCAACGAGTGATGAGG (24)
	reverse 3	CCAGAGACGGAAATCCATCGCTCG (24)

PCR reactions for each were carried out in PCR buffer with $MgCl_2$ with dNTP's using RedTaq DNA polymerase. The PCR products were resolved on a 2% agarose gel containing 1:40,000 ethidium bromide and visualised with an Infra-red imaging system.

2.2.24 siRNA knockdown of CaMKK-β

Reverse transfection of siRNA constructs against CaMKK-β were carried out according to protocols detailed in the Ambion™ siRNA starter kit. Briefly, transfection reagent (siPORT) was diluted 1 in 20 in Opti-MEM medium and allowed to incubate for 10 minutes. Meanwhile, cells were trypsinised for 5 minutes and the trypsin quenched with complete media. siRNA (obtained from Ambion, Life Technologies) was diluted in Opti-MEM to a final concentration of 5nM. siRNA and diluted transfection reagent were then mixed and incubated for 10 minutes. The siRNA- siPORT mixture was added to 6 well plates and cells were seeded into the 6-well plates. The plates were returned to the incubator for 24 hours, following which treatment with vehicle or drugs was carried out for 18 hours. Knockdown was confirmed by Western blotting.

2.2.25 Cell Cycle Analysis

Cells were seeded in 6 cm dishes until 40-80% confluence and treated for 16-18 hours. Cells were trypsinised until detached from the base of the dish and the trypsin was then quenched with media. The cells were pelleted, transferred into 5 ml falcon tubes and washed with PBS containing 1% FCS and 0.1mM EDTA. The cells were then fixed with ice cold 70% ethanol for atleast 2 hours. The cells were then washed twice in the PBS buffer and then stained with PBS containing propidium iodide (diluted 1 in 20 in the PBS buffer) and RNAse to digest RNA. The cell cycle analysis was performed on the Calibur flowcytometer and analysis performed using Flow Jo software.

2.2.26 Cell Survival Assay

Cells were seeded into $25cm^3$ flasks at equal density and treated at 40-80% confluence with control and different concentrations of drug for 24 hours. Cells were trypsinised in 3 mls of trypsin EDTA for 5 minutes and then quenched with 5 mls complete media. The cells in the control flask were counted using a haemocytometer under a microscope and 2000-5000 cells seeded in triplicate into 10 cm dishes containing 10 mls of media. The same volume of media containing cells was aspirated from the treated flasks and seeded in triplicate into 10 cm dishes also containing 10 mls of media. The dishes were placed at 37ºC in an incubator with an atmosphere containing 5% CO_2 for 7-10 days. The media was changed once during this period. At the end of the incubation period, the media was aspirated; the cells were fixed in ice-cold methanol for 10 minutes and stained with 0.4% (w/v) Giemsa in methanol for 10 minutes. The dishes were washed with de-ionised water and the number of colonies was counted manually.

2.2.27 Immunofluorescence Microscopy

Cells were grown on glass coverslips in 6-well dishes until 40-80% confluence. They were then treated with control or different concentrations of various drugs for a set period of time. The coverslips were then washed in PBS thrice, fixed in 4% Paraformaldehyde made up in PBS for 20 minutes and washed again with PBS three times. The cells were then permeabilised in 0.2% Triton in PBS for 5 minutes. The coverslips were again washed in PBS. The coverslips were then placed in blocking buffer (PBS containing 0.2% Fish skin gelatin) for 1 hour to block non-specific antibody binding. Coverslips were then stained with primary antibody (1:300- 1:1000

dilution in blocking buffer) for 30 minutes. After the coverslips were washed in blocking buffer, the coverslips were again stained with fluorescent secondary antibody (1:200 dilution in blocking buffer) for 30 minutes. The coverslips were then washed in PBS twice, mounted onto slides using Vectashield and then sealed with nail varnish. The slides were imaged on the Deltavision deconvolution microscope and images acquired and deconvolved using the SoftWorx program.

2.2.28 Live Cell Imaging

Cells were grown on glass bottom dishes (Willco Wells) until 40-80% confluence. Cells were then loaded with 1 μM Fluo4-AM dye for 20-30 minutes. The cells were then washed with PBS and fresh media added to the dish. The Willco dish was mounted onto a stage pre-heated to 37 degrees and enclosed with a lid to deliver 5% CO_2 to the cells. Calcium flux was measured using the Zeiss LSM-710 confocal system with fluorescence measured at 488nm using 63X magnification objective. Image analysis and quantification was done using Volocity 5.5.1 software.

2.2.29 Real-time PCR

Real time PCR was used to analyse and compare the mRNA expression of genes in mice thymocytes which lacked PTEN ± AMPK to that of wild type thymocytes. First, RNA was extracted from the thymocytes using the QIAGEN RNeasy Kit, according to the manufacturer's instructions. Cell pellets of thymocytes, previously frozen at -80°C were resuspended and lysed in RLT buffer (QIAGEN) before being passed through QIA shredders. Nucleic acids were precipitated by adding 70% ethanol. The mixture was passed through RNeasy spin columns, which bound nucleic acids. Genomic DNA was

then digested on the column with DNase I. Following a series of wash steps, RNA was eluted in RNase-free water. The RNA was quantitated using the nanodrop.

cDNA was then synthesised using the Quanta cDNA synthesis kit, according to the manufacturer's instructions. Briefly 500ng of RNA was added to qScript reaction mix, which contained primers and nucleotides, before the addition of qScript reverse transcriptase. The final volume of this reaction was 20 μls. The cDNA was synthesised by placing this mixture in a thermal cycler programmed as follows: 1 cycle at 22°C for 5 minutes, 1 cycle at 42°C for 30 minutes and 1 cycle at 85°C for 5 minutes, before being cooled to 4°C. 80 μls of DEPC water was then added to the PCR product.

PCR reactions were then performed in triplicate with the cDNA as a template along with specific primers for various genes (See Table 5), along with the reaction mixes containing nucleotides and SyBr green which stained double stranded DNA. The PCR reactions were performed in a real-time PCR machine, according to a standardized programme, which measured the intensity of SyBr green signal as a measure of the amount of DNA synthesised. The number of cycles to achieve a defined intensity of SyBr green by the different cDNA constructs was noted and normalized to the number of cycles required by a   housekeeping gene to achieve the same intensity of SyBr green.

Table 5: List of primers used for RT-PCR

1)	$S1P_1$	forward	5'-GTG TAG ACC CAG AGT CCT GCG-3'
	$S1P_1$	reverse	5'-AGC TTT TCC TTG GCT GGA GAG-3'
2)	HPRT	forward	5'-TGA TCA GTC AAC GGG GGA CA-3'
	HPRT	reverse	5'-TTC GAG AGG TCC TTT TCA CCA-3'
3)	CD62L	forward	5'- CCT GTA GCC GTC ATG GTC AC-3'
	CD62L	reverse	5'- GAA TCA GTA TGG ATC ATC CAT C -3'

4) CCR7 forward 5'- CAG CCT TCC TGT GTG ATT TCT ACA-3'

  CCR7 reverse 5'- ACC ACC AGC ACG TTT TTC CT-3'

5) CD69 forward 5'- AAC TGA CTG CTA ATC ACA TCA AGG-3'

  CD69 reverse 5'- GTC ATT CGG CAA TAA ATA GTA ACT CTA G-3'

2.2.30 Statistical Analysis

Statistical analysis was carried out using GraphPad Prism software version 5. Student t-test was used to compare 2 groups and ANOVA used to compare three or more groups. Where applicable, the Newman-Keuls post-test was used, which assumes equal variance. In cases where a large number of samples were compared, then a Bonferroni test was used. Statistical significance was determined by calculating p values and represented as follows- $p < 0.05$ (represented in some figures as *), $p < 0.01$ (represented in some figures as **) and $p < 0.001$ (represented in some figures as ***).

CHAPTER THREE: ACTIVATION OF AMPK BY AGENTS THAT CAUSE DOUBLE STRANDED DNA BREAKS

3.1 INTRODUCTION

3.1.1 DNA Damage response pathways

Endogenous DNA damage occurs at high frequency in normal cells. For example, base loss due to spontaneous hydrolysis of DNA glycosyl bonds occurs at a frequency of 10^4 events per mammalian cell per day (Lindahl and Nyberg, 1972). These defects need to be detected and repaired rapidly to allow the cell to divide and pass on the correct complement of genomic material (Rouse and Jackson, 2002). Different types of DNA damage occur on exposure to different agents, for instance, exposure to ultraviolet radiation causes single strand DNA breaks (Reynolds and Friedberg, 1981), while ionising radiation, reactive oxygen species and exposure to topoisomerase inhibitors (e.g. etoposide) cause double strand DNA breaks (Povirk, 2006, Heisig, 2009). Of all the various genotoxic stresses the cell undergoes, double stranded DNA breaks are the most deleterious. To counter DNA damage, cells have evolved complex responses, with a network of distinct, but interacting pathways that are defined by the type of DNA damage (Lord and Ashworth, 2012). The different pathways involved with specific types of DNA damage are summarised in Figure 3.1. The rest of this introductory section deals with double strand breaks caused by etoposide and focusses on activation of the *Ataxia-Telangiectasia Mutated* (ATM) kinase.

3.1.2. The PIKK family of proteins

The phosphatidyl inositol 3-kinase-like kinases (PIKKs) are a family of six kinases of unusually large molecular weight (300-500 KDa), which play an important role in dealing with cellular stress (Abraham, 2004b). They include three protein kinases, namely, *A*taxia-*T*elangiectasia *M*utated (ATM), ATM and Rad-3 related kinase (ATR) and DNA- dependent protein kinase (DNA- PK), which share sequence identity and are involved in the DNA damage response (Durocher and Jackson, 2001). Two other kinases in this group include the mammalian *T*arget-*of-R*apamycin (mTOR), which regulates protein synthesis, cell growth and cell proliferation in response to the availability of nutrients and mitogenic growth factors, and *S*uppressor of *M*orphogenesis in *G*enitalia-1 (SMG-1), which may also be involved in genotoxic stress as well as in mRNA surveillance pathways (Abraham, 2004a). The sixth and final member of this family, *T*ransformation/*T*ranscription domain *a*ssociated *p*rotein (TRRAP) retains the PI 3-kinase related catalytic domain, but possesses no intrinsic phospho-transferase activity (Mcmahon et al., 1998).
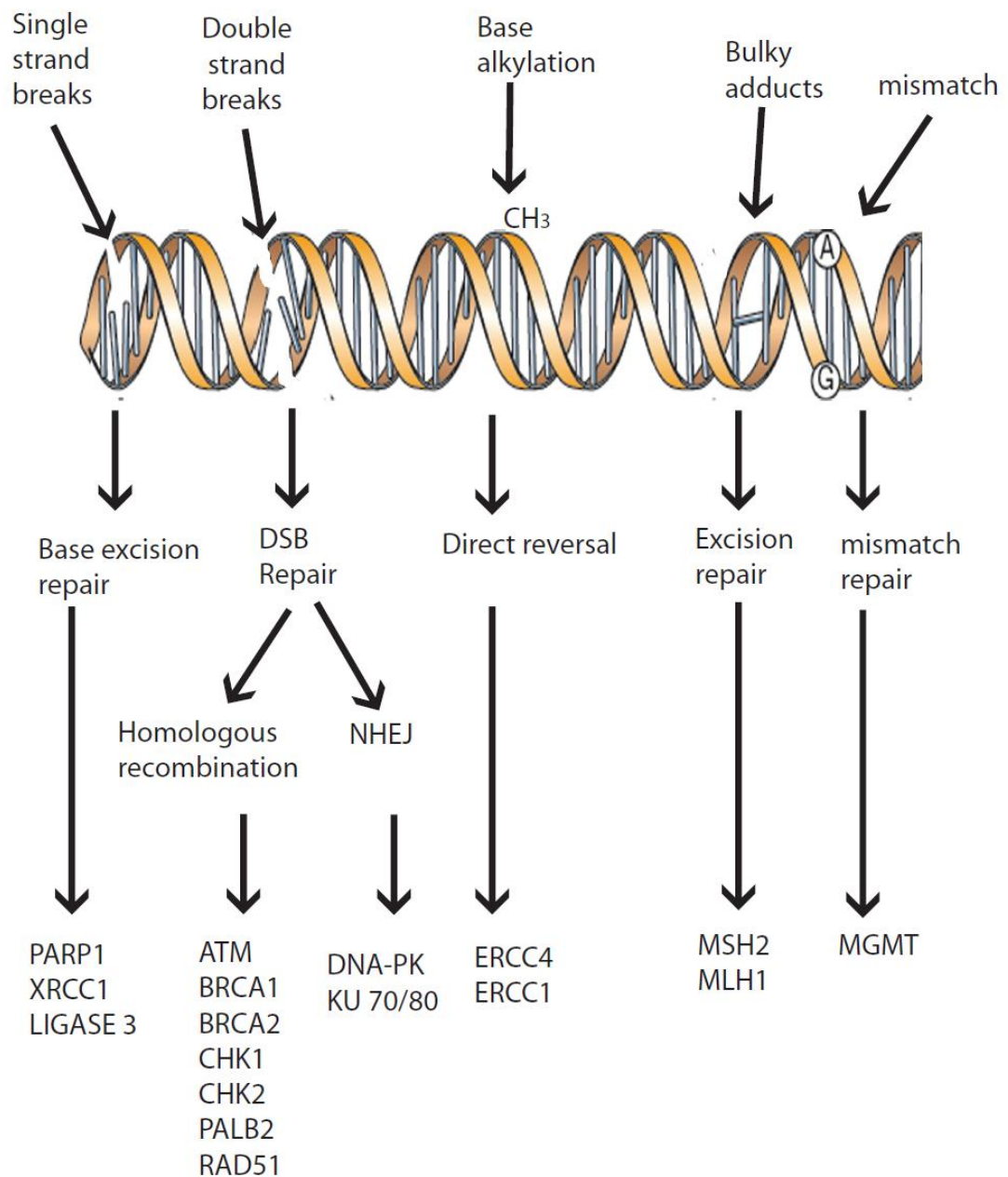
Figure 3.1: DNA Damage response pathways

The type of genotoxic insult determines the type of DNA repair, and different components of the DNA damage response are activated or recruited to sites of DNA damage in each case. Adapted from (Lord and Ashworth, 2012).

NHEJ: Non-homologous end joining

3.1.3 ATM Kinase

ATM kinase, encoded by the ATM gene is a 370 KD protein. ATM is activated by double stranded DNA breaks (DSBs). Mutations in or loss of the ATM gene are associated with the Ataxia Telangiectasia, an autosomal recessive human disorder, characterised by gait abnormalities, mainly ataxia, dilated blood vessels (telangiectasia), immune deficiency and predisposition to cancer and diabetes mellitus (Lavin and Shiloh, 1997). Under basal conditions, ATM exists as an inactive dimer. In response to DNA damage, it undergoes auto-phosphorylation on Ser-1981, forms monomers and is activated (Bakkenist and Kastan, 2003). It is then recruited to sites of DNA damage by the *M*re11- *R*ad50- *N*BS1 (MRN) complex (Carson et al., 2003), and NBS1 activation by ATM-dependent phosphorylation further strengthens the association of ATM to these sites (Berkovich et al., 2007). Once activated, ATM phosphorylates several downstream targets involved in the repair of DSBs and regulation of the cell cycle. The optimal ATM substrate motif is a serine or threonine followed by glutamine (S/TQ) and large scale proteomics analysis reveals that ATM and ATR may phosphorylate as many as 900 sites on 700 different proteins (Matsuoka et al., 2007).

One target for ATM is the checkpoint kinase Chk2, which is phosphorylated on Thr-68 (Ahn et al., 2000). Chk2, in turn, phosphorylates and inactivates the protein phosphatases Cdc-25A and Cdc-25C, thereby causing a cell cycle arrest at the G2/M phase (Ahn et al., 2004). Another key protein that is phosphorylated by ATM is the p53 tumour suppressor. The p53 protein regulates the cell cycle by causing a G1/S arrest and also promotes apoptosis. ATM phosphorylates p53 on Ser-15 (Canman et al., 1998, Banin et al., 1998). This phosphorylation promotes a second phosphorylation on p53 by ATM at Thr-18, which disrupts its interaction with Mdm2 and enhances its transcriptional activity (Schon et al., 2002). ATM also phosphorylates Mdm2 and

Mdmx and destabilises them, further enhancing p53 activity (Meulmeester et al., 2005). As the cell cycle needs to be stalled in order to repair DNA damage, the two distinct phases in which cell cycle arrest occurs also determine which type of DNA repair takes place. The error-prone Non-homologous end joining (NHEJ) repair occurs in the G0/G1 phase when non-replication DSBs occur while homologous recombination can only occur in S/G2phase (Bekker-Jensen and Mailand, 2010).

Two other well characterised ATM substrates are the histone family member X (H2AX), which is phosphorylated on Ser-139 (when it is termed γ-H2AX) and *S*tructural *M*aintainence of *C*hromosome-1 (SMC-1), which is phosphorylated on Ser-966 (Fernandez-Capetillo et al., 2004, Kitagawa et al., 2004). ATM phosphorylates SMC-1 on two sites, Ser-957 and Ser-966 and these phosphorylation events have been shown to be necessary for S phase arrest in cells (Kitagawa et al., 2004). Antibodies against these phosphorylated ATM substrates have been used in the experiments detailed in this chapter as markers of ATM activation.

3.1.4 Etoposide causes double stranded DNA breaks

Etoposide (VP-16) is a potent anti-cancer drug used as a chemotherapeutic agent in cancers of the lung (Mascaux et al., 2000), testes (Loehrer, 2006), ovaries (Bruzzone et al., 2011), lymphoma (Bauer et al., 2011) and glioblastoma multiformae (Francesconi et al., 2010). It is a topoisomerase II (Top II) inhibitor derived from 40-demethylepipodophyllin benzylidene glucoside, a naturally occurring compound found in the Podophyllum plant root. Topoisomerase II is an enzyme that mediates transient double strand breaks in DNA, which allows the helix to unwind before replication. The same enzyme is also involved in the re-ligation of the disrupted DNA double strand.

Etoposide binds to topoisomerase II and stabilises the Topoisomerase II-DNA complex, preventing re-ligation of the broken DNA strands and thus increases the steady state concentration of double stranded DNA breaks (Hande, 1998, Montecucco and Biamonti, 2007). Although etoposide has been in clinical use for over twenty years, and its action on topoisomerase II delineated over thirty years ago, the cellular responses to etoposide remain poorly understood.

3.1.5 Activation of AMPK by DNA damage: Relationship between ATM and AMPK

ATM and ATR have been shown to phosphorylate LKB1 on its C-terminal tail on Thr-366 in cell free assay. Also, HeLa cells stably expressing wild type LKB1 and treated with ionising radiation, showed increased nuclear signal when stained with anti-phosphoThr-366 antibody compared to untreated cells. This nuclear localisation was lost in the cells expressing non-phosphorylatable alanine mutant (T366A) (Sapkota et al., 2002b). Etoposide has also been reported to activate AMPK, involving phosphorylation at Thr-172 within the activation loop (Fu, 2008). These authors reported that reduction in ATM levels by siRNA- mediated silencing reduced AMPK activation following etoposide treatment in HeLa cells, suggesting that the effect involves ATM. This is an interesting observation, as HeLa cells lack LKB1 and therefore this effect cannot have been mediated by phosphorylation of Thr-172 on AMPK by LKB1. Moreover the first paper (Sapkota et al., 2002b) was published before LKB1 had been identified as the main upstream kinase for AMPK and therefore the role of ATM-mediated LKB1 phosphorylation on activation of AMPK activity was not tested.

ATM is also activated by oxidative stress. ATM in the cytoplasm is activated by reactive oxygen species (ROS) and this leads to an LKB1-dependent activation of AMPK, and subsequent repression of the mTOR pathway via phosphorylation of TSC2 (Alexander et al., 2010). This activation of ATM is distinct from that caused by ionising radiation-induced DSBs, which occur in the nucleus and where activated ATM forms monomers. Activation of ATM in the cytoplasm by oxidative stress involves the formation of disulphide-linked dimers (Guo et al., 2010). The catalytic α subunits of AMPK lack the S/Q or T/Q motif required for ATM phosphorylation (Matsuoka et al., 2007), so the mechanism underlying etoposide induced AMPK activation remained unclear. The role of LKB1 in this process was also not defined. The role of AMPK activation in the overall cellular response to etoposide had also not been studied, apart from the observation that NRF-1 transcription in response to etoposide may be regulated by AMPK in an ATM-dependent manner (Fu, 2008).

Finally, large scale genome wide association studies have linked ATM with AMPK. Single nucleotide polymorphisms in a region of linkage disequilibrium containing the ATM locus are associated with an enhanced response to metformin (Pearson, 2011).

3.2 AIMS

The main aim of the chapter was to delineate the mechanism by which AMPK was activated following double strand breaks, clarify the relationship between ATM and AMPK and to examine if C-terminal phosphorylation of LKB1on Thr-366 by ATM was involved in regulating AMPK activity. Intact cells were treated with etoposide and endogenous AMPK was immunoprecipitated from the lysate and effects on its function examined. Western blotting was used to look for activation of ATM substrates as well as phosphorylation of Thr-172 on AMPK. Immunofluorescence microscopy was performed to detect subcellular localisation of activated ATM and AMPK.

The second aim of this chapter was to see if AMPK activation affected the cellular response to DNA damage. Clonogenic cell survival assays were utilised to examine whether activating AMPK using agents such as A-769662 and the calcium ionophore A23187 prior to DNA damage by etoposide, affected cell survival. Changes in the cell cycle in response to these treatments were also examined.

3.3 RESULTS

3.3.1 Etoposide activates AMPK in an LKB1-independent manner

Recent evidence suggests that etoposide activates AMPK and this causes increased mitochondrial biogenesis (Fu, 2008). In order to assess the mechanism behind this activation, several cell lines, namely HEK 293, H4IIe, HeLa, Mouse embryonic fibroblasts and G361 melanoma cells were treated with control (DMSO) or increasing concentrations of etoposide for varying lengths of time from one hour to 24 hours. HEK 293 cells and H4IIe cells failed to activate AMPK in response to etoposide (data not shown). However, HeLa cells (Figure 3.2 A) and G361 cells (Figure 3.3.B), both of which lack LKB1, showed a two- to three-fold increase in AMPK activity on immunoprecipitation kinase assays when treated with 30 μM etoposide for 18 hours, which is a concentration similar to that achieved by therapeutic oral or intravenous dosing in humans. This increase in AMPK activity was associated with an increase in phosphorylation of AMPK at Thr-172 detected by western blotting (Figure 3.2.B). It is important to note that these cells have very low basal AMPK activities as they lack LKB1, the main upstream kinase for AMPK. Interestingly, treatment of mouse embryonic fibroblasts, which have LKB1 with etoposide also resulted in a greater than two fold increase in AMPK (Figure 3.3 C and D).

A.
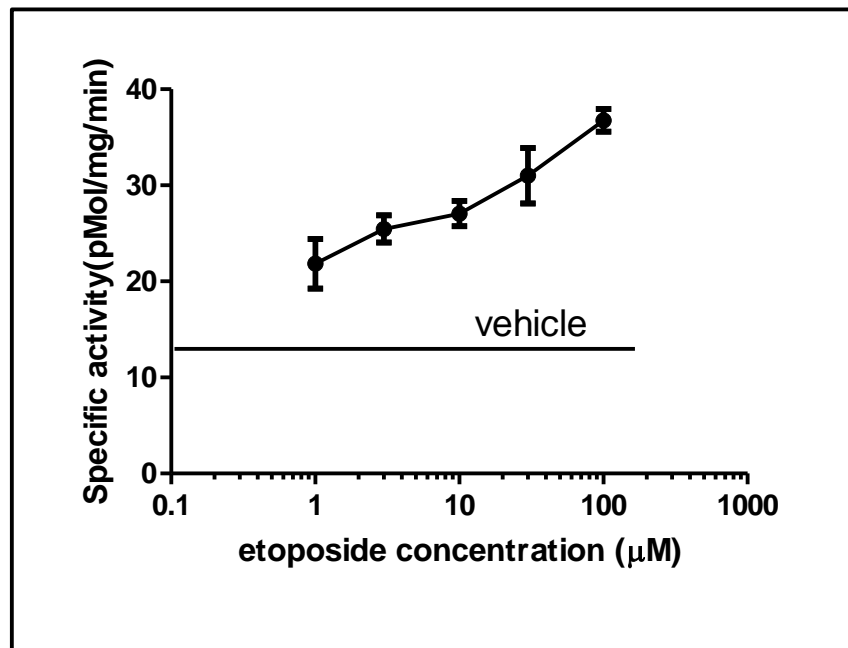
B.
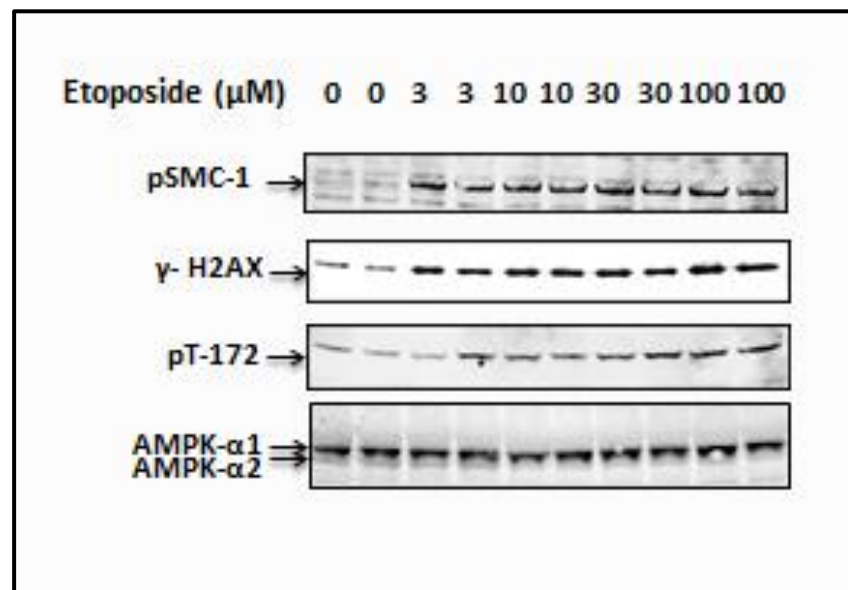
Figure 3.2: Etoposide activates AMPK

(A) HeLa cells were treated with increasing concentrations of etoposide for 18 hours, Endogenous AMPK was immunoprecipitated from the cell lysate and AMPK activity measured using the *AMARA* peptide substrate. Results shown are mean ± SEM (n=3, each replicate was a mean of two individual values of duplicate assay samples) and are representative of three independent experiments.

(B) Cell lysates from HeLa cells were subject to Western blotting with anti- AMPK-α1 and -α2 and anti- pT172 antibodies. Anti- pSMC-1 and γ- H2AX antibodies were used as markers of ATM activation. .

A.

HeLa cells

B.

G361 cells

C.

Mouse Embryonic Fibroblasts

D.
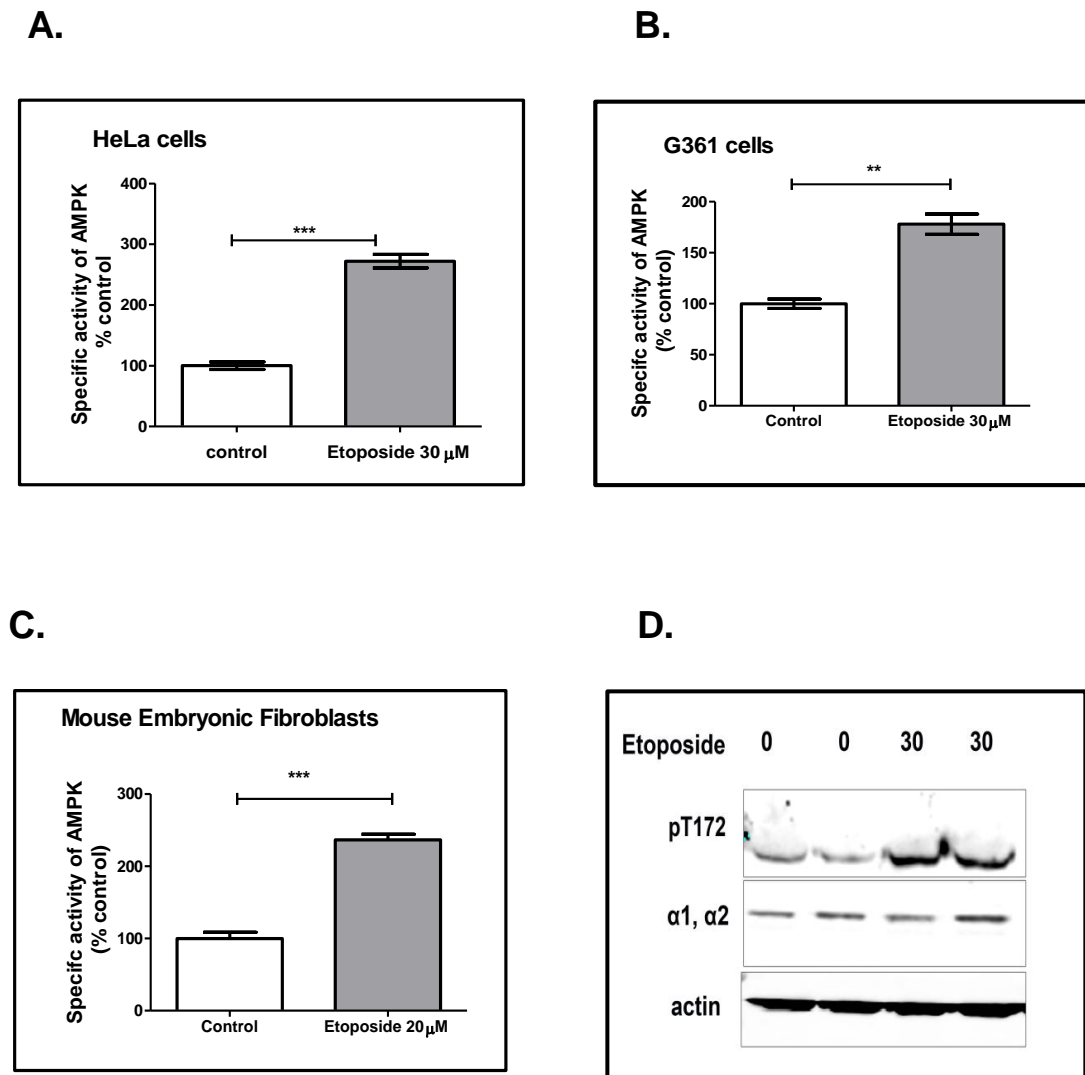
Figure 3.3: Etoposide activates AMPK independently of LKB1

Three different cell lines were treated with etoposide and endogenous AMPK was immunoprecipitated from the cell lysates and AMPK activity measured using the *AMARA* peptide substrate. The dose of etoposide and the duration of treatment used were different in different cell lines as some cell lines such as MEFs were very sensitive to the dose used and prolonged treatment caused cell death. Results shown are mean ± SEM (n=3) and are representative of three independent experiments. Student t-test was used to measure significance (p<0.01-**, p<.0001-***).

(A) HeLa cells (which lack LKB1) were treated with 30 µM etoposide for 18 hours
(B) G361 cells (which also lack LKB1) were treated with 30 µM etoposide for 18 hours
(C) MEF cells (which have LKB1) were treated with 20 µM etoposide for 2 hours
(D) Cell lysates from MEFs were subject to Western blotting with anti- AMPK-α1 and -α2 and with anti-pT-172 antibodies. Actin was used as a loading control.

In order to determine if AMPK activation by etoposide was isoform-specific, lysates subjected to western blotting were immunoblotted with pT-172, followed by infra-red secondary antibody read at 680nM (shown in red in Figure 3.4) and either anti-α1 or anti-α2 antibodies, followed by infra-red secondary antibody read at 800nM (shown in green in Figure 3.4) on the Li-Cor Odyssey imaging system . When treated with etoposide, HeLa cells showed activation of the α1 isoform of AMPK, as evidenced by colocalisation of the red and green fluorescence, which appeared as a yellow signal in the blots stained with anti-pT-172 and anti-AMPK-α1. In contrast, two separate bands were seen in the blots stained with anti-pT-172 and anti-AMPK-α2. This result shows that the activated AMPK was entirely AMPK-α1, with no activation of AMPK-α2.
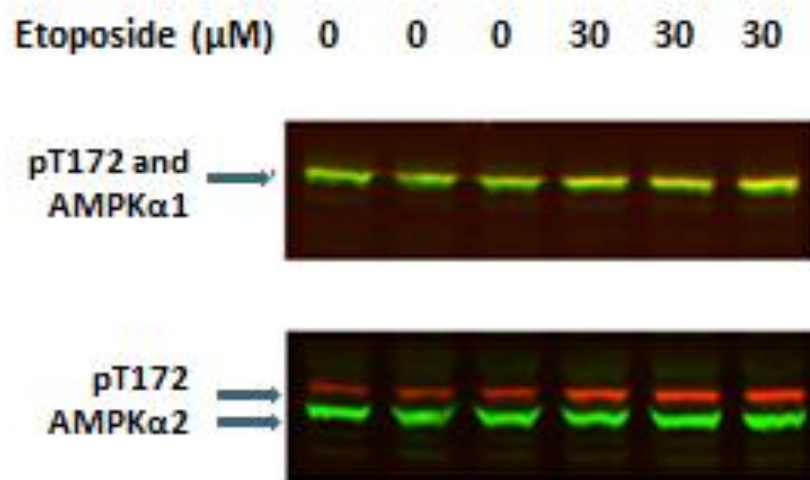
Figure 3.4: Etoposide treatment activates AMPK-α1 but not -α2

Cell lysates from HeLa cells treated with vehicle (DMSO) or etoposide were subject to Western blotting with anti- AMPK-α1 and -α2 and anti- pT172 antibodies. The Li-Cor Odyssey system was used for dual immunoblotting , with anti-pT172 antibody coupled to a Infra-red secondary antibody (read at 680nM and seen in red) and the anti- AMPK-α1 and -α2 antibodies were coupled to a second Infra-red secondary antibody (read at 800nM and seen in green). The top panel shows colocalisation of the anti-pT172 signal with anti- AMPK-α1 (seen as a yellow signal) and increased phosphorylation in the etoposide treated lanes (seen as brighter bands), while the bottom panel shows two distinct non-overlapping red and green bands of anti-pT172 and anti- AMPK-α2. This suggests that the α1 isoform of AMPK is selectively phosphorylated following etoposide treatment.

3.3.2. Etoposide activates AMPK in a CaMKK-β−dependent manner

3.3.2.1 The CaMKK inhibitor STO-609 abolishes etoposide-induced AMPK activation

As LKB1 was not required for AMPK activation in response to etoposide, we examined whether CaMKKβ, the alternative upstream kinase for AMPK was involved. We used both STO-609, a pharmacological inhibitor of CaMKK-α and CaMKK-β and siRNA- mediated knock down of CaMKK-β before treatment with etoposide to see whether AMPK activation was affected when CaMKK activity was inhibited. Immunoprecipitate kinase assays for AMPK activity were performed on the cell lysates which showed that inhibition of CaMKK-β by STO-609 significantly reduced etoposide-induced AMPK activation in HeLa cells (Figure 3.5.A) suggesting that AMPK activation in response to etoposide is dependent on CaMKK. However, as the fold change between STO-609 treated cells and cells treated with STO-609 and etoposide was almost the same as cells treated with vehicle and etoposide, it may be possible that another kinase may also be involved. Western blotting was also performed on the lysates. Following etoposide treatment, phosphorylation of SMC-1 (structural maintainence of chromosome-1) on Ser -966, which is mediated by ATM was detected using a phospho-specific antibody with no change in total SMC-1 confirming that ATM was activated. Western blotting also showed that phosphorylation of AMPK on Thr-172 in response to etoposide treatment was abolished by pre-treatment with STO-609, despite increase in pSMC-1 following etoposide treatment in cells treated with both STO-609 and etoposide (Figure 3.5.B). Interestingly, etoposide treatment did not cause an increase in phosphorylation of ACC on Ser-79, a known downstream target of AMPK, despite the increase in activity and Thr-172 phosphorylation on AMPK.

Phosphorylation of ACC, which was not increased by AMPK activation with etoposide,

was also not affected by treatment with STO-609.
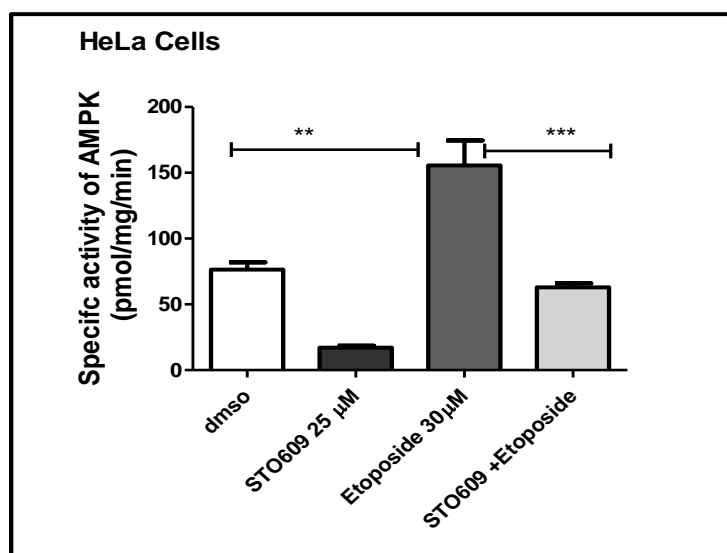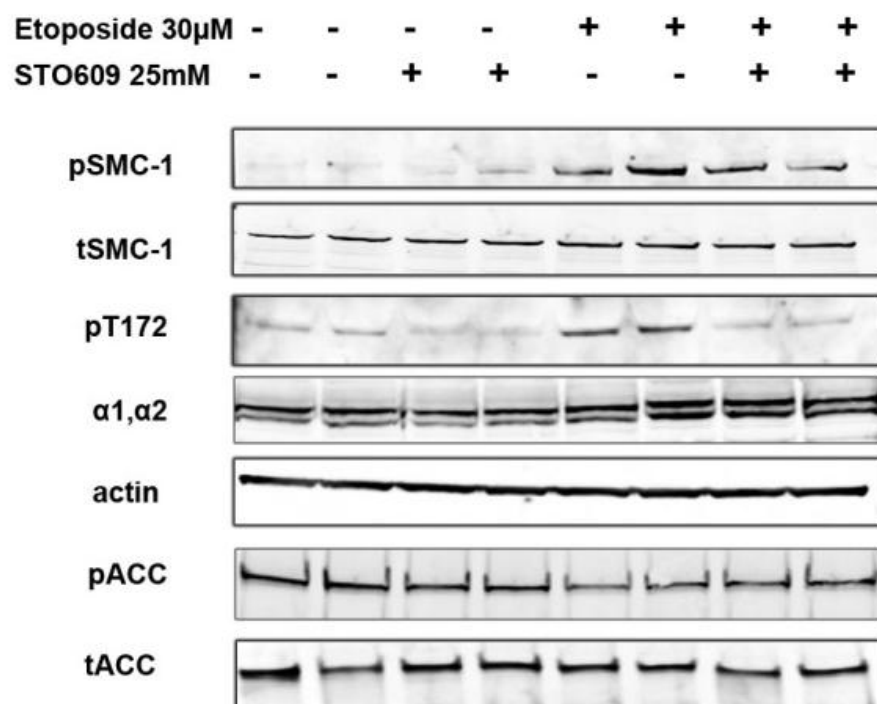
Figure 3.5: Etoposide activates AMPK in a CaMKK– dependent manner

HeLa Cells were treated with 30 µM etoposide for 18 hours with or without 1 hour pre-treatment with 25 µM STO-609.

(A) Endogenous AMPK was immunoprecipitated from the cell lysate and AMPK activity measured using the AMARA peptide substrate. Results shown are mean ± SEM (n=3) and are representative of three independent experiments done in triplicate. ($p < 0.01$-**, $p < .0001$-***).

(B) Cell lysates from HeLa cells were subject to Western blotting with anti- AMPK-$\alpha 1$ and -$\alpha 2$, anti-pT-172 antibodies, anti- pSMC-1and anti-SMC-1, Anti-pACC and biotinylated total ACC was detected with Streptavidin.

3.3.2.2 siRNA- mediated Knock down of CaMKK-β also abolishes etoposide- induced AMPK activation

siRNA-mediated knockdown was carried out in HeLa cells as a second approach to see whether reducing levels of CaMKK-β resulted in a loss of AMPK activation by etoposide. Scrambled negative control siRNA and CaMKK-β-specific siRNAs were reverse transfected into HeLa cells 24 hours before treatment with vehicle or etoposide. The Ca^{2+} ionophore A23187 was used as a positive control in these experiments. A 70% knock-down of endogenous CaMKK-β was achieved by this process (Figure 3.6.B). As expected, knock down of CaMKK-β resulted in a marked decrease in Thr-172 phosphorylation on AMPK on western blotting following treatment with A23187 (Figure 3.6.A) and this was confirmed by a marked reduction in the AMPK in immunoprecipitate kinase assays (Figure 3.6.C). Also, the fold change difference between vehicle and A23187 treated cells in the scrambled and siRNA knock-down cells was different with a lower degree of fold-change in the siRNA treated cells. Knock down of CaMKK-β completely abolished etoposide-induced AMPK activation on immunoprecipitate kinase assays (Figure 3.7.A) and also abolished Thr-172 phosphorylation on AMPK on western blotting (Figure 3.7.B), confirming that CaMKK-β was the main upstream kinase phosphorylating AMPK in response to etoposide-induced double strand breaks.
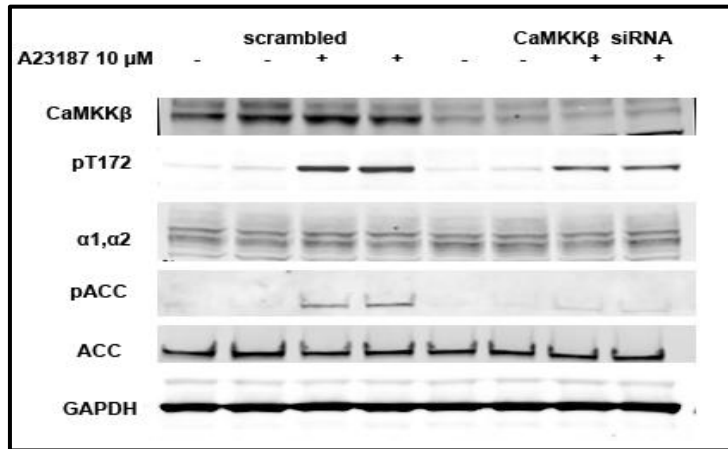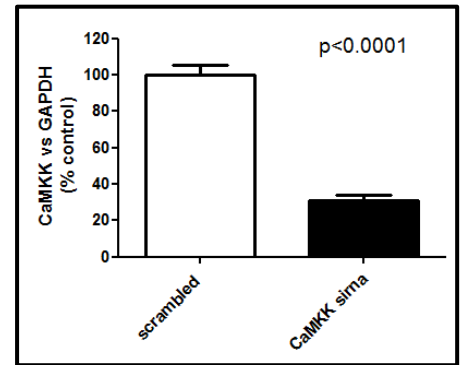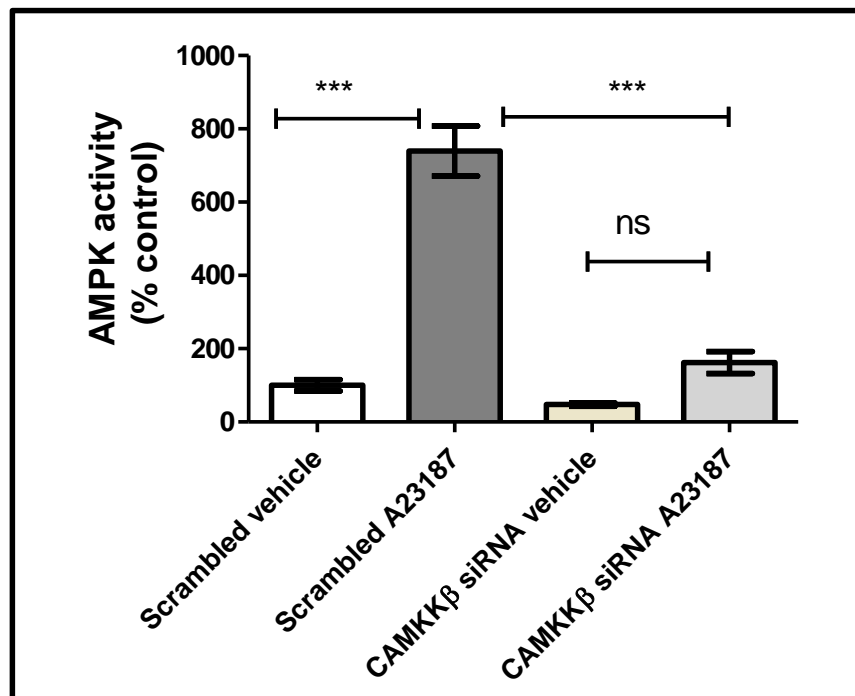
Figure 3.6: siRNA-mediated knock down of CaMKKβ reduces AMPK activation following treatment with A23187

siRNA-mediated knock-down of CaMKKβ was performed in HeLa cells by reverse transfection 24 hours before treatment with 10 μM A23187 for 1 hour

(A) Cell lysates were subject to Western blotting with anti- CaMKKβ, anti-pT-172, anti-AMPK-α1, -α2 and anti- pACC. Total ACC is a biotin enzyme and was detected by streptavidin. GAPDH was used as a loading control.

(B) The extent of knockdown of CaMKK is represented as the ratio of signal intensity of CaMKKβ to the signal intensity of GAPDH between the replicates treated with negative

control siRNA and the CaMKKβ- specific siRNA (n=4). 80% knockdown of CaMKKβ was achieved using this construct when measured against GAPDH signal intensity

(C) Immunoprecipitate kinase assays were performed on the cell lysates and the data plotted as shown. Results shown are mean ± SEM (n=3) and are representative of two independent experiments. (p<.0001-***).

A.
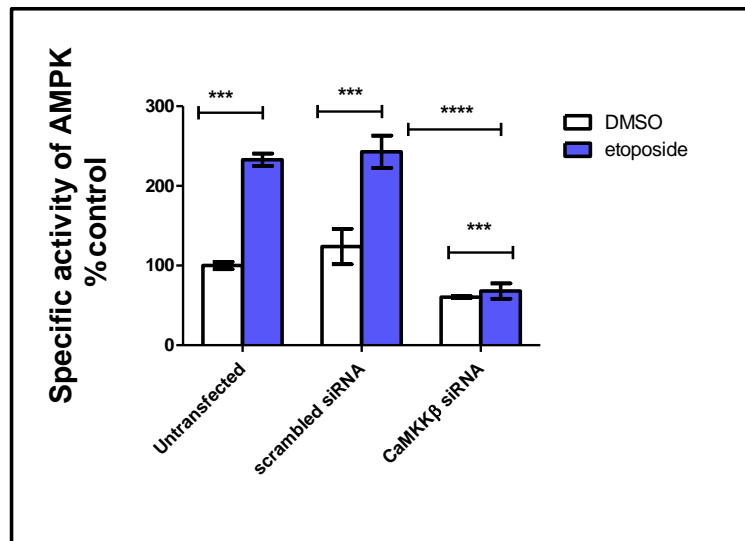
B.
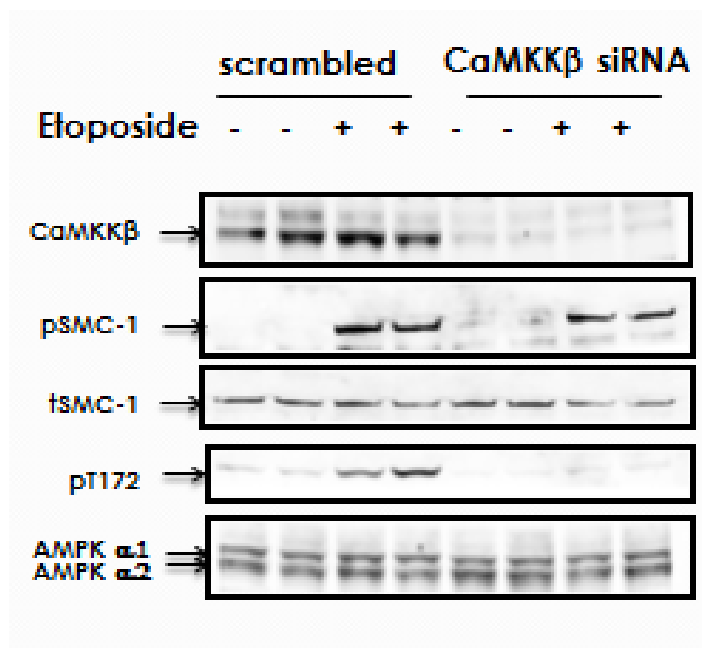
Figure 3.7: siRNA-mediated Knock down of CaMKKβ abolishes AMPK activation following treatment with etoposide

siRNA-mediated knock-down of CaMKKβ was performed in HeLa cells by reverse transfection 24 hours before treatment with 30 μM etoposide for 18 hrs

(A)   Immunoprecipitate kinase assays were performed on the cell lysates. Untransfected cells and cells transfected with negative control siRNA were used as controls. Results shown are mean ± SEM (n=3) and are representative of two independent experiments in triplicate (p<.0001-***).

(B)   Cell lysates were immunoblotted with anti- CaMKKβ, anti-phospho Thr-172, anti-AMPK α1, α2, pSMC-1 and tSMC-1 to confirm knockdown of CaMKKβ and to confirm lack of AMPK activation.

3.3.3 ATM inhibition reduces but does not abolish AMPK activation

The selective ATM inhibitor KU-55933 (Hickson et al., 2004) was used to examine whether ATM was involved in etoposide- induced AMPK activation. Whilst this inhibitor can inhibit other members of the PIKK family, at the doses that the treatments was carried out, it selectively inhibited only ATM (Hickson et al., 2004). Cells were pre-treated with 10 μM KU-55933 one hour before treatment with etoposide for 16 hours. Pre-treatment with KU-55933 caused a 30% reduction in etoposide- induced AMPK activity (Fig 3.8A). Western blotting showed that although the KU-55933 effectively inhibited ATM as evidenced by the marked reduction in phosphorylation of its substrate SMC-1 on Ser-966, there was only a very slight reduction in Thr-172 phosphorylation in the KU-55933 pre-treated cells when compared to cells treated with etoposide alone (Fig 3.8 B). This suggests that ATM may not be involved in this process. siRNA- mediated knock-down of ATM expression also showed a similar effect, although only 50% reduction of ATM expression could be achieved by this process (data not shown).

A.

B.
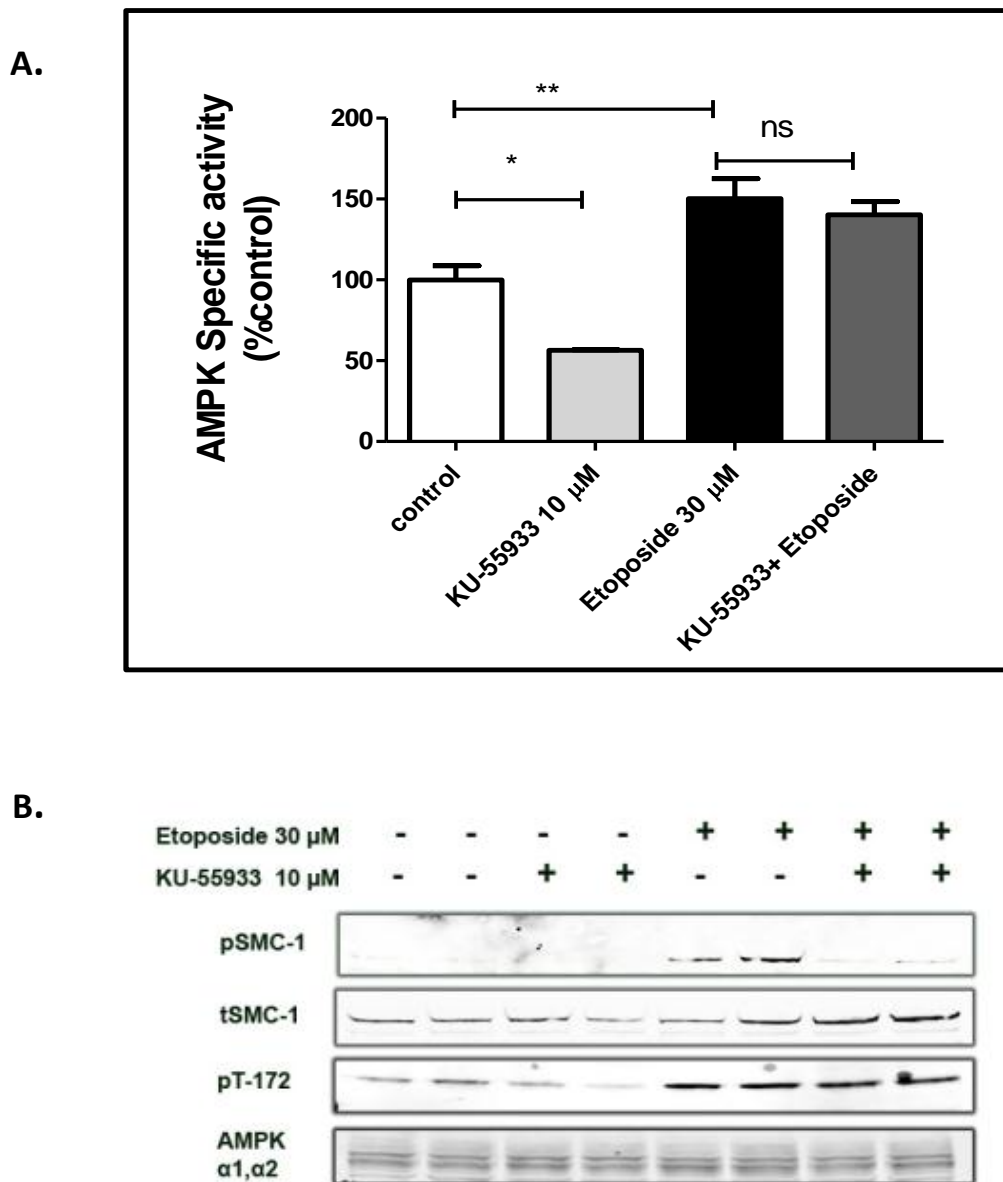
Figure 3.8: The ATM inhibitor KU-55933 reduces but does not abolish etoposide–induced AMPK activation

HeLa Cells were treated with 30 µM etoposide for 18 hours with or without 1hour pre-treatment with 10 µM KU-55933.

(A) Endogenous AMPK was immunoprecipitated from the cell lysate and AMPK activity measured using the AMARA peptide substrate. Results shown are mean ± SEM and are representative of three independent experiments done in triplicate (p<0.05-*, p<.001-**).

(B) Cell lysates from HeLa cells were immunoblotted with anti- AMPK α1 and α2, anti-pT-172 antibodies, anti- phospho SMC-1 and anti-SMC-1. The ATM inhibitor abolishes pSMC-1 signal but does not affect the phosphorylation of AMPK.

3.3.4 Etoposide-induced AMPK activation occurs in the nucleus

A surprising observation was that etoposide-induced activation of AMPK was not accompanied by a concomitant increase in its downstream substrate Acetyl CoA Carboxylase (ACC). ACC phosphorylation on Ser-79 is usually obvious when AMPK is activated and has been used as a marker for AMPK activation in several well published studies. ACC is a cytoplasmic protein. This led us to consider whether AMPK was being selectively activated in the nucleus, which is the primary site of DNA damage. To examine this, immunofluorescence microscopy was used to localise the site of AMPK activation. HeLa cells were grown on coverslips in 6 well dishes, treated with etoposide, fixed and stained with phospho-specific antibodies against Thr-172 on AMPK and Ser-1981 on ATM, the auto-phosphorylation site on ATM, which becomes phosphorylated in response to double strand DNA breaks. These were then probed with fluorescent secondary antibody and imaged. DAPI was used to stain the nucleus.

The specificity of the commercially available anti-pT-172 AMPK antibody for immunohistochemistry was tested using Wild type (WT) and AMPK-α1, -α2 Knock-out MEFs. The cells were treated with control or various AMPK activators such as A-769662 (direct activator of AMPK), berberine and A23187 (Figure 3.9). WT MEFs showed increased signal following treatment with AMPK activators compared to the control (Figure 3.9), while the KO cells did not show any signal either in the control cells or the cells treated with AMPK activators (Figure 3.10). Thus the specificity of the antibody was validated. It was also interesting to note that A23187 caused an increase in nuclear signal for AMPK phosphorylated on Thr-172 in the WT MEFs compared to A-769662 which caused a diffuse, less intense increase in fluorescence.
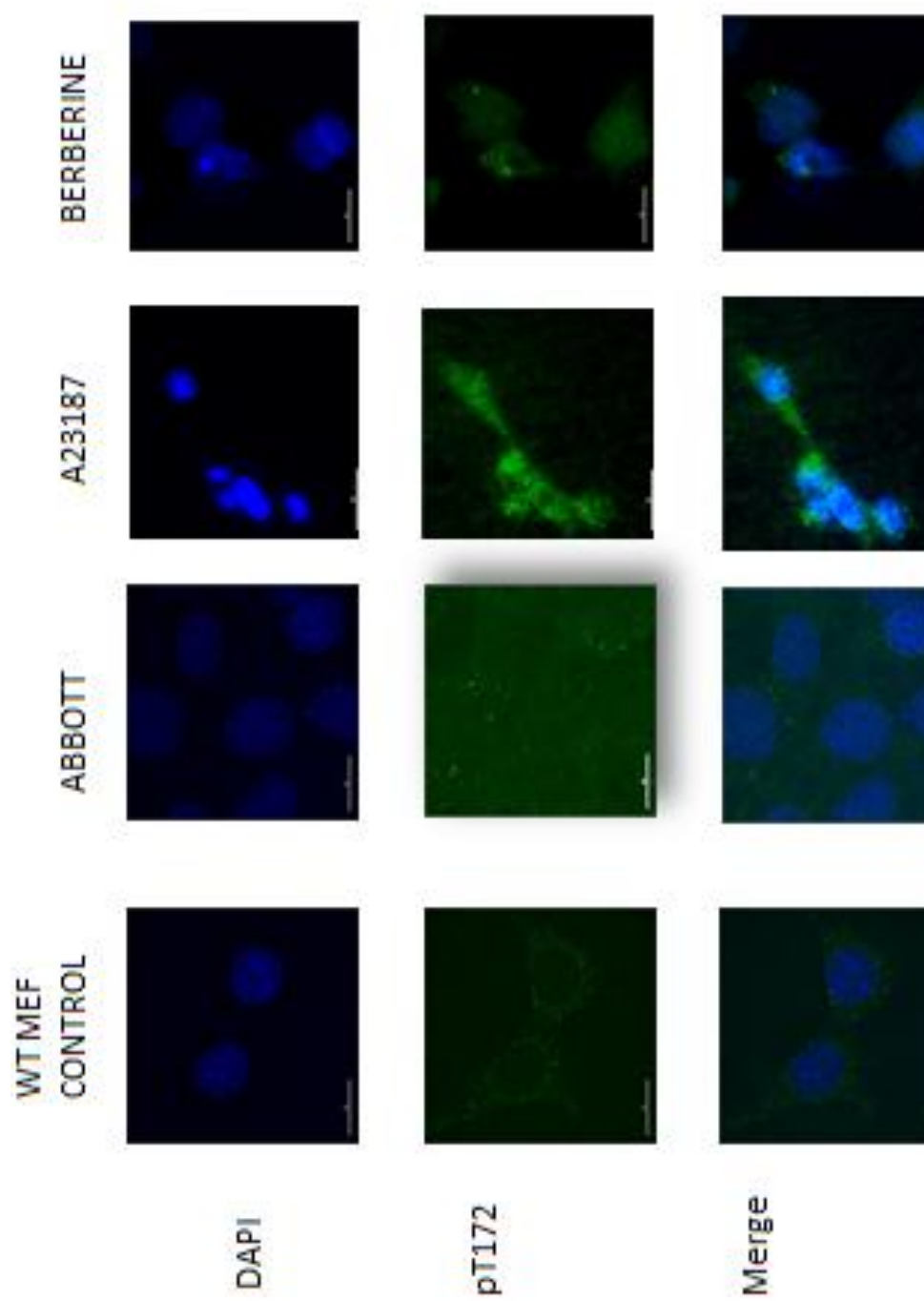
Figure 3.9: Validation of the anti-phospho Thr-172 AMPK antibody in WT MEFs.

AMPK α1, α2 WT MEFs grown on coverslips were treated with control or AMPK activators (A-769662 300 μM, Berberine 20 μM and A23187 10 μM for 1hour. The cells were fixed, permeabilised and stained with anti-pT172 AMPK antibody followed by a secondary FITC (green) antibody. DAPI was used as a nuclear stain. The results shown are representative of three independent experiments done in triplicate.
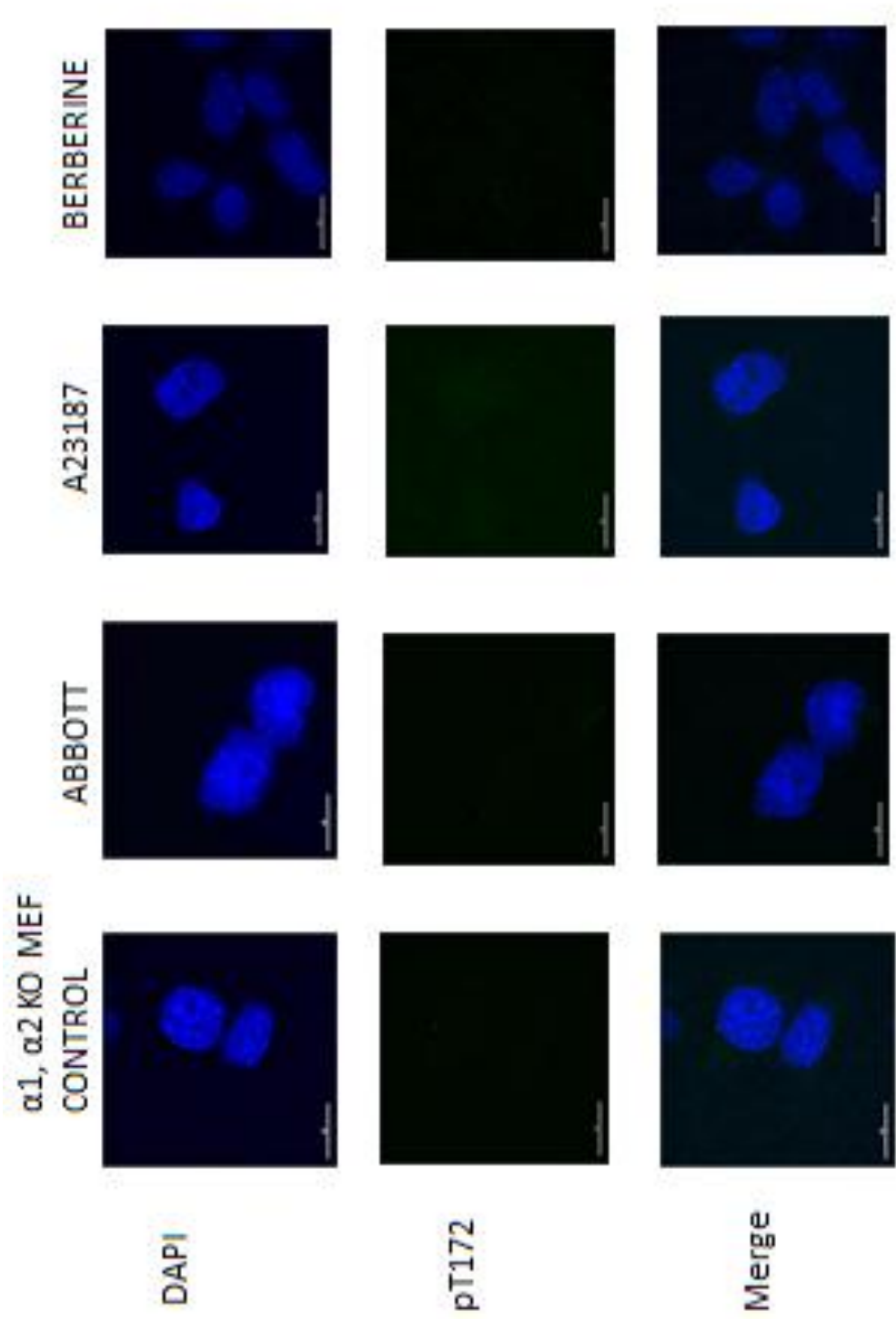
Figure 3.10: Validation of the anti-phosphoThr-172 AMPK antibody in AMPK α1, α2 KO MEFs.

AMPK α1, α2 knock-out MEFs grown on coverslips were treated with control or AMPK activators (A-769662 300 μM, Berberine 20 μM and A23187 10 μM for 1hour. The cells were fixed, permeabilised and stained with anti-pT172 AMPK antibody followed by a secondary FITC (green) antibody. DAPI was used as a nuclear stain. The results shown are representative of three independent experiments done in triplicate.

Once the anti-phosphoThr-172 AMPK antibody had been validated, we then performed the same staining on HeLa cells treated with control (DMSO) or etoposide. Cells were also stained for anti-phosphoSer-1981 on ATM to see whether AMPK was activated in the nucleus and if so, whether the pT-172 signal co-localised to sites of ATM activation. Robust nuclear activation of AMPK was seen following etoposide treatment in G361 cells (Figure 3.11 A and B) and Hela cells (Figure 3.11 C and D) when stained with the anti pT-172 phospho antibody alone.

Double staining with anti-pT-172 AMPK antibody and anti-pS-1981 ATM antibody showed that while both kinases were activated in the nucleus, they co-localised only partially (Figure 3.12). Nuclear and cytoplasmic fractionation was performed to try and further confirm this observation by two different methods. As most of the protocols involve osmotic stress followed by disruption of cell membranes, the basal activity levels of AMPK were greatly elevated following fractionation and meaningful comparison could not be made between the nuclear and cytoplasmic pools of AMPK between the control and etoposide treated cells (data not shown).

control   **etoposide 30 µM**

A.   B.

G361 cells

C.   D.
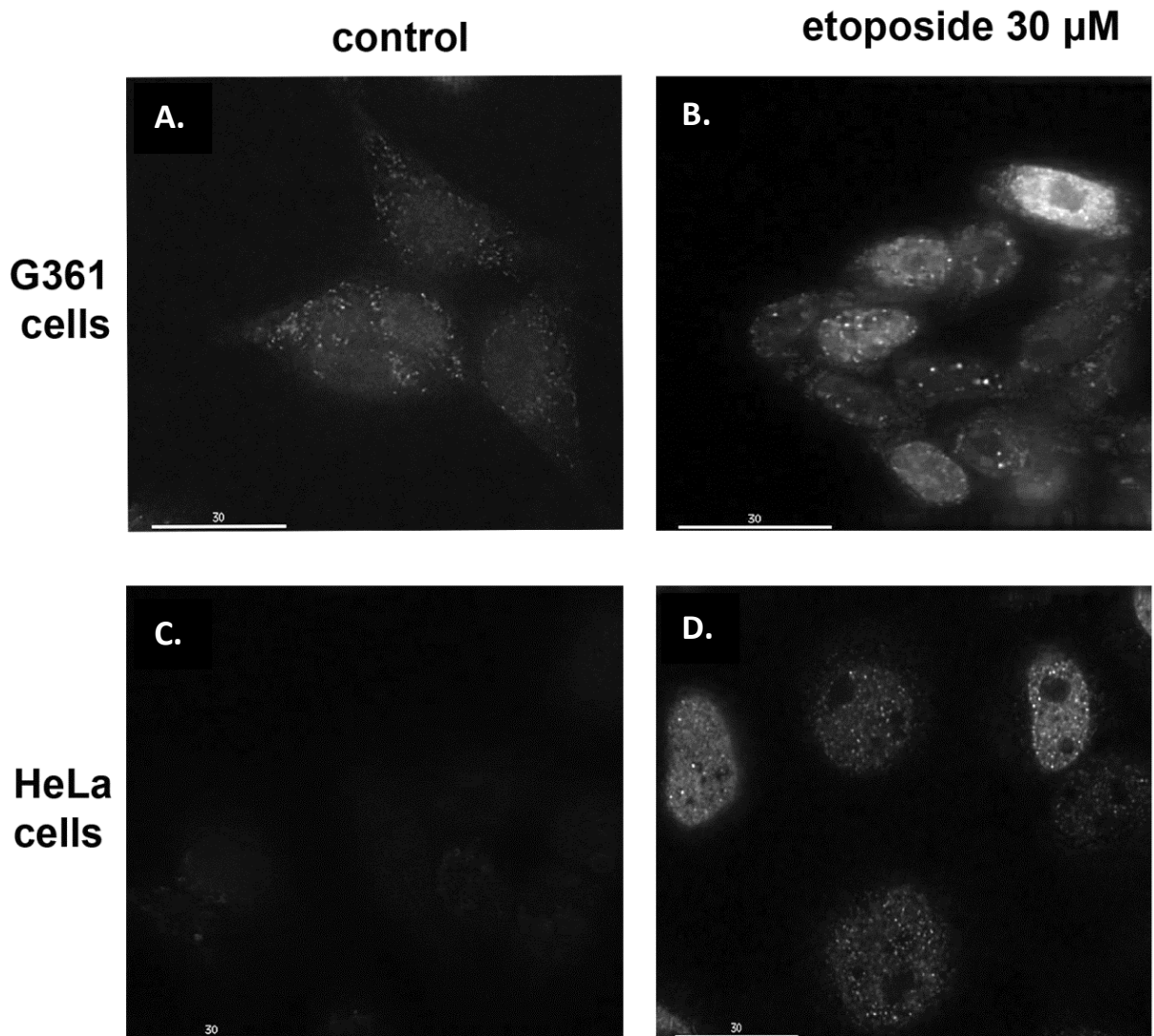
HeLa cells

Figure 3.11: Etoposide activates AMPK in the nucleus

G361 cells and HeLa cells were grown on glass slides in 6 well dishes and treated with DMSO (control) or etoposide 30 µM for 18 hours. The slides were then fixed with 4% paraformaldehyde, non-specific antibody binding blocked with fish skin gelatine and immuno-stained using the anti-pT-172 antibody and a FITC secondary antibody.

(A) G361 cells treated with DMSO
(B) G361 cells treated with etoposide
(C) HeLa cells treated with DMSO
(D) HeLa cells treated with etoposide.

The slides are representative and the experiment with G361 cells was performed twice in triplicate while the experiment in HeLa cells was repeated four times in triplicate.
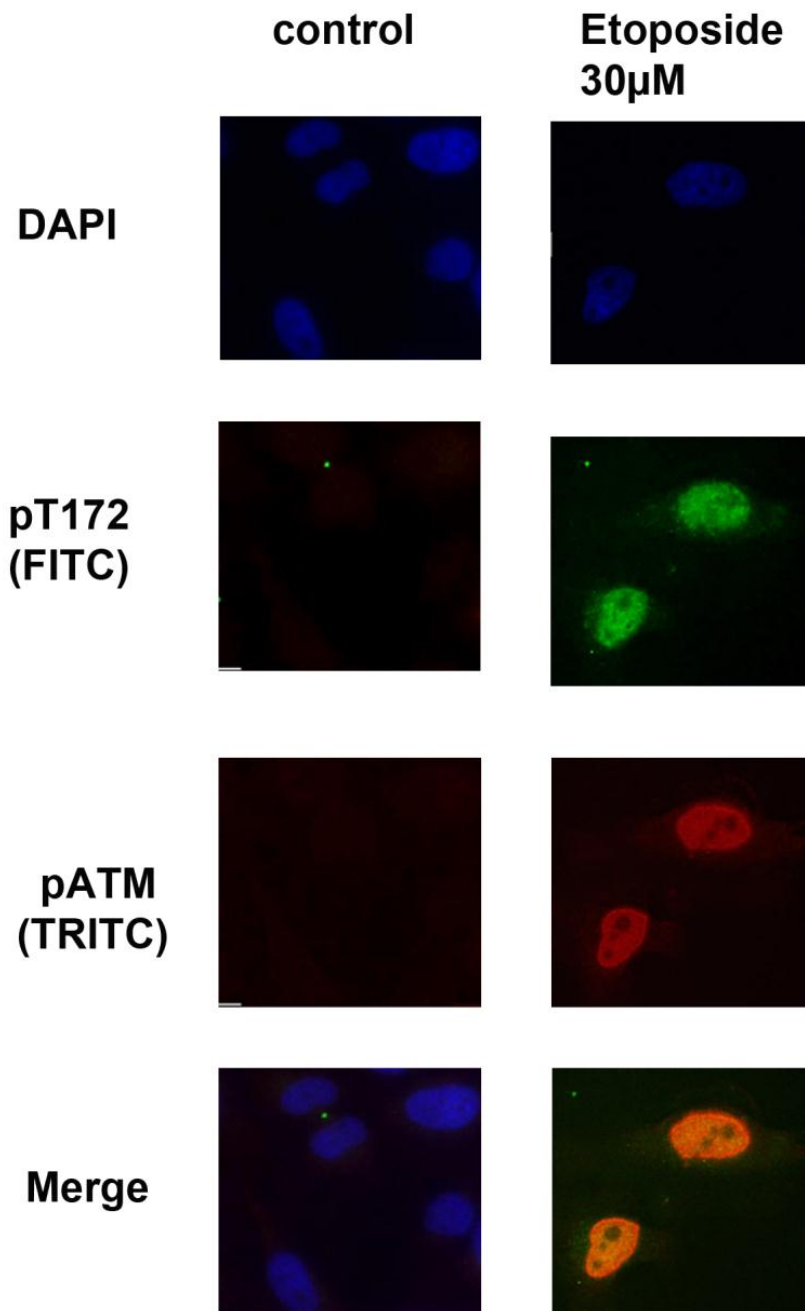
Figure 3.12: Activated AMPK partially co-localises with activated ATM in the nucleus

HeLa cells were grown on glass slides in 6 well dishes and treated with DMSO (control) or etoposide 30 µM for 18 hours. The slides were then fixed with 4% paraformaldehyde, non-specific antibody binding blocked with fish skin gelatine and immunostained using the anti-pT-172 antibody and a FITC secondary antibody and also the anti-pS-1981 ATM antibody and a fluorescent red secondary antibody. DAPI was used as the nuclear control. The first 3 rows show cells stained with DAPI, pT172 and pATM respectively. The bottom left panel shows a merged picture) with all three channels while the bottom   right panel shows the green and red fluorescence merged.

3.3.5 Etoposide treatment leads to an increase in intra-nuclear calcium in HeLa cells

The selective nuclear activation of AMPKα1 in response to etoposide was a new observation not reported previously with other agents. In order to explain the mechanism underlying this effect, nuclear calcium flux was measured using a pseudo ratiometric dye, Fluo-4AM. This dye binds calcium and increase in fluorescence intensity is used to measure increase in calcium within the cell (Gee et al., 2000). We observed an increase in nuclear calcium levels which was started around 3 hours and was maximal around 6-8 hours (Figure 3.13 A). This corresponds to when AMPK activation is first detected by immunoprecipitate kinase assays (Figure 3.13 B). This suggests that etoposide increases calcium ion concentration in the nucleus which then causes AMPK activation through activation of CaMKK-β.
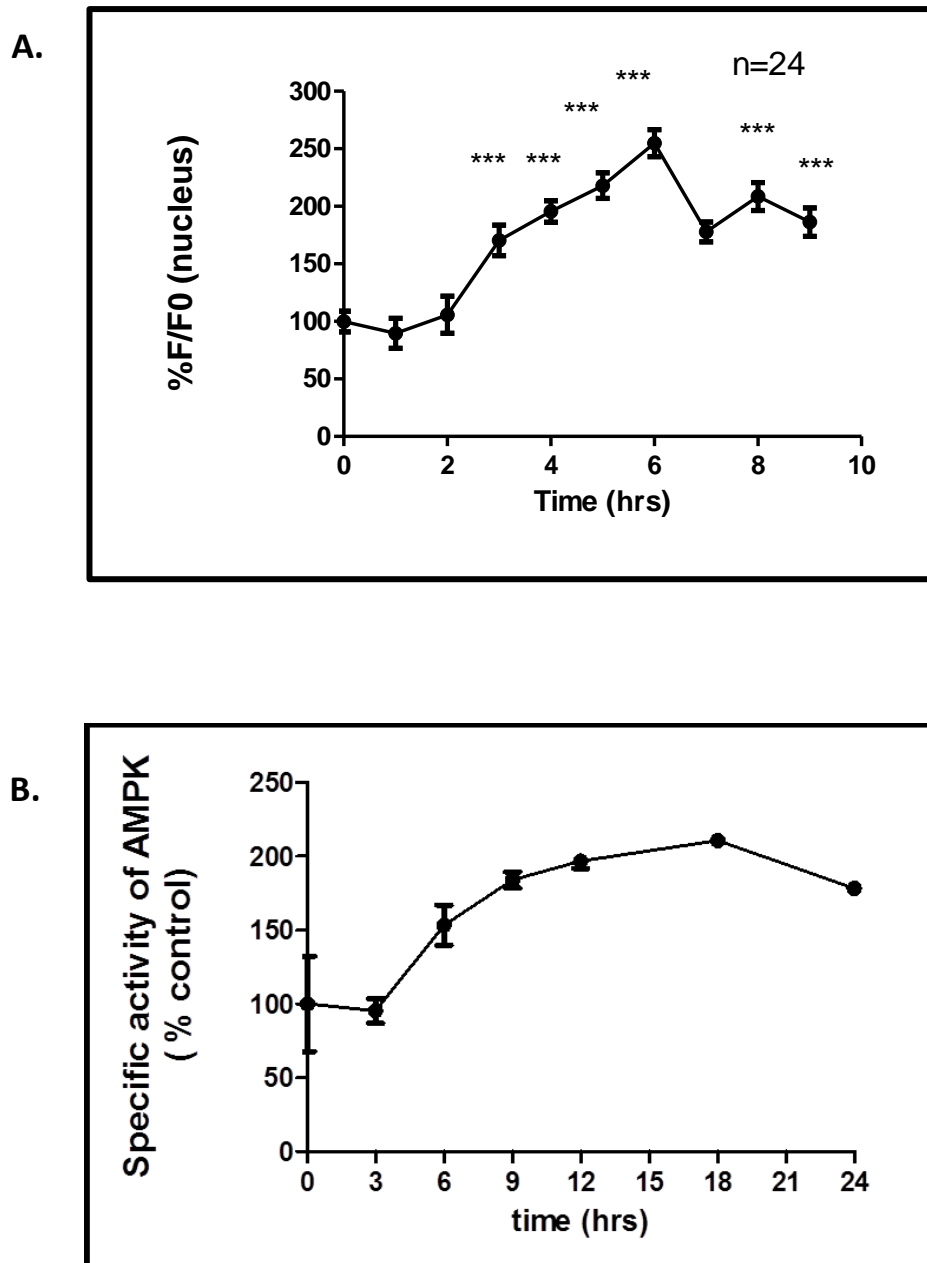
Figure 3.13: Etoposide treatment causes an increase in calcium flux which correlates with AMPK activation.

(A)   HeLa cells were loaded with the pseudo-ratiometric calcium-sensitive dye, Fluo-4 AM and the response to etoposide was measured in live cells using confocal microscopy. The nuclear fluorescence was expressed as a ratio of fluorescence intensity at a given time against the fluorescence intensity at time 0. One-way ANOVA was used to determine statistical significance ($p < 0.001$-***).

(B)   In parallel with the live imaging, HeLa cells treated with etoposide were harvested at different time points and immunoprecipitate kinase assays were performed on the lysates.

3.3.6 Activation of AMPK by A23187 affects cell survival in response to etoposide

In order to study the role of AMPK in genotoxic stress, clonogenic cell survival assays were carried out in MEF cells which were either WT for AMPK or lacked both AMPK $\alpha 1$ and $\alpha 2$. Cells grown in flasks were pre-treated with 300 nM calcium ionophore A23187. A lower concentration of A23187 was used as the total treatment duration was 24 hours. Two hours after pre-treatment, increasing concentrations of etoposide was added to the flasks in duplicate and incubated the cells for 24 hours. All flasks were trypsinised in the same volume of trypsin, the cells in the control flasks were counted and 5000 cells were seeded in triplicate into 10cm dishes. On the assumption that the agents had no effect, the other flasks would have the same number of cells. So the same volume of cells seeded in the control plates was aspirated from the trypsinised flasks and seeded into 10 cm dishes in triplicate. The assay was then performed as detailed in the methods section (2.2.25) and the results shown in Figure 3.14. WT MEFS had an IC_{50} of 39 nM etoposide while AMPK KO MEFs had an IC_{50} of 104nM (Figure 3.14 B). When pre-treated with A23187, survival in WT MEFs showed a five- fold increase (Figure 3.14 C), while AMPK KO MEFs did not show any increase in cell survival (Figure 3.14 D). This effect of AMPK activation on cell survival was not observed when other AMPK activators such as A-769662 were used (data not shown).
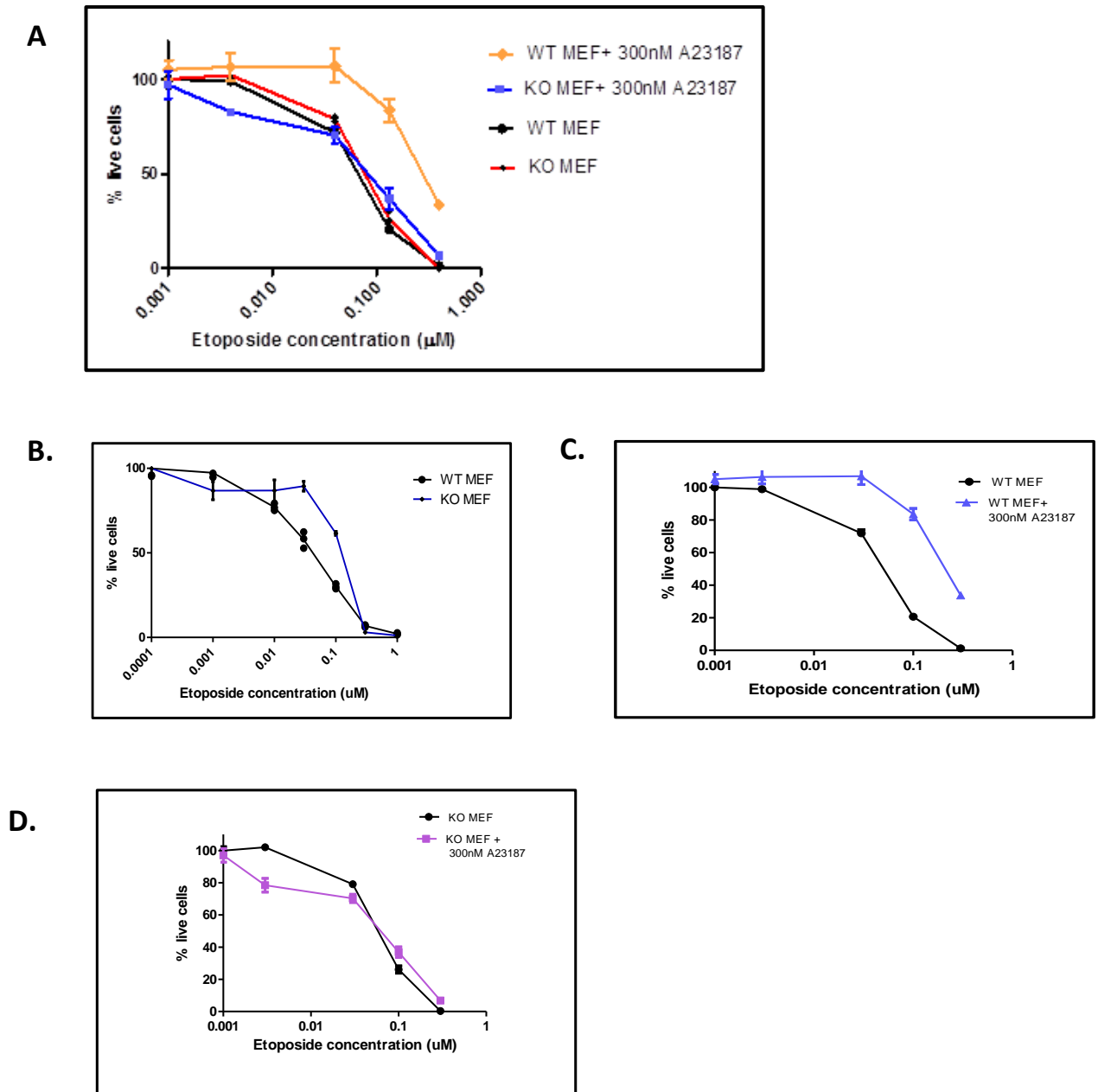
Figure 3.14: A23187 increases cell survival following etoposide treatment by activation of AMPK

Clonogenic cell survival assays were performed using wildtype (WT) and AMPKα1, α2 KO MEFS. The results were shown as a percentage of the number of colonies in the untreated controls. These results are representative of three experiments performed.

(A) WT and AMPKα1, α2 KO MEFS were treated with increasing concentrations of etoposide ± 300nM A23187.
(B) WT and AMPKα1, α2 KO MEFS were treated with increasing concentrations of etoposide.
(C) WT MEFs show increased survival when pre-treated with A23187 (re-plotted from Figure A).
(D) AMPKα1, α2 KO MEFS do not show increased survival when pre-treated with A23187 (re-plotted from Figure A).

3.3.7 A23187 increases cell survival by causing a cell cycle arrest

The selective increase in cell survival in cells pre-treated with A23187 before etoposide treatment suggests that the Ca^{2+}/ CaMKKβ- AMPK pathway activation protects against genotoxic stress. We know that cells are most vulnerable to genotoxic agents in the S phase and that DSB repair requires the cell to undergo cell cycle arrest. Previous data from our lab has shown that overexpression of constitutively active CaMKK-β or treatment of HeLa and G361 cells with A23187 causes a G1 arrest (Fogarty 2008 PhD thesis). The possibility that AMPK activation modulates the cell cycle in order to favour cell survival was therefore tested in G361 cells. These cells were first synchronised in G0/G1 by starving the cells of serum and L-glutamine overnight and then released into complete media with either control, etoposide, A23187 or both agents. The results are summarised in Figure 3.15 A. Serum and L-glutamine starvation led to nearly 80% of cells being synchronised to G0/G1 phase. Cells released into complete media rapidly progressed through the cell cycle. Treatment with A23187 leads to arrest of the cell cycle in G0/G1. Etoposide caused S-phase cell cycle arrest, while by pre-treatment with A23187 prevented this, with the cells arresting in the G0/G1 phase. These cells also showed increase in survival following etoposide treatment when pre-treated with A23187 (Figure 3.15 B). Thus A23187 may protect cells from irreversible S phase arrest leading to cell death, and in turn leads to increased cell survival.

A.

B.
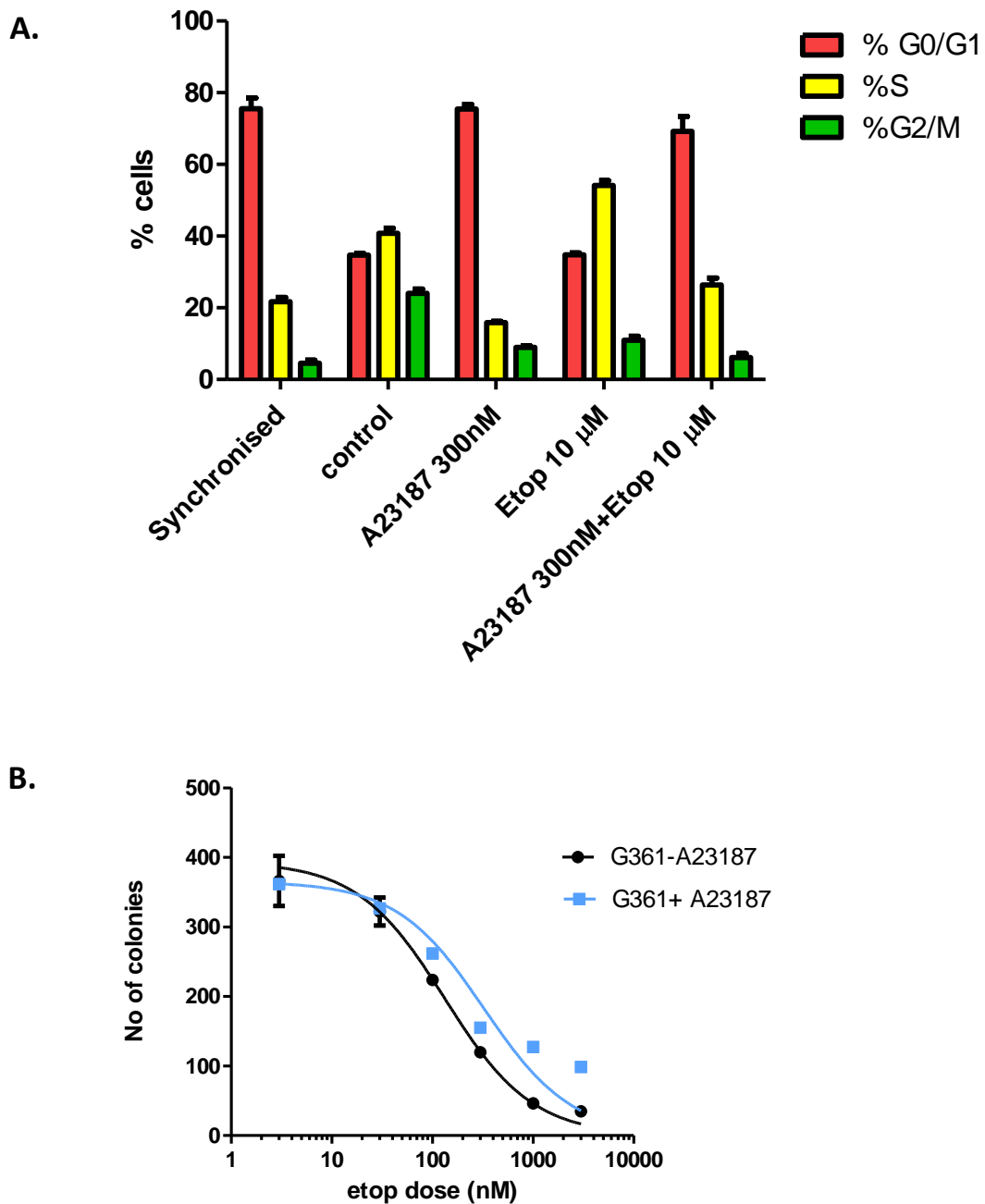
Figure3.15: A23187 causes a G1 cell cycle arrest and increases cell survival in G361 cells

(A)   G361 cells were synchronised in G0/G1 by serum and L-glutamine deprivation before being released into DMSO (control), A23187, etoposide or both. Cells were treated for 18 hours. Cell cycle analysis was performed in triplicate and the results shown are representative of three different experiments.

(B)   G361 cells were pre-treated with DMSO (control) or 300 nM A23187 2 hours before treatment with increasing concentrations of etoposide. Clonogenic cell survival assays were performed in triplicate. The results are representative of three individual experiments

3.4 DISCUSSION

Activation of AMPK in HeLa cells and G361 cells, which lack LKB1, demonstrates that etoposide-induced AMPK activation in these cells is an LKB1-independent process. This is consistent with the observations made by Fu et al that in HeLa cells, etoposide increases Thr-172 phosphorylation (Fu, 2008). Hela cells and G361 cells have very low basal AMPK activity as they lack the main upstream kinase LKB1.This may be the reason why a relatively modest increase in AMPK activation by etoposide was seen as a greater-fold change in HeLa cells and G361 cells. Also, HEK 293 cells and H4IIe cells have twenty times higher basal AMPK activity than HeLa cells and it is possible that this small increase in LKB1-independent AMPK activity caused by etoposide might have been missed in these cell lines . Interestingly, etoposide causes an increase in AMPK activity in mouse embryonic fibroblasts which have basal AMPK activity which is higher than that of HeLa cells, but is much lower than that of HEK 293 cells. Also the MEFs showed increased AMPK activity at a lower dose (20 µM) of etoposide than that required in HeLa cells (30 µM) and AMPK activation was apparent two hours after treatment compared to HeLa cells where the AMPK activation was measurable from around 6 hours after treatment.

CaMKK-β is the upstream kinase activating AMPK in HeLa cells (Hawley et al., 2005) and the requirement for CaMKK-β in increasing AMPK activity in response to etoposide was tested by two approaches, one involved pre-treatment of cells with the CaMKK inhibitor STO-609 and the second, silencing CaMKK-β expression using siRNA . Pharmacological inhibition of CaMKK-β by STO-609 causes a significant reduction in etoposide- induced AMPK activation. Knock-down of CaMKK-β by siRNA-mediated silencing completely abolishes AMPK-activation in response to

etoposide treatment. These results confirm that etoposide-induced AMPK activation is CaMKK-β-dependent.

The finding that phospho-ACC levels were not increased despite a two-three fold increase in AMPK activity was very interesting. ACC is a known substrate of AMPK, often used as a marker of AMPK activation. It is largely cytosolic in its localisation. DNA damage occurs in the nucleus and the mitochondria. Immunofluorescence microscopy was used to examine the subcellular localisation of AMPK. The anti-pT-172 antibody was first validated for immunocytochemistry using mouse embryonic fibroblasts expressing wild type AMPK and MEFs that lack AMPK-α1and -α2. Agents such as A-769662, a direct activator of AMPK caused a diffuse less intense fluorescence throughout the cytoplasm. The Ca^{2+} ionophore A23187 caused a more intense nuclear staining in addition to cytoplasmic staining. Following etoposide treatment in Hela and G361 cells, AMPK appeared to be activated mainly in the nucleus. Attempts to fractionate nuclear AMPK from cells has so far proven difficult as these methods rely on osmotic stress, which in itself activates AMPK, making it hard to meaningfully compare cytosolic and nuclear activity of AMPK, especially with the modest increases seen in AMPK activation in the whole cell lysates of cells treated with etoposide.

Fu et al have previously reported that etoposide-induced mitochondria biogenesis involved AMPK activation and that this process was ATM-dependent. However, the authors used siRNA mediated knock-down of ATM in HeLa cells to demonstrate loss of etoposide–induced AMPK activity. It is possible, that there might have been an off- target effect of the siRNA on either AMPK or CaMKK-β which may have caused this effect. While the authors of this paper had employed ATM+ and ATM-cells to look at mitochondrial biogenesis, AMPK activation in response to etoposide

was only seen in ATM+ cells. However, ATM- cells seemed to have several higher fold basal pT-172 signal on western blotting, which was not further increased by etoposide. Moreover, in the same paper, the authors have used AICAR and hydrogen peroxide to activate AMPK to demonstrate increased mitochondrial biogenesis and compound C, a rather non-specific inhibitor, which also inhibits AMPK, to show a reduction in ATM-dependent mitochondrial biogenesis. AICAR is converted to ZMP, which is an AMP analogue within cells and activates AMPK. The results detailed in this chapter clearly show that etoposide-induced AMPK activation is CaMKK-β-dependent and accompanied by change in intra-nuclear calcium levels.

Also, nuclear and cytoplasmic ATM activation may have different effects. The paper by Alexander et al suggests that ATM activation following oxidative stress induced by hydrogen peroxide, activates AMPK via an LKB1-dependent mechanism which is confined to the cytosol and is accompanied by increase in phospho-ACC (Alexander et al., 2010). The paper by Fu et al also showed that hydrogen peroxide treatment activated ATM and AMPK in HeLa cells and this was accompanied by increase in pACC levels. The immunohistochemistry data in this chapter clearly shows that etoposide-induced AMPK activation is limited to the nucleus and western blotting supports the nuclear localisation of activated AMPK by the lack of concomitant ACC phosphorylation. Moreover, activated AMPK did not co-localise completely with activated ATM. It has previously been shown that AMPK-α2 is the main nuclear isoform of AMPK (Salt et al., 1998). However, the data shows that only AMPK-α1 is activated by etoposide treatment. Western blotting shows no activation of AMPK-α2, although there is no detectable basal phosphorylation, either in the vehicle or etoposide treated cells. This was a very interesting result and is consistent with previous observations obtained with muscle-specific knockout (LKB1$^{fl/fl}$Cre$^{+/-}$) mice, in which AMPK-α1activity in muscle

under basal and AICAR stimulated conditions was undiminished compared to the

LKB1$^{fl/fl}$Cre$^{-/-}$ controls (Sakamoto et al., 2005). In contrast, basal and AICAR-

stimulated AMPK-α2 activity was markedly reduced in muscle-specific LKB1 knockout

compared to the LKB1$^{fl/fl}$ Cre$^{-/-}$ controls (Sakamoto et al., 2005).

Also in HeLa cells, the selective ATM inhibitor KU-55933 inhibited ATM

activation, as evidenced by a reduction in phosphoSMC-1 on Western blotting but did

not significantly reduce etoposide-induced AMPK activation. Conversely, treatment

with etoposide following CaMKK-β inhibition with STO-609 or reduction in CaMKK-β

levels by siRNA-mediated silencing caused loss of AMPK phosphorylation despite

increase in pSMC-1 levels. Thus, the data from this chapter suggests that DSB-induced

nuclear AMPK activation is not dependent on ATM activation. This is further supported

by the fact that neither CaMKK-β nor the catalytic α1 and α2 subunits of AMPK

contain the SQ/TQ motif which is an absolute requirement for phosphorylation by ATM

(Matsuoka et al., 2007).

The results from this chapter show that activation of AMPK by the calcium

ionophore A23187 increases cell survival in response to etoposide treatment. This effect

of increased cell survival is AMPK-dependent as it is not seen in AMPK-KO MEFs. It

has previously been reported that activation of the CaMKKβ-AMPK pathway by the

calcium ionophore A23187 causes a G1 cell cycle arrest in G361 cells (Fogarty 2008

PhD thesis). In these cells, etoposide causes an S phase arrest. A23187 may therefore,

protect cells from S phase arrest caused by etoposide. Moreover, arrest in G1 may allow

for DNA repair by non-homologous end-joining to occur, thereby increasing cell

survival. This mechanism of increased cell survival in response to DNA damaging

drugs has been reported with pre-treatment with other cell cycle inhibitors, particularly

CDK inhibitors such as flavopiridol, roscovitine and olomoucine (Cernak et al., 2005).

Flavopiridol and roscovitine cause a G1 arrest and increase cell survival in response to etoposide and doxorubicin (Di Giovanni et al., 2005, Crescenzi et al., 2005). The findings with A23187 suggest that activation of the CaMKKβ-AMPK pathway may enhance survival in tumour cells treated with etoposide. Conversely, it may be possible to selectively target tumour cells that have lost AMPK using drugs like etoposide and protect normal cells by using an AMPK activator. Given that metformin is now widely used in combination with chemotherapy which may involve DNA damaging drugs, further work in this area is warranted to ensure that beneficial effects alone are conferred to patients treated with these drugs.

CHAPTER FOUR: AMPK IS A TUMOUR SUPPRESSOR IN A T CELL-SPECIFIC PTEN KNOCKOUT TUMOUR MODEL

4.1 INTRODUCTION

4.1.1 The adaptive immune system

The immune system is composed of two main systems- the innate (or non-specific) and the adaptive (or specific) immune system. The adaptive immune system functions to prevent or eliminate growth of pathogens, including bacteria, viruses, fungi and parasites (Cooper and Alder, 2006). Elements of adaptive immunity are conserved throughout evolution; however, in jawed vertebrates and higher organisms, adaptive immunity is the cornerstone of the immune response (Danilova, 2012). The effectors of the adaptive immune response are highly specialised cells called lymphocytes, which have the ability to recognise and remember specific pathogens and to mount a stronger defence each time the pathogen is encountered. The two main types of lymphocyte are the T lymphocytes (T for thymus derived) and B lymphocytes (B for bursa or bone marrow derived), which effect cell-mediated and humoral immunity respectively. This introductory section focusses on the development, maturation and functions of T cells.

4.1.2 The thymus and its organogenesis in mice

The thymus is a bi-lobed organ located in the centre of the thoracic cavity in front of the heart and is the site of development of T cells(Osoba, 1966). The thymic anlage develops from the third pharyngeal pouch endoderm and surrounding neural crest cells

and lies adjacent to the developing parathyroid (Rodewald, 2008). At embryonic day 11.5, the pouch endoderm separates into the parathyroid and thymus-fated domains by the mutually exclusive expression of two transcription factors, *g*lial *m*issing *c*ells *h*omolog 2 (*gcm*2) and *f*orkhead *b*ox N1 (*foxn*1) (Ma et al., 2011 (epub ahead of print)). Around embryonic day 12, the thymus then undergoes differentiation, further separation from the parathyroid, it changes in morphology and migrates caudally into the thorax (Gordon et al., 2010). Along with the morphological changes of the whole organ, the cells within the thymus also undergo a series of developmental stages.

4.1.3 T cell development

T cells develop from haematopoetic stem cells which undergo a process of maturation and differentiation within the thymus. The hallmark of the T cell is the expression of the T cell receptor (TCR) (Hernandez et al., 2010). In order for a thymocyte to mature into a T lymphocyte, it has to undergo a series of maturational steps that have been summarised in the next section (Figure 4.1).
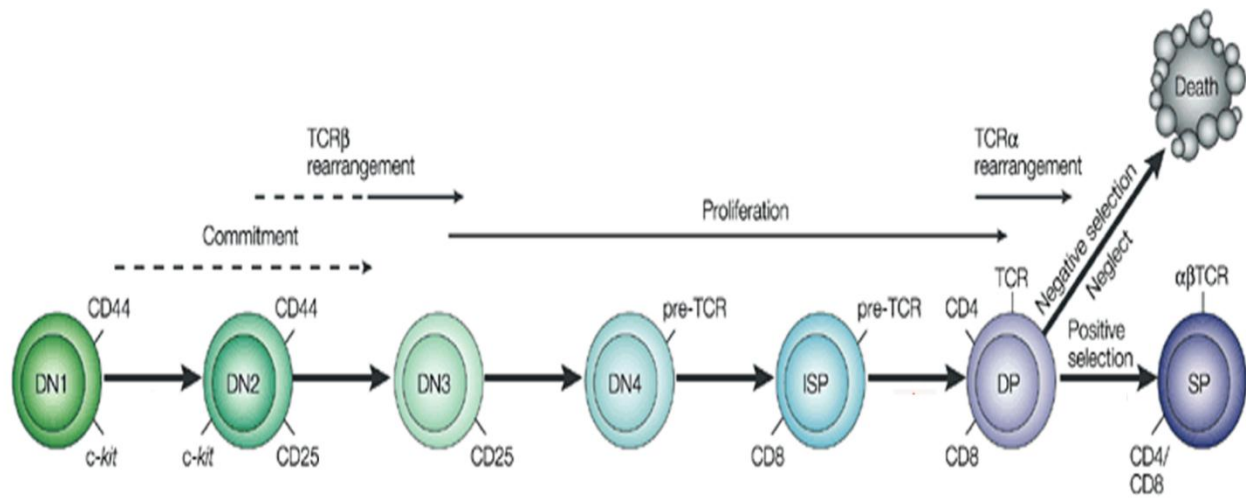
Figure 4.1: T cell development and differentiation

This schematic shows the development of T cells within the thymus from the double negative to the single positive stage. The immature thymocyte undergoes commitment to the T cell lineage, TCR rearrangement, and proliferation, positive and negative selection to form a single positive thymocyte. Adapted from (Engel and Murre, 2001).

4.1.3.1 T cell lineage commitment

Developing T cells in the thymus can be sub-divided into three main groups namely, double negative, double positive and single positive cells. T cell development begins with early thymocytes (also called thymic settling precursors), which enter the thymus from the bone marrow at the double negative (DN) stage (the term double negative indicates that the cells lack CD4 or CD8 receptors). The DN cells can be further sub-divided into 4 subsets, namely DN1, DN2, DN3 and DN4, based on the expression of CD117 (c-kit), CD44 and CD25 receptors (Godfrey et al., 1993). DN1 cells (CD117$^+$, CD44$^+$ and CD25$^-$) are not committed T cell precursors and can develop into other types of thymus-derived cells, such as B, T, dendritic and natural killer cells (Carlyle et al., 1997). Transition to DN2 occurs when cells start to express CD25 (DN2 cells are CD117$^+$, CD44$^+$ and CD25$^+$). The DN2 cells can give rise to T, dendritic and NK cells but lose the ability to give rise to B cells. Notch signalling is required for commitment of progenitor cells to the T cell lineage. Deletion of Notch1 leads to failure of T cell development with an accumulation of B cells (Radtke et al., 1999). Transition from the DN1 to DN2 stage is also accompanied by a series of events leading to a diverse TCR repertoire by V(D)J recombination of the four TCR receptor genes *Tcra*, *Tcrb*, *Tcrg* and *Tcrd* (Hernandez et al., 2010).

4.1.3.2. TCR rearrangement

V(D)J recombination is directed by RAG1 and RAG2 (*r*ecombination *a*ctivating *g*enes-1 and -2), which are lymphoid-specific recombinases that create double strand breaks at *r*ecombinant *s*ignal *s*equences (RSs) flanking the variable (V), diversity (D) and joining (J) segments of the TCR gene. These breaks are then repaired by non-

homologous end joining during which, the coding ends undergo nucleotide insertion or

deletion and the joining segments sometimes undergo inversion (Bassing et al., 2002).

This process leads to a large number of different TCR chains with the ability to

recognise a huge variety of antigens. Recombination of *Tcrb*, *Tcrg* and *Tcrd* occur in

the DN2 and DN3 (CD44$^-$ CD25$^+$) stages (Krangel, 2009). Recombination of *Tcrg* and

Tcrd results in expression of γδ TCR. Recombination of *Tcrb* with pre-Tα leads to

assembly of pre-TCR; this recombination is a pre-requisite for progression to the DN4

stage (CD44$^-$ CD25$^-$). When the β-chain is unable to pair with a pre-Tα chain, the cells

die; this process termed β-selection. Following β-selection, pre-TCR and Notch signals

cause down-regulation of recombinase expression followed by proliferation and

differentiation of thymocytes to the CD4$^+$CD8$^+$ double positive (DP) stage (Maillard et

al., 2006, Ciofani and Zúñiga-Pflücker, 2007). Signalling via the pre-TCR requires γ, ε,

and ζ chains of the CD3 complex and the Lck kinase (Von Boehmer et al., 1999).

4.1.3.3 Positive selection

Positive selection is initiated by TCR α-chain re-arrangement. This process

generates unique α-chains that pair up with the rearranged β-chain expressed on the cell

surface of a developing double positive cell. The re-arrangement of TCR-α chains

continues even after formation of an αβ heterodimer, thus ensuring that the same cell

expresses different α chains bound to the same β-chain, causing the expression of a

variety of αβ heterodimers on its surface (Borgulya et al., 1992). Formation of an

effective αβ heterodimer requires both the formation of a cell surface complex of the

two chains and the ability to recognise MHC-self antigen complexes presented by the

thymic epithelial cells, a process termed positive selection. The vast majority of

thymocytes that do not undergo positive selection die by neglect (almost 95%), while

those that do, stop further TCR α-chain re-arrangement by down-regulation of RAG-1

and RAG-2, developing into single positive (SP) cells (Borgulya et al., 1992). Two

models have been proposed for the development of single positive cells. The stochastic

model proposes that DP cells randomly commit to either CD4 or CD8 lineage, whereas,

the instructive model proposes that cells that express TCR with specificity for the Class

I MHC are biased towards developing into CD8^{+} T cells while those with specificity for

the Class II MHC are biased towards developing into CD4^{+} cells (Boehmer, 1986).

4.1.3.4 Negative selection

While positive selection ensures that the TCR is likely to recognise antigens

presented on MHC, negative selection (also known as clonal deletion) is essential to

prevent autoimmunity and eliminate self-reactive cells (Sant'angelo and Janeway,

2002). During negative selection, thymocytes migrate to the medulla where they come

into contact with medullary dendritic cells. Cells which express high avidity self-

reacting TCR against self- antigen interact with the self-antigen−self-MHC complex on

the dendritic cells (Sant'angelo and Janeway, 2002). This slows their migration,

allowing them to make prolonged contact with the DCs, after which they undergo

apoptosis (Le Borgne et al., 2009). Some self-reactive T cells escape negative selection

and undergo peripheral functional inactivation, a process also termed anergy

(Pacholczyk and Kern, 2008). Single positive cells that have survived negative selection

exit the thymus and await activation. Emigration requires recognition of the lipid

molecule sphingosine-1-phosphate (S1P) by the G-protein coupled receptor SIP_1, which

is expressed by the thymocytes in the final maturational stage. Blood and lymph have

high levels of SIP, drawing the lymphocytes expressing SIP_1 away from the thymus (Murphy, 2012). Mature thymocytes also express CD62L (L-selectin), a lymph node homing receptor that facilitates movement of mature naïve T cells to lymphoid organs (Murphy, 2012). These recent thymic emigrants (RTEs) are still immature compared to their more mature, yet naïve peripheral counterparts and further maturation of T cells occurs in the peripheral tissues (Fink and Hendricks, 2011).

4.1.4 T cell activation

T cells exit the thymus via the medullary vessels and circulate in the blood and lymphatics. In the spleen and lymph nodes, they come into contact with antigen presenting cells (APC) bearing processed foreign antigens as small peptides in the groove between the α1-α2 domains of the MHC Class I and α1-β1 domains of MHC Class II complexes (Greer John P et al., 2004). The αβ-TCR:CD3 complex recognises these short peptides on the MHC and this interaction of the TCR-MHC is accompanied by other interactions which strengthen adhesion, for example, the integrin LFA-1 (leukocyte function antigen 1) binds ICAM-1 (intercellular adhesion molecule 1) on the APC. Co-stimulatory interactions occur between CD28 on T cells and B7 on APC. This interaction between the two cells, primarily the TCR:MHC, initiates signal transduction and transcription of genes encoding cytokines in $CD4^+$ T cells and components of cellular lysis in $CD8^+$ T cells (Guy and Vignali, 2009).

Naïve T cells are small cells with scanty cytoplasm and synthesise little RNA or protein. On activation, they re-enter the cell cycle and divide rapidly into progeny that then differentiate into different subsets of effector cells. Activated T cells produce IL-2, which further stimulates their proliferation and differentiation (Murphy, 2012). T cells

are activated by three signals which lead to their clonal expansion and differentiation. The first signal is TCR:MHC binding, which activates the naïve T cell (Murphy, 2012). The second involves co-stimulatory signals, such as interaction of CD28 and CD80 and this promotes survival and clonal expansion of T cells (Jones and Thompson, 2007). The third signal is involved in directing T cell differentiation into subsets of effector T cells and involves the release of cytokines and growth factors by the APC.

The TCR relies on accessory proteins, such as CD3-γ,-ε,-δ and TCRζ. TCR initiates signalling by recruiting and activating protein tyrosine kinases (PTKs) of the Src, Syk and Tec families (Cantrell, 2002). The Src family PTK, Lck, phosphorylates the *i*mmunoreceptor *t*yrosine-based *a*ctivation *m*otifs (ITAM) on CD3, allowing ZAP-70 a Syk family PTK to bind to ITAMs via its SH2 (Src homology-2) domain. ITAM bound to ZAP-70 is then tyrosine phosphorylated by Lck, leading to its activation and subsequent phosphorylation of its downstream targets, SLP-76 (SH2 domain containing leukocyte protein of 76 KDa) and LAT (Linker for activation of T-cells). The tyrosine phosphatase CD45 antagonises TCR signalling (Cantrell, 2002). However, once TCR has bound to MHC, the large extracellular domain of CD45 excludes it from the proximity of the TCR:MHC complex.

SLP-76 and LAT function as scaffolds that assist the recruitment of additional PTK and scaffold proteins (Figure 4.2). Tyrosine phosphorylated motifs in the C-terminal tail of LAT bind to Grb2 (Growth factor receptor-bound protein 2) and its close relative Gads (Grb2-related adaptor downstream of SHc) (Zhang et al., 1998). This interaction recruits and localises Grb2-associated proteins such as SOS (named after Drosophila 's*on *o*f *s*evenless' protein) which functions as a guanine nucleotide exchange protein (GEF) for Ras. Tyrosine-phosphorylated LAT also interacts with the SH2 domain of phospholipase Cγ1 (PLCγ1), recruiting it to the plasma membrane

(Cantrell, 2002). TCR activation of PLCγ1 causes hydrolysis of phosphatidylinositol (4, 5) -bisphosphate [PtdIns (4,5) P2] and the production of inositol 1, 4, 5- trisphosphate which leads to release of intracellular calcium. PtdIns (4,5) P_2 breakdown generates the second messenger diacyl glycerol (DAG), which binds to specific domains of signalling proteins such as protein the kinase C family, protein kinase D and the Ras-GEF, GRP (Cantrell, 2002).

SLP-76 also binds to LAT via adapters such as Gads and Grf40 (Liu et al., 1999). SLP-76 has its own SH2 domain and helps recruit the protein Vav to the antigen-receptor complex. Vav proteins serve as GEFs for Rac1, Rac2 and RhoG in T cells, and also function as scaffolding proteins which contain SH2 and SH3 domains and undergo tyrosine phosphorylation following TCR activation (Tybulewicz, 2005). Vav1, one of three Vav isoforms, is essential for T cell development. Peripheral CD8$^+$ cells that lack Vav1 show no proliferation following antigen-receptor stimulation (Penninger et al., 1999, Gulbranson-Judge et al., 1999). SLP-76-mediated recruitment of proteins such as WASp (Wiskott- Aldrich Syndrome protein) via the adaptor Nck helps drive actin cytoskeletal rearrangement following TCR activation, leading to polarisation of the T cell towards the APC following the formation of the immunological synapse (Tybulewicz, 2005).
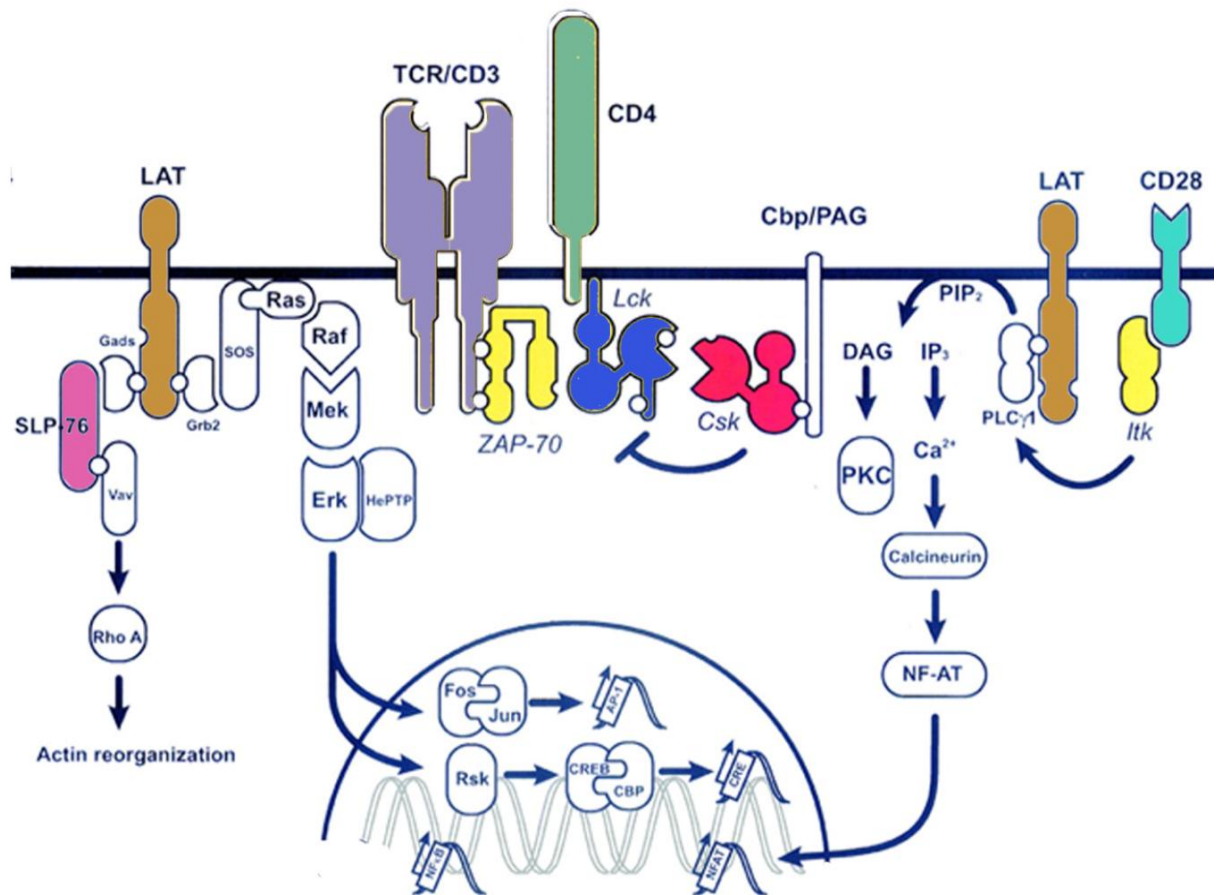
Figure 4.2: Signalling pathways downstream of TCR

This schematic shows the main downstream signalling events which occur following T cell activation. The αβTCR pairs with CD3 accessory chains and TCRζ which contain ITAM motifs. Lck phosphorylates the ITAM motifs which recruits ZAP-70. Once phosphorylated by Lck, ZAP-70 phosphorylates LAT and the SLP-76 complex. SLP-76 and ZAP-70 recruit and activate signalling molecules, leading to the activation of several pathways, including MAPK signalling, PtdIns (3, 4, 5) P3 signalling, calcium signalling and actin reorganisation. Adapted from (Mustelin and Taskén, 2003)

4.1.5. T cell sub-populations

Activation of the T cell response leads to the generation of effector and memory T cells. Several different subsets of effector T cells exist, each playing different roles in the immune system. Some of them are listed below. Apart from the γδ T cells, all other subsets express αβ TCR.

4.1.5.1 CD8⁺ cytotoxic T cells

Naïve CD8$^+$ T cells differentiate into CD8 cytotoxic T lymphocytes which kill their target cells, especially those that have been infected by viruses. Virus-infected cells display viral peptide on MHC Class I complexes, which are recognised by the CD8$^+$ T cells, triggering their proliferation into cytotoxic T lymphocytes (CTLs). Perhaps due to their destructive nature, naïve CD8 T cells require more co-stimulation to drive them to become activated CTLs than naïve CD4 T cells (Murphy, 2012). In some viral infections, mature dendritic cells, which have high intrinsic co-stimulatory activity, become activated and are sufficient to induce CD8 T cells to produce IL-2. However, in most cases, CD8 T cell activation requires additional signals provided by CD4 effector T cells (Zhai et al., 2007). Apart from viral infections, CTLs also play an important role in the response to intracellular bacterial pathogens. Mice that do not express Class I MHC and are unable to develop functional CD8$^+$ T cells, die rapidly when infected with *M*ycobacterium *t*uberculosis (Flynn et al., 1992).

The main mechanism of cytotoxicity of CTLs is calcium-dependent release of cytotoxic granules. These granules contain cytotoxic proteins such as perforin, which creates pores in the target cell membrane, serine proteases called granzymes that

activate caspases and granulysin, which in turn, induces apoptosis of target cells (Murphy, 2012).

4.1.5.2 CD4$^+$ T helper cells

CD4$^+$ T cells differentiate into several different subsets of effector T cells with different functions. The main classes are T_H1, T_H2, T_H17 and the regulatory T cells as well as T_{FH} cells, which help B cells in lymphoid follicles.

T_H1, T_H2, T_H17 T helper cells are defined on the basis of the cytokines they secrete. T_H1 cells help macrophages kill intra-vesicular pathogens such as *M. t*uberculosis. T_H1 and T_H2, as the names suggest, were the first two subsets to be identified. T_H1 cells, when activated, secrete interferon-γ (IFN-γ), IL-2, TNF-α and TNF-β (Mosmann et al., 1986). T_H2 cells help control infections by parasites, particularly helminths, and release IL-4, IL-5, IL-6, IL-13 and IL-25 following activation (Murphy, 2012). T_H17 cells were the third subset to be identified; they act to boost fungal defences and produce IL-17 (Harrington et al., 2005). T cell differentiation towards individual subsets is driven by the cytokines released into the environment of the naïve CD4$^+$ T cells. IL-12 released from DCs or macrophages favours T_H1 formation. IL-4 induces T_H2 formation (Murphy and Reiner, 2002). IL-6 and TGF-β promote T_H17 formation. IL-6 stimulation is required for T_{FH} cells, although the conditions required for their in vitro production have not yet been defined.

4.1.5.3 CD4$^+$ Treg cells

Regulatory T cells (Tregs) are a subset of CD4$^+$ T cells which are involved in immune suppression and the prevention of unwanted immune responses. Tregs are CD4$^+$ cells that highly express the IL-2 receptor α-chain, CD25. When CD25$^+$ cells were depleted from the CD4$^+$ cells and injected into lymphopenic mice, they developed autoimmune disease (Sakaguchi et al., 1995). Further evidence that Tregs were an independent population came with the identification of FoxP3 (also known as scurfin), a transcription factor which was highly expressed specifically in Tregs, and which regulated Treg function (Khattri et al., 2003). Mice deficient in FoxP3 develop progressive CD4$^+$- mediated autoimmunity. Tregs can be classified into two groups: natural Tregs (nTreg), which arise in the thymus and inducible Tregs (iTreg), which arise in the periphery.

4.1.5.4 NK T cells

NK T cells are characterised by the expression of an invariant T cell receptor α chain paired with one of three β chains. They share some markers expressed by NK cells such as CD161 (Godfrey and Kronenberg, 2004). They can recognise glycolipid antigens presented to them by the MHC-like molecule CD1 (Murphy, 2012). Following TCR stimulation they release IFN-γ, IL-4 and IL-13 and function as suppressors of the cell-mediated immune response (Godfrey and Kronenberg, 2004).

4.1.5.5 CD4⁻ CB8⁻ γδ T cells

γδ T cells, as the name suggests, bear an alternate TCR made up of γ and δ chains. γδ-TCR do not appear to be restricted to classical MHC Class I or II molecules. They appear to bind free antigens, such as bacterial heat shock protein, as well as antigens presented by non-classical MHC-like molecules (Murphy, 2012). They have been shown to play a role in the response to microbial infections such as *M. t*uberculosis and *M.a*vium and in co-infection with HIV (Chen and Letvin, 2003).

4.1.6. PI3K and PTEN in T cells

Phosphatidylinositol 3-kinase (PI3K) enzymes are lipid kinases that phosphorylate the 3' position of the inositol ring of phosphoinositides, resulting in the production of three lipid products, namely phosphatidylinositol (3)- monophosphate (PIP), phosphatidylinositol (3,4)-bisphosphate (PIP_2) and phosphatidylinositol (3,4,5)-trisphosphate (PIP_3) (Cantrell, 2001). Increases in PIP_3 levels within cells lead to the recruitment and activation of several pleckstrin homology (PH) domain containing proteins such as Akt, Tec, Vav, phospholipase Cγ1 and PDK1 (phosphoinositide-dependent kinase 1) (Buckler et al., 2008).

PI3Ks can be grouped into three main classes based on in-vitro substrate specificity, structure and mode of regulation (Curnock et al., 2002). Class IA PI3Ks can phosphorylate phosphatidylinositol (PtdIns), PtdIns (4) P and PtdIns (4,5) P2. They are heterodimers consisting of a 110 KDa catalytic subunit (of which there are three isoforms, p110α, p110β and p110δ) and an 85 KDa regulatory subunit (p85α, p85β and p55γ). Class IB PI3Ks associate with a unique p101 adaptor molecule, and are activated

by G protein βγ subunits. Class II PI3Ks (PI3K-C2α/β/γ) contain a C2 domain, and PtdIns and PtdIns(4)P are their main substrates (Curnock et al., 2002), while class III PI3Ks only phosphorylate PtdIns. Class IA and IB are the only classes that generate PIP_3, and are the best studied class in immune cells (Buckler et al., 2008). T cell activation is accompanied by a rapid increase in PIP_3 levels in the region of the immunological synapse. PI3K may be coupled to the TCR signals through p85 and its interactions with adaptor molecules with the canonical YxxM motif , or signalling molecules containing non-canonical tyrosine phosphorylation motifs , such as ZAP-70 and SLP-76 (Buckler et al., 2008).

PI3K is also activated downstream of CD28 co-stimulatory signals. CD28 has the YxxM motif on its cytoplasmic tail and when it is tyrosine-phosphorylated by Lck, provides a docking site for the SH2 domain of the p85 regulatory subunit of Class I PI3K, which then recruits the catalytic subunit to the membrane, leading to PI3K enzyme activity (Prasad et al., 1994).

Activation of PI3K pathways leads to activation of several downstream targets such as the Tec family of tyrosine kinases (comprising Itk, Tec and Btk), GTPases of the Rac and Rho families and serine/ threonine kinases of the AGC family (Ward and Cantrell, 2001). One of the key proteins of the AGC family that is activated by P13K is PDK1 (phosphoinositide dependent kinase-1), which binds to PIP_3 via its PH domain. PDK1 phosphorylates and activates the downstream protein kinases PKB (Akt), p70 S6kinase and p90RSK. PDK1 is required for normal T cell development (Kelly et al., 2007); the PDK1-PKB signalling axis regulates protein synthesis, cell growth and cell cycle progression (Rathmell et al., 2003).

The tumour suppressor PTEN is a 3'-PI phosphatase, which converts PIP_3 to PtdIns (4,5) P_2 and thus negatively regulates the PI3K signalling pathway. Cells lacking PTEN therefore have a constitutively active PI3K pathway. The importance of PTEN in T cell biology is demonstrated by studies showing that mice lacking PTEN in T cells develop lymphomas (Hagenbeek et al., 2004, Hagenbeek and Spits, 2007). These mice died at a median age of around 95 days (89-103 days) (Hagenbeek et al., 2004). The tumours arose in the thymus, but most mice also had peripheral tissue (spleen and lymph node) involvement (Hagenbeek and Spits, 2007). Most of the T cell-specific PTEN-null mice had larger thymi and contained significantly higher number of thymocytes compared to the control mice (Hagenbeek and Spits, 2007). These mice had similar distribution of cells expressing either CD4 or CD8 compared to wildtype controls, but had much larger populations of DP cells (Hagenbeek et al., 2004). The PI3K/PKB pathway was indeed constitutively active, as evidenced by increased PKB and FOXO phosphorylation in these mice. The PTEN-null T cells were resistant to apoptosis, which may account for the increase in proportion of DP cells. Some of these cells were deficient in the TCR-β receptor and would have normally been eliminated during β-selection, and are likely to have survived as a result of increased PI3K activity (Hagenbeek et al., 2004). Tumour formation in this model has been shown to be to be PDK1-dependent, as PTEN-null mice fail to develop tumours if PDK1 is also deleted (Finlay et al., 2009).

4.1.7. Role of AMPK in T cells

T cells express only the α1 isoform of the AMPK α subunit (Tamás et al., 2006). As discussed previously (in section 4.1.4) TCR activation causes an increase in intracellular

calcium, which also activates CaMKK-β. It has been shown that stimulation of TCR signalling by treatment of cells with anti-CD3 antibody activates AMPK and causes phosphorylation of its downstream target ACC (Tamás et al., 2006). This activation was abolished by pre-treatment with the CaMKK inhibitor, STO-609. Activation of AMPK in T cells can occur either in a LKB1-dependent manner as is seen in conditions of metabolic stress, or in a CaMKKβ-dependent manner downstream of TCR activation. The AMPK activation downstream of TCR is dependent on LAT and SLP-76 activation (Jurkat cells which do not express these two proteins fail to activate AMPK when treated with anti-CD3 antibody) and independently of PI3K signalling (since Jurkat cells also lack PTEN) (Tamás et al., 2006).

T cell-specific deletion of AMPKα1 increases the sensitivity of cells to metabolic stress, but does not affect development or differentiation of T cells or immune responses of both cytotoxic and helper T cells (Mayer et al., 2008). However, recent evidence suggests a role for AMPK in determining effector and memory cell fate of CD8^{+} T cells (Finlay and Cantrell, 2011).

4.2 AIMS AND METHODS

The main aim of the chapter was to test whether AMPK functions as a tumour suppressor. This project was carried out in collaboration with Prof. Doreen Cantrell's group. We utilised a previously described Cre/loxP system to delete PTEN, with or without deletion of AMPK in T cells of C57Bl/6 mice. We initially generated mice that were heterozygous for PTEN ± deletion of AMPK (PTEN$^{+/-}$ AMPK$^{+/+}$ and PTEN$^{+/-}$ AMPK$^{-/-}$), but then subsequently generated mice that were homozygous for PTEN ± deletion of AMPK (PTEN$^{-/-}$ AMPK$^{+/+}$ and PTEN$^{-/-}$ AMPK$^{-/-}$). These mice were then monitored to observe the development of lymphomas.

4.3 RESULTS

4.3.1 Generation of mice with T cell-specific deletion of AMPK and PTEN

T cell-specific PTEN knockout (KO) mice were generated by crossing PTEN$^{fl/fl}$ mice, where LoxP sequences were inserted in introns 4 and 5 flanking exon 5, with mice heterozygous for Cre recombinase driven by the Lck promoter (Lck-Cre). Expression of Cre recombinase from this promoter caused deletion of the floxed genes following TCRβ rearrangement in the DN stage. This model has been well established and used in previous studies (Marino et al., 2002, Hagenbeek et al., 2004, Hagenbeek and Spits, 2007, Finlay et al., 2009). The PTEN$^{fl/fl}$ mice were kind gifts from Prof. Hergen Spits. AMPKα1$^{fl/fl}$ mice were kind gifts from Dr. Benoit Viollet; the methods used to generate these mice have been previously described (Jørgensen et al., 2004)

As mentioned earlier α1 is the only AMPK-α isoform expressed in T cells. All of the strains of mice used were already established in Prof. Cantrell's group. Mice that had T cell-specific deletion of PTEN were bred with mice that had T cell-specific deletion of AMPK to generate mice that had reduced (heterozygous) expression of PTEN and with complete loss of AMPK-α1 (PTEN$^{+/-}$ AMPK$^{+/+}$ and PTEN$^{+/-}$ AMPK$^{-/-}$) (Figure 4.3). The frequency and onset of tumour formation were compared between the PTEN heterozygous mice that either expressed or lacked AMPK-α1. Mice with complete T cell-specific deletion of PTEN with or without complete T cell-specific deletion of AMPK-α1 (PTEN$^{-/-}$ AMPK$^{+/+}$ and PTEN$^{-/-}$ AMPK$^{-/-}$) were also generated (Figure 4.4). The frequency and onset of tumour formation was also compared between these two groups.
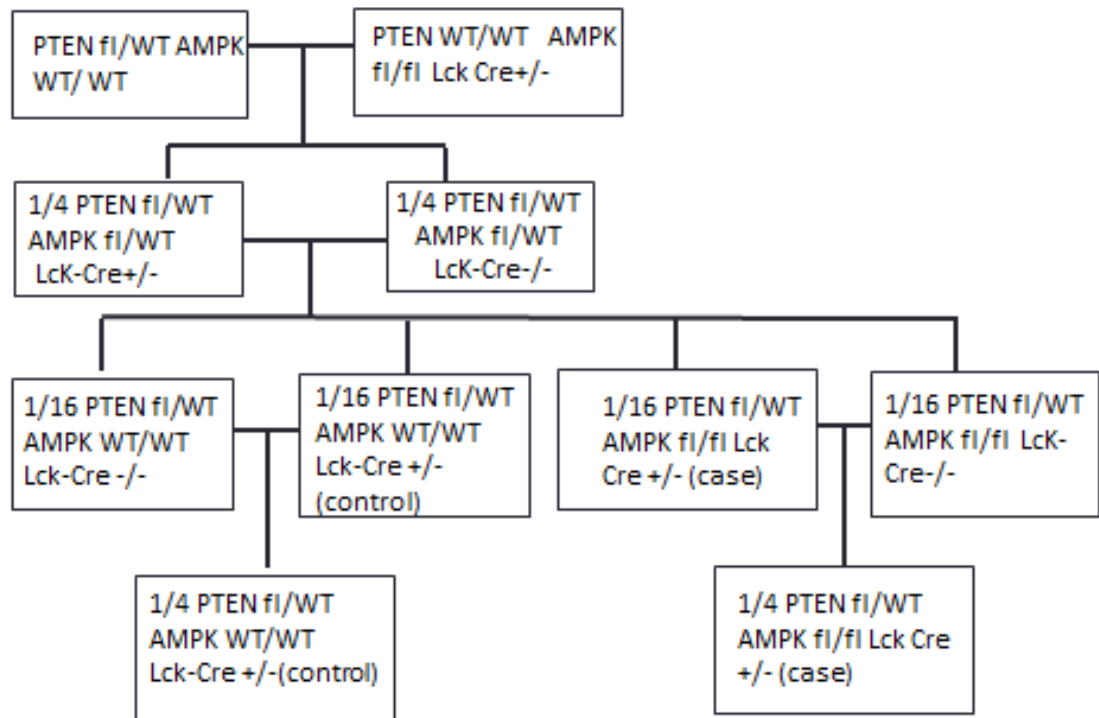
Figure 4.3: Schematic diagram showing generation of T cell-specific PTEN heterozygotes which lack or express AMPKα1

Mice that had T cell-specific deletion of PTEN were bred with mice that had T cell-specific deletion of AMPK to generate mice that had reduced (heterozygous) expression of PTEN and with complete loss of AMPK-α1 (PTEN$^{+/-}$ AMPK$^{+/+}$ and PTEN$^{+/-}$ AMPK$^{-/-}$). Once breeders had been established, there was a one-in-four chance of obtaining the desired genotype. The genotypes were confirmed by PCR.
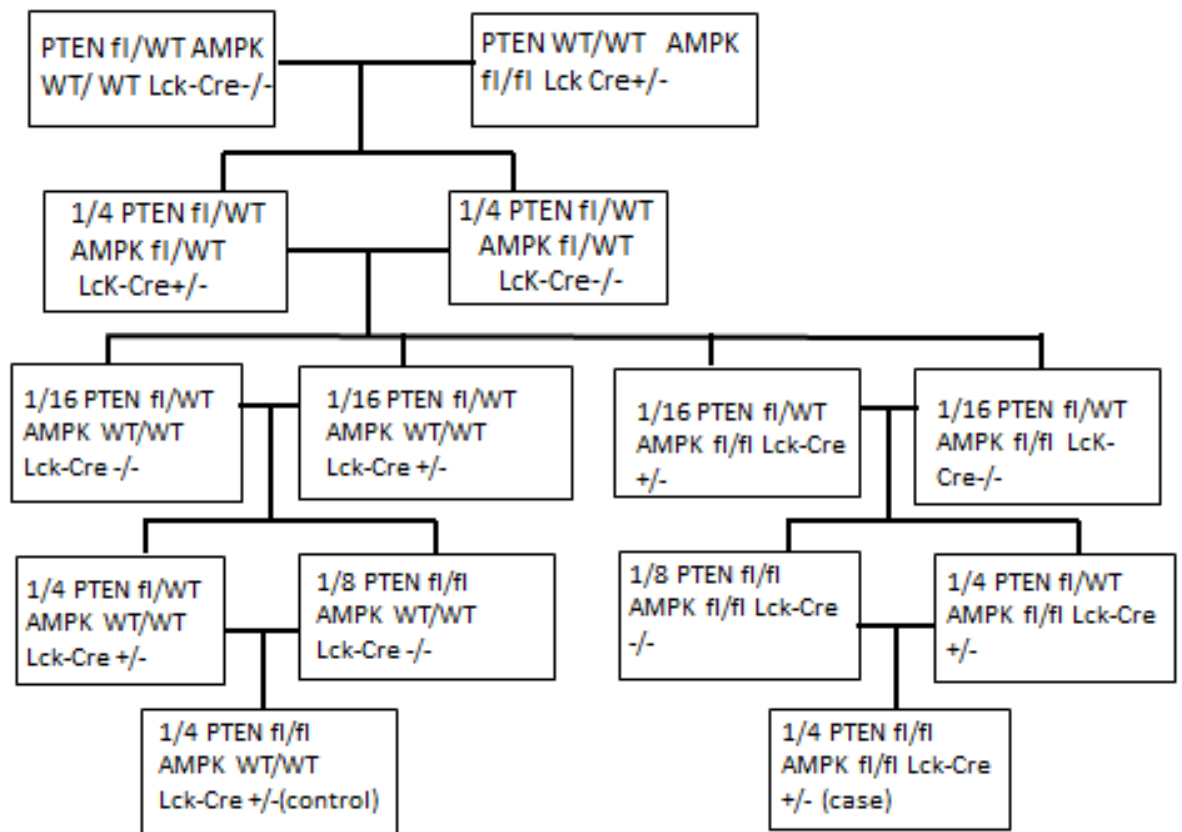
Figure 4.4 Schematic diagram showing generation of T cell-specific PTEN homozygotes which lack or express AMPKα1*

Mice with complete T cell-specific deletion of PTEN with or without complete T cell-specific deletion of AMPK-α1 (PTEN$^{-/-}$ AMPK$^{+/+}$ and PTEN$^{-/-}$ AMPK$^{-/-}$) were also generated. Cases and controls from the scheme used in Figure 4.3 were used to generate these mice. As PTEN fl/fl Lck-Cre+/- mice developed tumours early, they were not used as breeders. Instead PTEN fl/WT Lck-Cre+/- mice were crossed with PTEN fl/fl Lck-Cre-/- mice to obtain the desired cases and controls.

4.3.2 Phenotype of T cell-specific PTEN heterozygotes that lack or express AMPKα1

Mice with T cell-specific heterozygous deletion of PTEN expressing wildtype AMPK-α1 (PTEN $^{+/-}$ AMPK $^{+/+}$) or lacking AMPK α1 (PTEN$^{+/-}$ AMPK$^{-/-}$) were generated according to the schematic in Figure 4.3. Ear snips from three-week old mice were digested, genomic DNA was extracted and PCR was carried out as described in the Methods section to confirm the genotype. Despite reports that PTEN heterozygotes in mice develop lymphomas due to loss of heterozygosity in mice (Suzuki et al., 1998, Podsypanina et al., 1999) and observations in the T cell-specific PTEN heterozygotes of lymphomas (Finlay D, personal communication), we observed very few lymphomas in the PTEN heterozygotes we studied. Only 1 out of 12 mice developed lymphomas and even this low frequency of events took over a year to become apparent. There was a trend towards an increase in tumour incidence in the PTEN$^{+/-}$ mice that also lacked AMPK-α1 (4 out of 12 mice). However, as the numbers were small, no meaningful comparison could be made. One likely reason for this apparent discrepancy with the literature may be the difference in mouse strains used. The ES cells used for the generation of both AMPK and PTEN floxed mice were derived from 129 mice. The PTEN floxed mice were initially generated in a FVB-N line and back-crossed on a C57Bl/6 background. Since obtaining breeders, further backcrosses onto C57Bl/6 background had been carried out in the animal unit from 2008 onwards. C57Bl/6 mice are known to be relatively tumour-resistant and the low frequency of tumours in the PTEN heterozygous mice may be due to increasing influence of the C57Bl/6 background on the phenotype in successive generations of mice.

Mice that have T cell-specific deletion of PTEN develop lymphomas at a median age of 13-14 weeks (6-23 weeks) (Hagenbeek et al., 2004). Therefore, mice with homozygous T cell-specific PTEN deletion, with or without deletion of AMPK-α1 were generated and followed for formation of lymphomas.

4.3.3 AMPK suppresses tumour formation in the T cell-specific PTEN Knock-out mice

Mice with T cell specific homozygous deletion of PTEN expressing wildtype AMPK (hereafter termed PTEN KO mice) or lacking AMPK (hereafter termed PTEN AMPK double KO mice) were generated according to the breeding scheme in Figure 4.4. As T cells have been shown to express only the α1 isoform of AMPK-α, cohorts used for the earlier breeding scheme (PTEN $^{+/-}$ group) were used as breeders. Over the next 2-3 generations of breeding, desired genotypes were obtained and followed up for tumour formation. Mice were culled when they showed any signs of distress such as difficulty feeding, limping or lack of normal movements and presence of palpable lumps. As expected, mice with T cell-specific deletion of PTEN developed lymphomas around 85 days of age (12-13 weeks), around the same age as reported in previous studies (Hagenbeek et al., 2004, Finlay et al., 2009). Interestingly, mice that lacked PTEN and AMPK in the T cells, developed lymphomas at a median age of 65 days, much earlier than mice with T cell-specific deletion of PTEN alone (Figure 4.5). The difference in survival between the two groups was highly statistically significant (p<0.0001). This result strongly suggests that AMPK functions as a tumour suppressor in T cells when the PI3K pathway is overactive.
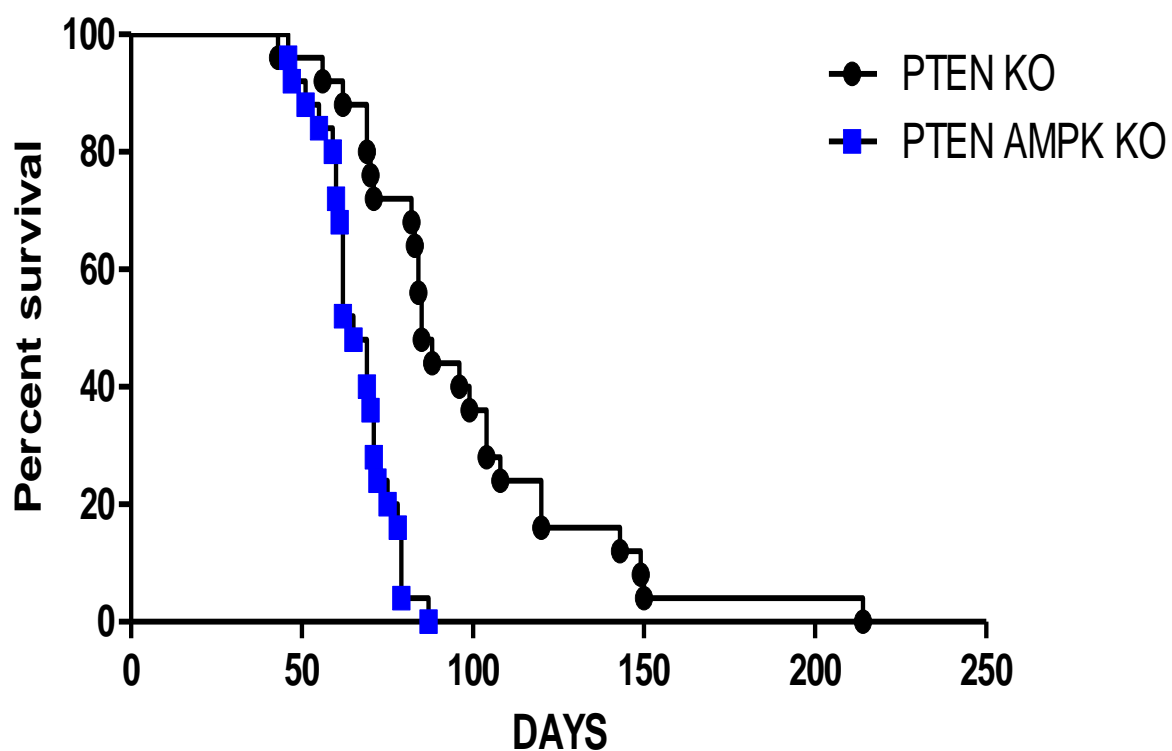
Figure 4.5: Survival analysis of T cell-specific PTEN homozygous KO mice which lack or express AMPK-α1

Mice that have T cell-specific deletion of PTEN (in black) had a median survival of 85 days. Mice that have T cell-specific deletion of PTEN and AMPK had a significantly shorter median survival of 65 days (p<0.0001, Hazard ratio=6.3 n=25 in each group).

4.3.4. Site- specific differences in tumour formation between the PTEN KO and PTEN AMPK KO MICE

PTEN KO mice developed T cell lymphomas that arise in the thymus. However, most of these mice also had peripheral lymphoid involvement as evidenced by enlargement of the lymph nodes and spleen (Figure 4.6). This was consistent with observations from previous studies (Hagenbeek et al., 2004, Hagenbeek and Spits, 2007). Strikingly, the PTEN AMPK double KO mice were often found dead, having shown no previous evidence of poor feeding or sickness. Examination of the PTEN AMPK double KO mice revealed the presence of massive thymomas in all mice, usually constricting the heart and adherent to the chest wall. Interestingly, very few PTEN AMPK double KO mice developed extra-thymic tumours. This difference in tumour location was statistically significant ($p<0.0001$). This suggests that AMPK deletion caused thymocytes or tumour cells to be confined to the thymus. This may also explain the reduction in lifespan in these mice as the massive thymomas would cause rapid deterioration in cardiac function while an enlarged spleen may not cause much discomfort until it outgrows its blood supply.

Thymocytes express several markers which facilitate emigration from the thymus (e.g. $S1P_1$) or that drive them towards peripheral lymph organs (e.g., L-selectin) .The expression of L-selectin in single thymocytes (measured by using fluorescent labelled L-selectin antibody and the signal measured using a flowcytometer) did not differ significantly between the PTEN KO and the PTEN AMPK double KO thymocytes (data not shown). However, the expression of $S1P_1$ mRNA (measured using real-time PCR) in the PTEN AMPK double KO thymocytes was significantly reduced

compared to wildtype thymocytes obtained from 4 week old mice (Fig 4.7A). mRNA levels of CCR7 (Chemokine receptor 7, which is expressed by naïve T cells and also facilitates entry into lymph nodes) were also significantly lower in the PTEN AMPK double KO thymocytes compared to wild type thymocytes (Figure 4.7B). CCR7 levels were also found to be lower in PTEN KO thymocytes and the PTEN AMPK double KO thymocytes had lower CCR7 levels than the PTEN KO thymocytes (Figure 4.7B).
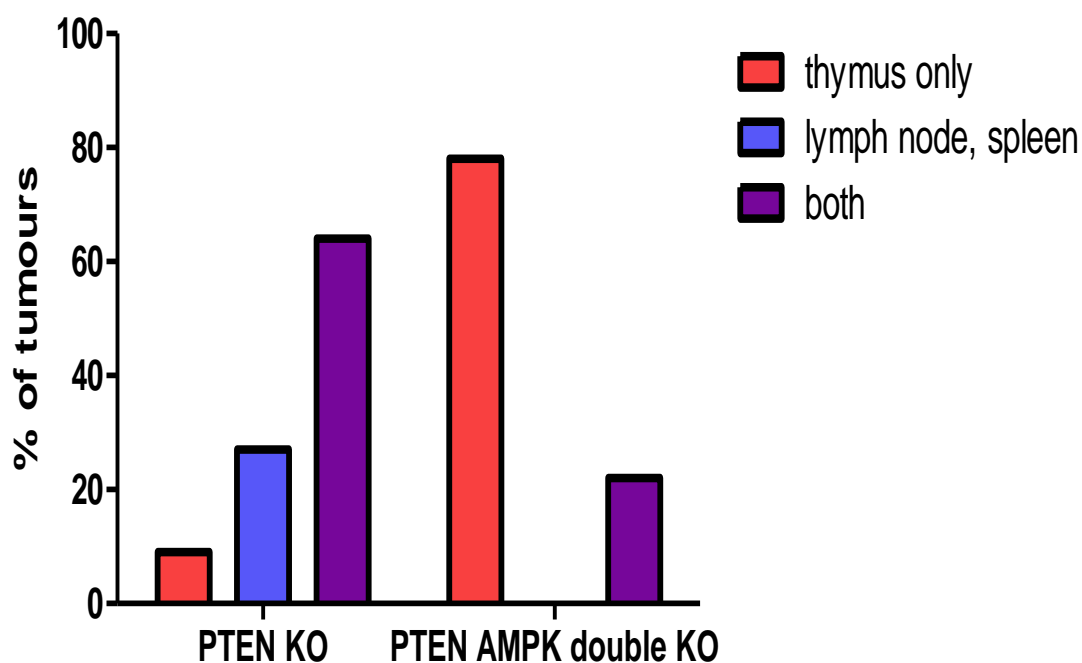
Figure 4.6 Distribution of tumours in PTEN KO and PTEN AMPK double KO mice

PTEN KO mice developed T cell lymphomas arising in the thymus. Most mice also had enlarged/infiltrated lymph nodes and spleen. Examination of the PTEN AMPK double KO mice revealed the presence of massive thymomas in all mice, while very few developed extra-thymic tumours. This difference in tumour location was statistically significant ($p < 0.0001$ determined using Chi square and Fisher's exact test),n=23 mice in each group.

A

S1P$_1$

B
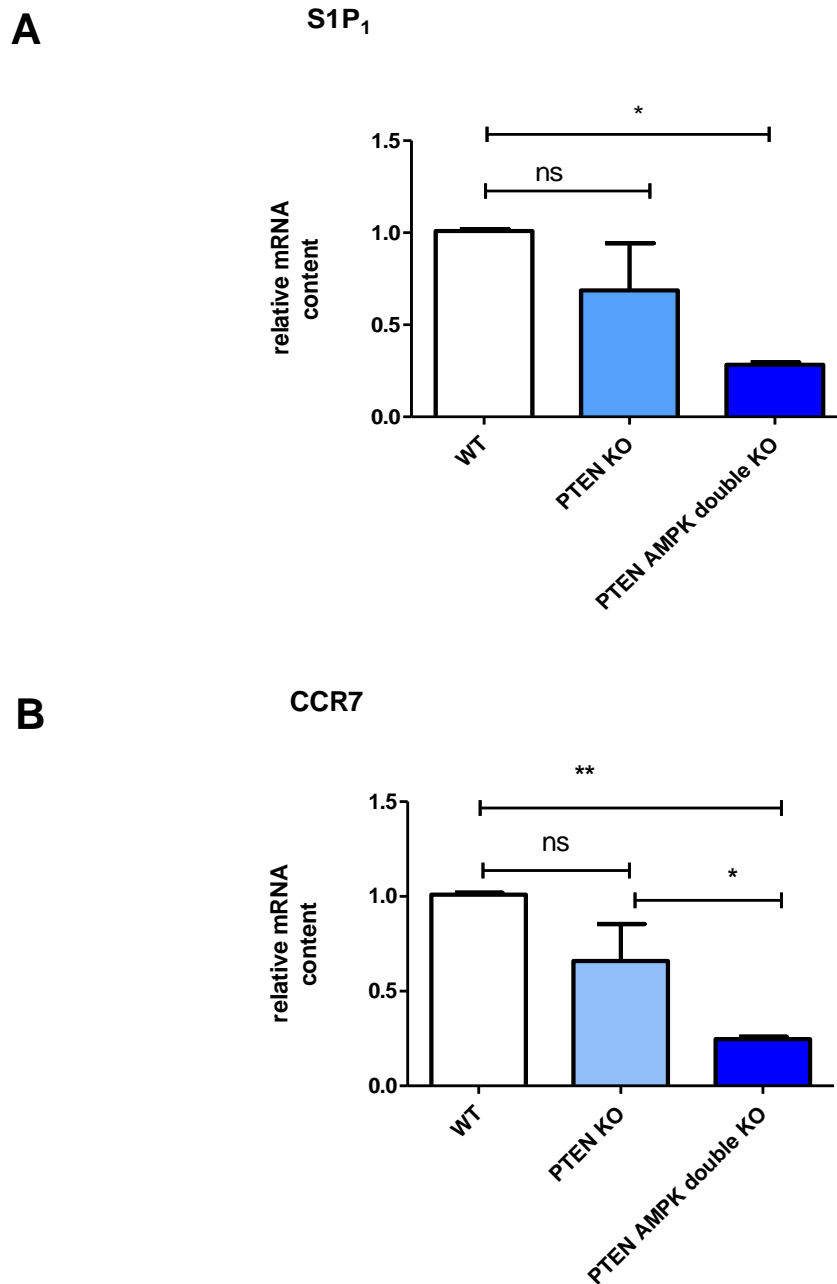
CCR7

Figure 4.7: mRNA expression levels of S1P$_1$ and CCR7 in wild type, PTEN KO and PTEN AMPK double KO thymocytes

mRNA levels of (A) Sphingosine-1-phosphate receptor 1 (S1P$_1$) and (B) Chemokine receptor 7 (CCR7) were measured by real-time quantitative PCR by calculating the number of cycles required to obtain a defined signal intensity of the DNA binding dye SyBr green and normalised to the housekeeping gene HPRT. The figure shows results obtained in triplicate from three individual mice from each genotype. One-way ANOVA was used to compare the different groups.

4.3.5 T cell development in PTEN KO and PTEN AMPK double KO mice

Flowcytometric analysis of T cell development and differentiation showed no difference in the development of thymocytes obtained from four week old PTEN KO and PTEN AMPK double KO mice (data not shown). Both groups had cells expressing high levels of TCRβ and had similar distribution of DN, DP and SP cells (data not shown). Expression of cell surface receptors such as CD62L (L-selectin) and CD69 did not differ between PTEN KO and PTEN AMPK double KO mice. However, PTEN AMPK KO thymocytes had increased cell size compared to wildtype and PTEN KO thymocytes overall (Figure 4.8). The predominant cells in the thymus at 4 weeks are the double positive cells and these cells are likely to contribute to the increased cell size. We aim to measure this in future by sorting DPs and measuring cell size and quantifying total protein content of cells from each genotype.
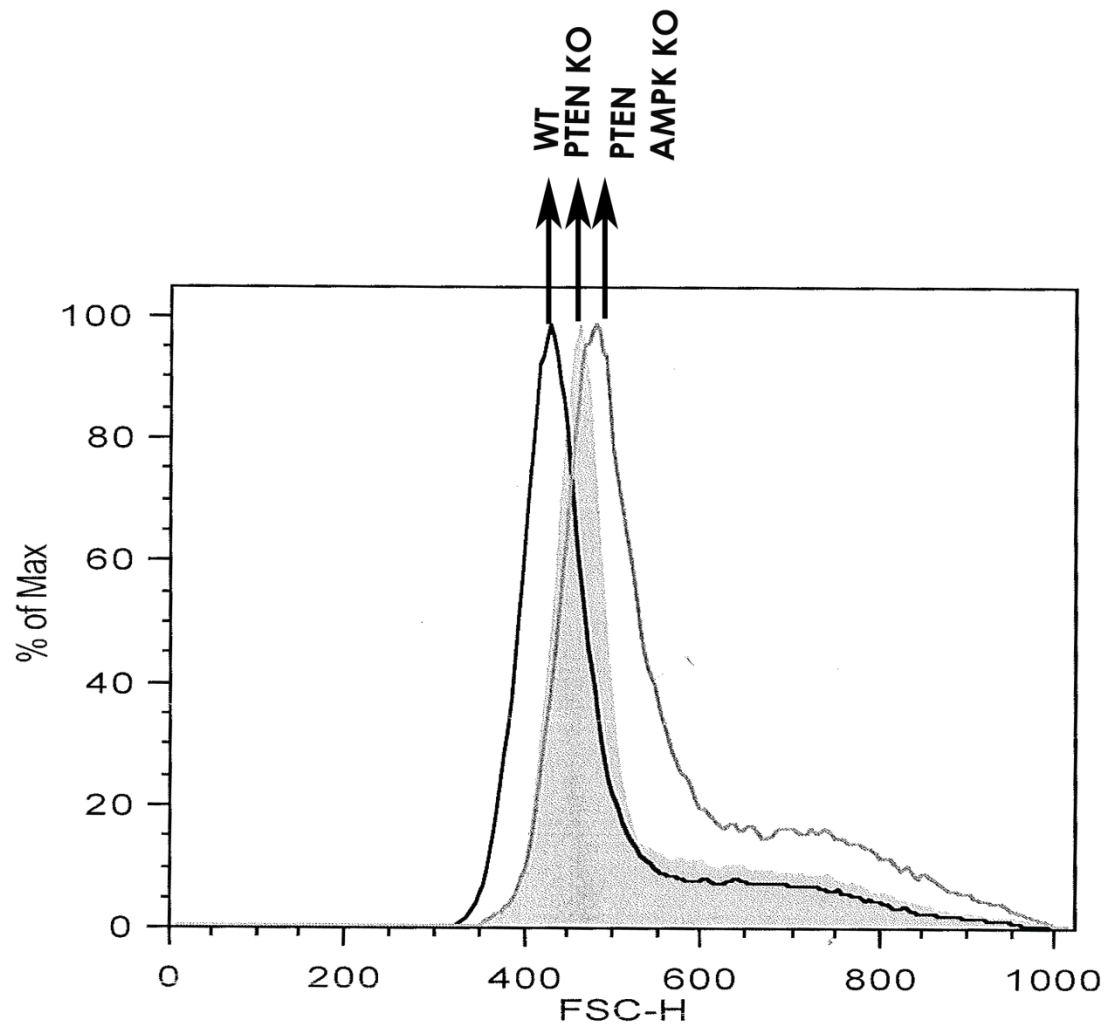
Figure 4.8: Difference in cell size in thymocytes from mice expressing different genotypes

Cell size (forward scatter or FSC-H) of wildtype (WT), PTEN KO and PTEN AMPK double KO thymocytes was measured and their distribution represented. The PTEN AMPK double KO cells were larger than the PTEN KO cells and the wildtype cells. This result is representative of four experiments performed.

4.3.6 AMPK antagonises the mTOR pathway in a subset of cells in this tumour model

Lysates of thymocytes obtained from 4-5 week old wild type, PTEN KO and PTEN AMPK double KO mice were subjected to SDS-PAGE and blots probed for proteins downstream of the PI3K/PKB and the mTOR pathways. PTEN KO mice showed increased activation of PKB compared to wild type mice, as evidenced by phosphorylation of two of its key regulatory residues, namely Thr-308 and Ser-473, as well as increased phosphorylation of FOXO-1 and -3A, which are known to be downstream of PDK1 and PKB. This is consistent with previous studies (Hagenbeek and Spits, 2007, Finlay et al., 2009). PTEN AMPK double KO cells also showed an increase in phosphorylation of PKB and FOXO compared to wildtype controls and the levels were comparable to those observed in the PTEN KO thymocytes (Figure 4.9). However, PTEN AMPK double KO cells showed markedly increased levels of phosphorylated ribosomal protein S6 compared to both wildtype controls and PTEN KO cells (Figures 4.9 and 4.10). This suggests that loss of AMPK in conjunction with increased PI3K signalling in thymocytes causes activation of signalling pathways downstream of mTOR. But as discussed earlier, the cells within the thymus can be sub-divided into several different sub-sets. At 4-5 weeks of age, the vast majority of thymocytes are the DPs, wherein S6 activity is down-regulated. It is likely that increased S6 phosphorylation is limited to a small sub-set of DPs that fail to down-regulate pS6 levels.
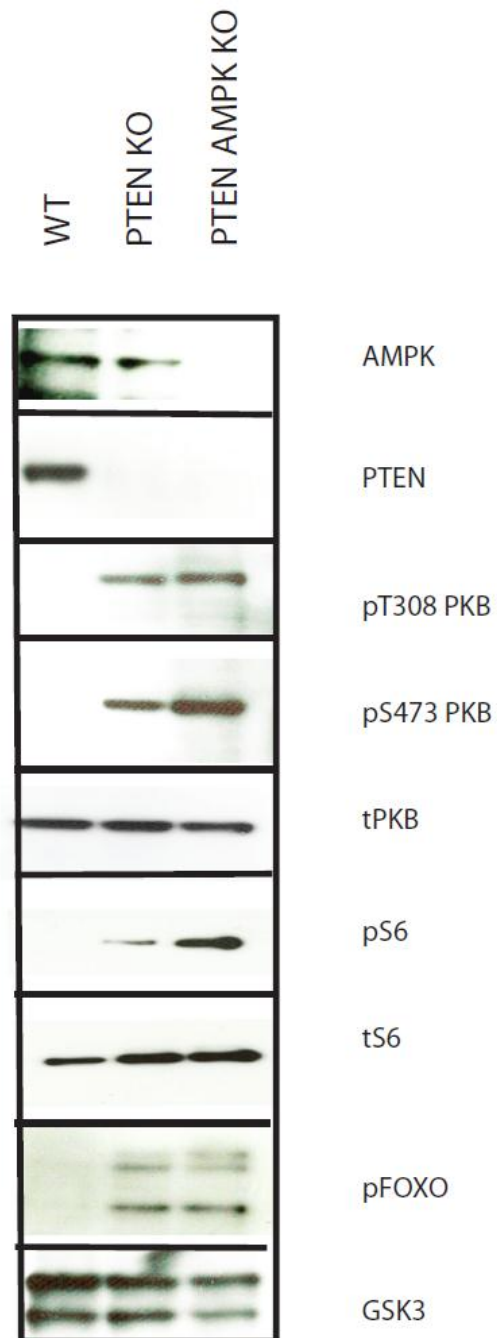
Figure 4.9: Activation of signalling pathways in PTEN KO and PTEN AMPK double KO mice

Wildtype thymocytes as well as thymocytes from PTEN KO and PTEN AMPK double KO mice were lysed and subjected to SDS-PAGE and immunoblotted with antibodies against phosphorylated PKB (anti-pT-308 and anti-pS-473), pFOXO-1, -3A and -4 and pS6 (Ser235/236). Deletion of PTEN and AMPK was also confirmed.

A.
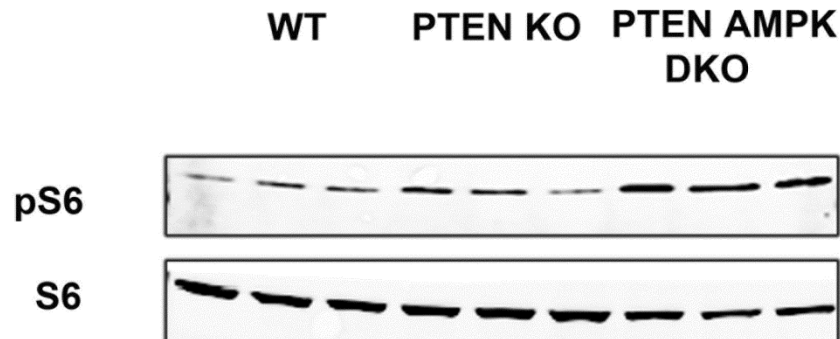
B.
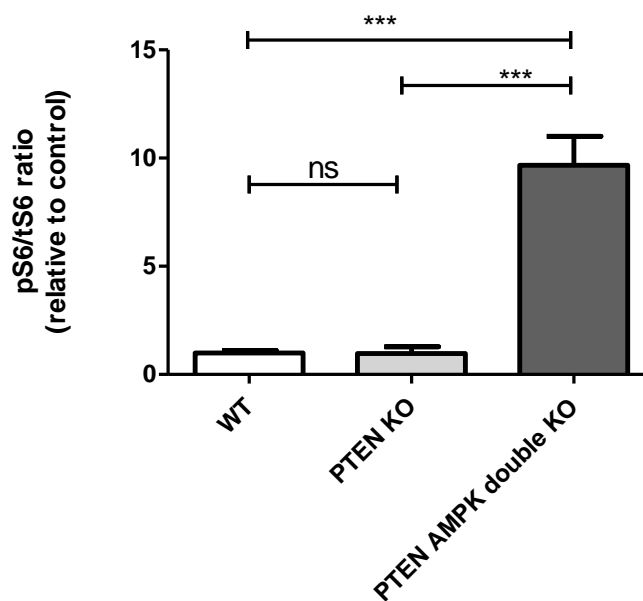
Figure 4.10: PTEN AMPK double KO cells have high pS6 levels when compared to wild type or PTEN KO cells

(A)   Thymocytes were harvested from three wildtype, PTEN KO and PTEN AMPK KO mice. The cells were lysed and subjected to SDS-PAGE electrophoresis and immunoblotted with antibodies against pS6 (Ser 235/236) and total S6.

(B)   The intensity of the bands was quantified using the Li-Cor Odyssey imager and the results plotted as ratio of pS6:S6 (relative to control). One way ANOVA was used to compare the groups (p<0.001-***).

To determine the sub-set of cells expressing high levels of pS6, staining of single cells using anti-pS6 antibodies as well as staining for CD4 and CD8 was carried out, followed by flow cytometric analysis. Staining for phospho-S6 using thymocytes treated with vehicle versus rapamycin (mTOR inhibitor) provided an estimate of mTOR-dependent phosphorylation of S6. Phosphorylation of S6 by mTOR is lost following rapamycin treatment and any positive staining in this group is taken as background staining. Staining in cells treated with vehicle was corrected for the background staining to compare mTOR-dependent phospho-S6 levels in wild type, PTEN KO and PTEN AMPK double KO mice. PTEN KO cells showed an increase in the proportion of pS6 staining cells, which was increased further in the PTEN AMPK KO cells (Figure 4.11). Both PTEN KO and PTEN AMPK double KO mice had higher percentages of DP cells in the thymus compared to the wild type mice and it is likely that a subset of DPs had up-regulation of mTOR leading to increased phospho-S6 staining.

Total Thymocytes

phospho-S6$^{S235/6}$
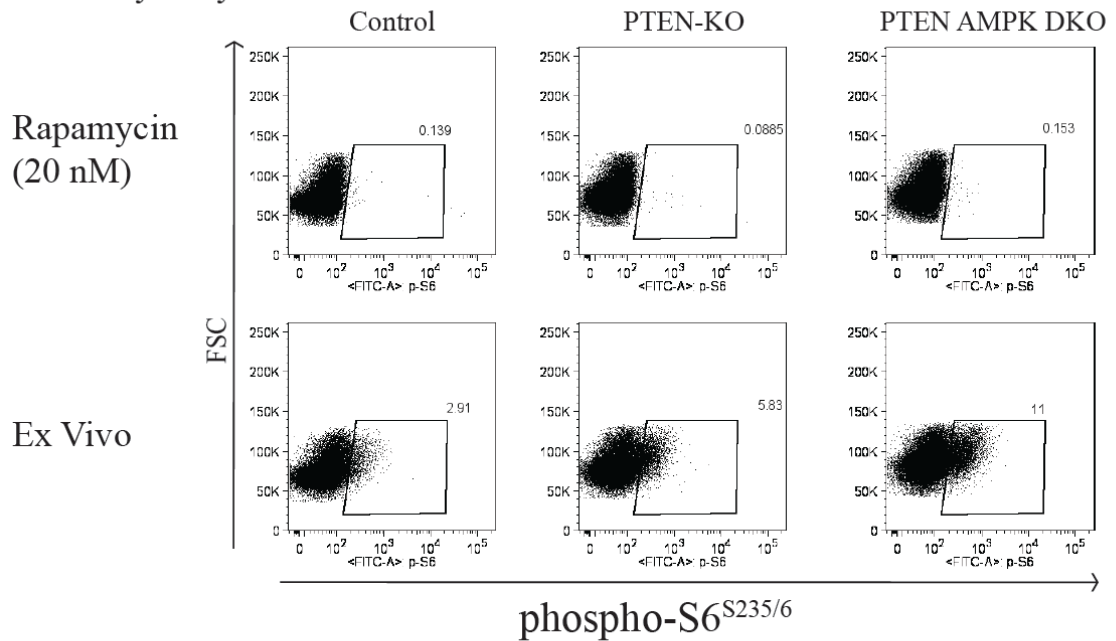
Gated on pS6^{pos} cells

CD8
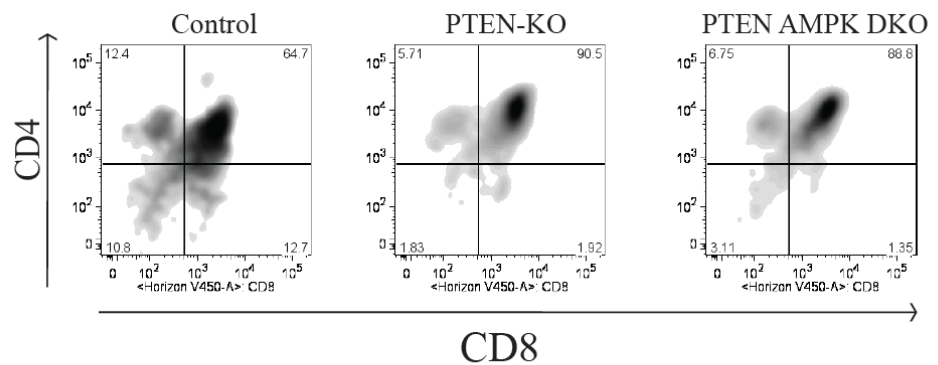
Figure 4.11: Distribution of phospho-S6 positive cells in thymocytes obtained from wild type, PTEN KO and PTEN AMPK double KO mice

Thymocytes obtained from wildtype, PTEN KO and PTEN AMPK double KO mice were treated with vehicle or rapamycin and then fixed in methanol and stained with anti-pS6 antibody followed by fluorescent-labelled secondary antibody. The proportion of phospho-S6 positive cells in each sample was measured and expressed as a percentage of total cells. The distribution of DN, DP and SP cells among the phospho-S6 positive cells was also determined. This experiment was carried out by Rosie Clarke, Flowcytometry Manager, College of Life Sciences, University of Dundee.

4.4 DISCUSSION

In recent years, it has been found that AMPK is downstream of the tumour suppressor LKB1 (Hawley et al., 2003, Woods et al., 2003, Shaw et al., 2004b). This has led many research groups to suggest that, AMPK may, atleast in part, modulate some of the tumour suppressive actions of LKB1(Corradetti et al., 2004, Shaw et al., 2004a, Carretero et al., 2007). There is evidence that the AMPK signalling pathway is down-regulated in some tumours (Hadad et al., 2009). Epidemiological studies also show that that treatment of diabetics with the AMPK-activating drug metformin is associated with a lower incidence of cancer (Evans, 2005, Bowker et al., 2006a). These results suggest that AMPK may itself be a tumour suppressor, although direct evidence has so far been lacking.

This study provides the first genetic evidence that AMPK functions as a tumour suppressor in vivo. T cell-specific deletion of PTEN and AMPK in mice resulted in death from lymphoma formation significantly earlier than that observed in mice with T cell-specific deletion of PTEN alone. The time of initial onset of tumour formation in the PTEN AMPK double KO mice is similar to that of the PTEN KO mice, but the former had more aggressive tumour growth and died much sooner. The striking difference in tumour location between the PTEN KO and the PTEN AMPK double KO mice was an interesting and unexpected result. While it has been established in previous studies that PTEN-null lymphomas involve the thymus as well as the liver and spleen, lymphomas in PTEN AMPK double KO mice were almost always confined to the thymus. This suggests a role for AMPK in promoting the exit of tumour cells from the thymus. Measurement of thymocyte mRNA levels by RT-PCR showed a significant reduction in $S1P_1$ mRNA in PTEN AMPK double KO mice, when normalised to

expression of a housekeeping gene. This decrease was not accompanied by up-regulation of CD69, which is known to cause a down-regulation of $S1P_1$ following activation of naïve T cells (data not shown). This suggests a role for AMPK in controlling the expression of $S1P_1$, a receptor that is vital for the egress of thymocytes from the thymus into the peripheral lymph organs and blood.

PTEN AMPK double KO mice also have larger cells in the thymus compared to wild type or PTEN KO mice. . However, further analyses of the different T cell sub-sets is required to determine which cells are enlarge or indeed if there is any delay in transition from DN to DP stage which may explain this observed difference in cell size. As wildtype thymus has very few DN cells at 4 weeks, we would probably need to pool thymocytes from 5-10 mice of each genotype and sort the DN cells to achieve this.

Another interesting observation was the increase in phospho-S6 levels in the PTEN AMPK double KO thymocytes, before the onset of tumours. At 4 weeks of age, only around 2% of wild type thymocytes exhibit detectable phospho-S6. The PTEN KO thymus had a greater percentage of cells expressing detectable phospho-S6 and this is doubled in PTEN AMPK double KO mice. Moreover, the PTEN KO mice seemed to have higher S6 protein levels, so that when pS6: S6 ratios were estimated, the wildtype and PTEN KO thymocytes had similar ratios. However, the PTEN AMPK double KO thymocytes had a ten-fold higher pS6:S6 ratio compared to either of the other two groups. This suggests a role for AMPK in down-regulation of mTOR- dependent S6 phosphorylation in a sub-set of thymocytes. This may also reflect a difference in sub-populations of thymocytes at 4 weeks between the different genotypes.

Further work is required to delineate the pathways activated in thymocytes following deletion of AMPK in this model and micro array analysis of thymocytes from

these mice would be useful. However, before that is done, we would need to identify the sub-set of thymocytes which have been transformed into tumour cells and try to dissect which signalling pathways have been altered in these cells.

CHAPTER FIVE: THE ROLE OF PHOSPHORYLATION OF THE C-TERMINAL TAIL OF LKB1 ON AMPK ACTIVATION

5.1 INTRODUCTION

5.1.1 Identification of LKB1 and Peutz Jeghers syndrome

LKB1 (Liver Kinase B1) was first identified as part of a screen for new kinases by researchers at Chugai Research Institute, the results of which were not published (Alessi et al., 2006). Genetic linkage studies then showed that mutations in the gene encoding LKB1 were responsible for 11 out of 12 cases of Peutz-Jeghers syndrome (PJS), a rare inherited cancer syndrome (Hemminki et al., 1998). Parallel studies by a different group also confirmed that PJS was caused by mutations in the same gene which they had termed serine threonine kinase 11(STK11) (Jenne et al., 1998).

Peutz-Jeghers syndrome is a rare, autosomal dominant, inherited cancer syndrome, characterised by the development of benign hamartomatous polyps and marked pigmentation of mucous membranes (Alessi et al., 2006). The syndrome is named after Peutz, who first described this condition in 1921 and Jegher, who characterised it as an autosomal dominant condition in 1949 (Hemminki, 1999). Patients with PJS have a markedly increased risk of cancer, especially colon, stomach, small intestinal and pancreatic cancer (Hemminki, 1999). In addition to germ line mutations that cause PJS, sporadic loss of LKB1 has also been reported in tumours of the lung and cervix (Vaahtomeri and Mäkelä, 2011). 144 different mutations in LKB1 have been identified in patients with PJS and from sporadic tumours, with a substantial proportion being truncating mutations in the catalytic domain resulting in loss of kinase function

(Alessi et al., 2006). However, some point mutations have been identified in the C-terminal tail of LKB1 in PJS patients and in sporadic tumours, suggesting a role for this region in regulating LKB1 activity (Alessi et al., 2006).

5.1.2 LKB1 structure and post-translational modifications

LKB1 is a 50 KDa protein that exists as two splice variants as described in Section 5.1.6. The LKB1 gene is located on chromosome 19 at 19p13 locus in humans and chromosome 10 in mice and is composed of ten exons, nine of which encode the LKB1 protein (Hemminki et al., 1998, Smith et al., 1999). Human LKB1 has 433 and murine LKB1 has 436 amino acids. LKB1 has unique N- and C-terminal regions that are unrelated to other proteins and possess no identifiable functional domains (Alessi et al., 2006). The N-terminus has a nuclear localisation sequence and over-expression of LKB1 leads to nuclear localisation of the protein (Smith et al., 1999).

LKB1 is phosphorylated on at least 8 residues (Figure 5.1) (Alessi et al., 2006). Four of these, namely Thr-185, Thr-189, Thr-336 and Ser-404 appear to be auto-phosphorylation sites (Karuman et al., 2001, Baas et al., 2003, Sapkota et al., 2002a). Ser-31and Ser-325 are phosphorylated by an as yet unidentified upstream kinase, although, Ser-31 lies within an AMPK consensus motif, while Ser-325 lies in a proline-rich region and is likely to be phosphorylated by a proline-directed kinase (Alessi et al., 2006). Thr-366 phosphorylation on LKB1 was shown to be increased when cells were treated with ionising radiation. It was then shown that this site was phosphorylated by *A*taxia-*t*elangiectasia *m*utated (ATM) kinase (Sapkota et al., 2002b). Ser-431 is phosphorylated by p90 *r*ibosomal *S*6 kinase (p90RSK) and cyclic-AMP-dependent protein kinase (also termed protein kinase A or PKA), in response to agents such as

forskolin and glucagon, that activate these kinases (Sapkota et al., 2001, Boudeau et al., 2003, Collins et al., 2000).

LKB1 terminates with the sequence Cys-Lys-Gln- Gln (-CKQQ), which is an optimal motif for protein prenylation, a type of post-translational modification. LKB1 was shown to be prenylated on its C-terminus using 14-C mevalonic acid labelling (Collins et al., 2000). Mutation of the Cys residue abolished prenylation (Collins et al., 2000). Mass spectrometry showed LKB1 was modified by farnesylation (a type of prenylation) on Cys-433 (Sapkota et al., 2001). The figure below (Figure 5.1) shows the domains contained in LKB1 and the sites that are modified by phosphorylation and farnesylation.
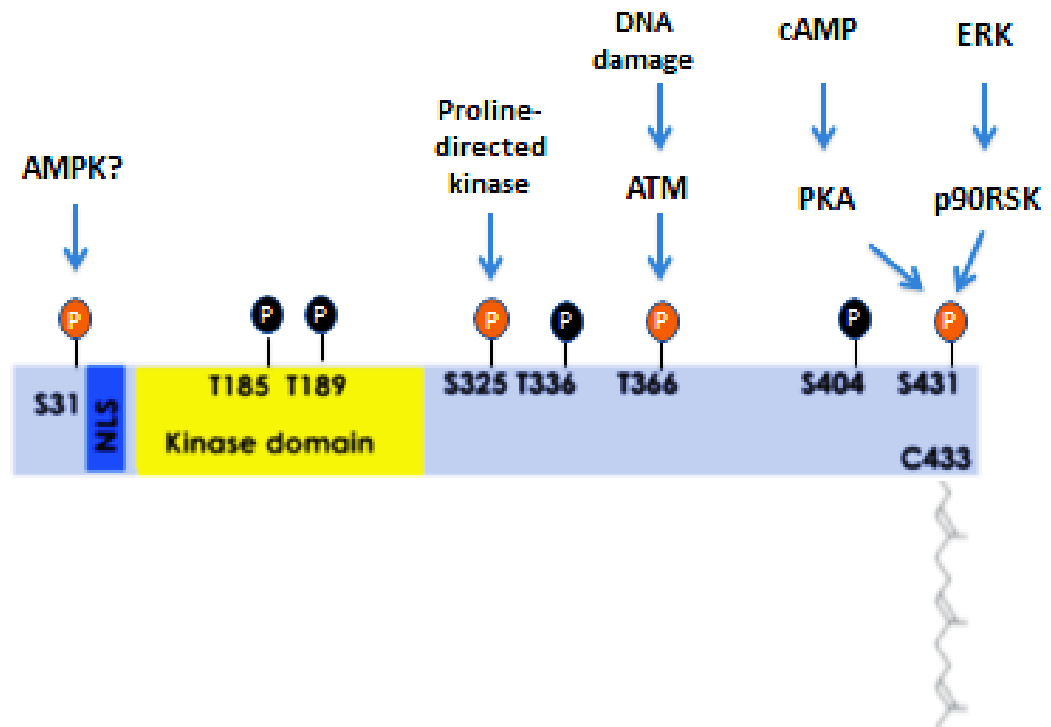
Figure 5.1: Schematic of the murine LKB1 sequence showing residues modified by post-translational modification

Murine LKB1 has 436 amino acids. The protein has an N-terminal domain, a kinase domain and a regulatory C-terminal tail. Multiple phosphorylation sites have been identified on the protein: four of these, namely, Thr-185, Thr-189, Thr-336 and Ser-404 are auto-phosphorylation sites. Thr-366 is phosphorylated by ATM, Ser-431 by PKA and p90RSK. Ser-325 lies in a proline-rich region and is likely to be phosphorylated by a proline- directed kinase. Ser-31 lies within an AMPK consensus recognition motif (Alessi et al., 2006).

5.1.3. The LKB1:STRAD:MO25 complex

LKB1 exists in a complex with two other proteins, the pseudokinase STRAD (Ste-20 related adapter protein) and the helical repeat protein MO25 (Mouse protein 25) (Alessi et al., 2006). Yeast two-hybrid screens using Kinase-dead LKB1 as bait, identified STRAD as an interacting protein (Baas et al., 2003). LKB1 was also detected in immunoprecipitates obtained from cell lysate using anti-STRAD monoclonal antibody (Baas et al., 2003). STRAD is classed as a pseudokinase, because although it bears similarity to the Ste-20 family of kinases, it lacks key residues required for catalytic activity. STRAD has two isoforms, namely, STRAD-α and STRAD-β. The STRAD-α gene is located on chromosome 17, while the STRAD-β gene is located on chromosome 2 in humans and the protein has a molecular weight of ~50 KDa (Baas et al., 2003). Binding of STRAD to LKB1 greatly enhances auto-phosphorylation of LKB1. LKB1 also phosphorylates STRAD at Thr-329 and Thr-419 (Baas et al., 2003). Binding of STRAD alters the sub-cellular localisation of LKB1. LKB1 alone, when expressed in cells localises to the nucleus, whilst co-expression of STRAD with LKB1 alters its localisation to the cytoplasm (Baas et al., 2003).

MO25 also has two isoforms, namely, MO25-α and MO25-β, which are highly similar, but lack homology to other proteins (Baas et al., 2003). MO25 was first identified as a gene that was expressed at the early cleavage stage in mouse embryogenesis (Miyamoto et al., 1993). When FLAG-tagged LKB1 was stably expressed in HeLa cells and the tagged protein was immunoprecipitated with anti-FLAG antibodies, the immunoprecipitate also showed the presence of MO25, suggesting that MO25 formed part of the LKB1 complex (Boudeau et al., 2003). MO25 is an armadillo-like, helical repeat protein with a concave protein binding surface. It

binds to STRAD by interacting with the WEF motif on its C-terminus, and this binding is abolished when the last 3 amino acids on STRAD are deleted (Boudeau et al., 2003, Milburn et al., 2004). However, binding of LKB1 to STRAD creates new binding sites for MO25, as it is able to bind to truncated STRAD mutants complexed with LKB1(Boudeau et al., 2003). Binding of MO25 stabilises the STRAD:LKB1 complex and further increases LKB1 activity (Boudeau et al., 2003).

The structure of the LKB1:STRAD:MO25 complex reveals that STRAD-α, although catalytically inactive, binds ATP and adopts a closed conformation like that of active kinases (Zeqiraj et al., 2009b). Also, unlike other kinases that are usually activated by phosphorylation, LKB1 is allosterically activated by binding to STRAD. This interaction is further strengthened by MO25 binding to STRAD though multiple residues on its concave surface (Zeqiraj et al., 2009a, Zeqiraj et al., 2009b). Mutations in the ATP binding pocket of STRAD have been shown to reduce LKB1 activity. Several mutations in LKB1 seen in patients with PJS were shown to affect its ability to bind STRAD and MO25, impairing the assembly and stability of the LKB1 complex, thereby affecting its activity (Zeqiraj et al., 2009a).

5.1.4 LKB1 is a master upstream kinase

LKB1 is the main upstream kinase that activates AMPK (Woods et al., 2003, Hawley et al., 2003, Shaw et al., 2004b). Apart from AMPK-α1 and AMPK-α2, LKB1 is known to phosphorylate 12 other protein kinases (BRSK1, BRSK2, NUAK1, NUAK2, QIK, QSK, SIK, MARK1, MARK2, MARK3, MARK4, and SNRK) that are located in the same branch of the human kineome dendrogram as AMPK, and share significant sequence homology with it within the kinase domain (Alessi et al., 2006). LKB1

phosphorylates key residues in the activation loop of these kinases, causing a 50-fold increase in their activity (Lizcano et al., 2004, Jaleel et al., 2005). These kinases are therefore much less active when expressed in LKB1-deficient cell lines. The *m*icrotubule-*a*ffinity *r*egulating *k*inases MARK1, MARK2, MARK3 and MARK4, which are orthologues of Par-1 in C. *elegans,* regulate cell polarity (Böhm et al., 1997, Drewes et al., 1997). NUAK 2, which is induced by cellular stresses and TNF, interacts with and phosphorylates *m*yosin *p*hosphatase *t*arget *s*ubunit-1 (MYPT-1) (Yamamoto et al., 2008). NUAK1 (also called *A*MPK *r*elated *k*inase-5 or ARK5) also interacts with MYPT-1 and has been reported to regulate cell adhesion by interacting with myosin phosphatases (Zagorska et al., 2010). The brain specific kinases BRSK1 and BRSK2, which (as their names suggest) are mainly expressed in the brain, regulate polarisation of neuronal cells (Kishi et al., 2005). Mice deficient in both these kinases (also called SAD-B and SAD-A), die due to the inability to polarise neurons into axons and dendrites (Kishi et al., 2005). The *s*alt *i*nducible *k*inases SIK 1 and SIK 2, phosphorylate TORC2 (also called CRTC2) at Ser-171, a site that is also phosphorylated by AMPK (Katoh et al., 2004, Screaton et al., 2004). Phosphorylation of CRTC2 on this site leads to its cytoplasmic sequestration, thereby preventing CREB-dependent transcription (Screaton et al., 2004). SIK2 is present mainly in adipose tissue and has been shown to phosphorylate *i*nsulin *r*eceptor *s*ubstrate-1 (IRS-1) on Ser-794 and may play a role in regulating adipocyte metabolism (Katoh et al., 2004, Horike et al., 2003).

5.1.5 LKB1 is a tumour suppressor

LKB1 is critically important in embryonic development as deletion of both LKB1 alleles leads to embryonic lethality at mid-gestation (embryonic day 8.5 to 11). The non-viable LKB1-null embryos had severe neural tube defects and vascular abnormalities (Ylikorkala et al., 2001, Jishage et al., 2002). LKB1$^{+/-}$ embryos were viable, but showed polyp formation at around 10 months of age. These polyps, although found in the stomach, were histologically similar to intestinal polyps seen in patients with PJS (Jishage et al., 2002, Bardeesy et al., 2002). LKB1$^{+/-}$ mice also developed spontaneous hepatocellular carcinoma (Miyoshi et al., 2009). These studies suggested that haplo-insufficiency was sufficient to cause polyp formation (Miyoshi et al., 2009, Jishage et al., 2002). However, another study showed complete loss of the LKB1 protein in the polyps, suggesting epigenetic inactivation of the second allele (Bardeesy et al., 2002). LKB1$^{fl/fl}$ hypomorphic mice expressing five to ten fold less LKB1 than wild type mice did not develop tumours spontaneously, also suggesting that complete loss of LKB1 was required for tumour formation (Huang et al., 2008). Moreover, over-expression of wildtype LKB1 in LKB1-deficient cell lines such as HeLa and G361 melanoma cells lines leads to a G1 cell cycle arrest (Tiainen et al., 1999). These findings, taken together, emphasise the role of LKB1 as a tumour suppressor.

5.1.6 Splice variants of LKB1

During purification from rat liver, two forms of the LKB1:STRAD:MO25 complex were resolved. The LKB1 polypeptide in the two forms showed differing mobilities on SDS-PAGE (Hawley et al., 2003). These two forms were identified by tryptic peptide

mass fingerprinting to be splice variants derived from the *STK11* gene encoding LKB1, and were termed LKB1$_L$ (long) and LKB1$_S$ (short) (Towler et al., 2008). Both LKB1$_L$ and LKB1$_S$ share the first 373 residues, which are encoded by exons 1-8. Due to alternative splicing, LKB1$_S$, has a unique 39 residue sequence at its C-terminus, encoded by exon 9A, whereas, LKB1$_L$ has a distinct 63 residue sequence encoded by exon 9B. The LKB1$_L$ protein has 436 amino acids, while LKB1$_S$ has 412 amino acid residues. Therefore LKB1$_S$ lacks two sites of post-translational modification, namely, Ser-431 and the farnesylation site on Cys-433. LKB1$_L$ was the predominant isoform found in most tissues, although LKB1$_S$ could also be detected ubiquitously, albeit at lower levels (Towler et al., 2008). Interestingly, LKB1$_S$ has been shown to be required for spermiogenesis, as male mice unable to generate LKB1$_S$ are sterile with 98% reduction in the number of sperm found in the epididymis compared to wild type mice (Towler et al., 2008). GST-LKB1$_S$ expressed and purified from HEK 293 cells, was able to phosphorylate a GST-fused kinase domain of AMPK α1 more rapidly than GST-LKB1$_L$ (Towler et al., 2008). However, both proteins had similar substrate specificity against AMPK and the ARKs (Towler et al., 2008).

5.1.7 The C-terminal tail of LKB1 and its effect on AMPK activity

Although LKB1 is required for activation of AMPK and ARKs in most cells, most evidence available suggests that it is constitutively active. However, there are now many indications that the C-terminal tail of LKB1 is a regulatory region whose phosphorylation affects AMPK activation. Mutations in the C-terminal region of LKB1 in some cases of PJS and sporadic tumours have been shown to be associated with reduced AMPK phosphorylation as well as impaired polarisation of intestinal cells

(Forcet et al., 2005). Interestingly, two of these mutations, namely P324L and T367M, were adjacent to the Ser-325 and Thr-363 (equivalent to Thr-366 in mouse LKB1) phosphorylation sites. This suggested that these mutations might interfere with phosphorylation of these residues. These LKB1 mutants also activated AMPK to a lower extent than the wild type protein (Forcet et al., 2005). LKB1 is phosphorylated on Ser-431 by agonists that activate p90RSK and PKA (Sapkota et al., 2001). Phosphorylation on this site was initially shown to be required to inhibit cell growth , as wild type LKB1 expressed in G361 melanoma cells caused inhibition of cell growth, whereas, cells expressing an LKB1 mutant, where Ser-431 was mutated to alanine were unable suppress cell growth (Sapkota et al., 2001). Phosphorylation of Ser-431 by protein kinase Cζ was also reported to be required for phosphorylation of Thr-172 on AMPK in bovine aortic endothelial cells in response to metformin treatment (Xie et al., 2008). However, our laboratory found that LKB1 truncated to residue 343 (which lacks most of the C-terminal tail), is still able to form a complex with STRAD and MO25. This mutant is able to activate AMPK in cell free assays as well as in intact cells (Fogarty S 2008, PhD thesis). Moreover, expression of $LKB1_S$ (the short splice variant of murine LKB1 containing residues 1-412 which also lacks the Ser-431 residue) or $LKB1_L$ (full length murine LKB1 containing 436 amino acid residues) or $LKB1_L$ where the Ser-431 site was mutated to alanine in HeLa cells, all caused a similar increase in AMPK activity compared to cells expressing the empty vector (Fogarty and Hardie, 2009). Our laboratory also showed that Ser-431 phosphorylation was not required for cell cycle arrest, although the effect of this mutation on cell survival and growth was not tested (Fogarty and Hardie, 2008).

Zheng et al have reported that Ser-325 and Ser-431 on the C-terminal tail of LKB1 are phosphorylated in melanoma cells carrying the V600E mutation in B-RAF

(present in -50% of malignant melanomas) (Zheng et al., 2009). The authors of the paper proposed that Ser-325 was phosphorylated by ERK and Ser-431 by p90RSK respectively, downstream of the RAF-MEK-ERK pathway that is activated by the V600E mutation (Figure 5.2). The melanoma cells carrying the B-RAF V600E mutation also exhibited reduced AMPK activity and it was proposed that this was caused by phosphorylation of the C-terminal sites in LKB1. However, as the Ser-325 site is flanked by multiple proline residues, a proline-directed kinase has been proposed as the likely upstream kinase that phosphorylates this site (Alessi et al., 2006).
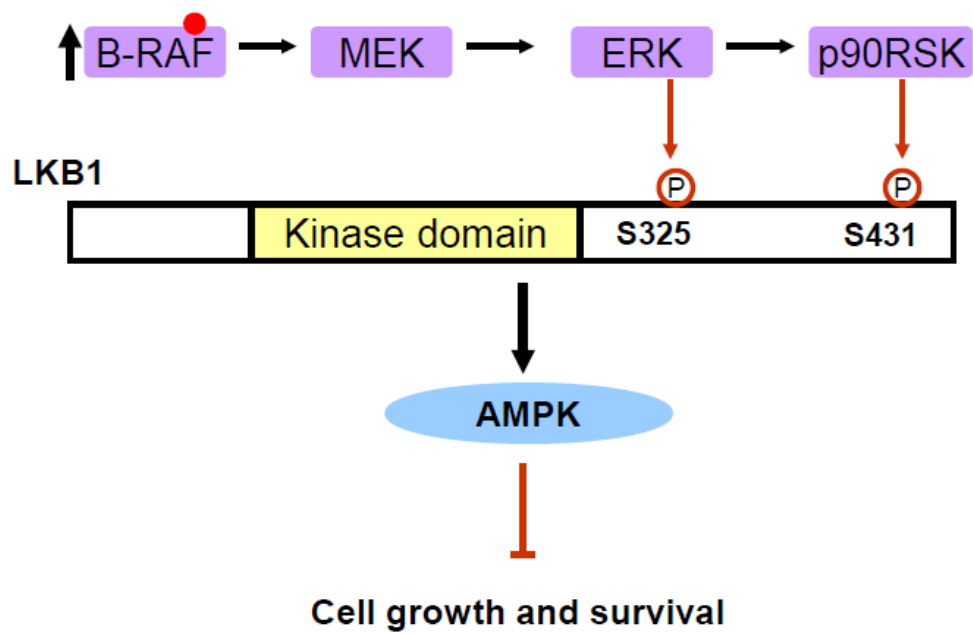
Figure 5.2: Schematic showing the proposed effect of C-terminal phosphorylation of LKB1 on AMPK activity

This model proposes that Ser-325 is phosphorylated by ERK in melanoma cells expressing the B-RAF (V600E) mutation, which renders B-RAF constitutively active. This in turn activates MEK and ERK, leading to phosphorylation of both Ser-325 and Ser-431 on LKB1. LKB1, phosphorylated on both these sites is then less effective at activating AMPK compared to the wildtype protein in these cells (Zheng et al., 2009).

5.2 AIMS

The main aim of the chapter was to test whether Ser-325 and Ser-431 phosphorylation on LKB1 affected AMPK activity. The requirement for Ser-325 and Ser-431 on LKB1 was initially tested by mutating these to non-phosphorylatable alanine residues. These mutants were expressed in HeLa cells and purified and the ability of these mutants to activate bacterially expressed AMPK heterotrimer was measured using a cell-free assay system.

We also aimed to test whether ERK2 phosphorylated Ser-325 on LKB1 and to determine the stoichiometry of the phosphorylation in a cell free system. We then aimed to phosphorylate Ser-325 and Ser-431 in a recombinant LKB1 complex (expressed in HeLa cells) by ERK2 and p90RSK and test the ability of this LKB1 complex to phosphorylate a bacterially expressed AMPK complex in a reconstituted cell free system.

5.3 RESULTS

5.3.1 Cloning and expression of GST- tagged wild type and mutant LKB1 complexes

Rat LKB1 fused to Glutathione-S-transferase (hereafter termed GST-LKB1$_{WT}$) was a gift from Sarah Fogarty, a former PhD student in the lab. Site-specific, non-phosphorylatable alanine mutants for the Ser-325 (GST-LKB1$_{S325A}$) and Ser-431 (GST-LKB1$_{S431A}$) sites were generated by site-directed mutagenesis of the wild type DNA, as described in the Methods section (section 2.2.1). In addition a double-alanine mutant, where both the sites were mutated (GST-LKB1$_{S325A/S431A}$ or GST-LKB1$_{AA}$) was also generated. HeLa cells, which lack LKB1, were transfected with the wild type and mutant GST-LKB1, along with its accessory proteins, namely STRAD-α, which contained a FLAG tag and MO25-α, which contained a myc tag. The LKB1 complex was detected in the cell lysate obtained 36 hours after transfection by probing Western blots for the GST, FLAG and myc tags respectively (Figure 5.3). As expected, non-transfected HeLa cells lacked all components of the LKB1 complex. GST-LKB1, FLAG-STRAD and myc-MO25 were detected in HeLa cells transfected with GST-LKB1$_{WT}$, GST-LKB1$_{S325A}$, GST-LKB1$_{S431A}$ and GST-LKB1$_{AA}$ constructs. The S325A and S431A mutants were expressed to a similar extent as the wild type LKB1 protein. The expression of the GST-LKB1$_{AA}$ protein was, however, slightly lower than that of the wild type protein.
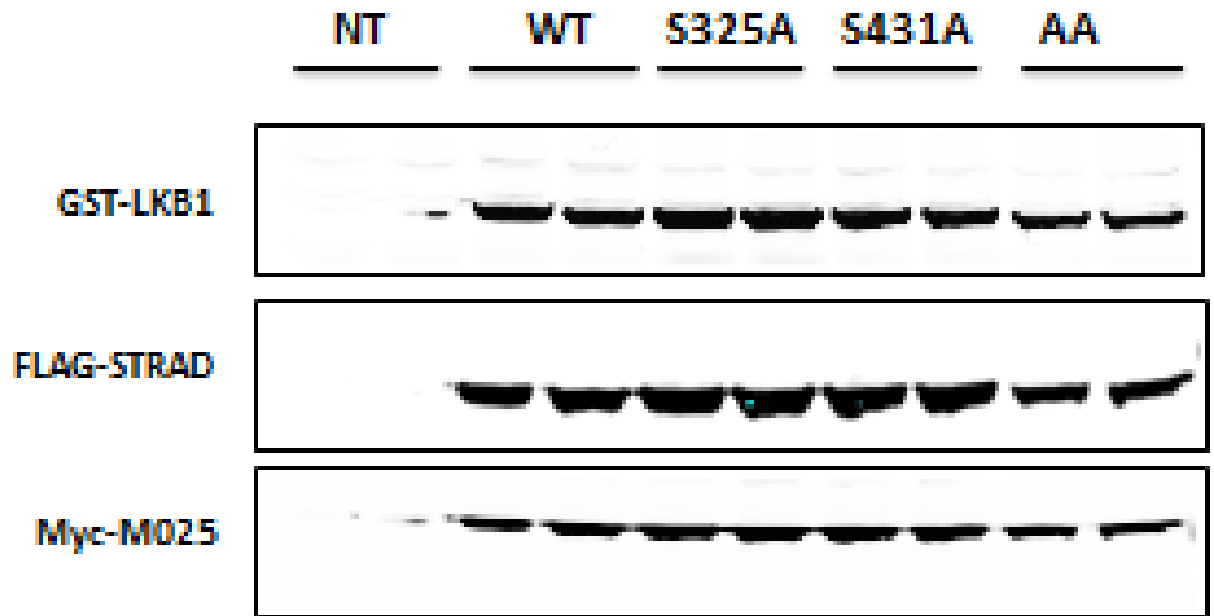
Figure 5.3: Expression of wild type and mutant LKB1 in HeLa cells

GST-tagged wild type LKB1, as well as S325A, S431A and AA mutants were expressed along with FLAG-STRAD and myc-MO25 in HeLa cells. Non-transfected cells were used as negative controls. LKB1 was detected by anti- GST, STRAD was detected by anti- FLAG and MO25 was detected by anti-myc antibodies respectively.

5.3.2 Affinity purification of LKB1 using glutathione- Sepharose

Following expression of GST-LKB1$_{WT}$, GST-LKB1$_{S325A}$, GST-LKB1$_{S431A}$ and GST-LKB1$_{AA}$ with STRAD and MO25 in HeLa cells, the LKB1 complexes were purified by incubating the cell lysates with glutathione-Sepharose beads, which bind GST. Following a number of washing steps to remove unbound proteins, GST-LKB1 protein was then eluted in buffer containing glutathione, which displaces the GST-tagged protein from the glutathione-Sepharose beads. GST-LKB1 was therefore, highly enriched in the eluate (Figure 5.4). As expected, STRAD and MO25 were also detected in the purified eluate. However, while most of the GST-LKB1 was bound to the beads and very little was detectable in the supernatant or wash, only a proportion of the STRAD and MO25 initially present in the lysate was detectable in the eluate. Most of the expressed STRAD and MO25 could be detected in the supernatant. This was probably due to overexpression of STRAD and MO25, relative to LKB1. Due to competition for expression between the three expression vectors for the same biosynthetic pathways in cells, it is likely that the smaller proteins, namely STRAD and MO25, were expressed more efficiently. Also, only the fraction of STRAD and M025 bound to LKB1 would be present in the eluate. Coomasie staining was performed to ensure that the eluate was free from contamination by other proteins. The relative amount of LKB1 in the eluate obtained from cells expressing LKB1 mutants was similar to that obtained from cells expressing wild type LKB1 when quantified with bovine serum albumin standards (5ng of LKB1/ µl of eluate).
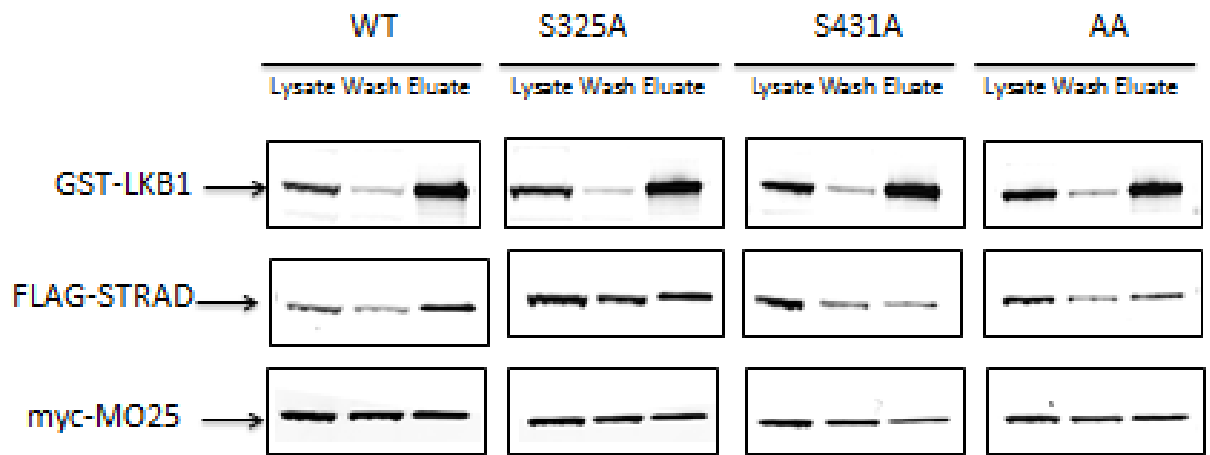
Figure 5.4: Purification of the LKB1:STRAD:MO25 complex from cell lysates

GST-LKB1$_{WT}$, GST-LKB1$_{S325A}$, GST-LKB1$_{S431A}$ and GST-LKB1$_{AA}$ constructs were transfected along with FLAG-STRAD and myc-MO25 in HeLa cells. The LKB1 complex was purified by incubating the cell lysate with glutathione-Sepharose beads. The LKB1 complex was then eluted in buffer containing glutathione. Anti-GST, anti-Flag and anti-myc antibodies were used to detect LKB1, STRAD and MO25 in the lysate, supernatant (wash) and the eluate.

5.3.3 Phosphorylation of Ser-325 and Ser-431on LKB1 does not affect AMPK activity

The effect of Ser-325 and Ser-431 phosphorylation on the ability of LKB1 to phosphorylate AMPK was tested in a cell-free system. GST-LKB1$_{WT}$, GST-LKB1$_{S325A}$, GST-LKB1$_{S431A}$ and GST-LKB1$_{AA}$, in complex with STRAD and MO25, purified as described in the previous section, was used to phosphorylate bacterially expressed AMPK heterotrimer (5 µg AMPK per 20 µl reaction). AMPK activity was then measured by its ability to phosphorylate its peptide substrate *AMARA*. GST-LKB1$_{S325A}$, GST- LKB1$_{S431A}$ and GST-LKB1$_{AA}$, were able to phosphorylate AMPK to a similar extent, which was similar to GST-LKB1$_{WT}$ (Figure 5.5). These results suggest that in a cell-free system, phosphorylation of Ser-325 and Ser-431 residues of LKB1 did not significantly affect its ability to activate AMPK. This result is consistent with previous results from our laboratory showing that GST-LKB1$_{S431A}$ activated the GST-AMPKα1 kinase domain to a similar extent as GST-LKB1$_{WT}$ (Fogarty and Hardie, 2009).
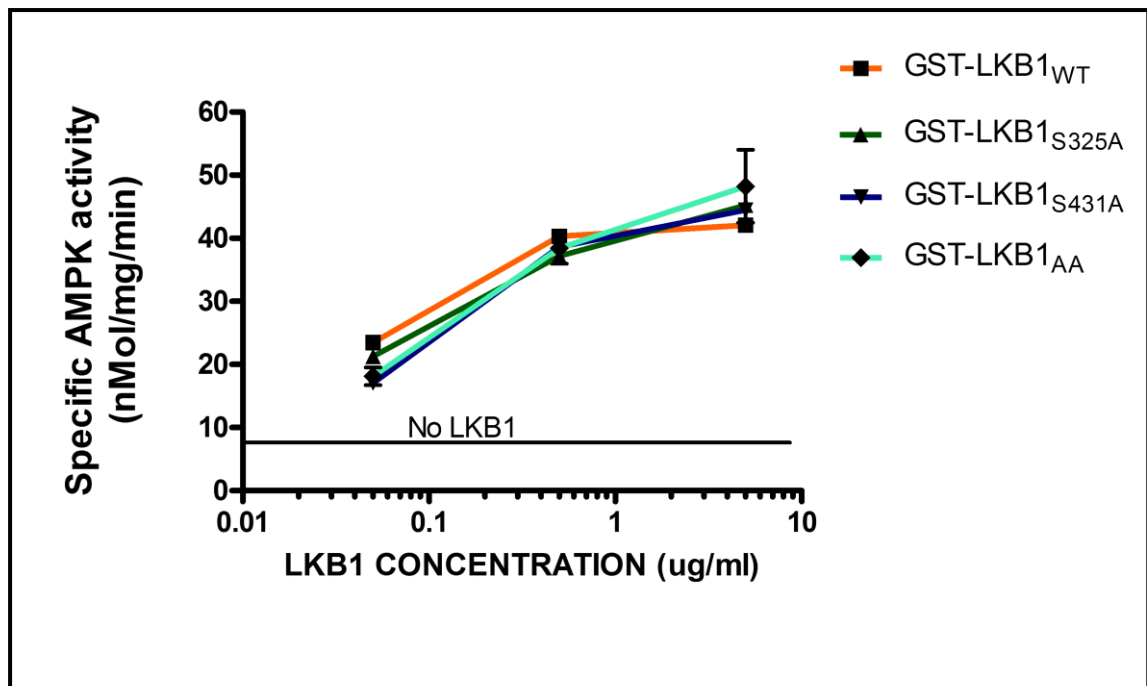
Figure 5.5: Activity of GST-LKB1$_{WT}$, GST-LKB1$_{S325A}$, GST-LKB1$_{S431A}$ and GST-LKB1$_{AA}$

HeLa cells were transfected with GST-LKB1$_{WT}$ or GST-LKB1$_{S325A}$ or GST-LKB1$_{S431A}$ or GST-LKB1$_{AA}$, along with FLAG-STRAD and myc-MO25. LKB1 complexes were purified from cell lysate using glutathione-Sepharose. The activity of GST-LKB1$_{WT}$, GST-LKB1$_{S325A}$, GST-LKB1$_{S431A}$ and GST-LKB1$_{AA}$ was measured by assessing their ability to activate bacterially expressed AMPK heterotrimer using the *AMARA* peptide substrate. Results shown are representative of three individual experiments.

5.3.4 Phosphorylation of Ser-431 on LKB1 by p90RSK does not affect AMPK activity

The ability of GST-LKB1$_{S431A}$ to activate the isolated AMPK kinase domain in a cell-free system was shown to be similar to that of GST-LKB1$_{WT}$ (Fogarty and Hardie, 2009). Moreover, HeLa cells transfected with GST-LKB1$_{WT}$ and treated with forskolin, which activated p90RSK, had similar activity to transfected cells treated with vehicle (Fogarty and Hardie, 2009). The aim of the next experiment was to test if phosphorylation of LKB1 on Ser-431 by p90RSK affected its ability to phosphorylate bacterially expressed AMPK heterotrimer in a cell-free system. The first step was to verify that recombinant p90RSK, produced in insect cells (obtained from the Division of Signal Transduction Therapy, University of Dundee) phosphorylated Ser-431 on LKB1 and to test the specificity of the anti-phosphoSer-431 (anti-pS431) antibody (also obtained from the Division of Signal Transduction Therapy, University of Dundee). GST-LKB1$_{WT}$, as well as GST-LKB1$_{S325A}$, GST-LKB1$_{S431A}$ and GST-LKB1$_{AA}$ complexes were incubated with p90RSK in the presence of Mg-ATP at 30°C for 30 minutes on a shaker. The reaction was stopped by adding LDS buffer and the proteins resolved by SDS-PAGE. The blots were then probed with anti-pS431 antibody, as well as total LKB1 (Figure 5.6). p90RSK phosphorylated GST-LKB1$_{WT}$, as well as GST-LKB1$_{S325A}$, but not GST-LKB1$_{S431A}$ and GST-LKB1$_{AA}$ in a concentration-dependent manner. This result was consistent with published studies and also confirmed the specificity of the anti-pS431 antibody. Despite the undetectable phospho-signal on western blotting, it is possible that some phosphorylation of the Ser-431 residue was present under basal conditions, which has not been quantified, A better approach would have been to pre-treat LKB1 with phosphatase before incubation with p90RSK.
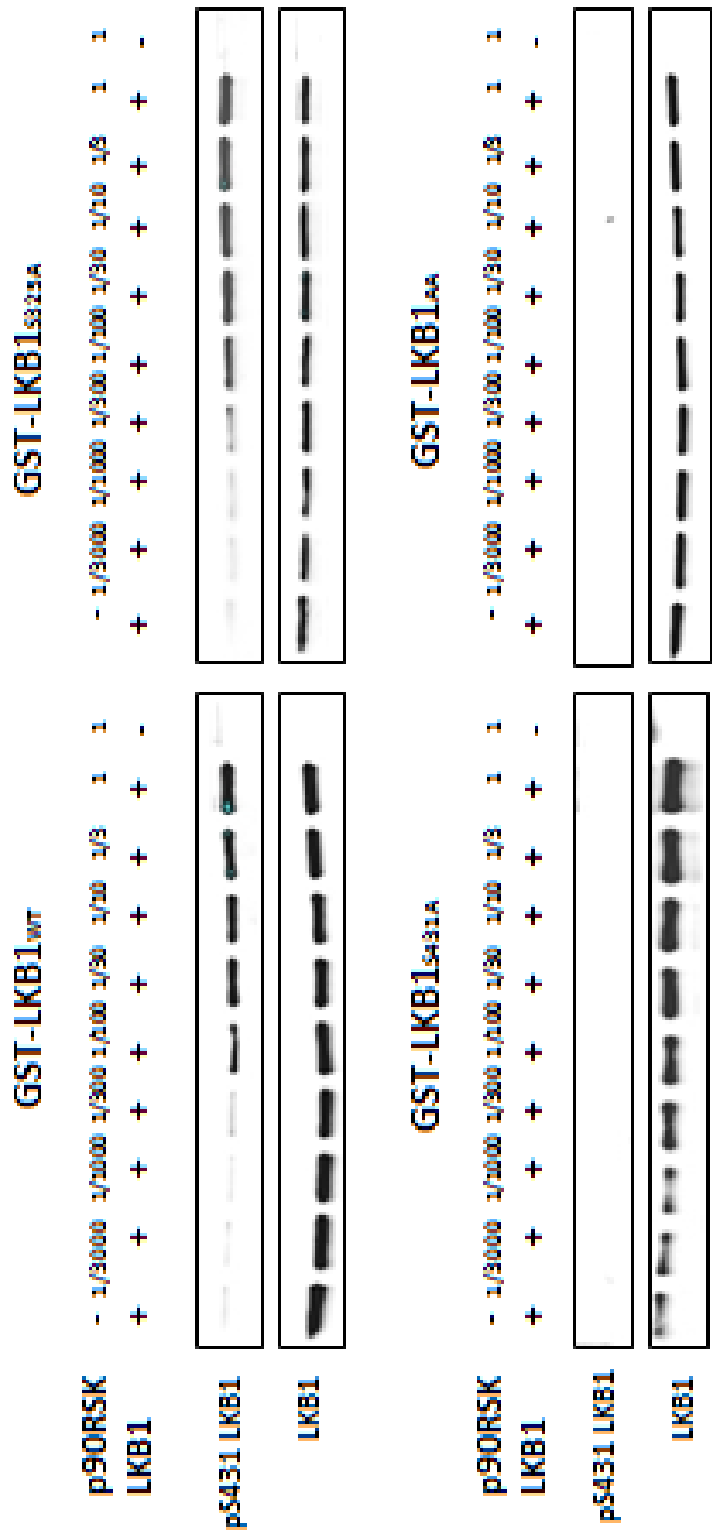
Figure 5.6: LKB1 is phosphorylated on Ser-431 by p90RSK

GST-LKB1$_{WT}$, GST-LKB1$_{S325A}$, GST-LKB1$_{S431A}$ and GST-LKB1$_{AA}$ were expressed in HeLa cells along with FLAG-STRAD and myc-MO25 and cell lysates purified using glutathione-Sepharose beads. The LKB1 complexes were incubated with increasing concentrations of p90RSK for 30 minutes at 30°C and the reaction stopped by adding LDS. The proteins were resolved by SDS-PAGE and the blots probed with anti-pS431 and anti-LKB1 antibodies.

After ascertaining that LKB1 was phosphorylated on Ser-431 by p90RSK, its effect on AMPK activity was measured. As this involved three serial phosphorylation reactions, namely, p90RSK phosphorylating LKB1, LKB1 phosphorylating AMPK which in turn phosphorylates *AMARA,* and this effect had to be measured at varying concentrations of LKB1, the first reaction was performed during the purification of recombinant LKB1 complexes. HEK 293 cells were transfected with GST-LKB1$_{WT}$ or GST-LKB1$_{S431A}$ or GST-LKB1$_{AA}$, along with FLAG- STRAD and myc-MO25. The LKB1 complex was purified using glutathione-Sepharose. While the LKB1 complex was still bound to the Sepharose beads, the beads were incubated with recombinant p90RSK in the presence of Mg^{2+} and ATP at 30°C for 30 minutes on a shaker. A 1: 30 dilution of p90RSK (which maximally phosphorylated LKB1 as shown in Figure 5.6) or buffer (with no p90RSK) was used to phosphorylate GST-LKB1$_{WT}$, GST-LKB1$_{S431A}$ and GST-LKB1$_{AA}$. The reaction was stopped by spinning the beads down and aspirating the supernatant (containing p90RSK), followed by several wash steps. The LKB1 complex was then eluted in buffer containing glutathione and quantified using BSA standards. Varying concentrations of the eluate were then used to phosphorylate bacterially expressed AMPK heterotrimer. Ser-431 phosphorylation on GST-LKB1$_{WT}$ was confirmed by Western blotting and probing blots using anti-pS431 antibody (Figure 5.7). As expected, p90RSK phosphorylated the Ser-431site on GST-LKB1$_{WT,}$ but not on GST-LKB1$_{S431A}$ or GST-LKB1$_{AA,}$ which lacked the serine residue.

Different concentrations of the GST-LKB1$_{WT}$ and GST-LKB1$_{S431A}$ complexes, which had or had not been incubated with p90RSK, were then used to phosphorylate AMPK heterotrimer in the presence of Mg-ATP, following which, the activity of the AMPK heterotrimer in each reaction was measured using the *AMARA* peptide substrate (Figure 5.8). Phosphorylation of Ser-431 did not affect the ability of GST-LKB1$_{WT}$ to

activate AMPK. GST-LKB1$_{S431A}$, which cannot be phosphorylated by p90RSK, activated AMPK to a similar extent as the GST-LKB1$_{WT}$. As expected, the activity of GST-LKB1$_{S431A}$ was not affected by incubation with p90RSK.

A.
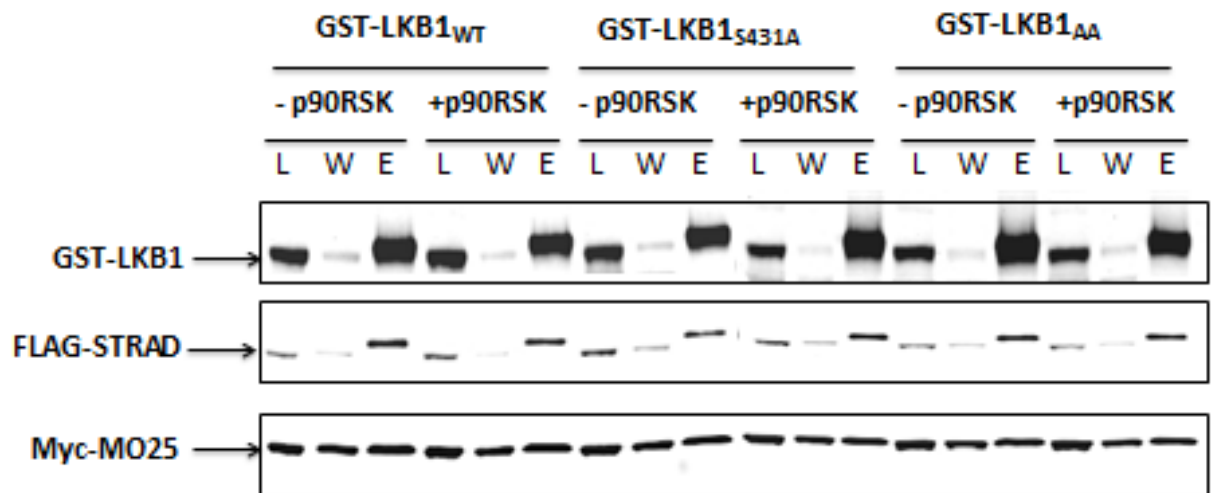
B.
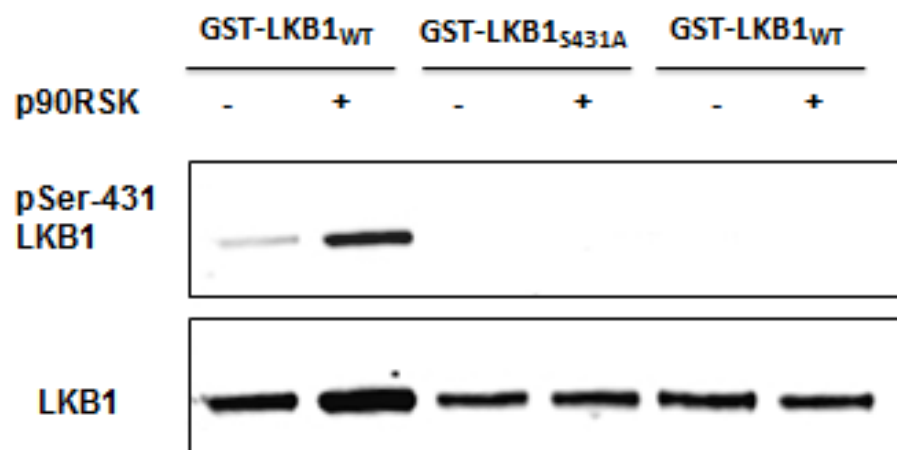
Figure 5.7: Recombinant p90RSK phosphorylates Ser-431 on LKB1 in a cell-free system

(A)   HEK293 cells were transfected with GST-LKB1$_{WT}$, GST- LKB1$_{S431A}$ or GST- LKB1$_{AA}$, along with FLAG-STRAD and myc-MO25. The LKB1 complex was purified using glutathione-Sepharose. LKB1 complexes bound to the Sepharose beads were incubated with recombinant p90RSK in the presence of Mg- ATP. The LKB1 complex was then eluted with buffer containing glutathione. The lysate (L), wash (W) and eluate (E) were subjected to Western blotting. Anti-GST, anti-FLAG and anti-myc antibodies were used to detect LKB1, STRAD and MO25.

(B)   The eluate containing LKB1 complexes were subjected to Western blotting. Anti-pS431 and anti-LKB1 antibodies were used to detect phosphorylation of LKB1 on Ser-431.
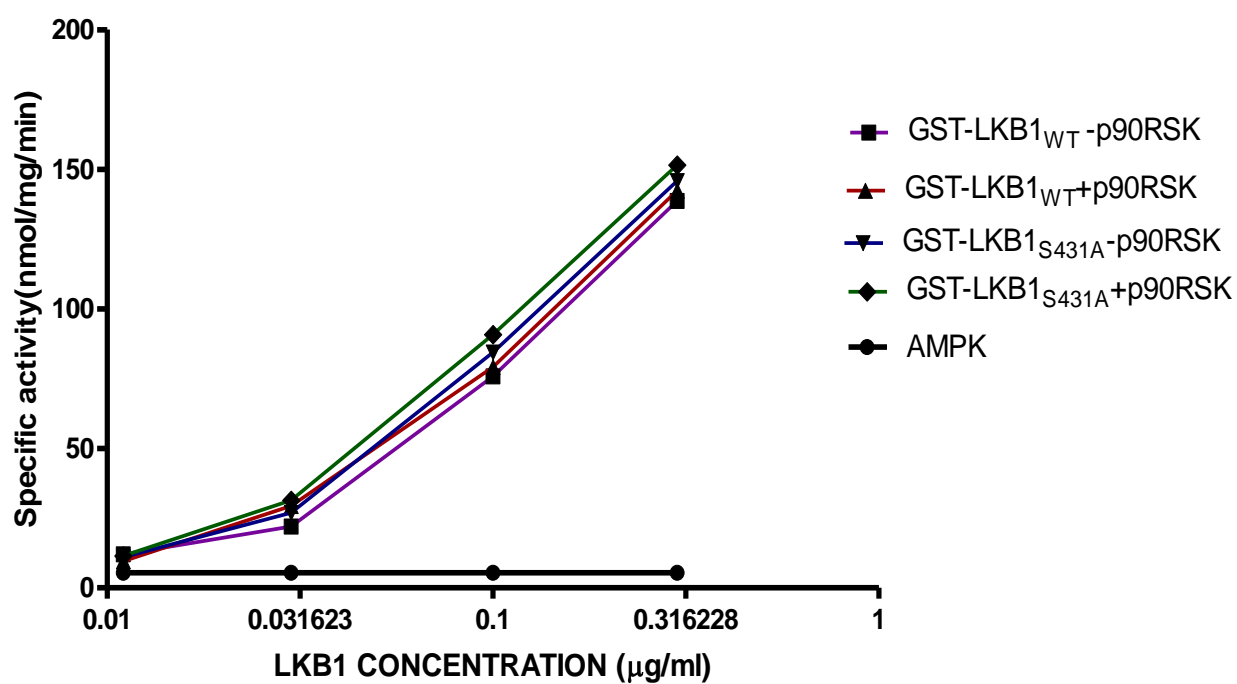
Figure 5.8: Phosphorylation of LKB1 on Ser-431 by p90RSK does not affect AMPK activity

GST-LKB1$_{WT}$ or GST-LKB1$_{S431A}$ complex, which either had or had not been incubated with p90RSK, were used to phosphorylate AMPK heterotrimer in the presence of Mg- ATP, following which, the activity of the AMPK heterotrimer in each reaction was measured using the *AMARA* peptide substrate.

5.3.5 ERK does not stoichiometrically phosphorylate Ser-325 on LKB1

As mentioned earlier in the chapter, Zheng et al published results showing that the MAP kinase ERK2 phosphorylated LKB1 on Ser-325 (Zheng et al., 2009). However, the authors did not clarify the stoichiometry of this reaction, which would serve as a measure of the functional role of this modification on LKB1, as well as whether ERK was effective as an upstream kinase phosphorylating LKB1. The main aim of the experiments detailed in this section was to confirm the stoichiometry of this phosphorylation reaction. Wild type human GST-LKB1 (GST-LKB1$_{WT}$) and kinase-dead mutant LKB1 (GST-LKB1$_{KD}$) were kinds gift from Prof. Dario Alessi. Site-directed mutagenesis was used to generate site-specific alanine mutants of both of these proteins (GST-LKB1$_{S325A}$ and GST-LKB1$_{KD/S325A}$). The GST-LKB1$_{KD}$ was expressed in HeLa cells, which lack endogenous LKB1, and was purified as detailed previously. After the protein was bound to glutathione-Sepharose, the beads were treated with protein phosphatase to dephosphorylate the protein, followed by wash steps before elution of the GST-LKB1$_{KD}$. HeLa cells were also transfected with DNA encoding GST-ERK2 (obtained from the Division of Signal Transduction Therapy, University of Dundee) and were then treated with phorbol 12-myristate 13-acetate (PMA), a phorbol ester that activates ERK in cells. The cells were then lysed and the GST-ERK2 was purified using glutathione-Sepharose beads as previously described. Varying concentrations of GST-ERK2 were then incubated with dephosphorylated GST-LKB1$_{KD}$ in the presence of ATP and Mg^{2+} at 30°C on a shaker for 15 minutes. The kinase-dead LKB1 mutant was used instead of the wild type protein to prevent auto-phosphorylation. The reaction was then stopped by adding LDS buffer and boiling the

samples. SDS-PAGE was then carried out and the membrane probed with anti-pS325 antibody. Unfortunately no signal was seen (data not shown). This either meant that the antibody was unable to detect phosphoSer-325 or that ERK2 did not phosphorylate this site; therefore phosphorylation using $[\gamma^{32}P]$-ATP followed by autoradiography was performed. The experiment was repeated by incubating the GST-ERK2 with GST-LKB1$_{KD}$ in the presence of $[\gamma^{32}P]$-ATP and Mg^{2+} and the reaction was stopped by adding LDS buffer. The reaction mixes were resolved using SDS-PAGE, the gel was dried and autoradiography performed. Most of the signal obtained corresponded to GST-ERK2 and the intensity increased with increasing ERK concentration, suggesting auto-phosphorylation of GST-ERK2. A very faint band was seen corresponding to GST-LKB1$_{KD}$, which took 24 hour exposure to become evident (Figure 5.9). The bands were then cut out and the $[\gamma^{32}P]$-ATP incorporation in the samples as well as a standard was measured using a scintillation counter. The stoichiometry of phosphorylation was then calculated to be 0.1 mol/mol, suggesting that ERK2 only weakly phosphorylated LKB1 in this cell-free system. However, this experiment could be improved by repeating this experiment with a known ERK2 substrate in parallel as a positive control.

As ERK2 did not seem to phosphorylate LKB1 on Ser-325 significantly in a cell-free system, the likelihood of its ability to phosphorylate LKB1 on Ser-325 in intact cells seemed very low. Therefore due to the lack of promising results, further experiments to test whether maximal phosphorylation on both sites, Ser-325 and Ser-431, by ERK2 and p90RSK activation, affected AMPK activity were not carried out.
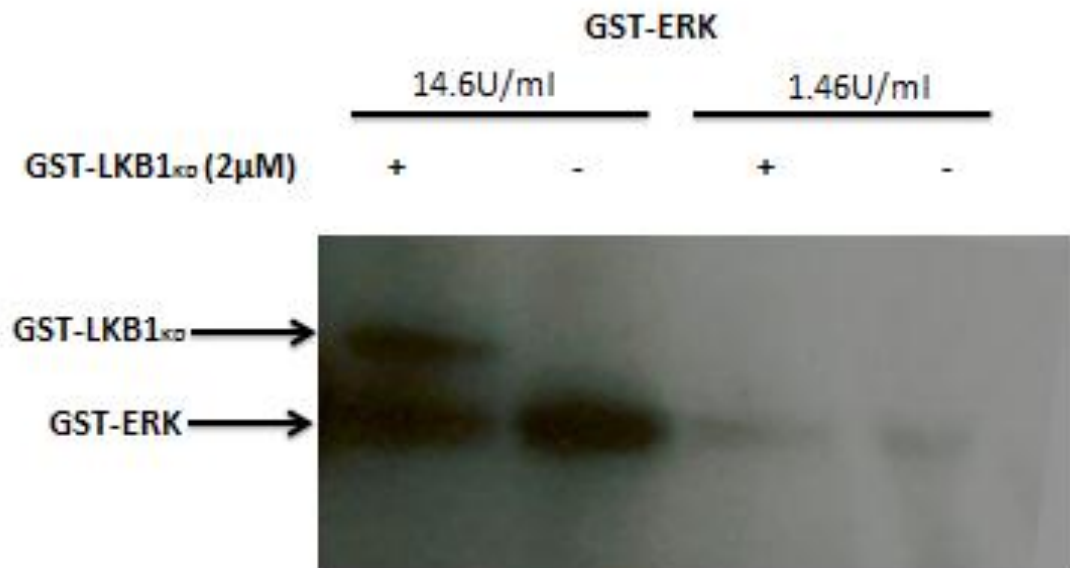
Figure 5.9: GST-ERK weakly phosphorylates GST-LKB1$_{KD}$

GST-ERK2 was incubated with GST-LKB1$_{KD}$ in the presence of Mg^{2+} and [γ^{32}P]-ATP. The reaction mixes were resolved using SDS-PAGE, the gel was dried and autoradiography performed. The bands were cut and [γ^{32}P]-ATP incorporation measured in a scintillation counter to calculate the stoichiometry of phosphorylation.

5.4 DISCUSSION

PJS syndrome is caused by mutations in the LKB1 gene, which mainly affect its catalytic activity. However Forcet et al reported that some C-terminal tail mutations, notably P324L and T367M, while not affecting the sub-cellular localisation of LKB1 or its binding of STRAD, reduced its ability to phosphorylate and activate AMPK (Forcet et al., 2005). The P324L mutation lies adjacent to Ser-325, which is likely to be phosphorylated by a proline-directed kinase and T367M is close to the ATM phosphorylation site (Thr-363 in human LKB1). Previous reports also suggested that Ser-431 phosphorylation was required for LKB1-mediated cell cycle arrest (Sapkota et al., 2001). However, our laboratory found that Ser-431 phosphorylation was not required for cell cycle arrest (Fogarty and Hardie, 2009). Moreover, the non-phosphorylatable alanine mutant LKB1$_{S431A}$ activated the isolated AMPK-α kinase domain to a similar extent as wild type LKB1 (Fogarty and Hardie, 2009).

The possible regulatory role of the C-terminal tail of LKB1 was again emphasised by observations that melanoma cells with constitutive activation of B-RAF, caused by the V600E mutation in the latter, had reduced AMPK activity. The authors proposed that the MEK-ERK-p90RSK pathway was activated downstream of the activated B-RAF, and that ERK2 phosphorylated Ser-325 and p90RSK phosphorylated Ser-431 on LKB1. Phosphorylation of LKB1 on both of these sites was claimed to reduce AMPK activity (Zheng et al., 2009). The main aim of the chapter was to test whether phosphorylation of Ser-325 was indeed mediated by ERK, as although LKB1 has a proline residue after the serine at the 325 position, it does not possess the typical ERK phosphorylation motif, which in addition to Ser/Pro at the phosphorylation site,

would normally require the presence of a DEF motif (F-X-F-P) or D-domain (which are ERK binding motifs) (Fernandes and Allbritton, 2009).

The aim of the first experiment was to test whether phosphorylation of Ser-325 and Ser-431 affected AMPK activity. The ability of LKB1 containing complexes GST-LKB1$_{WT}$, GST-LKB1$_{S325A}$, GST-LKB1$_{S431A}$ or GST-LKB1$_{AA}$ to activate AMPK heterotrimer was tested in a cell-free system. All of the mutants activated AMPK to the same degree as that of the wild type LKB1, suggesting that phosphorylation of the C-terminal tail of LKB1 on Ser-325 and Ser-431 did not affect its ability to AMPK in a cell-free system.

It had previously been demonstrated in our laboratory that Ser-431 phosphorylation on LKB1did not affect activation of the isolated recombinant AMPK kinase domain (Fogarty and Hardie, 2009). The result that GST-LKB1$_{WT}$, GST-LKB1$_{S431A}$ and GST-LKB1$_{AA}$, all activated AMPK heterotrimer to the same extent was consistent with the published results. Moreover, p90RSK-mediated Ser-431 phosphorylation on GST- LKB1$_{WT}$ activated AMPK heterotrimer to the same extent as GST-LKB1$_{WT}$ that had not been phosphorylated by p90RSK.

The next step was to test whether ERK2 significantly phosphorylated the Ser-325 site. Phosphorylation using unlabelled Mg-ATP, followed by Western blotting did not give conclusive results, because no signal was detectable using the anti-pS325 antibody. Therefore, incorporation of [γ^{32}P]-ATP into GST-LKB1$_{KD}$ by ERK2 was measured using autoradiography. The stoichiometry of phosphorylation was also estimated. Most of the γ^{32}P was incorporated into GST-ERK itself rather than LKB1, suggesting auto-phosphorylation. This auto-phosphorylation was concentration-dependent. It took a very long exposure time of around 24 hours before the LKB1 band

became visible after autoradiography, and even after this time, the stoichiometry of phosphorylation was very low. This suggested that ERK2, which was maximally activated by treatment of cells with PMA, only weakly phosphorylated LKB1 on Ser-325. This was in contrast to the results of Zheng et al, which demonstrated phosphorylation of LKB1 on Ser-325 by ERK2. However, the authors did not report the stoichiometry of phosphorylation in that experiment. Despite the difference in our observations, the conclusion that ERK was not a good upstream kinase for the Ser-325 site in a cell-free system meant that the likely effect of this reaction would be negligible in intact cells. Due to results that were not very promising, the intended final experiment using both ERK and p90RSK to phosphorylate Ser-325 and Ser-431 on LKB1, and testing its effect on AMPK activity was not carried out. It appears therefore, that although in melanoma cells with the B-RAF V600E mutation, AMPK activation has been shown to be impaired, the site-specific alanine mutations did not seem to have reduced AMPK activity when tested in a cell-free system. It is plausible that a different kinase, likely to phosphorylate LKB1 on Ser-325 better than ERK2, may also be activated in the melanoma cells expressing the B-RAFV600Emutation, which may account for the reduced ability of LKB1 to activity AMPK. Due to the lack of time, the testing of this hypothesis was beyond the scope of this study.

CHAPTER SIX: CONCLUSIONS AND PERSPECTIVES

6.1 INTRODUCTION

This thesis explores the role of AMPK in cancer and in the DNA damage response. The aim was to test the role of AMPK, both as a tumour suppressor and as a modulator of cell survival in conditions of genotoxic stress. Data presented in this thesis provides evidence that AMPK functions as a tumour suppressor in vivo, delaying death from lymphomas in mice that lack PTEN in their T cells. By contrast, it increases the survival of cells treated with chemotherapeutic agents such as etoposide that cause double stranded DNA breaks. Thus AMPK appears to act as a "double-edged sword" in cancer, providing protection against the development of tumours, while protecting tumour cells against the effects of cancer therapy once tumours have become established. Our data also suggests that AMPK activation occurs in the nucleus in response to genotoxic stress. One of the initial aims of the thesis was to explore the regulatory role of the C-terminal tail of LKB1 on AMPK activity. However, Thr-366 phosphorylation of LKB1 by ATM, in the context of DNA damage, did not appear to play a role in AMPK activation, as this process has been shown in this thesis to be independent of LKB1 and dependent instead on CaMKK-β. This chapter discusses the implications of the findings reported in this thesis and suggests areas for future research.

6.2 AMPK is activated by agents that cause double strand DNA breaks

The work done in this thesis was prompted by reports from other groups suggesting that AMPK was activated in conditions of genotoxic stress (Fu, 2008, Sanli et al., 2010). It has been known for some time that ATM phosphorylates Thr-366 on LKB1, when cells were treated with ionising radiation (Sapkota et al., 2002b). It therefore seemed plausible that genotoxic stress might activate AMPK downstream of this ATM-LKB1 pathway. However, data from the thesis shows that AMPK activation, in response to etoposide, occurs in an LKB1-independent manner. Two different cell lines that lacked LKB1, namely HeLa and G361 cells, showed a 2-to-3 fold activation of AMPK in response to etoposide. By contrast, inhibition of CaMKK-β, either by reducing its expression using siRNA- mediated gene silencing, or by pharmacological inhibition using STO-609, resulted in a marked reduction of etoposide-induced AMPK activation. These results showed that the AMPK activation in these cells was mediated by CaMKK-β. Interestingly, only the AMPK-α1 isoform was shown to be activated with little or no activation of AMPK-α2. This was an interesting result and may serve, in part to explain previous observations obtained with muscle-specific knockout (LKB1$^{fl/fl}$ Cre$^{+/-}$) mice, in which AMPK-α1 activity in muscle under basal and AICAR stimulated conditions was undiminished compared to the LKB1$^{fl/fl}$ Cre$^{-/-}$ controls (Sakamoto et al., 2005). In contrast, basal and AICAR-stimulated AMPK-α2 activity was markedly reduced in muscle-specific LKB1 knockout compared to the LKB1$^{fl/fl}$ Cre$^{-/-}$ controls (Sakamoto et al., 2005).

Data from the thesis also suggests that AMPK activation in response to etoposide is independent of ATM. Treatment of cells with the specific ATM inhibitor,

KU-55933, although inhibiting phosphorylation of ATM substrates, did not reduce AMPK activation. This is in contrast to previous reports showing impaired AMPK activation in response to etoposide in cells that lack ATM (Fu, 2008). However, the data in that paper showed that ATM-null cells have much higher basal levels of phosphorylated AMPK compared to ATM+ cells, and that this was not further increased with etoposide. ATM+ cells, when maximally activated with etoposide have pT-172 signal intensity comparable to that seen in untreated ATM-null cells. This is an area which needs clarification, ideally in LKB1-null cells which express or lack ATM. siRNA-mediated ATM silencing in HeLa cells was attempted during this study. However, the efficacy of ATM knockdown was only about 50%, and a reduction in AMPK activation in ATM-knock-down cells treated with etoposide was not observed.

Perhaps one of the most intriguing findings in this study was the lack of concomitant ACC activation, despite AMPK activation in HeLa and G361 cells treated with etoposide. Immunohistochemistry revealed that AMPK was activated almost exclusively in the nucleus following etoposide treatment. It has been shown that the α2 isoform, but not the α1 isoform of AMPK is enriched in the nucleus (Salt et al., 1998). However, our data shows that only AMPK-α1 is activated by etoposide treatment. This was a very interesting result and may serve, in part to explain previous observations obtained with muscle-specific knockout (LKB1$^{fl/fl}$Cre$^{+/-}$) mice, in which AMPK-α1activity in muscle under basal and AICAR stimulated conditions was undiminished compared to the LKB1$^{fl/fl}$Cre$^{-/-}$ controls (Sakamoto et al., 2005). In contrast, basal and AICAR-stimulated AMPK-α2 activity was markedly reduced in muscle-specific LKB1 knockout compared to the LKB1$^{fl/fl}$Cre$^{-/-}$ controls (Sakamoto et al., 2005).

Two different anti- AMPK-α1 and anti-AMPK-α2 antibodies were tested for staining in HeLa cells, but the antibodies were unfortunately not specific enough for

immunocytochemistry. Sub-cellular fractionation was also attempted, but as the osmotic stress used for cell lysis activated AMPK, the small increase in nuclear AMPK by etoposide treatment may have been obscured by the large increase in AMPK activation due to the osmotic stress. It would be interesting to test whether leptomycin, an agent that prevents nuclear import of proteins, abolished activation of nuclear AMPK in response to etoposide treatment. If confirmed, this would suggest nuclear translocation of activated AMPK-α1 from the cytoplasm.

Activation of AMPK in cells treated with etoposide is temporally associated with an increase in nuclear calcium. This provides a mechanism by which CaMKK-β, and subsequently AMPK is activated, which is independent of signalling via ATM. However, testing whether other agents that cause double stranded DNA breaks such as topotecan and irinotecan also cause similar increase in nuclear calcium flux would add strength to this hypothesis. At present, we do not know the source of the increased nuclear calcium ions, the mechanism by which they are released in response to etoposide treatment, and whether it occurs in response to DNA damage or in response to some other side effect of etoposide.

6.3 AMPK activation confers resistance to DNA-damaging drugs such as etoposide

Epidemiological studies show that diabetics on metformin have a reduced risk of cancer compared to diabetics on other treatments (Evans, 2005, Bowker et al., 2006a). However, there have been conflicting reports in the literature about the role of AMPK as a therapeutic target in cancer. Some reports suggest that AMPK activation using

metformin sensitises cells to ionising radiation (Sanli et al., 2010). Agents such as aspirin have also been shown to activate AMPK, and this activation partially mediated suppression of the mTOR pathway in colorectal cancer cells (Din et al., 2012). However, data from our study shows that CaMKKβ-mediated activation of AMPK by the calcium ionophore A23187 increased cell survival of wild type MEFs in response to etoposide treatment, while this effect was not seen in MEFs lacking AMPK-α1 and -α2. The increased survival may be due to G1 cell cycle arrest mediated by AMPK activation, which protected cells from prolonged S phase arrest caused by etoposide. Cells are more vulnerable to DNA damage during the S phase when their DNA is being replicated and topoisomerases are active. This effect is similar to other agents such as roscovitine and flavopiridol, which cause G1 arrest and also protect against DNA damage (Crescenzi et al., 2005, Di Giovanni et al., 2005). This may have implications for combination chemotherapy where agents that activate AMPK, when used in combination with DSB-inducing drugs, may lead to poor response to chemotherapy.

6.4 AMPK functions as a tumour suppressor in vivo

Perhaps the most significant result in this thesis is the direct evidence that AMPK functions as a tumour suppressor in vivo. The data clearly demonstrates that T cell-specific deletion of PTEN and AMPK causes death of mice from lymphomas significantly earlier than in mice with T cell-specific deletion of PTEN alone. The location of the lymphomas were also significantly different in the PTEN AMPK double KO mice with almost all tumours being limited to the thymus, whereas in the PTEN KO mice, spleen and lymph node involvement was usually seen in addition to involvement

of the thymus. The study also showed a marked reduction in $S1P_1$ mRNA levels in the PTEN AMPK double KO cells, which suggests a role for AMPK in mediating egress of mature thymocytes into peripheral lymph organs. The data also suggested that the PTEN AMPK double KO thymocytes were larger than PTEN KO thymocytes. PTEN AMPK double KO thymocytes also had markedly increased phosphorylation of ribosomal protein S6 compared to the other two groups, which indicated a role for AMPK in down-regulation of mTOR in thymocytes with increased PI3K activity.

Future work to understand the biological role of AMPK would require identification of the subset of cells that become tumour cells, subsequent to the deletion of PTEN and AMPK. Work from this study suggests that the transition from the DN to the DP cells, and the egress of tumour cells may be two important areas, where further work to delineate AMPK-dependent signalling changes in this tumour model may yield interesting results that might explain how AMPK deletion affects tumour formation.

6.5 C-terminal phosphorylation of LKB1and AMPK activity

The last chapter in the thesis briefly explored the role of C-terminal phosphorylation on two sites of LKB1, namely Ser-325 and Ser-431. This was prompted by reports suggesting that, in melanoma cells carrying the B-RAF V600E mutation, there was activation of ERK and p90RSK, which caused phosphorylation of these two sites on LKB1, inhibiting its ability to activate AMPK (Zheng et al., 2009). Previous reports suggest that Ser-431 phosphorylation does not affect AMPK activation (Fogarty and Hardie, 2009). The data from this thesis shows that mutation of both Ser-325 and Ser-431 to alanine also does not affect the ability of LKB1 to activate AMPK in a cell-free

system. Moreover, ERK does not stoichiometrically phosphorylate Ser-325 on LKB1. Future experiments to investigate the role of LKB1 phosphorylation might involve construction of stable cell lines of G361 or HeLa cells expressing wild type LKB1 or various phosphorylation site mutants.

6.7 Final summary

Overall, the results presented in this thesis dissect the role played by AMPK in cancer. AMPK appears to function in two very different ways; on the one hand AMPK functions as a tumour suppressor delaying tumour onset in mice with T cell-specific PTEN deletion, while in tumour cells treated with DNA damaging agents, AMPK activation confers increased cell survival. AMPK activation therefore, may delay tumour formation; however, once a cancer is established, AMPK activation may be detrimental to therapy. However, this may depend on the type of cancer and the signalling pathways that have been activated or suppressed, either causally, or as a consequence of the cancer. Further work is required to determine tissue and cellular responses to AMPK activation and inhibition, in different cancers to evaluate the potential therapeutic benefit of modulating AMPK activity as an adjunct to existing treatments for cancer. This is an exciting area likely to yield real benefit to cancer patients.

REFERENCES

Abraham, R. T. 2004a. The ATM-related kinase, hSMG-1, bridges genome and RNA surveillance pathways. *DNA Repair,* 3**,** 919-925.

Abraham, R. T. 2004b. PI 3-kinase related kinases: 'big' players in stress-induced signaling pathways. *DNA Repair,* 3**,** 883-887.

Abu-Elheiga, L., Brinkley, W., Zhong, L., Chirala, S., Woldegiorgis, G. & Wakil, S. 2000. The subcellular localization of acetyl-CoA carboxylase 2. *Proc Natl Acad Sci USA,* 97**,** 1444 - 1449.

Abu-Elheiga, L., Matzuk, M., Abo-Hashema, K. & Wakil, S. 2001. Continuous fatty acid oxidation and reduced fat storage in mice lacking acetyl-CoA carboxylase 2. *Science,* 291**,** 2613 - 2616.

Ahn, J.-Y., Schwarz, J. K., Piwnica-Worms, H. & Canman, C. E. 2000. Threonine 68 Phosphorylation by Ataxia Telangiectasia Mutated Is Required for Efficient Activation of Chk2 in Response to Ionizing Radiation. *Cancer Research,* 60**,** 5934-5936.

Ahn, J., Urist, M. & Prives, C. 2004. The Chk2 protein kinase. *DNA Repair,* 3**,** 1039-1047.

Akman, H. O., Sampayo, J. N., Ross, F. A., Scott, J. W., Wilson, G., Benson, L., Bruno, C., Shanske, S., Hardie, D. G. & Dimauro, S. 2007. Fatal Infantile Cardiac Glycogenosis with Phosphorylase Kinase Deficiency and a Mutation in the [ggr]2-Subunit of AMP-Activated Protein Kinase. *Pediatr Res,* 62**,** 499-504.

Alessi, D. R., Sakamoto, K. & Bayascas, J. R. 2006. LKB1-Dependent Signaling Pathways. *Annual Review of Biochemistry,* 75**,** 137-163.

Alexander, A., Cai, S.-L., Kim, J., Nanez, A., Sahin, M., Maclean, K. H., Inoki, K., Guan, K.-L., Shen, J., Person, M. D., Kusewitt, D., Mills, G. B., Kastan, M. B. & Walker, C. L. 2010. ATM signals to TSC2 in the cytoplasm to regulate mTORC1 in response to ROS. *Proceedings of the National Academy of Sciences,* 107**,** 4153-4158.

Altarejos, J. Y., Taniguchi, M., Clanachan, A. S. & Lopaschuk, G. D. 2005. Myocardial Ischemia Differentially Regulates LKB1 and an Alternate 5'-AMP-activated Protein Kinase Kinase. *Journal of Biological Chemistry,* 280**,** 183-190.

Aschenbach, W. G., Sakamoto, K. & Goodyear, L. J. 2004. 5' Adenosine Monophosphate-Activated Protein Kinase, Metabolism and Exercise. *Sports Medicine,* 34**,** 91-103.

Baas, A. F., Boudeau, J., Sapkota, G. P., Smit, L., Medema, R., Morrice, N. A., Alessi, D. R. & Clevers, H. C. 2003. Activation of the tumour suppressor kinase LKB1 by the STE20-like pseudokinase STRAD. *EMBO J,* 22**,** 3062-3072.

Bakkenist, C. J. & Kastan, M. B. 2003. DNA damage activates ATM through intermolecular autophosphorylation and dimer dissociation. *Nature,* 421**,** 499-506.

Banin, S., Moyal, L., Shieh, S.-Y., Taya, Y., Anderson, C. W., Chessa, L., Smorodinsky, N. I., Prives, C., Reiss, Y., Shiloh, Y. & Ziv, Y. 1998. Enhanced Phosphorylation of p53 by ATM in Response to DNA Damage. *Science,* 281**,** 1674-1677.

Bardeesy, N., Sinha, M., Hezel, A. F., Signoretti, S., Hathaway, N. A., Sharpless, N. E., Loda, M., Carrasco, D. R. & Depinho, R. A. 2002. Loss of the Lkb1 tumour suppressor provokes intestinal polyposis but resistance to transformation. *Nature,* 419**,** 162-167.

Bassing, C. H., Swat, W. & Alt, F. W. 2002. The Mechanism and Regulation of Chromosomal V(D)J Recombination. *Cell,* 109**,** S45-S55.

Bateman, A. 1997. The structure of a domain common to archaebacteria and the homocystinuria disease protein. *Trends in Biochemical Sciences,* 22**,** 12-13.

Bauer, K., Skoetz, N., Monsef, I., Engert, A. & Brillant, C. 2011. Comparison of chemotherapy including escalated BEACOPP versus chemotherapy including ABVD for patients with early unfavourable or advanced stage Hodgkin lymphoma. *Cochrane Database of*

Systematic Reviews [Online]. Available: http://www.mrw.interscience.wiley.com/cochrane/clsysrev/articles/CD007941/frame.html.

Beg, Z., Allmann, D. & Gibson, D. 1973. Modulation of 3-hydroxy-3-methylglutaryl coenzyme A reductase activity with cAMP and wth protein fractions of rat liver cytosol. *Biochem Biophys Res Commun,* 54**,** 1362-1369.

Bekker-Jensen, S. & Mailand, N. 2010. Assembly and function of DNA double-strand break repair foci in mammalian cells. *DNA Repair,* 9**,** 1219-1228.

Bergeron, R., Ren, J. M., Cadman, K. S., Moore, I. K., Perret, P., Pypaert, M., Young, L. H., Semenkovich, C. F. & Shulman, G. I. 2001. Chronic activation of AMP kinase results in NRF-1 activation and mitochondrial biogenesis. *American Journal of Physiology - Endocrinology and Metabolism,* 281.

Berkovich, E., Monnat, R. J. & Kastan, M. B. 2007. Roles of ATM and NBS1 in chromatin structure modulation and DNA double-strand break repair. *Nat Cell Biol,* 9**,** 683-690.

Boehmer, H. V. 1986. The selection of the α,β heterodimeric T-cell receptor for antigen. *Immunology Today,* 7**,** 333-336.

Böhm, H., Brinkmann, V., Drab, M., Henske, A. & Kurzchalia, T. V. 1997. Mammalian homologues of C. elegans PAR-1 are asymmetrically localized in epithelial cells and may influence their polarity. *Current biology : CB,* 7**,** 603-606.

Borgulya, P., Kishi, H., Uematsu, Y. & Von Boehmer, H. 1992. Exclusion and inclusion of α and β T cell receptor alleles. *Cell,* 69**,** 529-537.

Boudeau, J., Baas, A. F., Deak, M., Morrice, N. A., Kieloch, A., Schutkowski, M., Prescott, A. R. & Alessi, D. R. 2003. MO25α/β interact with STRADα/β enhancing their ability to bind , activate and localize LKB1 in the cytoplasm. *EMBO Journal,* 22**,** 5102-5114.

Boudeau, J., Miranda-Saavedra, D., Barton, G. J. & Alessi, D. R. 2006. Emerging roles of pseudokinases. *Trends in Cell Biology,* 16**,** 443-452.

Bowker, S., Majumdar, S., Veugelers, P. & Johnson, J. 2006a. Increased cancer-related mortality for patients with type 2 diabetes who use sulfonylureas or insulin. *Diabetes Care,* 29**,** 254 - 258.

Bowker, S. L., Majumdar, S. R., Veugelers, P. & Johnson, J. A. 2006b. Increased Cancer-Related Mortality for Patients With Type 2 Diabetes Who Use Sulfonylureas or Insulin. *Diabetes Care,* 29**,** 254-258.

Breitkreutz, A., Choi, H., Sharom, J. R., Boucher, L., Neduva, V., Larsen, B., Lin, Z.-Y., Breitkreutz, B.-J., Stark, C., Liu, G., Ahn, J., Dewar-Darch, D., Reguly, T., Tang, X., Almeida, R., Qin, Z. S., Pawson, T., Gingras, A.-C., Nesvizhskii, A. I. & Tyers, M. 2010. A Global Protein Kinase and Phosphatase Interaction Network in Yeast. *Science,* 328**,** 1043-1046.

Brown, M. S., Brunschede, G. Y. & Goldstein, J. L. 1975. Inactivation of 3-hydroxy-3-methylglutaryl coenzyme A reductase in vitro. An adenine nucleotide-dependent reaction catalyzed by a factor in human fibroblasts. *Journal of Biological Chemistry,* 250**,** 2502-2509.

Bruzzone, M., Centurioni, M. G., Giglione, P., Gualco, M., Merlo, D. F., Miglietta, L., Cosso, M., Giannelli, F., Cristoforoni, P. & Ferrarini, M. 2011. Second-Line Treatment with Intravenous Gemcitabine and Oral Etoposide in Platinum-Resistant Advanced Ovarian Cancer Patients: Results of a Phase II Study. *Oncology,* 80**,** 238-246.

Buckler, J. L., Liu, X. & Turka, L. A. 2008. Regulation of T-cell responses by PTEN. *Immunological Reviews,* 224**,** 239-248.

Burwinkel, B., Scott, J. W., Bührer, C., Van Landeghem, F. K. H., Cox, G. F., Wilson, C. J., Grahame Hardie, D. & Kilimann, M. W. 2005. Fatal Congenital Heart Glycogenosis Caused by a Recurrent Activating R531Q Mutation in the [3]2-Subunit of AMP-Activated Protein Kinase (PRKAG2), Not by Phosphorylase Kinase Deficiency. *American journal of human genetics,* 76**,** 1034-1049.

Canman, C. E., Lim, D.-S., Cimprich, K. A., Taya, Y., Tamai, K., Sakaguchi, K., Appella, E., Kastan, M. B. & Siliciano, J. D. 1998. Activation of the ATM Kinase by Ionizing Radiation and Phosphorylation of p53. *Science,* 281**,** 1677-1679.

Cantrell, D. A. 2001. Phosphoinositide 3-kinase signalling pathways. *Journal of Cell Science,* 114**,** 1439-1445.

Cantrell, D. A. 2002. T-cell antigen receptor signal transduction. *Immunology,* 105**,** 369-374.

Carling, D., Aguan, K., Woods, A., Verhoeven, A. J. M., Beri, R. K., Brennan, C. H., Sidebottom, C., Davison, M. D. & Scott, J. 1994. Mammalian AMP-activated protein kinase is homologous to yeast and plant protein kinases involved in the regulation of carbon metabolism. *Journal of Biological Chemistry,* 269**,** 11442-11448.

Carling, D., Clarke, P. R., Zammit, V. A. & Hardie, D. G. 1989. Purification and characterization of the AMP-activated protein kinase. *European Journal of Biochemistry,* 186**,** 129-136.

Carling, D., Zammit, V. A. & Hardie, D. G. 1987. A common bicyclic protein kinase cascade inactivates the regulatory enzymes of fatty acid and cholesterol biosynthesis. *FEBS Letters,* 223**,** 217-222.

Carlson, C. A. & Kim, K.-H. 1973. Regulation of Hepatic Acetyl Coenzyme A Carboxylase by Phosphorylation and Dephosphorylation. *Journal of Biological Chemistry,* 248**,** 378-380.

Carlyle, J. R., Michie, A. M., Furlonger, C., Nakano, T., Lenardo, M. J., Paige, C. J. & Zúñiga-Pflücker, J. C. 1997. Identification of a Novel Developmental Stage Marking Lineage Commitment of Progenitor Thymocytes. *The Journal of Experimental Medicine,* 186**,** 173-182.

Carretero, J., Medina, P. P., Blanco, R., Smit, L., Tang, M., Roncador, G., Maestre, L., Conde, E., Lopez-Rios, F., Clevers, H. C. & Sanchez-Cespedes, M. 2006. Dysfunctional AMPK activity, signalling through mTOR and survival in response to energetic stress in LKB1-deficient lung cancer. *Oncogene,* 26**,** 1616-1625.

Carretero, J., Medina, P. P., Blanco, R., Smit, L., Tang, M., Roncador, G., Maestre, L., Conde, E., Lopez-Rios, F., Clevers, H. C. & Sanchez-Cespedes, M. 2007. Dysfunctional AMPK activity, signalling through mTOR and survival in response to energetic stress in LKB1-deficient lung cancer. *Oncogene,* 26**,** 1616-1625.

Carson, C. T., Schwartz, R. A., Stracker, T. H., Lilley, C. E., Lee, D. V. & Weitzman, M. D. 2003. The Mre11 complex is required for ATM activation and the G2/M checkpoint. *EMBO J,* 22**,** 6610-6620.

Cernak, I., Stoica, B. A., Byrnes, K. R., Giovanni, S. D. & Faden, A. I. 2005. Role of the Cell Cycle in the Pathobiology of Central Nervous System Trauma. *Cell Cycle,* 4**,** 1286-1293.

Chen, L., Jiao, Z.-H., Zheng, L.-S., Zhang, Y.-Y., Xie, S.-T., Wang, Z.-X. & Wu, J.-W. 2009. Structural insight into the autoinhibition mechanism of AMP-activated protein kinase. *Nature,* 459**,** 1146-1149.

Chen, S., Murphy, J., Toth, R., Campbell, D. G., Morrice, N. A. & Mackintosh, C. 2008. Complementary regulation of TBC1D1 and AS160 by growth factors, insulin and AMPK activators. *Biochemical Journal,* 409**,** 449-459.

Chen, Z. W. & Letvin, N. L. 2003. Vγ2Vδ2+ T cells and anti-microbial immune responses. *Microbes and Infection,* 5**,** 491-498.

Cheung, P. C. F., Salt, I. P., Davies, S. P., Hardie, D. G. & Carling, D. 2000. Characterization of AMP-activated protein kinase γ-subunit isoforms and their role in AMP binding. *Biochemical Journal,* 346**,** 659-669.

Ciofani, M. & Zúñiga-Pflücker, J. C. 2007. The Thymus as an Inductive Site for T Lymphopoiesis. *Annual Review of Cell and Developmental Biology,* 23**,** 463-493.

Cohen, P. 2002. The origins of protein phosphorylation. *Nat Cell Biol,* 4**,** E127-E130.

Collins, S. P., Reoma, J. L., Gamm, D. M. & Ulher, M. D. 2000. LKB1, a novel serine/threonine protein kinase and potential tumour suppressor, is phosphorylated by cAMP-

dependent protein kinase (PKA) and prenylated in vivo. . *Biochemical Journal,* 345**,** 673-80.

Cooper, M. D. & Alder, M. N. 2006. The Evolution of Adaptive Immune Systems. *Cell,* 124**,** 815-822.

Corradetti, M. N., Inoki, K., Bardeesy, N., Depinho, R. A. & Guan, K. L. 2004. Regulation of the TSC pathway by LKB1: Evidence of a molecular link between tuberous sclerosis complex and Peutz-Jeghers syndrome. *Genes and Development,* 18**,** 1533-1538.

Corton, J. M., Gillespie, J. G. & Hardie, D. G. 1994. Role of the AMP-activated protein kinase in the cellular stress response. *Current biology : CB,* 4**,** 315-324.

Corton, J. M., Gillespie, J. G., Hawley, S. A. & Hardie, D. G. 1995. 5-Aminoimidazole-4-carboxamide ribonucleoside. A specific method for activating AMP-activated protein kinase in intact cells? *European Journal of Biochemistry,* 229**,** 558-565.

Crescenzi, E., Palumbo, G. & Brady, H. J. M. 2005. Roscovitine Modulates DNA Repair and Senescence: Implications for Combination Chemotherapy. *Clinical Cancer Research,* 11**,** 8158-8171.

Crute, B. E., Seefeld, K., Gamble, J., Kemp, B. E. & Witters, L. A. 1998. Functional Domains of the α1 Catalytic Subunit of the AMP-activated Protein Kinase. *Journal of Biological Chemistry,* 273**,** 35347-35354.

Curnock, A. P., Logan, M. K. & Ward, S. G. 2002. Chemokine signalling: pivoting around multiple phosphoinositide 3-kinases. *Immunology,* 105**,** 125-136.

Dale, S., Wilson, W. A., Edelman, A. M. & Hardie, D. G. 1995. Similar substrate recognition motifs for mammalian AMP-activated protein kinase, higher plant HMG-CoA reductase kinase-A, yeast SNF1, and mammalian calmodulin-dependent protein kinase I. *FEBS Letters,* 361**,** 191-195.

Daniel, T. & Carling, D. 2002. Functional analysis of mutations in the γ2 subunit of AMP-activated protein kinase associated with cardiac hypertrophy and Wolff-Parkinson-White syndrome. *Journal of Biological Chemistry,* 277**,** 51017-51024.

Danilova, N. 2012. The Evolution of Adaptive Immunity: Self and Nonself. Springer US.

Davies, S., Carling, D., Munday, M. & Hardie, D. 1992. Diurnal rhythm of phosphorylation of rat liver acetyl-CoA carboxylase by the AMP-activated protein kinase, demonstrated using freeze-clamping. Effects of high fat diets. *Eur J Biochem,* 203**,** 615 - 623.

Davies, S. P., Carling, D. & Hardie, D. G. 1989. Tissue distribution of the AMP-activated protein kinase, and lack of activation by cyclic-AMP-dependent protein kinase, studied using a specific and sensitive peptide assay. *European Journal of Biochemistry,* 186**,** 123-128.

Davies, S. P., Hawley, S. A., Woods, A., Carling, D., Haystead, T. a. J. & Hardie, D. G. 1994. Purification of the AMP-activated protein kinase on ATP-γ-Sepharose and analysis of its subunit structure. *European Journal of Biochemistry,* 223**,** 351-357.

Davies, S. P., Helps, N. R., Cohen, P. T. W. & Hardie, D. G. 1995. 5'-AMP inhibits dephosphorylation, as well as promoting phosphorylation, of the AMP-activated protein kinase. Studies using bacterially expressed human protein phosphatase-2Cα and native bovine protein phosphatase-2C. *FEBS Letters,* 377**,** 421-425.

Di Giovanni, S., Movsesyan, V., Ahmed, F., Cernak, I., Schinelli, S., Stoica, B. & Faden, A. I. 2005. Cell cycle inhibition provides neuroprotection and reduces glial proliferation and scar formation after traumatic brain injury. *Proceedings of the National Academy of Sciences of the United States of America,* 102**,** 8333-8338.

Din, F. V. N., Valanciute, A., Houde, V. P., Zibrova, D., Green, K. A., Sakamoto, K., Alessi, D. R. & Dunlop, M. G. 2012. Aspirin Inhibits mTOR Signaling, Activates AMP-Activated Protein Kinase, and Induces Autophagy in Colorectal Cancer Cells. *Gastroenterology,* 142**,** 1504-1515.e3.

Drewes, G., Ebneth, A., Preuss, U., Mandelkow, E.-M. & Mandelkow, E. 1997. MARK, a Novel Family of Protein Kinases That Phosphorylate Microtubule-Associated Proteins and Trigger Microtubule Disruption. *Cell,* 89**,** 297-308.

Durocher, D. & Jackson, S. P. 2001. DNA-PK, ATM and ATR as sensors of DNA damage: variations on a theme? *Current Opinion in Cell Biology,* 13**,** 225-231.

Egan, D. F., Shackelford, D. B., Mihaylova, M. M., Gelino, S., Kohnz, R. A., Mair, W., Vasquez, D. S., Joshi, A., Gwinn, D. M., Taylor, R., Asara, J. M., Fitzpatrick, J., Dillin, A., Viollet, B., Kundu, M., Hansen, M. & Shaw, R. J. 2011. Phosphorylation of ULK1 (hATG1) by AMP-Activated Protein Kinase Connects Energy Sensing to Mitophagy. *Science,* 331**,** 456-461.

Engel, I. & Murre, C. 2001. The function of E- and id proteins in lymphocyte development. *Nat Rev Immunol,* 1**,** 193-199.

Esteve-Puig, R., Canals, F., Colomã©, N., Merlino, G. & Recio, J. Ã. 2009. Uncoupling of the LKB1-AMPK energy sensor pathway by growth factors and oncogenic BRAFV600E. *PLoS ONE,* 4.

Evans, J. M. M., Donnelly,L.A., Emslie-Smith, A.M., Alessi, D.R., Morris, A.D. 2005. Metformin and reduced risk of cancer in diabetic patients *British Medical Journal,* 330**,** 1304-1305.

Fernandes, N. & Allbritton, N. L. 2009. Effect of the DEF motif on phosphorylation of peptide substrates by ERK. *Biochemical and Biophysical Research Communications,* 387**,** 414-418.

Fernandez-Capetillo, O., Lee, A., Nussenzweig, M. & Nussenzweig, A. 2004. H2AX: the histone guardian of the genome. *DNA Repair,* 3**,** 959-967.

Ferrer, A., Caelles, C., Massot, N. & Hegardt, F. G. 1985. Activation of rat liver cytosolic 3-hydroxy-3-methylglutaryl Coenzyme A reductase kinase by adenosine 5'-monophosphate. *Biochemical and Biophysical Research Communications,* 132**,** 497-504.

Fink, P. J. & Hendricks, D. W. 2011. Post-thymic maturation: young T cells assert their individuality. *Nat Rev Immunol,* 11**,** 544-549.

Finlay, D. & Cantrell, D. A. 2011. Metabolism, migration and memory in cytotoxic T cells. *Nat Rev Immunol,* 11**,** 109-117.

Finlay, D. K., Sinclair, L. V., Feijoo, C., Waugh, C. M., Hagenbeek, T. J., Spits, H. & Cantrell, D. A. 2009. Phosphoinositide-dependent kinase 1 controls migration and malignant transformation but not cell growth and proliferation in PTEN-null lymphocytes. *The Journal of Experimental Medicine,* 206**,** 2441-2454.

Fischer, E. H. & Krebs, E. G. 1955. CONVERSION OF PHOSPHORYLASE b TO PHOSPHORYLASE a IN MUSCLE EXTRACTS. *Journal of Biological Chemistry,* 216**,** 121-132.

Flynn, J. L., Goldstein, M. M., Triebold, K. J., Koller, B. & Bloom, B. R. 1992. Major histocompatibility complex class I-restricted T cells are required for resistance to Mycobacterium tuberculosis infection. *Proceedings of the National Academy of Sciences,* 89**,** 12013-12017.

Fogarty, S. & Hardie, D. 2008. C-terminal phosphorylation of LKB1 is not required for regulation of AMPK, BRSK1, BRSK2, or cell cycle arrest. *J Biol Chem,* 284**,** 77 - 84.

Fogarty, S. & Hardie, D. G. 2009. C-terminal phosphorylation of LKB1 Is not required for regulation of AMP-activated protein kinase, BRSK1, BRSK2, or cell cycle arrest. *Journal of Biological Chemistry,* 284**,** 77-84.

Fogarty, S., Hawley, S. A., Green, K. A., Saner, N., Mustard, K. J. & Hardie, D. G. 2010. Calmodulin-dependent protein kinase kinase-β activates AMPK without forming a stable complex: synergistic effects of Ca2+ and AMP *Biochemical Journal,* 426**,** 109-118.

Forcet, C., Etienne-Manneville, S., Gaude, H., Fournier, L., Debilly, S., Salmi, M., Baas, A., Olschwang, S., Clevers, H. & Billaud, M. 2005. Functional analysis of Peutz-Jeghers

mutations reveals that the LKB1 C-terminal region exerts a crucial role in regulating both the AMPK pathway and the cell polarity. *Human Molecular Genetics,* 14**,** 1283-1292.

Foretz, M., Hébrard, S., Leclerc, J., Zarrinpashneh, E., Soty, M., Mithieux, G., Sakamoto, K., Andreelli, F. & Viollet, B. 2010. Metformin inhibits hepatic gluconeogenesis in mice independently of the LKB1/AMPK pathway via a decrease in hepatic energy state. *The Journal of Clinical Investigation,* 120**,** 2355-2369.

Francesconi, A. B., Dupre, S., Matos, M., Martin, D., Hughes, B. G., Wyld, D. K. & Lickliter, J. D. 2010. Carboplatin and etoposide combined with bevacizumab for the treatment of recurrent glioblastoma multiforme. *Journal of Clinical Neuroscience,* 17**,** 970-974.

Fryer, L. G. D., Parbu-Patel, A. & Carling, D. 2002. The anti-diabetic drugs rosiglitazone and metformin stimulate AMP-activated protein kinase through distinct signaling pathways. *Journal of Biological Chemistry,* 277**,** 25226-25232.

Fu, X., Wan S., Lyu ,Y.L., Liu, L.F., and Qi, H., 2008. Etoposide Induces ATM-Dependent Mitochondrial Biogenesis through AMPK Activation. *PLoS ONE,* 3.

Gao, G., Widmer, J., Stapleton, D., Teh, T., Cox, T., Kemp, B. E. & Witters, L. A. 1995. Catalytic subunits of the porcine and rat 5'-AMP-activated protein kinase are members of the SNF1 protein kinase family. *Biochimica et Biophysica Acta - Molecular Cell Research,* 1266**,** 73-82.

Gee, K. R., Brown, K. A., Chen, W. N. U., Bishop-Stewart, J., Gray, D. & Johnson, I. 2000. Chemical and physiological characterization of fluo-4 Ca2+-indicator dyes. *Cell Calcium,* 27**,** 97-106.

Godfrey, D. I., Kennedy, J., Suda, T. & Zlotnik, A. 1993. A developmental pathway involving four phenotypically and functionally distinct subsets of CD3-CD4-CD8- triple-negative adult mouse thymocytes defined by CD44 and CD25 expression. *The Journal of Immunology,* 150**,** 4244-52.

Godfrey, D. I. & Kronenberg, M. 2004. Going both ways: Immune regulation via CD1d-dependent NKT cells. *The Journal of Clinical Investigation,* 114**,** 1379-1388.

Gollob, M. H., Seger, J. J., Gollob, T. N., Tapscott, T., Gonzales, O., Bachinski, L. & Roberts, R. 2001. Novel PRKAG2 Mutation Responsible for the Genetic Syndrome of Ventricular Preexcitation and Conduction System Disease With Childhood Onset and Absence of Cardiac Hypertrophy. *Circulation,* 104**,** 3030-3033.

Gordon, J., Patel, S. R., Mishina, Y. & Manley, N. R. 2010. Evidence for an early role for BMP4 signaling in thymus and parathyroid morphogenesis. *Developmental Biology,* 339**,** 141-154.

Greer John P, Foerster John, Lukens John N, Rodgers, G. M., Paraskevas Frixos & Glader, B. 2004. Wintrobe's Clinical Hematology (11th Edition).

Gulbranson-Judge, A., Tybulewicz, V. L. J., Walters, A. E., Toellner, K.-M., Maclennan, I. C. M. & Turner, M. 1999. Defective immunoglobulin class switching in Vav-deficient mice is attributable to compromised T cell help. *European Journal of Immunology,* 29**,** 477-487.

Guo, Z., Kozlov, S., Lavin, M. F., Person, M. D. & Paull, T. T. 2010. ATM Activation by Oxidative Stress. *Science,* 330**,** 517-521.

Guy, C. S. & Vignali, D. a. A. 2009. Organization of proximal signal initiation at the TCR:CD3 complex. *Immunological Reviews,* 232**,** 7-21.

Gwinn, D., Shackelford, D., Egan, D., Mihaylova, M., Mery, A., Vasquez, D., Turk, B. & Shaw, R. 2008. AMPK phosphorylation of raptor mediates a metabolic checkpoint. *Mol Cell,* 30**,** 214 - 226.

Hadad, S., Baker, L., Quinlan, P., Robertson, K., Bray, S., Thomson, G., Kellock, D., Jordan, L., Purdie, C., Hardie, D., Fleming, S. & Thompson, A. 2009. Histological evaluation of AMPK signalling in primary breast cancer. *BMC Cancer,* 9**,** 307.

Hagenbeek, T. J., Naspetti, M., Malergue, F., Garçon, F., Nunès, J. A., Cleutjens, K. B. J. M., Trapman, J., Krimpenfort, P. & Spits, H. 2004. The Loss of PTEN Allows TCR αβ Lineage Thymocytes to Bypass IL-7 and Pre-TCR–mediated Signaling. *The Journal of Experimental Medicine,* 200**,** 883-894.

Hagenbeek, T. J. & Spits, H. 2007. T-cell lymphomas in T-cell-specific Pten-deficient mice originate in the thymus. *Leukemia,* 22**,** 608-619.

Hande, K. R. 1998. Etoposide: Four decades of development of a topoisomerase II inhibitor. *European Journal of Cancer,* 34**,** 1514-1521.

Hardie, D. G. 2007a. AMP-activated/SNF1 protein kinases: conserved guardians of cellular energy. *Nat Rev Mol Cell Biol,* 8**,** 774-785.

Hardie, D. G. 2007b. AMP-activated/SNF1 protein kinases:conserved guardians of cellular energy *Nature Reviews: Molecular Cell biology,* 8**,** 774-785.

Hardie, D. G. 2011a. AMP-activated protein kinase—an energy sensor that regulates all aspects of cell function. *Genes & Development,* 25**,** 1895-1908.

Hardie, D. G. 2011b. Sensing of energy and nutrients by AMP-activated protein kinase. *The American Journal of Clinical Nutrition,* 93**,** 891S-896S.

Hardie, D. G., Carling, D. & Gamblin, S. J. 2011. AMP-activated protein kinase: also regulated by ADP? *Trends in Biochemical Sciences,* 36**,** 470-477.

Hardie, D. G. & Hawley, S. A. 2001. AMP-activated protein kinase: the energy charge hypothesis revisited. *BioEssays,* 23**,** 1112-1119.

Hardie, D. G., Ross, F. A. & Hawley, S. A. 2012. AMPK: a nutrient and energy sensor that maintains energy homeostasis. *Nat Rev Mol Cell Biol,* 13**,** 251-262.

Harrington, L. E., Hatton, R. D., Mangan, P. R., Turner, H., Murphy, T. L., Murphy, K. M. & Weaver, C. T. 2005. Interleukin 17-producing CD4+ effector T cells develop via a lineage distinct from the T helper type 1 and 2 lineages. *Nat Immunol,* 6**,** 1123-1132.

Hawley, S., Boudeau, J., Reid, J., Mustard, K., Udd, L., Makela, T., Alessi, D. & Hardie, D. 2003. Complexes between the LKB1 tumor suppressor, STRAD alpha/beta and MO25 alpha/beta are upstream kinases in the AMP-activated protein kinase cascade. *J Biol,* 2**,** 28.

Hawley, S. A., Davison, M., Woods, A., Davies, S. P., Beri, R. K., Carling, D. & Hardie, D. G. 1996. Characterization of the AMP-activated Protein Kinase Kinase from Rat Liver and Identification of Threonine 172 as the Major Site at Which It Phosphorylates AMP-activated Protein Kinase. *Journal of Biological Chemistry,* 271**,** 27879-27887.

Hawley, S. A., Fullerton, M. D., Ross, F. A., Schertzer, J. D., Chevtzoff, C., Walker, K. J., Peggie, M. W., Zibrova, D., Green, K. A., Mustard, K. J., Kemp, B. E., Sakamoto, K., Steinberg, G. R. & Hardie, D. G. 2012. The Ancient Drug Salicylate Directly Activates AMP-Activated Protein Kinase. *Science*.

Hawley, S. A., Pan, D. A., Mustard, K. J., Ross, L., Bain, J., Edelman, A. M., Frenguelli, B. G. & Hardie, D. G. 2005. Calmodulin-dependent protein kinase kinase-β is an alternative upstream kinase for AMP-activated protein kinase. *Cell Metabolism,* 2**,** 9-19.

Hawley, S. A., Ross, F. A., Chevtzoff, C., Green, K. A., Evans, A., Fogarty, S., Towler, M. C., Brown, L. J., Ogunbayo, O. A., Evans, A. M. & Hardie, D. G. 2010. Use of Cells Expressing γ Subunit Variants to Identify Diverse Mechanisms of AMPK Activation. *Cell Metabolism,* 11**,** 554-565.

Hawley, S. A., Selbert, M. A., Goldstein, E. G., Edelman, A. M., Carling, D. & Hardie, D. G. 1995. 5'-AMP activates the AMP-activated protein kinase cascade, and Ca2+/calmodulin activates the calmodulin-dependent protein kinase I cascade, via three independent mechanisms. *Journal of Biological Chemistry,* 270**,** 27186-27191.

Heisig, P. 2009. Type II topoisomerases—inhibitors, repair mechanisms and mutations. *Mutagenesis,* 24**,** 465-469.

Hemminki, A. 1999. The molecular basis and clinical aspects of Peutz-Jeghers syndrome. *Cellular and Molecular Life Sciences,* 55**,** 735-750.

Hemminki, A., Markie, D., Tomlinson, I., Avizienyte, E., Roth, S., Loukola, A., Bignell, G., Warren, W., Aminoff, M., Hoglund, P., Jarvinen, H., Kristo, P., Pelin, K., Ridanpaa, M., Salovaara, R., Toro, T., Bodmer, W., Olschwang, S., Olsen, A. S., Stratton, M. R., De La Chapelle, A. & Aaltonen, L. A. 1998. A serine/threonine kinase gene defective in Peutz-Jeghers syndrome. *Nature,* 391**,** 184-187.

Hernandez, J. B., Newton, R. H. & Walsh, C. M. 2010. Life and death in the thymus—cell death signaling during T cell development. *Current Opinion in Cell Biology,* 22**,** 865-871.

Herrero-Martin, G., Hoyer-Hansen, M., Garcia-Garcia, C., Fumarola, C., Farkas, T., Lopez-Rivas, A. & Jaattela, M. 2009. TAK1 activates AMPK-dependent cytoprotective autophagy in TRAIL-treated epithelial cells. *EMBO J,* 28**,** 677-685.

Hickson, I., Zhao, Y., Richardson, C., Green, S., Martin, N., Orr, A. & Smith , G. 2004. Identification and characterisation of a novel and specific inhibitor of the Ataxia telangectasia mutated kinase ATM. *Cancer Research,* 64**,** 9152-9159.

Hong, S. P., Leiper, F. C., Woods, A., Carling, D. & Carlson, M. 2003. Activation of yeast Snf1 and mammalian AMP-activated protein kinase by upstream kinases. *Proceedings of the National Academy of Sciences of the United States of America,* 100**,** 8839-8843.

Horike, N., Takemori, H., Katoh, Y., Doi, J., Min, L., Asano, T., Sun, X. J., Yamamoto, H., Kasayama, S., Muraoka, M., Nonaka, Y. & Okamoto, M. 2003. Adipose-specific Expression, Phosphorylation of Ser794 in Insulin Receptor Substrate-1, and Activation in Diabetic Animals of Salt-inducible Kinase-2. *Journal of Biological Chemistry,* 278**,** 18440-18447.

Huang, X., Wullschleger, S., Shpiro, N., Mcguire, V. A., Sakamoto, K., Woods, Y. L., Mcburnie, W., Fleming, S. & Alessi, D. R. 2008. Important role of the LKB1–AMPK pathway in suppressing tumorigenesis in PTEN-deficient mice. *Biochemical Journal* 412 211-221.

Hudson, E. R., Pan, D. A., James, J., Lucocq, J. M., Hawley, S. A., Green, K. A., Baba, O., Terashima, T. & Hardie, D. G. 2003. A novel domain in AMP-activated protein kinase causes glycogen storage bodies similar to those seen in hereditary cardiac arrhythmias. *Current Biology,* 13**,** 861-866.

Hurley, R. L., Anderson, K. A., Franzone, J. M., Kemp, B. E., Means, A. R. & Witters, L. A. 2005. The Ca2+/calmodulin-dependent protein kinase kinases are AMP-activated protein kinase kinases. *Journal of Biological Chemistry,* 280**,** 29060-29066.

Ikematsu, N., Dallas, M. L., Ross, F. A., Lewis, R. W., Rafferty, J. N., David, J. A., Suman, R., Peers, C., Hardie, D. G. & Evans, A. M. 2011. Phosphorylation of the voltage-gated potassium channel Kv2.1 by AMP-activated protein kinase regulates membrane excitability. *Proceedings of the National Academy of Sciences,* 108**,** 18132-18137.

Imamura, K., Ogura, T., Kishimoto, A., Kaminishi, M. & Esumi, H. 2001. Cell Cycle Regulation via p53 Phosphorylation by a 5′-AMP Activated Protein Kinase Activator, 5-Aminoimidazole- 4-Carboxamide-1-β-d-Ribofuranoside, in a Human Hepatocellular Carcinoma Cell Line. *Biochemical and Biophysical Research Communications,* 287**,** 562-567.

Ingebritsen, T. S. & Cohen, P. 1983. The Protein Phosphatases Involved in Cellular Regulation. *European Journal of Biochemistry,* 132**,** 255-261.

Inoki, K., Li, Y., Xu, T. & Guan, K.-L. 2003. Rheb GTPase is a direct target of TSC2 GAP activity and regulates mTOR signaling. *Genes & Development,* 17**,** 1829-1834.

Iseli, T. J., Walter, M., Van Denderen, B. J. W., Katsis, F., Witters, L. A., Kemp, B. E., Michell, B. J. & Stapleton, D. 2005. AMP-activated Protein Kinase β Subunit Tethers α and γ Subunits via Its C-terminal Sequence (186–270). *Journal of Biological Chemistry,* 280**,** 13395-13400.

Jäger, S., Handschin, C., St.-Pierre, J. & Spiegelman, B. M. 2007. AMP-activated protein kinase (AMPK) action in skeletal muscle via direct phosphorylation of PGC-1α. *Proceedings of the National Academy of Sciences,* 104**,** 12017-12022.

Jaleel, M., Mcbride, A., Lizcano, J. M., Deak, M., Toth, R., Morrice, N. A. & Alessi, D. R. 2005. Identification of the sucrose non-fermenting related kinase SNRK, as a novel LKB1 substrate. *FEBS Letters,* 579**,** 1417-1423.

Jenne, D. E., Reomann, H., Nezu, J.-I., Friedel, W., Loff, S., Jeschke, R., Muller, O., Back, W. & Zimmer, M. 1998. Peutz-Jeghers syndrome is caused by mutations in a novel serine threoninekinase. *Nat Genet,* 18**,** 38-43.

Jishage, K.-I., Nezu, J.-I., Kawase, Y., Iwata, T., Watanabe, M., Miyoshi, A., Ose, A., Habu, K., Kake, T., Kamada, N., Ueda, O., Kinoshita, M., Jenne, D. E., Shimane, M. & Suzuki, H. 2002. Role of Lkb1, the causative gene of Peutz–Jegher's syndrome, in embryogenesis and polyposis. *Proceedings of the National Academy of Sciences,* 99**,** 8903-8908.

Jones, R. G. & Thompson, C. B. 2007. Revving the Engine: Signal Transduction Fuels T Cell Activation. *Immunity,* 27**,** 173-178.

Jørgensen, S. B., Viollet, B., Andreelli, F., Frøsig, C., Birk, J. B., Schjerling, P., Vaulont, S., Richter, E. A. & Wojtaszewski, J. F. P. 2004. Knockout of the α2 but Not α1 5'-AMP-activated Protein Kinase Isoform Abolishes 5-Aminoimidazole-4-carboxamide-1-β-4-ribofuranosidebut Not Contraction-induced Glucose Uptake in Skeletal Muscle. *Journal of Biological Chemistry,* 279**,** 1070-1079.

Kahn, B. B., Alquier, T., Carling, D. & Hardie, D. G. 2005. AMP-activated protein kinase: Ancient energy gauge provides clues to modern understanding of metabolism. *Cell Metabolism,* 1**,** 15-25.

Karuman, P., Gozani, O., Odze, R. D., Zhou, X. C., Zhu, H., Shaw, R., Brien, T. P., Bozzuto, C. D., Ooi, D., Cantley, L. C. & Yuan, J. 2001. The Peutz-Jegher Gene Product LKB1 Is a Mediator of p53-Dependent Cell Death. *Molecular Cell,* 7**,** 1307-1319.

Katoh, Y., Takemori, H., Horike, N., Doi, J., Muraoka, M., Min, L. & Okamoto, M. 2004. Salt-inducible kinase (SIK) isoforms: their involvement in steroidogenesis and adipogenesis. *Molecular and Cellular Endocrinology,* 217**,** 109-112.

Kazgan, N., Williams, T., Forsberg, L. J. & Brenman, J. E. 2010. Identification of a Nuclear Export Signal in the Catalytic Subunit of AMP-activated Protein Kinase. *Molecular Biology of the Cell,* 21**,** 3433-3442.

Kelly, A. P., Finlay, D. K., Hinton, H. J., Clarke, R. G., Fiorini, E., Radtke, F. & Cantrell, D. A. 2007. Notch-induced T cell development requires phosphoinositide-dependent kinase 1. *EMBO J,* 26**,** 3441-3450.

Khattri, R., Cox, T., Yasayko, S.-A. & Ramsdell, F. 2003. An essential role for Scurfin in CD4+CD25+ T regulatory cells. *Nat Immunol,* 4**,** 337-342.

Kim, J., Kundu, M., Viollet, B. & Guan, K.-L. 2011. AMPK and mTOR regulate autophagy through direct phosphorylation of Ulk1. *Nat Cell Biol,* 13**,** 132-141.

Kishi, M., Pan, Y. A., Crump, J. G. & Sanes, J. R. 2005. Mammalian SAD Kinases Are Required for Neuronal Polarization. *Science,* 307**,** 929-932.

Kitagawa, R., Bakkenist, C. J., Mckinnon, P. J. & Kastan, M. B. 2004. Phosphorylation of SMC1 is a critical downstream event in the ATM–NBS1–BRCA1 pathway. *Genes & Development,* 18**,** 1423-1438.

Koo, S.-H., Flechner, L., Qi, L., Zhang, X., Screaton, R. A., Jeffries, S., Hedrick, S., Xu, W., Boussouar, F., Brindle, P., Takemori, H. & Montminy, M. 2005. The CREB coactivator TORC2 is a key regulator of fasting glucose metabolism. *Nature,* 437**,** 1109-11.

Krangel, M. S. 2009. Mechanics of T cell receptor gene rearrangement. *Current Opinion in Immunology,* 21**,** 133-139.

Laplante, M. & Sabatini, David m. 2012. mTOR Signaling in Growth Control and Disease. *Cell,* 149**,** 274-293.

Lavin, M. F. & Shiloh, Y. 1997. THE GENETIC DEFECT IN ATAXIA-TELANGIECTASIA. *Annual Review of Immunology,* 15**,** 177-202.

Le Borgne, M., Ladi, E., Dzhagalov, I., Herzmark, P., Liao, Y. F., Chakraborty, A. K. & Robey, E. A. 2009. The impact of negative selection on thymocyte migration in the medulla. *Nat Immunol,* 10**,** 823-830.

Leclerc, I., Lenzner, C., Gourdon, L., Vaulont, S., Kahn, A. & Viollet, B. 2001. Hepatocyte Nuclear Factor-4α Involved in Type 1 Maturity-Onset Diabetes of the Young Is a Novel Target of AMP-Activated Protein Kinase. *Diabetes,* 50**,** 1515-1521.

Lee, K.-H. & Kim, K.-H. 1977. Regulation of Rat Liver Acetyl Coenzyme A Carboxylase: Evidence for Interconversion between active and inactive forms of enzyme by phosphorylation and dephosphorylation. *Journal of Biological Chemistry,* 252**,** 1748-1751.

Li, Y., Xu, S., Mihaylova, M. M., Zheng, B., Hou, X., Jiang, B., Park, O., Luo, Z., Lefai, E., Shyy, John y. J., Gao, B., Wierzbicki, M., Verbeuren, Tony j., Shaw, Reuben j., Cohen, Richard a. & Zang, M. 2011. AMPK Phosphorylates and Inhibits SREBP Activity to Attenuate Hepatic Steatosis and Atherosclerosis in Diet-Induced Insulin-Resistant Mice. *Cell Metabolism,* 13**,** 376-388.

Liang, J., Shao, S. H., Xu, Z.-X., Hennessy, B., Ding, Z., Larrea, M., Kondo, S., Dumont, D. J., Gutterman, J. U., Walker, C. L., Slingerland, J. M. & Mills, G. B. 2007. The energy sensing LKB1-AMPK pathway regulates p27kip1 phosphorylation mediating the decision to enter autophagy or apoptosis. *Nat Cell Biol,* 9**,** 218-224.

Lindahl, T. & Nyberg, B. 1972. RATE OF DEPURINATION OF NATIVE DEOXYRIBONUCLEIC ACID. *Biochemistry,* 11**,** 3610-&.

Liu, S. K., Fang, N., Koretzky, G. A. & Jane Mcglade, C. 1999. The hematopoietic-specific adaptor protein Gads functions in T-cell signaling via interactions with the SLP-76 and LAT adaptors. *Current biology : CB,* 9**,** 67-75.

Lizcano, J. M., Goransson, O., Toth, R., Deak, M., Morrice, N. A., Boudeau, J., Hawley, S. A., Udd, L., Makela, T. P., Hardie, D. G. & Alessi, D. R. 2004. LKB1 is a master kinase that activates 13 kinases of the AMPK subfamily, including MARK/PAR-1. *EMBO Journal,* 23**,** 833-843.

Loehrer, P. J. 2006. Etoposide therapy for testicular cancer. *Cancer,* 67**,** 220-224.

Lord, C. J. & Ashworth, A. 2012. The DNA damage response and cancer therapy. *Nature,* 481**,** 287-294.

Ma, D., Wei, Y. & Liu, F. 2011 (epub ahead of print). Regulatory mechanisms of thymus and T cell development. *Developmental & Comparative Immunology*.

Maillard, I., Tu, L., Sambandam, A., Yashiro-Ohtani, Y., Millholland, J., Keeshan, K., Shestova, O., Xu, L., Bhandoola, A. & Pear, W. S. 2006. The requirement for Notch signaling at the β-selection checkpoint in vivo is absolute and independent of the pre–T cell receptor. *The Journal of Experimental Medicine,* 203**,** 2239-2245.

Manning, G., Whyte, D. B., Martinez, R., Hunter, T. & Sudarsanam, S. 2002. The Protein Kinase Complement of the Human Genome. *Science,* 298**,** 1912-1934.

Marino, S., Krimpenfort, P., Leung, C., Van Der Korput, H. a. G. M., Trapman, J., Camenisch, I., Berns, A. & Brandner, S. 2002. PTEN is essential for cell migration but not for fate determination and tumourigenesis in the cerebellum. *Development,* 129**,** 3513-3522.

Marsin, A. S., Bertrand, L., Rider, M. H., Deprez, J., Beauloye, C., Vincent, M. F., Van Den Berghe, G., Carling, D. & Hue, L. 2000. Phosphorylation and activation of heart PFK-2 by AMPK has a role in the stimulation of glycolysis during ischaemia. *Current Biology,* 10**,** 1247-1255.

Marsin, A. S., Bouzin, C., Bertrand, L. & Hue, L. 2002. The stimulation of glycolysis by hypoxia in activated monocytes is mediated by AMP-activated protein kinase and inducible 6-phosphofructo-2-kinase. *Journal of Biological Chemistry,* 277**,** 30778-30783.

Mascaux, C., Paesmans, M., Berghmans, T., Branle, F., Lafitte, J. J., LemaîTre, F., Meert, A. P., Vermylen, P. & Sculier, J. P. 2000. A systematic review of the role of etoposide and cisplatin in the chemotherapy of small cell lung cancer with methodology assessment and meta-analysis. *Lung Cancer,* 30**,** 23-36.

Matsumoto, S., Iwakawa, R., Takahashi, K., Kohno, T., Nakanishi, Y., Matsuno, Y., Suzuki, K., Nakamoto, M., Shimizu, E., Minna, J. D. & Yokota, J. 2007. Prevalence and specificity of LKB1 genetic alterations in lung cancers. *Oncogene,* 26**,** 5911-5918.

Matsuoka, S., Ballif, B. A., Smogorzewska, A., Mcdonald, E. R., Hurov, K. E., Luo, J., Bakalarski, C. E., Zhao, Z., Solimini, N., Lerenthal, Y., Shiloh, Y., Gygi, S. P. & Elledge, S. J. 2007. ATM and ATR Substrate Analysis Reveals Extensive Protein Networks Responsive to DNA Damage. *Science,* 316**,** 1160-1166.

Mayer, A., Denanglaire, S., Viollet, B., Leo, O. & Andris, F. 2008. AMP-activated protein kinase regulates lymphocyte responses to metabolic stress but is largely dispensable for immune cell development and function. *European Journal of Immunology,* 38**,** 948-956.

Mcbride, A., Ghilagaber, S., Nikolaev, A. & Hardie, D. G. 2009. The Glycogen-Binding Domain on the AMPK ² Subunit Allows the Kinase to Act as a Glycogen Sensor. *Cell Metabolism,* 9**,** 23-34.

Mccrimmon, R. J., Shaw, M., Fan, X., Cheng, H., Ding, Y., Vella, M. C., Zhou, L., Mcnay, E. C. & Sherwin, R. S. 2008. Key Role for AMP-Activated Protein Kinase in the Ventromedial Hypothalamus in Regulating Counterregulatory Hormone Responses to Acute Hypoglycemia. *Diabetes,* 57**,** 444-450.

Mcmahon, S. B., Van Buskirk, H. A., Dugan, K. A., Copeland, T. D. & Cole, M. D. 1998. The Novel ATM-Related Protein TRRAP Is an Essential Cofactor for the c-Myc and E2F Oncoproteins. *Cell,* 94**,** 363-374.

Merrill, G. F., Kurth, E. J., Hardie, D. G. & Winder, W. W. 1997. AICA riboside increases AMP-activated protein kinase, fatty acid oxidation, and glucose uptake in rat muscle. *American Journal of Physiology - Endocrinology and Metabolism,* 273.

Meulmeester, E., Pereg, Y., Shiloh, Y. & Jochemsen, A. G. 2005. ATM-Mediated Phosphorylations Inhibit Mdmx/Mdm2 Stabilization by HAUSP in Favor of p53 Activation. *Cell Cycle,* 4**,** 1166-1170.

Michell, B. J., Stapleton, D., Mitchelhill, K. I., House, C. M., Katsis, F., Witters, L. A. & Kemp, B. E. 1996. Isoform-specific Purification and Substrate Specificity of the 5'-AMP-activated Protein Kinase. *Journal of Biological Chemistry,* 271**,** 28445-28450.

Mihaylova, M. M., Vasquez, D. S., Ravnskjaer, K., Denechaud, P. D., Yu, R. T., Alvarez, J. G., Downes, M., Evans, R. M., Montminy, M. & Shaw, R. J. 2011. Class IIa Histone Deacetylases Are Hormone-Activated Regulators of FOXO and Mammalian Glucose Homeostasis. *Cell,* 145**,** 607-621.

Milburn, C. C., Boudeau, J., Deak, M., Alessi, D. R. & Van Aalten, D. M. F. 2004. Crystal structure of MO25[alpha] in complex with the C terminus of the pseudo kinase STE20-related adaptor. *Nat Struct Mol Biol,* 11**,** 193-200.

Minokoshi, Y., Alquier, T., Furukawa, H., Kim, Y. B., Lee, A., Xue, B., Mu, J., Foufelle, F., Ferre, P., Birnbaum, M. J., Stuck, B. J. & Kahn, B. B. 2004. AMP-kinase regulates food intake by responding to hormonal and nutrient signals in the hypothalamus. *Nature,* 428**,** 569-574.

Minokoshi, Y., Kim, Y. B., Peroni, O. D., Fryer, L. G. D., Müller, C., Carling, D. & Kahn, B. B. 2002. Leptin stimulates fatty-acid oxidation by activating AMP-activated protein kinase. *Nature,* 415**,** 339-343.

Mitchelhill, K. I., Michell, B. J., House, C. M., Stapleton, D., Dyck, J., Gamble, J., Ullrich, C., Witters, L. A. & Kemp, B. E. 1997. Posttranslational modifications of the 5'-AMP-

activated protein kinase β1 subunit. *Journal of Biological Chemistry,* 272**,** 24475-24479.

Mitchelhill, K. I., Stapleton, D., Gao, G., House, C., Michell, B., Katsis, F., Witters, L. A. & Kemp, B. E. 1994. Mammalian AMP-activated protein kinase shares structural and functional homology with the catalytic domain of yeast Snf1 protein kinase. *Journal of Biological Chemistry,* 269**,** 2361-2364.

Miyamoto, H., Matsushiro, A. & Nozaki, M. 1993. Molecular cloning of a novel mRNA sequence expressed in cleavage stage mouse embryos. *Mol Reprod Dev,* 34**,** 1-7.

Miyoshi, H., Deguchi, A., Nakau, M., Kojima, Y., Mori, A., Oshima, M., Aoki, M. & Taketo, M. M. 2009. Hepatocellular carcinoma development induced by conditional β-catenin activation in Lkb1+/− mice. *Cancer Science,* 100**,** 2046-2053.

Momcilovic, M., Hong, S.-P. & Carlson, M. 2006. Mammalian TAK1 Activates Snf1 Protein Kinase in Yeast and Phosphorylates AMP-activated Protein Kinase in Vitro. *Journal of Biological Chemistry,* 281**,** 25336-25343.

Montecucco, A. & Biamonti, G. 2007. Cellular response to etoposide treatment. *Cancer Letters,* 252**,** 9-18.

Mosmann, T. R., Cherwinski, H., Bond, M. W., Giedlin, M. A. & Coffman, R. L. 1986. Two types of murine helper T cell clone. I. Definition according to profiles of lymphokine activities and secreted proteins. *The Journal of Immunology,* 136**,** 2348-57.

Munday, M. R., Campbell, D. G., Carling, D. & Hardie, D. G. 1988. Identification by amino acid sequencing of three major regulatory phosphorylation sites on rat acetyl-CoA carboxylase. *European Journal of Biochemistry,* 175**,** 331-338.

Murphy, K. (ed.) 2012. *Janeway's Immunobiology*: Garland Science.

Murphy, K. M. & Reiner, S. L. 2002. The lineage decisions of helper T cells. *Nat Rev Immunol,* 2**,** 933-944.

Mustelin, T. & Taskén, K. 2003. Positive and negative regulation of T-cell activation through kinases and phosphatases. *Biochem. J.,* 371**,** 15-27.

Oakhill, J. S., Chen, Z.-P., Scott, J. W., Steel, R., Castelli, L. A., Ling, N., Macaulay, S. L. & Kemp, B. E. 2010. β-Subunit myristoylation is the gatekeeper for initiating metabolic stress sensing by AMP-activated protein kinase (AMPK). *Proceedings of the National Academy of Sciences,* 107**,** 19237-19241.

Oakhill, J. S., Steel, R., Chen, Z.-P., Scott, J. W., Ling, N., Tam, S. & Kemp, B. E. 2011. AMPK Is a Direct Adenylate Charge-Regulated Protein Kinase. *Science,* 332**,** 1433-1435.

Osoba, D. 1966. Functions of the thymus. *Canad. Med. Ass. J.,* 94**,** 488-97.

Pacholczyk, R. & Kern, J. 2008. The T-cell receptor repertoire of regulatory T cells. *Immunology,* 125**,** 450-458.

Pang, T., Xiong, B., Li, J.-Y., Qiu, B.-Y., Jin, G.-Z., Shen, J.-K. & Li, J. 2007. Conserved α-Helix Acts as Autoinhibitory Sequence in AMP-activated Protein Kinase α Subunits. *Journal of Biological Chemistry,* 282**,** 495-506.

Pearson, E. R. 2011. Common variants near ATM are associated with glycemic response to metformin in type 2 diabetes. *Nat Genet,* 43**,** 117-120.

Penninger, J. M., Fischer, K. D., Sasaki, T., Kozieradzki, I., Le, J., Tedford, K., Bachmaier, K., Ohashi, P. S. & Bachmann, M. F. 1999. The oncogene product Vav is a crucial regulator of primary cytotoxic T cell responses but has no apparent role in CD28-mediated co-stimulation. *European Journal of Immunology,* 29**,** 1709-1718.

Plowman, G. D., Sudarsanam, S., Bingham, J., Whyte, D. & Hunter, T. 1999. The protein kinases of Caenorhabditis elegans: A model for signal transduction in multicellular organisms. *Proceedings of the National Academy of Sciences,* 96**,** 13603-13610.

Podsypanina, K., Ellenson, L. H., Nemes, A., Gu, J., Tamura, M., Yamada, K. M., Cordon-Cardo, C., Catoretti, G., Fisher, P. E. & Parsons, R. 1999. Mutation of Pten/Mmac1 in mice

causes neoplasia in multiple organ systems. *Proceedings of the National Academy of Sciences,* 96**,** 1563-1568.

Polekhina, G., Gupta, A., Michell, B. J., Van Denderen, B., Murthy, S., Feil, S. C., Jennings, I. G., Campbell, D. J., Witters, L. A., Parker, M. W., Kemp, B. E. & Stapleton, D. 2003. AMPK β Subunit Targets Metabolic Stress Sensing to Glycogen. *Current Biology,* 13**,** 867-871.

Polekhina, G., Gupta, A., Van Denderen, B. J. W., Feil, S. C., Kemp, B. E., Stapleton, D. & Parker, M. W. 2005. Structural Basis for Glycogen Recognition by AMP-Activated Protein Kinase. *Structure (London, England : 1993),* 13**,** 1453-1462.

Povirk, L. 2006. Biochemical mechanisms of chromosomal translocations resulting from double- strand breaks. *DNA Repair (Amst),* 5**,** 1199-212.

Prasad, K. V., Cai, Y. C., Raab, M., Duckworth, B., Cantley, L., Shoelson, S. E. & Rudd, C. E. 1994. T-cell antigen CD28 interacts with the lipid kinase phosphatidylinositol 3-kinase by a cytoplasmic Tyr(P)-Met-Xaa-Met motif. *Proceedings of the National Academy of Sciences,* 91**,** 2834-2838.

Radtke, F., Wilson, A., Stark, G., Bauer, M., Van Meerwijk, J., Macdonald, H. R. & Aguet, M. 1999. Deficient T Cell Fate Specification in Mice with an Induced Inactivation of Notch1. *Immunity,* 10**,** 547-558.

Rathmell, J. C., Elstrom, R. L., Cinalli, R. M. & Thompson, C. B. 2003. Activated Akt promotes increased resting T cell size, CD28-independent T cell growth, and development of autoimmunity and lymphoma. *European Journal of Immunology,* 33**,** 2223-2232.

Reynolds, R. J. & Friedberg, E. C. 1981. Molecular Mechanisms of Pyrimidine Dimer Excision in Saccharomyces cerevisiae: Incision of Ultraviolet-Irradiated Deoxyribonucleic Acid In Vivo. *Journal of Bacteriology,* 146**,** 692-704.

Rodewald, H.-R. 2008. Thymus Organogenesis. *Annual Review of Immunology,* 26**,** 355-388.

Ross, F. A., Rafferty, J. N., Dallas, M. L., Ogunbayo, O., Ikematsu, N., Mcclafferty, H., Tian, L., Widmer, H., Rowe, I. C. M., Wyatt, C. N., Shipston, M. J., Peers, C., Hardie, D. G. & Evans, A. M. 2011. Selective Expression in Carotid Body Type I Cells of a Single Splice Variant of the Large Conductance Calcium- and Voltage-activated Potassium Channel Confers Regulation by AMP-activated Protein Kinase. *Journal of Biological Chemistry,* 286**,** 11929-11936.

Rouse, J. & Jackson, S. P. 2002. Interfaces Between the Detection, Signaling, and Repair of DNA Damage. *Science,* 297**,** 547-551.

Sakaguchi, S., Sakaguchi, N., Asano, M., Itoh, M. & Toda, M. 1995. Immunologic self-tolerance maintained by activated T cells expressing IL-2 receptor alpha-chains (CD25). Breakdown of a single mechanism of self-tolerance causes various autoimmune diseases. *The Journal of Immunology,* 155**,** 1151-64.

Sakamoto, K., Mccarthy, A., Smith, D., Green, K. A., Hardie, D. G., Ashworth, A. & Alessi, D. R. 2005. Deficiency of LKB1 in skeletal muscle prevents AMPK activation and glucose uptake during contraction. *EMBO Journal,* 24**,** 1810-1820.

Salt, I., Celler, J. W., Hawley, S. A., Prescott, A., Woods, A., Carling, D. & Hardie, D. G. 1998. AMP-activated protein kinase: Greater AMP dependence, and preferential nuclear localization, of complexes containing the α2 isoform. *Biochemical Journal,* 334**,** 177-187.

Sanchez-Cespedes, M., Parrella, P., Esteller, M., Nomoto, S., Trink, B., Engles, J. M., Westra, W. H., Herman, J. G. & Sidransky, D. 2002. Inactivation of LKB1/STK11 Is a Common Event in Adenocarcinomas of the Lung. *Cancer Research,* 62**,** 3659-3662.

Sanders, M. J., Grondin, P. O., Hegarty, B. D., Snowden, M. A. & Carling, D. 2007. Investigating the mechanism for AMP activation of the AMP-activated protein kinase cascade. *Biochemical Journal,* 403**,** 139-148.

Sanli, T., Rashid, A., Liu, C., Harding, S., Bristow, R. G., Cutz, J.-C., Singh, G., Wright, J. & Tsakiridis, T. 2010. Ionizing Radiation Activates AMP-Activated Kinase (AMPK): A Target

for Radiosensitization of Human Cancer Cells. *International Journal of Radiation Oncology*Biology*Physics,* 78**,** 221-229.

Sant'angelo, D. B. & Janeway, C. A. 2002. Negative selection of thymocytes expressing the D10 TCR. *Proceedings of the National Academy of Sciences,* 99**,** 6931-6936.

Sapkota, G. P., Boudeau, J., Deak, M., Kieloch, A., Morrice, N. A. & Alessi, D. R. 2002a. Identification and characterization of four novel phosphorylation sites (Ser31, Ser325, Thr336 and Thr366) on LKB1/STK11, the protein kinase mutated in Peutz-Jeghers cancer syndrome. . *Biochemical Journal,* 362**,** 481-90.

Sapkota, G. P., Deak, M., Kieloch, A., Morrice, N., Goodarzi, A. A., Smythe, C., Shiloh, Y., Lees-Miller, S. P. & Alessi, D. R. 2002b. Ionizing radiation induces ataxia telangiectasia mutated kinase (ATM)-mediated phosphorylation of LKB1/STK11 at Thr-366. *Biochem J. ,* 368(Pt 2)**,** 507-16.

Sapkota, G. P., Lizcano, J. M., Lain, S., Arthur, J. S. C., Deak, M., Morrice, N. & Alessi, D. R. 2001. Phosphorylation of the Protein Kinase Mutated in Peutz-Jeghers Cancer Syndrome, LKB1/STK11, at Ser431 by p90RSK and cAMP-dependent Protein Kinase, but Not Its Farnesylation at Cys433, Is Essential for LKB1 to Suppress Cell Growth. *Journal of Biological Chemistry,* 276**,** 19469-19482.

Schon, O., Friedler, A., Bycroft, M., Freund, S. M. V. & Fersht, A. R. 2002. Molecular Mechanism of the Interaction between MDM2 and p53. *Journal of Molecular Biology,* 323**,** 491-501.

Scott, J. W., Hawley, S. A., Green, K. A., Anis, M., Stewart, G., Scullion, G. A., Norman, D. G. & Hardie, D. G. 2004. CBS domains form energy-sensing modules whose binding of adenosine ligands is disrupted by disease mutations. *The Journal of Clinical Investigation,* 113**,** 274-284.

Scott, J. W., Norman, D. G., Hawley, S. A., Kontogiannis, L. & Hardie, D. G. 2002. Protein kinase substrate recognition studied using the recombinant catalytic domain of AMP-activated protein kinase and a model substrate. *Journal of Molecular Biology,* 317**,** 309-323.

Scott, J. W., Van Denderen, B. J. W., Jorgensen, S. B., Honeyman, J. E., Steinberg, G. R., Oakhill, J. S., Iseli, T. J., Koay, A., Gooley, P. R., Stapleton, D. & Kemp, B. E. 2008. Thienopyridone Drugs Are Selective Activators of AMP-Activated Protein Kinase [2]1-Containing Complexes. *Chemistry & biology,* 15**,** 1220-1230.

Screaton, R. A., Conkright, M. D., Katoh, Y., Best, J. L., Canettieri, G., Jeffries, S., Guzman, E., Niessen, S., Yates, J. R., Takemori, H., Okamoto, M. & Montminy, M. 2004. The CREB Coactivator TORC2 Functions as a Calcium- and cAMP-Sensitive Coincidence Detector. *Cell,* 119**,** 61-74.

Shackelford, D. B. & Shaw, R. J. 2009. The LKB1-AMPK pathway: Metabolism and growth control in tumour suppression. *Nature Reviews Cancer,* 9**,** 563-575.

Shaw, R., Lamia, K., Vasquez, D., Koo, S., Bardeesy, N., Depinho, R., Montminy, M. & Cantley, L. 2005. The kinase LKB1 mediates glucose homeostasis in liver and therapeutic effects of metformin. *Science,* 310**,** 1642 - 1646.

Shaw, R. J., Bardeesy, N., Manning, B. D., Lopez, L., Kosmatka, M., Depinho, R. A. & Cantley, L. C. 2004a. The LKB1 tumor suppressor negatively regulates mTOR signaling. *Cancer Cell,* 6**,** 91-99.

Shaw, R. J., Kosmatka, M., Bardeesy, N., Hurley, R. L., Witters, L. A., Depinho, R. A. & Cantley, L. C. 2004b. The tumor suppressor LKB1 kinase directly activates AMP-activated kinase and regulates apoptosis in response to energy stress. *Proceedings of the National Academy of Sciences of the United States of America,* 101**,** 3329-3335.

Smith, A. C., Bruce, C. R. & Dyck, D. J. 2005. AMP kinase activation with AICAR further increases fatty acid oxidation and blunts triacylglycerol hydrolysis in contracting rat soleus muscle. *The Journal of Physiology,* 565**,** 547-553.

Smith, D. P., Spicer, J., Smith, A., Swift, S. & Ashworth, A. 1999. The Mouse Peutz-Jeghers Syndrome Gene Lkbl Encodes a Nuclear Protein Kinase. *Human Molecular Genetics,* 8**,** 1479-1485.

Stapleton, D., Mitchelhill, K. I., Gao, G., Widmer, J., Michell, B. J., Teh, T., House, C. M., Fernandez, C. S., Cox, T., Witters, L. A. & Kemp, B. E. 1996. Mammalian AMP-activated Protein Kinase Subfamily. *Journal of Biological Chemistry,* 271**,** 611-614.

Steinberg, G. R. & Kemp, B. E. 2009. AMPK in Health and Disease. *Physiological Reviews,* 89**,** 1025-1078.

Sun, G., Tarasov, A., Mcginty, J., Mcdonald, A., Da Silva Xavier, G., Gorman, T., Marley, A., French, P., Parker, H., Gribble, F., Reimann, F., Prendiville, O., Carzaniga, R., Viollet, B., Leclerc, I. & Rutter, G. 2010. Ablation of AMP-activated protein kinase α1 and α2 from mouse pancreatic beta cells and & RIP2.Cre neurons suppresses insulin release in vivo. *Diabetologia,* 53**,** 924-936.

Suter, M., Riek, U., Tuerk, R., Schlattner, U., Wallimann, T. & Neumann, D. 2006. Dissecting the role of 5' AMP for allosteric stimulation, activation, and deactivation of AMP-activated protein kinase. *Journal of Biological Chemistry,* 281**,** 32207-32216.

Sutherland, C. M., Hawley, S. A., Mccartney, R. R., Leech, A., Stark, M. J. R., Schmidt, M. C. & Hardie, D. G. 2003. Elm1p Is One of Three Upstream Kinases for the Saccharomyces cerevisiae SNF1 Complex. *Current biology : CB,* 13, 1299-1305.

Suzuki, A., De La Pompa, J. L., Stambolic, V., Elia, A. J., Sasaki, T., Barrantes, I. D. B., Ho, A., Wakeham, A., Ltie, A., Khoo, W., Fukumoto, M. & Mak, T. W. 1998. High cancer susceptibility and embryonic lethality associated with mutation of the PTEN tumor suppressor gene in mice. *Current biology : CB,* 8**,** 1169-1178.

Tamás, P., Hawley, S. A., Clarke, R. G., Mustard, K. J., Green, K., Hardie, D. G. & Cantrell, D. A. 2006. Regulation of the energy sensor AMP-activated protein kinase by antigen receptor and Ca2+ in T lymphocytes. *The Journal of Experimental Medicine,* 203**,** 1665-1670.

Thomson, D. M., Porter, B. B., Tall, J. H., Kim, H. J., Barrow, J. R. & Winder, W. W. 2007. Skeletal muscle and heart LKB1 deficiency causes decreased voluntary running and reduced muscle mitochondrial marker enzyme expression in mice. *American Journal of Physiology - Endocrinology and Metabolism,* 292.

Thornton, C., Snowden, M. A. & Carling, D. 1998. Identification of a novel AMP-activated protein kinase β subunit isoform that is highly expressed in skeletal muscle. *Journal of Biological Chemistry,* 273**,** 12443-12450.

Tiainen, M., Ylikorkala, A. & Mäkelä, T. P. 1999. Growth suppression by Lkb1 is mediated by a G1 cell cycle arrest. *Proceedings of the National Academy of Sciences,* 96**,** 9248-9251.

Towler, M. C., Fogarty, S., Hawley, S. A., Pan, D. A., Martin, D. M. A., Morrice, N. A., Mccarthy, A., Galardo, M. N., Meroni, S. B., Cigorraga, S. B., Ashworth, A., Sakamoto, K. & Hardie, D. G. 2008. A novel short splice variant of the tumour suppressor LKB1 is required for spermiogenesis. *Biochem J,* 416**,** 1-14.

Towler, M. C. & Hardie, D. G. 2007. AMP-activated protein kinase in metabolic control and insulin signaling. *Circulation Research,* 100**,** 328-341.

Tybulewicz, V. L. J. 2005. Vav-family proteins in T-cell signalling. *Current Opinion in Immunology,* 17**,** 267-274.

Vaahtomeri, K. & Mäkelä, T. P. 2011. Molecular mechanisms of tumor suppression by LKB1. *FEBS Letters,* 585**,** 944-951.

Viana, R., Towler, M. C., Pan, D. A., Carling, D., Viollet, B., Hardie, D. G. & Sanz, P. 2007. A Conserved Sequence Immediately N-terminal to the Bateman Domains in AMP-activated Protein Kinase γ Subunits Is Required for the Interaction with the β Subunits. *Journal of Biological Chemistry,* 282**,** 16117-16125.

Viollet, B., Andreelli, F., Jorgensen, S. B., Perrin, C., Geloen, A., Flamez, D., Mu, J., Lenzner, C., Baud, O., Bennoun, M., Gomas, E., Nicolas, G., Wojtaszewski, J. F. P., Kahn, A., Carling, D., Schuit, F. C., Birnbaum, M. J., Richter, E. A., Burcelin, R. & Vaulont, S. 2003. The AMP-activated protein kinase α2 catalytic subunit controls whole-body insulin sensitivity. *Journal of Clinical Investigation,* 111**,** 91-98.

Von Boehmer, H., Aifantis, I., Feinberg, J., Lechner, O., Saint-Ruf, C., Walter, U., Buer, J. & Azogui, O. 1999. Pleiotropic changes controlled by the pre-T-cell receptor. *Current Opinion in Immunology,* 11**,** 135-142.

Walsh, D. A., Perkins, J. P. & Krebs, E. G. 1968. An Adenosine 3',5'-Monophosphate-dependant Protein Kinase from Rabbit Skeletal Muscle. *Journal of Biological Chemistry,* 243**,** 3763-3765.

Warburg, O. 1956. On the origin of cancer cells. *Science,* 123**,** 309-14.

Ward, S. G. & Cantrell, D. A. 2001. Phosphoinositide 3-kinases in T lymphocyte activation. *Current Opinion in Immunology,* 13**,** 332-338.

Warden, S. M., Richardson, C., O'donnell J, Jr., Stapleton, D., Kemp, B. E. & Witters, L. A. 2001. Post-translational modifications of the β-1 subunit of AMP-activated protein kinase affect enzyme activity and cellular localization. *Biochemical Journal,* 354**,** 275-283.

Weekes, J., Ball, K. L., Caudwell, F. B. & Hardie, D. G. 1993. Specificity determinants for the AMP-activated protein kinase and its plant homologue analysed using synthetic peptides. *FEBS Letters,* 334**,** 335-339.

Winder, W., Wilson, H., Hardie, D., Rasmussen, B., Hutber, C., Call, G., Clayton, R., Conley, L., Yoon, S. & Zhou, B. 1997. Phosphorylation of rat muscle acetyl-CoA carboxylase by AMP-activated protein kinase and protein kinase A. *J Appl Physiol,* 82**,** 219 - 225.

Winder, W. W. & Hardie, D. G. 1996. Inactivation of acetyl-CoA carboxylase and activation of AMP-activated protein kinase in muscle during exercise. *American Journal of Physiology - Endocrinology and Metabolism,* 270**,** E299-E304.

Winder, W. W., Holmes, B. F., Rubink, D. S., Jensen, E. B., Chen, M. & Holloszy, J. O. 2000. Activation of AMP-activated protein kinase increases mitochondrial enzymes in skeletal muscle. *Journal of Applied Physiology,* 88**,** 2219-2226.

Wingo, S. N., Gallardo, T. D., Akbay, E. A., Liang, M.-C., Contreras, C. M., Boren, T., Shimamura, T., Miller, D. S., Sharpless, N. E., Bardeesy, N., Kwiatkowski, D. J., Schorge, J. O., Wong, K.-K. & Castrillon, D. H. 2009. Somatic <italic>LKB1</italic> Mutations Promote Cervical Cancer Progression. *PLoS ONE,* 4**,** e5137.

Wojtaszewski, J. F. P., Jârgensen, S. B., Hellsten, Y., Grahame Hardie, D. & Richter, E. A. 2002. Glycogen-dependent effects of 5-aminoimidazole-4-carboxamide (AICA)-riboside on AMP-activated protein kinase and glycogen synthase activities in rat skeletal muscle. *Diabetes,* 51**,** 284-292.

Wojtaszewski, J. F. P., Nielsen, P., Hansen, B. F., Richter, E. A. & Kiens, B. 2000. Isoform-specific and exercise intensity-dependent activation of 5'-AMP-activated protein kinase in human skeletal muscle. *Journal of Physiology,* 528**,** 221-226.

Woods, A., Cheung, P. C. F., Smith, F. C., Davison, M. D., Scott, J., Beri, R. K. & Carling, D. 1996a. Characterization of AMP-activated Protein Kinase and Subunits. *Journal of Biological Chemistry,* 271**,** 10282-10290.

Woods, A., Cheung, P. C. F., Smith, F. C., Davison, M. D., Scott, J., Beri, R. K. & Carling, D. 1996b. Characterization of AMP-activated protein kinase β and γ subunits Assembly of the heterotrimeric complex in vitro. *Journal of Biological Chemistry,* 271**,** 10282-10290.

Woods, A., Dickerson, K., Heath, R., Hong, S. P., Momcilovic, M., Johnstone, S. R., Carlson, M. & Carling, D. 2005. Ca2+/calmodulin-dependent protein kinase kinase-β acts upstream of AMP-activated protein kinase in mammalian cells. *Cell Metabolism,* 2**,** 21-33.

Woods, A., Johnstone, S. R., Dickerson, K., Leiper, F. C., Fryer, L. G. D., Neumann, D., Schlattner, U., Wallimann, T., Carlson, M. & Carling, D. 2003. LKB1 Is the Upstream Kinase in the AMP-Activated Protein Kinase Cascade. *Current Biology,* 13**,** 2004-2008.

Woods, A., Munday, M. R., Scott, J., Yang, X., Carlson, M. & Carling, D. 1994. Yeast SNF1 is functionally related to mammalian AMP-activated protein kinase and regulates acetyl-CoA carboxylase in vivo. *Journal of Biological Chemistry,* 269**,** 19509-19515.

Xiao, B., Heath, R., Saiu, P., Leiper, F. C., Leone, P., Jing, C., Walker, P. A., Haire, L., Eccleston, J. F., Davis, C. T., Martin, S. R., Carling, D. & Gamblin, S. J. 2007. Structural basis for AMP binding to mammalian AMP-activated protein kinase. *Nature,* 449**,** 496-500.

Xiao, B., Sanders, M. J., Underwood, E., Heath, R., Mayer, F. V., Carmena, D., Jing, C., Walker, P. A., Eccleston, J. F., Haire, L. F., Saiu, P., Howell, S. A., Aasland, R., Martin, S. R., Carling, D. & Gamblin, S. J. 2011. Structure of mammalian AMPK and its regulation by ADP. *Nature,* 472**,** 230-233.

Xie, M., Zhang, D., Dyck, J. R. B., Li, Y., Zhang, H., Morishima, M., Mann, D. L., Taffet, G. E., Baldini, A., Khoury, D. S. & Schneider, M. D. 2006. A pivotal role for endogenous TGF-β-activated kinase-1 in the LKB1/AMP-activated protein kinase energy-sensor pathway. *Proceedings of the National Academy of Sciences,* 103**,** 17378-17383.

Xie, Z., Dong, Y., Scholz, R., Neumann, D. & Zou, M.-H. 2008. Phosphorylation of LKB1 at Serine 428 by Protein Kinase C-ζ Is Required for Metformin-Enhanced Activation of the AMP-Activated Protein Kinase in Endothelial Cells. *Circulation,* 117**,** 952-962.

Yamamoto, H., Takashima, S., Shintani, Y., Yamazaki, S., Seguchi, O., Nakano, A., Higo, S., Kato, H., Liao, Y., Asano, Y., Minamino, T., Matsumura, Y., Takeda, H. & Kitakaze, M. 2008. Identification of a novel substrate for TNFα-induced kinase NUAK2. *Biochemical and Biophysical Research Communications,* 365**,** 541-547.

Yamauchi, T., Kamon, J., Minokoshi, Y., Ito, Y., Waki, H., Uchida, S., Yamashita, S., Noda, M., Kita, S., Ueki, K., Eto, K., Akanuma, Y., Froguel, P., Foufelle, F., Ferre, P., Carling, D., Kimura, S., Nagai, R., Kahn, B. B. & Kadowaki, T. 2002. Adiponectin stimulates glucose utilization and fatty-acid oxidation by activating AMP-activated protein kinase. *Nature Medicine,* 8**,** 1288-1295.

Yang, W., Hong, Y. H., Shen, X.-Q., Frankowski, C., Camp, H. S. & Leff, T. 2001. Regulation of Transcription by AMP-activated Protein Kinase. *Journal of Biological Chemistry,* 276**,** 38341-38344.

Ylikorkala, A., Rossi, D. J., Korsisaari, N., Luukko, K., Alitalo, K., Henkemeyer, M. & Mäkelä, T. P. 2001. Vascular Abnormalities and Deregulation of VEGF in Lkb1-Deficient Mice. *Science,* 293**,** 1323-1326.

Zagorska, A., Deak, M., Campbell, D. G., Banerjee, S., Hirano, M., Aizawa, S., Prescott, A. R. & Alessi, D. R. 2010. New Roles for the LKB1-NUAK Pathway in Controlling Myosin Phosphatase Complexes and Cell Adhesion. *Sci. Signal.,* 3**,** ra25-.

Zeqiraj, E., Filippi, B. M., Deak, M., Alessi, D. R. & Van Aalten, D. M. F. 2009a. Structure of the LKB1-STRAD-MO25 Complex Reveals an Allosteric Mechanism of Kinase Activation. *Science,* 326**,** 1707-1711.

Zeqiraj, E., Filippi, B. M., Goldie, S., Navratilova, I., Boudeau, J., Deak, M., Alessi, D. R. & Van Aalten, D. M. F. 2009b. ATP and MO25α Regulate the Conformational State of the STRADα Pseudokinase and Activation of the LKB1 Tumour Suppressor. *PLoS Biol,* 7**,** e1000126.

Zhai, Y., Wang, Y., Wu, Z. & Kupiec-Weglinski, J. W. 2007. Defective Alloreactive CD8 T Cell Function and Memory Response in Allograft Recipients in the Absence of CD4 Help. *The Journal of Immunology,* 179**,** 4529-4534.

Zhang, W., Sloan-Lancaster, J., Kitchen, J., Trible, R. P. & Samelson, L. E. 1998. LAT: The ZAP-70 Tyrosine Kinase Substrate that Links T Cell Receptor to Cellular Activation. *Cell,* 92**,** 83-92.

Zheng, B., Jeong, J. H., Asara, J. M., Yuan, Y. Y., Granter, S. R., Chin, L. & Cantley, L. C. 2009. Oncogenic B-RAF Negatively Regulates the Tumor Suppressor LKB1 to Promote Melanoma Cell Proliferation. *Molecular Cell,* 33**,** 237-247.

Zhou, G., Myers, R., Li, Y., Chen, Y., Shen, X., Fenyk-Melody, J., Wu, M., Ventre, J., Doebber, T., Fujii, N., Musi, N., Hirshman, M. F., Goodyear, L. J. & Moller, D. E. 2001. Role of AMP-activated protein kinase in mechanism of metformin action. *Journal of Clinical Investigation,* 108**,** 1167-1174.

Zong, H., Ren, J. M., Young, L. H., Pypaert, M., Mu, J., Birnbaum, M. J. & Shulman, G. I. 2002. AMP kinase is required for mitochondrial biogenesis in skeletal muscle in response to chronic energy deprivation. *Proceedings of the National Academy of Sciences of the United States of America,* 99**,** 15983-15987.